Scuola Normale Superiore

Tesi di Perfezionamento in Fisica

Dynamic Critical Behavior of Non-Equilibrium Systems

Candidate
Andrea Gambassi

Supervisor
Prof. Sergio Caracciolo

Ph.D. Thesis
Pisa, November 2002

Contents

Chapter 1

Introduction

At present, the statistical mechanics of systems in thermal equilibrium is well established on firm basis. A wealth of results concerning the macroscopic behavior of statistical systems have been obtained by means of both analytical and numerical works, and in many cases very good agreement with experiments has been found. The description of statistical systems in equilibrium relies on the fact that, once the microscopic interactions are known, the macroscopic properties of the system could be determined in terms of suitable statistical *ensembles*. In this approach there is no reference at all to the specific dynamical processes by means of which the system reaches the thermal equilibrium. Averages over time evolutions may be computed simply as ensemble averages. Even non-trivial collective behaviors, emerging in some cases, may be accounted for in this framework. In the case of second order phase transitions further progresses have been made thank to the observed universality which characterizes them. In most of these cases the powerful methods of *renormalization group* (RG) have been applied with striking successes.

For non-equilibrium system such a complete framework is lacking. Very useful and basic concepts in equilibrium, as the entropy and thermodynamic potentials, can not be defined in a clear way, resulting in many difficulties also when attempting a very crude description of non-equilibrium behavior[1]. Despite some recent and very interesting progresses [26], there are still many things to be understood.

Of course, in nature, equilibrium is the exception rather than the rule. For this reason it is worthwhile devoting many efforts to study non-equilibrium systems. There are many reasons for which a system, although in contact with an environment (acting as a *reservoir* of energy, particles, etc.), does not manage to equilibrate with it. Basically we can distinguish between those cases (a) in which some external sources (of energy, particles, etc.) prevent the system from achieving equilibrium with the environment (thermal bath, particle reservoir, etc.), and those (b) in which this fact is due to dynamical reasons and no external perturbations act on the system. The former class is well represented in many physical realizations, for example the heat (current) conduction in conducting materials, liquids under shear, growing interfaces and crystals, etc., and it is studied by means of simplified models of, say, driven diffusion on a lattice. Usually all these systems eventually settle in a *non-equilibrium steady state* (NESS), characterized by stationary properties and time-translational invariant dynamics of fluctuations. The class (b) mentioned above is realized in all those systems with *slow dynamics*. With this expression we simply mean that the system evolves according to a dynamics which is so slow that the relaxation towards equilibrium does not take place even after very long time has elapsed since the last external perturbation on the system. At

[1] In some cases non-equilibrium systems may display very counterintuitive properties. For a pedagogical introduction see Ref. [25].

variance with case (a), dynamical properties do not become stationary as time goes by. There are many possible examples of systems that, in our schematic classification, belong to this class: Supercooled fluids, spin glasses, non-disordered magnets developing order through domain coarsening, etc. We note that there are also very interesting cases in which the presence of a slow dynamics is due to the action of external fields. This is, for example, the case of granular material. In the absence of driving forces they are blocked in metastable states but when energy is injected in the system (by means of shearing forces or vibrations) a slow relaxation towards configurations with higher density takes place, with non-stationary properties.

1.1 Time-reversal Symmetry and Detailed Balance

It should be clear from the examples mentioned above that dynamics plays a very different role in equilibrium and non-equilibrium systems. In the former it describes only the way in which the system thermalizes and which equilibrium evolution should be expected for small fluctuations. In the latter it does determine in an *a priori* unknown way which stationary state will be reached by the system.

How does this difference emerge from the microscopic point of view? A possible way to distinguish between equilibrium and non-equilibrium is to look at the condition of *microscopic reversibility*. It is intimately related to the idea of time-reversal symmetry[2] of dynamical quantities when the system has reached the stationary state, even if some attention should be paid when establishing such a connection rigorously[3]. Indeed the very difference between a NESS (case (a)) and an equilibrium state, both characterized by time-translational invariance of observables, is that in the latter time-reversal is a symmetry of the dynamics, while in the former it is not. When the system relaxes with slow dynamics and for this reason the equilibrium state is not reached (case (b)), both time homogeneity and time-reversal symmetry are broken. These ideas can be very simply illustrated in the case of Markov chains. We do not want to treat this issue in full generality, but make very simple observation to illustrate the ideas mentioned above. For this reason we will restrict to the case of (continuous time) Markov chains on a finite space, without any attempt to discuss the problem of thermodynamic limit (we note that when considering a finite space, whatever the initial configuration is, the convergence to equilibrium is exponentially fast, and thus we can not discuss the problem of slow dynamics). Consider a finite state space $\mathcal{C}$ (for example the space of configurations of a lattice gas on finite lattice, see Sect. 2.1) and a set of non-negative transition rates $W : \mathcal{C} \times \mathcal{C} \mapsto \mathbb{R}^+$, where $W[C' \mapsto C]$ specifies the rate of the transition from the configuration C' to the configuration C. The Markov process can now be defined by means of the *Master Equation* (or Fokker-Planck equation)

$$\partial_t P(C,t|C_0,t_0) = \sum_{C' \in \mathcal{C}} \{W[C' \mapsto C]P(C',t|C_0,t_0) - W[C \mapsto C']P(C,t|C_0,t_0)\} , \tag{1.1}$$

where $P(C,t|C_0,t_0)$ is the conditional probability that the configuration of the system is C at time t, starting from an initial configuration $C_0 \in \mathcal{C}$ at time t_0. If the chain is aperiodic and irreducible (see, e.g., Ref. [78] for details) then there is a unique stationary solution $P^s(C)$ of Eq. (1.1) towards which the system evolves independently of the initial configuration chosen. In which sense is the time-reversal symmetry represented in this framework? Of course a very natural definition is as follows. Consider a trajectory in the configuration space $\{C_t\}_t$, $t \in [t_1, t_2]$, then it has a given

[2] In the following, whenever dealing with time-reversal symmetry, we assume that there are no external fields breaking it. An extension to these cases may be done.

[3] Recently it has been pointed out that in some cases microscopic irreversibility may be lost when considering macroscopic averages [28].

probability to be realized during the stochastic evolution in the stationary state (we assume that the system has already relaxed towards it). If time-reversal symmetry holds we expect that the time-reversed trajectory $\{C_t^*\}_t \equiv \{C_{-t+t_1+t_2}\}_t$ has the same probability to be realized. This, in turn, implies that (it is sufficient to consider a trajectory visiting only two configurations),

$$W[C' \mapsto C]P^s(C') = W[C \mapsto C']P^s(C) \;, \qquad \forall C, C' \in \mathcal{C} \;, \tag{1.2}$$

which is the so called *detailed balance* condition for the stationary measure P^s. If this condition is satisfied, then each single term of the sum in Eq. (1.1) vanishes (of course not all the stationary solutions satisfy the detailed balance). While Eq. (1.2) requires the explicit knowledge of P^s in order to verify the detailed balance condition, we can use an equivalent condition (see, e.g, Ref. [78]) based only on the transition rates. Indeed if, for any set of configurations $\{C_1, C_2, \ldots, C_n\} \subset \mathcal{C}$,

$$W[C_1 \mapsto C_2]W[C_2 \mapsto C_3]\cdots W[C_n \mapsto C_1] = W[C_1 \mapsto C_n]W[C_n \mapsto C_{n-1}]\cdots W[C_2 \mapsto C_1] \;, \tag{1.3}$$

then there exists a (stationary) probability distribution $P^*(C)$ satisfying the detailed balance condition. It is possible, by virtue of the irreducibility of the chain, to determine the function $P^*(C)$. Indeed, once its value is given in some point of the parameter space, using the condition of detailed balance, it can be defined on all $\mathcal{C}$ (and it is also well defined in the sense that the value assigned to a configuration is unique). Summing up, the time-reversal symmetry implies detailed balance for the stationary measure, which, by virtue of this symmetry, has to be regarded as an equilibrium distribution. We remark that in the case of physical systems of interacting particles, the equilibrium distribution is *a priori* known once the interaction Hamiltonian has been specified. In these cases the detailed balance condition give a (quite loose) constraint on the choice of transition rates, in order to be sure that the system will eventually reach the correct stationary (equilibrium) distribution, whatever the initial one is (this idea is behind all dynamic Monte Carlo simulations of statistical systems).

From the discussion above it should be clear that any violation of detailed balance condition would produce very unexpected results, given one is entering the realm of non-equilibrium systems. Lots of models have been introduced in order to capture some of the features of more complex real out-of-equilibrium systems and among them we quote percolation, directed or not, reaction-diffusion processes (with or without absorbing states), lattice gases, cellular automata, etc.

Even more intriguing is, in the context of systems reaching a NESS, the problem of phase transitions, and the effect of the violation of detailed balance on critical dynamics (see the recent overview in Ref. [23]). On the one hand it is numerically evident that non-equilibrium systems may undergo phase transitions. On the other many aspects concerning the interpretation of numerical data are still unclear, despite many efforts to analyze them. Well-established concepts applied when dealing with critical phenomena, as, for example, universality, are controversial in NESS. Therefore, it seems worthwhile to study even very simple models which are out of thermal equilibrium. Among them, one of the simples but non-trivial, was introduced at the beginning of the eighties by Katz, Lebowitz, and Spohn [36], who studied the stationary state of a lattice gas under the action of an external drive. The model, hereafter called *driven lattice gas* (DLG), may be considered as the "Ising model" for non-equilibrium critical phenomena, given its simplicity and richness. Indeed although not in thermal equilibrium, the DLG has a stationary state and shows a finite-temperature phase transition, which is however different in nature from its equilibrium counterpart[4]. In Chap. 2 we recall the definition and the properties of the DLG, which we will deal with in the first part of this work (Chapters 2–6). We review also, in Section 2.3, some general features of critical phenomena occurring in NESS, in order to show the novelties (and the difficulties) with respect to the

[4]For an extensive presentation of the DLG and of many generalizations, see Refs. [21, 35].

usual equilibrium critical behavior. Despite its simplicity, the DLG has not been solved exactly[5]. Nonetheless, many results have been obtained by means of Monte Carlo (MC) simulations and by using field-theoretical methods. This latter approach is reviewed in Chap. 3. Several computer simulations studied the critical behavior of the DLG in two and three dimensions. These simulations provided good support to the field-theoretical predictions, once it was understood that the highly anisotropic character of the transition required some kind of anisotropic finite-size scaling (FSS, discussed in Chapter 4).

Recently some doubts have been casted on the field theory that should be used to describe the critical properties of the DLG. The resulting debate is still open and we review it in Sect. 3.3. In spite of the extensive numerical work, there are no direct studies of the correlation length so far, essentially because it is not easy to define it. Thus, our first concern will be the definition of a finite-volume transverse correlation length (see Section 2.4.2). Once this have been done, we can use the FSS method discussed in Section 4.3 to determine critical exponents. Our aim is to provide evidences that could contribute to settle the debate about the universality class of the DLG, and account for some of the disappointing numerical results that heat it. In Chapter 5 we discuss the informations we can derive from our MC simulations and present also some preliminary results. In Chapter 6 we summarize the work, concerning the DLG, that we have done so far and its main perspectives.

1.2 The Fluctuation-Dissipation Theorem

It has been known since long that the time-reversal symmetry of an equilibrium state has the remarkable consequence that there is a precise relation between the correlations of spontaneous fluctuations and those externally induced in the linear response regime (Green-Kubo relations, see Ref. [8] for a classical introduction). This is essentially the content of the fluctuation-dissipation theorem (FDT). Before going on in the discussion of this subject we mention that recently much attention has been paid to the so called "fluctuation theorems" [27]. They concern the distribution of entropy production (suitably defined) in the long-time dynamics of driven out-of-equilibrium systems and reduce to the FDT in the limit of vanishing drive (i.e. when the system recover equilibrium). Our aim is here to introduce the FDT in its simplest form, which will be considered in the following, i.e. for classical statistical systems (we are not interested in the effects of quantum fluctuations, see, e.g. Ref. [113]). The very first examples of the (static) FDT are the well-known relations between fluctuations of a thermodynamic observable of an equilibrium system at a given temperature β^{-1} and its linear susceptibility with respect to changes in the conjugated field. Indeed consider a system characterized by the Hamiltonian $\mathcal{H}_0$, in equilibrium with a thermal bath. Let us consider an observable $\mathcal{O}$ whose conjugated field is h, then

$$\chi_{\mathcal{O}} \equiv \left.\frac{\delta\langle\mathcal{O}\rangle_h}{\delta h}\right|_{h=0} = \beta(\langle\mathcal{O}^2\rangle - \langle\mathcal{O}\rangle^2) \,, \tag{1.4}$$

where the average $\langle\cdot\rangle_h$ is computed by using the Gibbs measure in the presence of the small external field h, i.e. with Hamiltonian $\mathcal{H} = \mathcal{H}_0 - h\mathcal{O}$. Of course, in the case of NESS, this relation no more generally holds, given that the form of the stationary measure is not known.

The more interesting case of the FDT is when one considers the dynamical properties. We do not want to be rigorous in our discussion, aiming at giving only an introduction to the subject (see Ref. [8] for details and references). For illustration purposes let us consider a system whose properties can be described in term of a set of variables, hereafter denoted by ϕ_i, labeled with index

[5]The DLG is solvable for infinite drive in the limit in which the ratio of jump rates parallel and perpendicular to the field direction becomes infinite [37].

i, such that they vanishes in the equilibrium state (these variables represent the fluctuations of the physical quantities with respect to their equilibrium values). The Hamiltonian of the system will be denoted by $\mathcal{H}[\phi]$. To study the evolution of small fluctuations around the equilibrium (linear regime) it is usually assumed that the relaxation process can be described by means of the Langevin equation (see, e.g., Ref. [9])

$$\partial_t \phi_i(t) = -\mathbb{D}_{ij} \frac{\delta \mathcal{H}[\phi]}{\delta \phi_j(t)} + \zeta_i(t) \ . \tag{1.5}$$

The $\mathbb{D}_{ij}$ are relaxation rates (diffusion constant in the case of density relaxation, conductivity for charge relaxation and so on), while $\zeta_i(t)$ is a Gaussian random noise with covariance $\langle \zeta_i(t)\zeta_j(t')\rangle = 2\mathbb{N}_{ij}\delta(t-t')$ (where $\langle\cdot\rangle$ stands for the mean over the possible realizations of the noise). We observe that Eq. (1.5) consists of a deterministic and a stochastic part, the former taking into account the tendency of the system to recover equilibrium, the latter summing up the effects of the microscopic fluctuations. From the Langevin equation it is possible to write down a Fokker-Planck partial differential equation for the probability distribution function $P[\{\phi_i\}, t]$ of ϕ_i at a given time t, starting from a specified initial condition (see, e.g., Ref. [4])

$$\partial_t P[\{\phi_i\}, t] = \frac{\delta}{\delta \phi_k} \left[\mathbb{N} \frac{\delta P}{\delta \phi_k} + \mathbb{D} \frac{\delta \mathcal{H}}{\delta \phi_k} \right] \ . \tag{1.6}$$

The stationary measure ($\partial_t P[\{\phi_i\}, t] = 0$) is $P^s[\{\phi_i\}] \propto e^{-\beta \mathcal{H}[\phi]}$[6] if and only if

$$\mathbb{D} = \beta \mathbb{N} \quad \text{(Einstein's relation)} \ . \tag{1.7}$$

Moreover, if ergodicity holds, whatever the initial condition for the Eq. (1.6) was, the long-time limit of $P[\{\phi_i\}, t]$ is $P^s[\{\phi_i\}]$. Thus if Eq. (1.5) should describe a dynamical process leading to the expected canonical distribution (proper to the specified Hamiltonian), Eq. (1.7) has to be satisfied. We remark that Eq. (1.7) is sometimes called fluctuation-dissipation theorem (FDT), see e.g. Ref. [35] (and also the discussion in Ref. [32]), although, in most cases, this name is used for the relation (1.12) we are going to derive. We observe that one generically expects, as we will discuss in more detail in Sect. 8.1, that for NESS $\mathbb{N} \not\propto \mathbb{D}$ (see Ref. [35] for details). It is not difficult to see by algebraic manipulations [4] that, given an arbitrary function of the noise, $F(\zeta)$

$$\langle F(\zeta)\zeta_i(t)\rangle = 2\mathbb{N}_{ij} \langle \frac{\delta F(\zeta)}{\delta \zeta_j(t)} \rangle \ , \tag{1.8}$$

where summation over repeated indices is understood. With this equation in mind we can give a heuristic argument to deduce the FDT[7]. First of all let us define the dynamical correlation function between fluctuations $C_{ij}(t,s) = \langle \phi_i(t)\phi_j(s)\rangle$ (again, $\langle\cdot\rangle$ stands for the mean over the stochastic dynamics) and the response function to an external field h_i coupled to ϕ_i in the Hamiltonian $\mathcal{H}$ (as discussed previously), given by

$$R_{ij}(t,s) = \langle \frac{\delta \phi_i(t)}{\delta h_j(s)} \rangle \Big|_{h=0} \tag{1.9}$$

We note that the presence of the external field h in Eq. (1.5) is equivalent to a shift in the noise $\delta\zeta_i(t) = \mathbb{D}_{ij}\, h_j(t)$, so that Eq. (1.9) may be written as

$$R_{ij}(t,s) = \mathbb{D}_{jk} \langle \frac{\delta \phi_i(t)}{\delta \zeta_k(s)} \rangle = \frac{1}{2} \mathbb{D}\mathbb{N}^{-1}_{jk} \langle \phi_i(t)\zeta_k(s)\rangle = \frac{\beta}{2} \langle \phi_i(t)\zeta_j(s)\rangle \tag{1.10}$$

[6] We are assuming that, for the given $\mathcal{H}$, $e^{-\beta\mathcal{H}[\phi]}$ makes sense as a probability distribution, see, e.g., Ref. [4] for further details.

[7] The argument in this form may be found in Ref. [118].

where we have used both the algebraic identity (1.8) and the condition (1.7). Let us remark that, due to the causality in the dynamics of physical systems, we expect that $\phi_i(t)$ does not depend on any of $\zeta_j(s)$ (or, equivalently on $h_j(s)$) whenever $t < s$. As a consequence $R_{ij}(t,s) \propto \theta(t-s)$. In the following we consider $t > s$, so $\langle \phi_i(s)\zeta_k(t)\rangle = 0$. Now it is easy to compute $(\partial_t - \partial_s)C_{ij}(t,s) = \langle \partial_t\phi_i(t)\phi_j(s)\rangle - \langle \phi_i(t)\partial_s\phi_j(s)\rangle$, and, by using the Eq. (1.5), we get

$$(\partial_t - \partial_s)C_{ij}(t,s) = -\langle \mathbb{D}_{ik}\frac{\delta\mathcal{H}[\phi]}{\delta\phi_k(t)}\phi_j(s)\rangle + \langle \phi_i(t)\mathbb{D}_{jk}\frac{\delta\mathcal{H}[\phi]}{\delta\phi_k(s)}\rangle - \langle \phi_i(t)\zeta_j(s)\rangle \ . \tag{1.11}$$

At equilibrium, the time-reversal symmetry implies that for two generic observables $\mathcal{O}_1(t)$ and $\mathcal{O}_2(t)$, $\langle \mathcal{O}_1(t)\mathcal{O}_2(s)\rangle = \langle \mathcal{O}_1(s)\mathcal{O}_2(t)\rangle$. Moreover equilibrium is also characterized by time homogeneity and thus general correlation functions are invariant under time translations, i.e. the generic two-time correlation function C satisfies $C(t,s) = C(t-s,0)$ (this is true also in the case of NESS) and therefore $(\partial_t - \partial_s)C_{ij}(t,s) = -2\partial_s C_{ij}(t,s)$. Keeping into account all these observation and Eq. (1.10), we conclude that

$$R_{ij}(t,s) = \theta(t-s)\ \beta\ \frac{\partial C_{ij}(t,s)}{\partial s} \ , \tag{1.12}$$

which is a possible form of the FDT (we explicit write down the causality constraint). Of course there are many possible ways to deduce this result, more or less rigorous (for example, a diagrammatic derivation in the perturbative expansion suited to study dynamic critical phenomena is given in S. K. Ma, Ref. [5], while a standard reference on the subject is Ref. [8]). In Section 8.1 the formalism of dynamical functional will be briefly discussed in order to study Langevin equations as Eq. (1.5), by the introduction of response fields. Extending further this formalism it is possible to group together both kind of fields into the so called superfield (it is necessary to introduce also Grassmann coordinates) and then derive the FDT as the Ward identity of the supersymmetry (SUSY) of the resulting theory [29]. Explicit breaking of the SUSY occurs in the case of NESS [30] while in the case of slow dynamics SUSY is *spontaneously* broken [31]. See Ref. [4] for details.

Whenever the system does not reach thermal equilibrium, we can not expect that a relation as Eq. (1.12) holds, and in this sense its validity may be considered as a signal of equilibrium dynamics of fluctuation. However we must pay attention when making such a statement given it may occur that the validity of FDT and detailed balance is recovered at macroscopic level even if they do not hold at the microscopic one. This may occurs both generically, as pointed out in Ref. [28], and just when the system is at its critical point [45]. In the latter case we can say that the terms in the Langevin equation breaking the detailed balance (and thus leading to a violation of FDT) are irrelevant in the renormalization-group sense. Keeping in mind this remark, we expect that for systems settling into a NESS, the FDT will be violated generically. More interesting is, instead, the case in which it is possible to study the onset of slow-dynamical behavior by looking at the violation of FDT (spontaneous breaking in the thermodynamic limit). In Sect. 7.2 and Chap. 8 we will consider the case of the relaxation process in ferromagnetic systems after a quench from a given initial state. As long as the quench is towards the high-temperature region, equilibration time is finite and equilibrium is recovered after a while, so FDT applies and no breaking occurs. When the system is quenched right at criticality, the relaxation time is infinite (at least when thermodynamic limit is considered) and the system evolves according a slow dynamic, characterized by an aging regime. This is the subject reviewed in Sect. 7. In these cases it is possible to introduce a quantity, called fluctuation-dissipation ratio (FDR, see Sect. 7.2.3) that has been proved to be universal (as critical exponents). For this reason we can use field-theoretical methods to compute it at criticality for various models of dynamics (see Chap. 9), finding, in some cases, a satisfactory agreement with numerical simulations. The main results of the investigation we have carried out are summed up in Sect. 9.5. By using the same methods it is also possible to compute universal scaling functions for

the response and correlation functions, and this allows us to check some predictions recently made assuming Local Scale Invariance (LSI, briefly introduced in Sect. 8.4).

Chapter 2

The Driven Lattice Gas

In this Chapter we provide the basic definitions and describe the relevant features of the DLG. *In particular §2.1 gives a brief overview of the Lattice Gas in order to make clear the framework into which the* DLG *is introduced. In §2.2 we give the very definition of the* DLG *in its basic form and we stress that the main difference with the undriven case is the lack of detailed balance. The consequences of this fact are described in §2.3 where the peculiar characteristic of the* NESS *into which the* DLG *eventually settles, are reviewed. Moreover they cause some difficulties when trying to analyze correlation functions and define correlation length. In §2.4 we introduce the observables we measured in* MC *simulations. In spite of the difficulties mentioned above, we succeeded in defining the transverse finite-volume correlation length that allows us to perform the* FSS *analysis described in Chapter 5.*

2.1 Lattice Gases

As a prelude to the DLG let us consider a simple lattice gas of interacting particles. A *lattice gas*[1] is a model of indistinguishable classical particles moving on a d-dimensional hypercubic lattice $\Lambda \subset \mathbb{Z}^d$. A configuration C of the system is completely described by the occupation numbers $n_{\mathbf{i}}$ of each site $\mathbf{i} \in \Lambda$. We will consider only models in which at most one particle may occupy a given site, then $n_{\mathbf{i}} \in \{0,1\}$ and the space of states is $\mathcal{C}(\Lambda) \equiv \{0,1\}^{\Lambda}$[2]. In some sense the lattice gas may be considered as a model for physical systems of particles interacting via a short-range potential with repulsive hard-core. The distance between $\mathbf{i},\mathbf{j} \in \Lambda$ will be denoted by $|\mathbf{i}-\mathbf{j}|$ and $|\mathbf{i}-\mathbf{j}| = 1$ when $\mathbf{i}$ and $\mathbf{j}$ are nearest neighbors (NN). Given a configuration $C \in \mathcal{C}$ ($C(\mathbf{i}) \equiv n_{\mathbf{i}}$) we will denote with $C_{\mathbf{ij}}$ the configuration

$$C_{\mathbf{ij}}(\mathbf{k}) \equiv \begin{cases} C(\mathbf{j}), & \text{if } \mathbf{k} = \mathbf{i}, \\ C(\mathbf{i}), & \text{if } \mathbf{k} = \mathbf{j}, \\ C(\mathbf{k}), & \text{otherwise}, \end{cases}$$

i.e. $C_{\mathbf{ij}}$ is obtained from C by exchanging site $\mathbf{i}$ with site $\mathbf{j}$. When Λ is finite (in the following we call $|\Lambda|$ the number of sites in Λ) we can define a Markov process on the state space $\mathcal{C}$ by means of

[1] Its simplest form was used as a model in seminal works on phase transitions [2, 3].

[2] Dynamics may restricts configuration to a subset of $\{0,1\}^{\Lambda}$.

the Master Equation (1.1), discussed in Sect. 1.1

$$\partial_t P(C,t|C_0,t_0) = \sum_{C' \in \mathcal{C}} \{W[C' \mapsto C]P(C',t|C_0,t_0) - W[C \mapsto C']P(C,t|C_0,t_0)\} \,, \tag{2.1}$$

where $P(C,t|C_0,t_0)$ is the conditional probability that the configuration of the system is C at time t, starting from an initial configuration $C_0 \in \mathcal{C}$ at time t_0. The function $W[C \mapsto C']$ is the transition rate from a generic state C to another state C', both in $\mathcal{C}$.

In the following we will be interested in dynamics allowing only for NN exchanges (Kawasaki dynamics [79]), i.e. we assume that $W[C \mapsto C'] = 0$ if C' is not derived from C by making an exchange between NN sites. It is a *conservative* dynamics given that the total number of particles is conserved by construction, i.e. the density

$$\rho_\Lambda(C) \equiv \frac{1}{|\Lambda|} \sum_{\mathbf{i} \in \Lambda} n_{\mathbf{i}}, \tag{2.2}$$

does not change in time. The configuration space may be splitted into invariant subspaces with different densities, i.e. $\mathcal{C} = \cup_\rho \mathcal{C}_\rho$, where $\mathcal{C}_\rho = \{C \in \mathcal{C} \,|\, \rho_\Lambda(C) = \rho\}$. The dynamics is now irreducible [78] in every $\mathcal{C}_\rho$, i.e. from any state it is possible to get to each other state by a finite number of allowed transitions. This is sufficient to ensure that there exists a unique invariant probability (i.e. a stationary solution of Eq. (2.1)) $P^s_\rho(C)$ in each $\mathcal{C}_\rho$ and that it is independent of the initial configuration chosen.

As already said in Sect. 1.1, among stationary solutions a special role is played by those satisfying the *detailed-balance* condition, given in Eq. (1.2). As discussed there, we can prove that, under some general assumptions, among which the time-reversal invariance of the dynamics, the stationary solutions of Eq. (2.1) for a classical or quantum isolated and close physical system satisfy Eq. (1.2) [9].

The dynamics of the system is then completely specified by the transition rates $W[C \mapsto C']$. If the lattice gas has to be a model of a system in thermodynamic equilibrium then transition rates cannot be arbitrary. Indeed general principles of statistical mechanics tell us that for a system in thermal equilibrium with an heat bath of a given temperature T, the equilibrium ensemble is the canonical one (or grancanonical if the system is also coupled to a particle reservoir), proper to the Hamiltonian $H_\Lambda[C]$ of the system, and detailed balance holds.

That is, we must require

$$\frac{W[C \mapsto C']}{W[C' \mapsto C]} = \frac{P^{eq}_\Lambda(C')}{P^{eq}_\Lambda(C)}, \qquad \text{with} \qquad P^{eq}_\Lambda(C) = \frac{e^{-\beta\, H_\Lambda[C]}}{Z_\Lambda(\beta)} \,,$$

where $Z_\Lambda(\beta)$ is the partition function of the system defined on Λ and at a given temperature $T = \beta^{-1}$. This relation implies that transition rates must satisfy

$$W[C \mapsto C'] = w(\beta \Delta H) \,, \quad \text{where} \quad \Delta H \equiv H_\Lambda[C'] - H_\Lambda[C] \tag{2.3}$$

is the difference in energy between the new (C') and the old (C) configuration. In Eq. (2.3) w is a real and positive function such that

$$w(-x) = e^x \, w(x) \,.$$

Different dynamics correspond to different choices for w. The equilibrium state of the resulting Markov process is, nevertheless, the same, irrespective of the specific choice[3].

[3]One popular choice for w is the Metropolis rate $w(x) = \min\{1; e^{-x}\}$.

In the following we will consider only the simplest case, namely that of NN interaction energy

$$H_\Lambda[C] = -4J \sum_{\langle \mathbf{i},\mathbf{j}\rangle \in \Lambda} n_\mathbf{i}\, n_\mathbf{j} \ , \tag{2.4}$$

where the sum runs over all the lattice nearest-neighbor pairs and the coupling J may be positive (*ferromagnetic* interaction, in spin language) or negative (*antiferromagnetic* one). It's easy to realize that the system has the same stationary measure as the Ising model with fixed magnetization $m = 2\rho - 1$, given a trivial mapping between the corresponding Hamiltonians. Then in dimensions $d \geq 2$, for $m = 0$ and $|\Lambda| \to \infty$ we expect a second-order phase transition occurring at a given finite temperature $T_c(J,d)$[4] (for $d = 2$, relevant in what follows, the critical temperature is the Onsager one $J\,\beta_c = \frac{1}{2}\ln(\sqrt{2}+1)$). This transition is of course well understood both from the thermodynamical point of view [4], and for what concerns dynamical effects [1].

It is possible to modify this very simple and well-known model of equilibrium dynamics to obtain models which mimic real systems driven out of equilibrium.

2.2 Driven Lattice Gas: Standard Model

Let us consider a lattice gas with a nearest-neighbor attractive (ferromagnetic, in spin language) Hamiltonian (2.4) where, without loss of generality, we assume $J = 1$. We consider, as before, discrete-time Kawasaki-type dynamics [79], which preserves the total number of particles N or, equivalently, the density (2.2). At each step, we choose randomly a lattice link $\langle \mathbf{i},\mathbf{j}\rangle$. If $n_\mathbf{i} = n_\mathbf{j}$, nothing happens. Otherwise, we propose a swap, i.e. a particle jump, which is accepted with probability given by Eq. (2.3) where C' is the configuration after the swap and C is the initial one.

The DLG is a generalization of the lattice gas previously described in which one introduces a uniform (in space and time) force field pointing along one of the axes of the lattice, say $\hat{\mathbf{x}}$, i.e. $\mathbf{E} = E\hat{\mathbf{x}}$. It favors (respectively unfavors) the particle jumps along (resp. opposite) to the $\hat{\mathbf{x}}$-direction while those transverse to it are not affected. If Λ is bounded by *rigid walls*, then $\mathbf{E}$ is a conservative field and it can be accounted for by adding a linear potential term to $H_\Lambda[C]$. Therefore, the system remains in thermal equilibrium: The net effect of $\mathbf{E}$ is simply to induce a particle concentration gradient in the equilibrium state.

Here, we will consider instead *periodic boundary conditions*[5]. In this case, the field $\mathbf{E}$ does not have a global potential and the system eventually reaches a stationary state which, however, is not in thermal equilibrium (NESS).

In the DLG, transition probabilities take into account the work done by the field during the particle jump from one site to one of its nearest neighbors. In this case, instead of (2.3), one accepts a proposed particle swap with probability

$$w(\beta\,\Delta H + \beta E \ell) \ , \tag{2.5}$$

with $\ell = (1, 0, -1)$ for jumps (along, transverse, opposite) to $\hat{\mathbf{x}}$.

For $E \neq 0$ and $\rho_\Lambda = 1/2$, the system shows a continuous phase transition (numerical evidences in $d = 2$ and $d = 3$, can be found in a lot of papers, see Refs. [21,35] for comprehensive reviews) at a temperature $T_c(E)$. Interestingly enough, $T_c(E)$ increases with E (somehow the opposite of what one could have expected, see footnote 1 of Chap. 1) and saturates to a finite $T_c(\infty)$ for diverging

[4]Given the equivalence, in the thermodynamic limit, of canonical and grancanonical ensemble, conservative (*diffusive*) and non-conservative dynamics lead to the same equilibrium properties.

[5]In principle, it is enough to consider periodic boundary conditions in the field direction. The boundary conditions in the transverse directions are largely irrelevant for the problems discussed here.

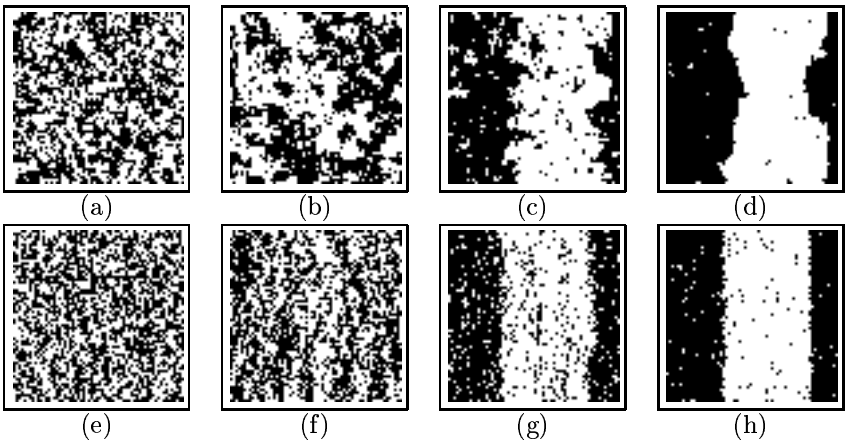

Figure 2.1: Configurations for a two dimensional lattice gas as showed up in numerical simulations, on square lattice 64×64. Pictures are ordered from left to right with decreasing temperature: (a,b,e,f) $T > T_c(E)$; (c,d,g,h) $T < T_c(E)$. (a,b,c,d) refer to ordinary lattice gas $E = 0$. (e,f,g,h) refer to DLG with a saturating electric field $E = \infty$, along the vertical direction (from Ref. [50]).

E. In two dimensions, $T_c(\infty) \simeq 1.4 T_c(0)$, where $T_c(0)$ is the Onsager critical temperature. For $T > T_c(E)$ (high-temperature phase) particles are homogeneously distributed in the lattice, while for $T < T_c(E)$ (low-temperature phase) the gas segregates in two regions, one almost full and the other almost empty, with interfaces parallel to $\mathbf{E}$, as shown in Figure 2.1

As stressed in Chap. 1, the key difference between non-equilibrium models as the DLG and the equilibrium ones is that the dynamics plays a different role in them. For the latter dynamics may either model or not physical processes, being used only to generate an equilibrium ensemble, *a priori* known (this is the case of standard dynamic Monte Carlo techniques). Dynamics is usually chosen to minimize the computational cost of simulations. For the former dynamics is crucial, given that the stationary solutions of the Master Equation are not *a priori* known, and one wishes to realize them by means of simulations. Changing dynamics may change the stationary distribution of the system and then physical properties [61].

Symmetries

Before going on with the description of the model, let us review briefly its symmetry properties, which will play a role when discussing the different field-theoretical approach proposed in the past (see Sect. 3.3). Let us define the following transformations for the DLG:

$$\begin{cases} C: & n_{\mathbf{i}} \overset{C}{\mapsto} 1 - n_{\mathbf{i}} \,, \quad \forall \mathbf{i} \in \Lambda \,, \\ R: & \mathbf{E} \overset{R}{\mapsto} -\mathbf{E} \,, \\ P: & \hat{\mathbf{x}} \overset{P}{\mapsto} -\hat{\mathbf{x}} \,. \end{cases} \tag{2.6}$$

It's easy to realize that transition rates (and so the model) are invariant for lattice translations of both initial and final configurations and for all possible pairings of the transformations (2.6), i.e. CR, CP and PR. Moreover any orthogonal transformation in the transverse space is a symmetry. These symmetries are of fundamental importance when trying to set up a mesoscopic description of the observed phase transition, as emerges from the discussion in Sections 3.1 and 3.3.

2.3 The DLG Steady State

To illustrate the novelties of the DLG let us briefly summarize the peculiar behavior of the system in its steady state (more generally some of the features we are going to describe are common to a wide class of non-equilibrium systems [21,22,24,35]).

2.3.1 Generic Long-Range Correlations

Let us consider the two-point function (see also Section 2.4), i.e.

$$G(\mathbf{x}-\mathbf{y}) = \langle n_{\mathbf{x}} n_{\mathbf{y}} \rangle \, ,$$

where $\langle \cdot \rangle$ denote the average in the steady state. This two point function has been studied by MC simulations and approximate analytic methods [21,35,51], shows a generic (i.e. not only at the critical point) power-law behavior

$$G(\mathbf{x}) \propto |\mathbf{x}|^{-d} \, , \tag{2.7}$$

and is not positive-definite (as a consequence of Eq. (2.7) and of the conservation law), as we can see from Fig. 2.2.

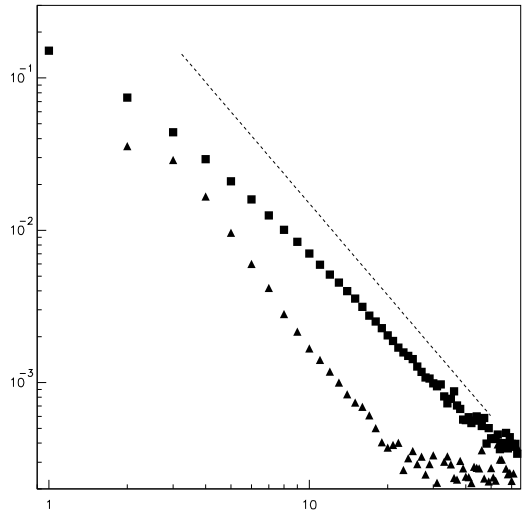

Figure 2.2: $G(\mathbf{x})$ for the DLG on a 2d 128×128 lattice in the high-temperature region ($\beta \ll 1$) and for $E = \infty$. (■) is $G(\mathbf{x})$ for $\mathbf{x} \| \mathbf{E}$; (▲) $-G(\mathbf{x})$ for $\mathbf{x} \perp \mathbf{E}$. Note that transverse correlations are negative. The dotted line has a slope of -2. From Ref. [50].

The algebraic, generic power-law decay of correlations, as expressed by Eq. (2.7) is related to the discontinuity of the static structure factor, defined as

$$\tilde{G}(\mathbf{k}) = \sum_{\mathbf{x} \in \Lambda} e^{i\mathbf{k}\cdot\mathbf{x}} G(\mathbf{x}) \, ,$$

for $\mathbf{k} = \mathbf{0}$. This discontinuity is quite evident in Fig. 2.3, where the numerical data for $\tilde{G}(\mathbf{k})$ of the two-dimensional 128×128 DLG are plotted in momentum space. Note that the conservation law and the initial condition $\rho_\Lambda = 1/2$ imply that $\tilde{G}(\mathbf{0}) = 0$. The discontinuity is made even stronger by another striking characteristic of the DLG steady state (of particular relevance when approaching the critical point), i.e. the strong anisotropy that we are going to describe in Sect. 2.3.2. Without entering into details, for which we refer to Ref. [35], it is possible to see that the discontinuity of the structure factor in the origin (leading to the generic long-range correlations) is a consequence of the conservative dynamics and of the violation of the condition $\mathbb{N} \propto \mathbb{D}$ (sometimes called fluctuation-dissipation theorem, see the remark at the end of Section 2 of Ref. [35] and Sect. 1.2 here).

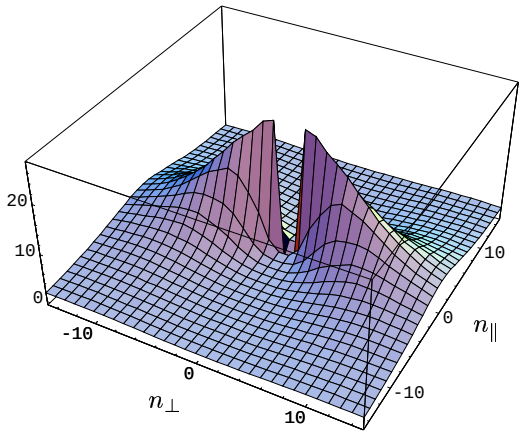

Figure 2.3: $\tilde{G}(\mathbf{k})$ for the DLG in $d = 2$, $L_\parallel \times L_\perp = 128 \times 128$ lattice. $n_\parallel, n_\perp$ are wave-numbers: $k_{\parallel,\perp} = 2\pi n_{\parallel,\perp}/L_{\parallel,\perp}$ where $\parallel, \perp$ denote directions parallel and transverse to $\mathbf{E}$.

From this peculiar behavior one problem arises: How can we define a correlation length for this system? Generally, in equilibrium systems, correlations decay exponentially with distance, at least in the high-temperature phase, so that a natural length scale emerges in that context. But here correlations *generically* decay following a power law and there is no evident emerging length scale. Nevertheless it is possible to show that if one considers the mean correlation of two points on the solid angle, an exponential decay is recovered (see Ref. [35] for details). In Section 2.4.2 we will define a *transverse correlation length*, suitable for our FSS analysis of the transition (see Sect. 5.2).

2.3.2 Strong Anisotropy

Another striking property of the DLG steady state in the critical region (i.e. when critical point is approached) is its *strong anisotropy*, emerging in a clear way from numerical simulations. In Fig. 2.4 we report some numerical data for the transverse and longitudinal susceptibility χ defined, as we will discuss below and in Sect. 2.4, by looking at the two-point correlation function for vanishing transverse and longitudinal momenta, respectively. We can easily see that, while $\chi_\perp$ seems to diverge when approaching the critical β, on the right of the figure, $\chi_\parallel$ does not display any anomalous behavior. Of course these are only qualitative considerations, given that also finite-size effects should be properly considered (see Chap. 4).

There are many examples of anisotropic systems also in equilibrium, as in the case of uniaxial one with long-range dipolar interactions [4], Lifshitz points [166], the Kasteleyn model of dimers

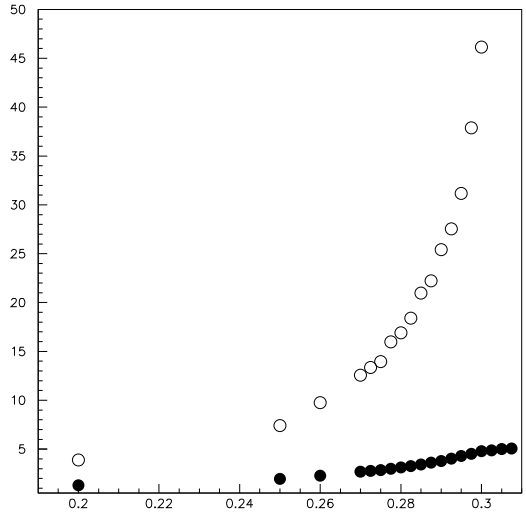

Figure 2.4: Comparison between $\chi_\perp$ ($\circ$) and $\chi_\parallel$ ($\bullet$) for various β on a 32×128 two-dimensional DLG.

on the brick lattice [88], etc. There are basically two different degrees of anisotropy. One is related to the fact that in scaling functions, different space directions scales with different amplitudes but with the same scaling exponent (this is usually the case of the simplest lattice spin systems with different coupling constants along different axes). The other, usually termed as *strong*, is realized when these exponents depend on the specific direction in space, as it is the case, e.g. for systems with strong (long-range) dipolar forces, for (short-range) anisotropic spin models (as the axial-next-nearest-neighbor Ising model – ANNNI) displaying a Lifshitz point (see Ref. [166] for a brief review), etc. We would discuss here, from a phenomenological point of view, the consequences of a strongly anisotropic scaling, in view also of the fact that it implies a doubling of the whole set of critical exponents. In the framework of scaling theory (see, e.g., Ref. [5]), the basic assumption is that when critical point is approached, the only physically relevant length scale is the correlation one $\xi \sim \tau^{-\nu}$, where $\tau \propto T - T_c$, T_c being the critical temperature. All the microscopic lengths do not influence the behavior in the critical limit, and thus the singular part of thermodynamic functions and observables will be homogeneous functions of ξ. Let us consider, thus, the dynamic structure factor $S(\mathbf{k}, t; \tau)$ (where t is the time), defined as the Fourier transform of the two-point correlation function. Introducing a momentum scale μ, the homogeneity of S may be expressed as

$$S(k_\parallel, \mathbf{k}_\perp, t; \tau) = \mu^{-2+\eta}\, S(k_\parallel/\mu^{1+\Delta}, \mathbf{k}_\perp/\mu, t\,\mu^z; \tau/\mu^{1/\nu})\ , \tag{2.8}$$

where the usual critical exponents have been introduced (see, e.g. Ref. [5]). To describe the strong anisotropy we have to introduce one more exponent, called *anisotropy exponent*, denoted by Δ in this scaling form. For isotropic or weakly anisotropic systems $\Delta = 0$ and both spatial directions scales with the same power of the momentum scale. A scaling form as Eq. (2.8) will emerge naturally from the field-theoretical models we discuss in Section 3.2 (once the requirement of anisotropy has been implemented in the theory). Here we would simply analyze its implications.

As a consequence of the scaling form (2.8), assuming $\mu = \tau^{\nu}$, it is possible to obtain

$$\mathbf{k}_{\perp} \sim \tau^{\nu} , \quad \text{and} \quad k_{\parallel} \sim \tau^{\nu(1+\Delta)} , \tag{2.9}$$

so that two different critical exponents ν naturally emerge as

$$\nu_{\perp} = \nu , \quad \text{and} \quad \nu_{\parallel} = \nu(1+\Delta) . \tag{2.10}$$

In a sense, the previous relation may be interpreted as the emergence of two different correlation lengths (long-range correlations may cause, as in the case of DLG, difficulties when trying to define them),

$$\xi_{\perp} \sim \tau^{-\nu_{\perp}} , \quad \text{and} \quad \xi_{\parallel} \sim \tau^{-\nu_{\parallel}} . \tag{2.11}$$

Considering long-time properties we can define two different dynamic critical exponents. Indeed, by setting $\mu = t^{-1/z}$ we get

$$\mathbf{k}_{\perp} \sim t^{-1/z} , \quad \text{and} \quad k_{\parallel} \sim t^{-(1+\Delta)/z} , \tag{2.12}$$

thus

$$z_{\perp} = z , \quad \text{and} \quad z_{\parallel} = z/(1+\Delta) . \tag{2.13}$$

Let us look at the exponent η. It is usually defined, from the scaling point of view (see Ref. [5]), from the momentum dependence of the critical scaling form (i.e. that with $\tau = 0$) of the static structure factor (for $t = 0$), as

$$S(k_{\parallel}, \mathbf{k}_{\perp}) = k_{\perp}^{-2+\eta_{\perp}} \Sigma_{\perp}(k_{\parallel}/k_{\perp}^{1+\Delta}) = k_{\parallel}^{-2+\eta_{\parallel}} \Sigma_{\parallel}(k_{\perp}/k_{\parallel}^{1/(1+\Delta)}) . \tag{2.14}$$

Thus, from Eq. (2.8), we get

$$\eta_{\perp} = \eta , \quad \text{and} \quad \eta_{\parallel} = \frac{\eta + 2\Delta}{1+\Delta} . \tag{2.15}$$

We note, however, that η may also be defined by looking at the space dependence of the static two-point correlation function. At variance with isotropic case, the η-like exponents so obtained differ from the previous ones. This is essentially due to the fact that when the Fourier transform of S is computed, to determine the two-point function $G(x_{\parallel}, \mathbf{x}_{\perp}, t; \tau)$, the integration measure $\mathrm{d}^d\mathbf{k} = \mathrm{d}^{d-1}\mathbf{k}_{\perp}\mathrm{d}k_{\parallel}$ scales as $\mu^{d+\Delta}$. Thus we expect

$$G(x_{\parallel}, \mathbf{x}_{\perp}, t, \tau) = \mu^{d+\Delta-2+\eta} G(\mu^{1+\Delta} x_{\parallel}, \mu\mathbf{x}_{\perp}, t\mu^{z}, \tau/\mu^{1/\nu}) . \tag{2.16}$$

For $t = 0$, $\tau = 0$, we can recognize the exponent η from the following scaling forms

$$G(x_{\parallel}, \mathbf{x}_{\perp}, t, \tau) = x_{\perp}^{-d+2-\eta'_{\perp}} g_{\perp}(x_{\parallel}/x_{\perp}^{1+\Delta}) = x_{\parallel}^{-d+2-\eta'_{\parallel}} g_{\parallel}(x_{\perp}/x_{\parallel}^{1/(1+\Delta)}) \tag{2.17}$$

resulting in two more η-like exponents, given by $\eta'_{\perp} = \eta + \Delta = \eta_{\perp} + \Delta$ and $\eta'_{\parallel} = (\eta - \Delta(d-3))/(1+\Delta)$, different from $\eta_{\perp}$ and $\eta_{\parallel}$. Attention should be paid whenever dealing with these exponents.

As far as the susceptibility χ is concerned, we can determine four different γ-like exponents, depending on how this quantity is defined. In equilibrium systems it is usually measured, by virtue of the fluctuation-dissipation theorem, as the low momentum behavior of the two-point correlation function. For general non-equilibrium systems, as remarked in Sect. 1.2, such a connection no more holds, but it is still useful *to define* the susceptibility as in equilibrium. Without relying on the

fluctuation-dissipation theorem this quantity should be defined in terms of the response function (according to the very definition of susceptibility), leading to two possible γ exponents, but it is usually quite difficult to measure it in numerical simulations.

So, according to the former definition, we have

$$\chi_\perp(\tau) \equiv S(k_\parallel = 0, \mathbf{k}_\perp \to \mathbf{0}, 0; \tau) \ , \quad \chi_\parallel(\tau) \equiv S(k_\parallel \to 0, \mathbf{k}_\perp = \mathbf{0}, 0; \tau) \ , \tag{2.18}$$

and thus we can generically introduce two γ-like exponents:

$$\chi_\parallel(\tau) \sim |\tau|^{-\gamma_\parallel} \quad \text{and} \quad \chi_\perp(\tau) \sim |\tau|^{-\gamma_\perp} \ . \tag{2.19}$$

Using Eq. (2.8) we find

$$\gamma_\parallel = \gamma_\perp = \nu(2 - \eta) = \gamma \ . \tag{2.20}$$

Let us remark that Fisher's scaling relation[6] is fulfilled also in the presence of anisotropy. Indeed, given the previous definitions

$$\nu_\parallel(2 - \eta_\parallel) = \nu_\perp(1 + \Delta)\left(2 - \frac{\eta_\perp + 2\Delta}{1 + \Delta}\right) = \nu_\perp(2 - \eta_\perp) \ , \tag{2.21}$$

and thus

$$\gamma_\parallel = \nu_\parallel(2 - \eta_\parallel) \quad \text{and} \quad \gamma_\perp = \nu_\perp(2 - \eta_\perp) \ . \tag{2.22}$$

Using standard arguments it is also possible to see that a generalized hyperscaling relation holds. We refer to Ref. [35] for a detailed illustration. We should stress here that the discussion above is based on very simple scaling arguments. These, of course, may fail to describe correctly the critical singularities whenever the amplitudes of the terms that would be generically the leading ones, vanish (scaling violations). In this sense the conclusion that $\chi_\perp$ and $\chi_\parallel$ diverge with the same exponent could not be true, as it seems to be in the DLG (see Fig. 2.4).

2.4 Observables

In this Section we define those observables we are interested in, which can be measured in numerical simulations and by means of which it is possible to describe the phase transition of the DLG [69]. Our principal concern is with two-dimensional ($d = 2$) model so we will refer to this case even though the definitions given can be readily generalized to generic d.

2.4.1 Order Parameter and Susceptibility

We consider a finite square lattice of size $L_\parallel \times L_\perp$ with periodic boundary conditions. We define a "spin" variable $s_\mathbf{j} \equiv 2n_\mathbf{j} - 1$ and its Fourier transform

$$\phi(\mathbf{k}) \equiv \sum_{\mathbf{j} \in \Lambda} e^{i\mathbf{k}\cdot\mathbf{j}} s_\mathbf{j} \ , \tag{2.23}$$

where the allowed momenta are

$$\mathbf{k}_{n,m} \equiv \left(\frac{2\pi n}{L_\parallel}, \frac{2\pi m}{L_\perp}\right) , \tag{2.24}$$

[6] It states that $\gamma = \nu(2 - \eta)$, see, e.g. Ref. [5].

with $(n,m) \in \mathbb{Z}_{L_\parallel} \times \mathbb{Z}_{L_\perp}$.

We consider the model at half filling, i.e. for $\rho_\Lambda = 1/2$. Then

$$\sum_{\mathbf{j}\in\Lambda} s_{\mathbf{j}} = 0 \,, \qquad \text{i.e.} \qquad \phi(\mathbf{k}_{0,0}) = 0 \,. \tag{2.25}$$

In the ordered phase $|\phi(\mathbf{k})|$ takes its maximum for $\mathbf{k} = \mathbf{k}_{0,1}$, and the expectation value on the steady state of its module

$$m(L_\parallel, L_\perp) \equiv \frac{1}{|\Lambda|}\langle |\phi(\mathbf{k}_{0,1})| \rangle \tag{2.26}$$

is a good order parameter. We remark that, given the ordered phase consists of a strip aligned with the field and placed somewhere in the finite system, $\phi(\mathbf{k}_{0,1})$ has a phase that changes randomly from sample to sample. To obtain a non-vanishing value we can get rid of this phase by considering the module of $\phi(\mathbf{k}_{0,1})$.

In momentum space the static structure factor

$$\tilde{G}(\mathbf{k}; L_\parallel, L_\perp) \equiv \frac{1}{|\Lambda|}\langle |\phi(\mathbf{k})|^2 \rangle \,, \tag{2.27}$$

vanishes at $\mathbf{k}_{0,0}$ because of Eq. (2.25) and is maximal at $\mathbf{k}_{0,1}$, so that it is natural to define the susceptibility as[7]

$$\chi(L_\parallel, L_\perp) \equiv \tilde{G}(\mathbf{k}_{0,1}; L_\parallel, L_\perp) \,. \tag{2.28}$$

Another interesting observable is the transverse Binder's cumulant $g(L_\parallel, L_\perp)$ defined as

$$g(L_\parallel, L_\perp) \equiv 2 - \frac{\langle |\phi(\mathbf{k}_{0,1})|^4 \rangle}{\langle |\phi(\mathbf{k}_{0,1})|^2 \rangle^2} \,. \tag{2.29}$$

Next, we would like to define a correlation length.

2.4.2 Finite-volume Correlation Length

Before discussing the problem of the definition of a finite-volume correlation length in the DLG let us briefly review, following Ref. [109], how this is usually done in (lattice) equilibrium systems. In infinite volume there are (at least) two possible definitions of the correlation length. In particular for systems with short-range interactions a long-distance exponential decay of correlations (and thus of the two-point correlation function $G(\mathbf{x})$) is expected generically. Equivalently this means that $\tilde{G}(\mathbf{k})$, the Fourier transform of $G(\mathbf{x})$, is an analytic function of $|\mathbf{k}|$ in a neighborhood of the origin. Thus one can define the *exponential* correlation length as

$$\xi_\infty^{(\exp)} \equiv - \lim_{|\mathbf{x}|\to\infty} \frac{|\mathbf{x}|}{\log G(\mathbf{x})} \,, \tag{2.30}$$

which is generally independent of the particular direction along which the limit is computed (at least as long as the hypercubic symmetry holds). The other natural definition is the *second moment*

[7] Let us remark again that the susceptibility defined by using the linear response theory does not coincide in non-equilibrium systems with that defined in terms of the Fourier transform of the two-point correlation function. Indeed these two definitions are connected by the fluctuation-dissipation theorem (see Sect. 1.2) which does not hold out of equilibrium.

correlation length (for a system on a d-dimensional hypercubic lattice)

$$\xi_\infty^{(2)} \equiv \left(\frac{1}{2d} \frac{\sum_{\mathbf{x}} |\mathbf{x}|^2 G(\mathbf{x})}{\sum_{\mathbf{x}} G(\mathbf{x})} \right)^{1/2} = \left[-\frac{1}{2d\tilde{G}(\mathbf{0})} \left. \frac{\mathrm{d}^2 \tilde{G}(\mathbf{q})}{\mathrm{d}q_\mu \, \mathrm{d}q_\mu} \right|_{q=0} \right]^{1/2} , \tag{2.31}$$

which extracts from $\tilde{G}^{-1}(\mathbf{q})$ for small q, the coefficient of the quadratic term in $\mathbf{q}$. Whenever $\tilde{G}(\mathbf{k})$ is dominated by a single pole (which then determines the exponential fall-off at large distances), $\xi_\infty^{(2)}$ and $\xi_\infty^{(\mathrm{exp})}$ are strictly related, usually differing, when approaching the critical point, only by a multiplicative constant.

In finite volume there is no *a priori* natural definition of the correlation length. Of course, as it has been defined, $\xi_\infty^{(\mathrm{exp})}$ cannot be generalized. In some cases one can resort to definitions based on spatial crossover between different behaviors of correlations, in such a way to identify a length scale (see, e.g., the discussion in Ref. [89]). The definition of $\xi_\infty^{(2)}$ can, instead, be easily extended to confined systems, but there is a great deal of arbitrariness in doing that. Indeed, for example, equally valid definitions are (with G_L we mean the finite-volume two-point correlation function)

$$\xi_L^{(2a)} \equiv \left[\frac{\tilde{G}_L(\mathbf{0}) - \tilde{G}_L(\mathbf{q}_{\min})}{\hat{\mathbf{q}}^2_{\min} \tilde{G}_L(\mathbf{q}_{\min})} \right]^{1/2} , \tag{2.32}$$

$$\xi_L^{(2b)} \equiv \left[\frac{\tilde{G}_L(\mathbf{0}) - \tilde{G}_L(\mathbf{q}_{\min})}{\hat{\mathbf{q}}^2_{\min} \tilde{G}_L(\mathbf{0})} \right]^{1/2} , \tag{2.33}$$

$$\xi_L^{(2c)} \equiv \left[\frac{\tilde{G}_L(\mathbf{0}) - \tilde{G}_L(\mathbf{q}_{\min})}{\hat{\mathbf{q}}^2_{\min} (2\tilde{G}_L(\mathbf{q}_{\min}) - \tilde{G}_L(\mathbf{0}))} \right]^{1/2} , \tag{2.34}$$

where $\mathbf{q}_{\min} = (2\pi/L, 0, \ldots, 0)$ (or one of the equivalent $2d$ definitions) is the minimum allowed non-vanishing momentum, and $\hat{\mathbf{q}}^2 = \sum_{\mu=1}^{d} 4 \sin^2(q_\mu/2)$ is the lattice momentum. From these definitions it is quite evident that, in the limit $L \to \infty$ and $t = (T - T_c)/T_c$ fixed,

$$\xi_L^{(2a)} \approx \xi_L^{(2b)} \approx \xi_L^{(2c)} \to \xi_\infty^{(2)} , \tag{2.35}$$

so that all of them are sensible finite-volume approximations of $\xi_\infty^{(2)}$. The question is, now, whether all of them have the correct FSS properties.

In Ref. [109] we deal with this problem by studying the large-N limit of the N-vector model. We show the existence of several constraints on the definitions of the finite-volume correlation length in order to have regular FSS functions and the correct anomalous behavior above the upper critical dimension. For example, in that model it is easy to realize that, even for finite L, $\xi_L^{(2c)}$ is defined only in a restricted range of temperatures, so that we can not expect regular FSS functions. Thus the first natural requirement is that the finite-volume correlation length has to be defined, for fixed L, for all temperatures. The other important point is that the correlation length should have the scaling behavior which is generally expected, on the basis of simple scaling arguments, above the upper critical dimension. This provides another constraint on the possible definitions and in Ref. [109] we explicitly show, for the model mentioned above, that some of those do not fulfill this requirement. Moreover these constraints also ensure the correct behavior taking into account the logarithmic corrections at the upper critical dimension [110].

Then, we study in detail the N-vector model ($N \to \infty$) in which the zero mode in prohibited, as for the lattice gas. In this case the definitions given in Eqs. (2.32), (2.33), and (2.34), can not

be used as they stand, given the constraint imposed by the conservation law. A sensible definition could be

$$\xi_L^{(2e)} \equiv \left[\frac{\tilde{G}_L(\mathbf{q}_{\min}) - \tilde{G}_L(\mathbf{q}_2)}{\tilde{G}_L(\mathbf{q}_2)(\hat{\mathbf{q}}_2^2 - \hat{\mathbf{q}}_{\min}^2)} \right]^{1/2} , \tag{2.36}$$

where $\mathbf{q}_i$, $i = 1, 2$ are two arbitrary non-vanishing momenta. One property of $\xi_L^{(2e)}$ in the case without zero mode is that, at least for the model considered in Ref. [109], it has the same universal scaling function as that of $\xi_L^{(2a)}$ in the case with zero mode. Other generalizations of the definitions previously given can not be defined in all the temperature range (see Ref. [109] for details). Also in the case of prohibited zero-mode, we find that the finite-volume correlation length must satisfy appropriate constraints in order to fulfill the requirements discussed above. What emerges from this analysis is that to have a sensible definition of correlation length there are additional conditions that are not, generally, obvious. Moreover good definitions for a model with zero mode can not be such when this mode is not allowed, see Ref. [109].

Having in mind the discussion above, let us face the problem of the definition of the finite-volume correlation length in the DLG.

First of all we note that, also in the thermodynamic limit, both the definitions (2.30) and (2.31) do not work for the DLG given that, as discussed in Section 2.3, the two-point function $\langle s_{\mathbf{x}} s_{\mathbf{0}} \rangle$ always decays *algebraically* with the distance, it is not positive-definite and in the infinite-volume limit (at fixed temperature) its Fourier transform (i.e. the static structure factor) $\tilde{G}(\mathbf{k})$ has a finite discontinuity at $\mathbf{k} = 0$.

Therefore, a different definition of the correlation length is necessary.

We observed, in Sect. 2.3.1, that the algebraic decay of correlations in the high-temperature phase of the DLG is described by Eq. (2.7) (see the numerical evidences in Ref. [51] for the two- and three-dimensional DLG, and Fig. 2.2). On the other hand we expect that approching the critical point, critical fluctuations will modify the exponent in Eq. (2.7) (as in Eq. (2.17) when considering transverse or longitudinal displacements). Then it should be possible to identify a lenght scale corresponding to which the crossover between this two different power-law behaviors occurs. By definition this length diverges (in the thermodynamic limit) when approaching the critical point, and for this reason it could be considered as a measure of the spatial extension of correlations. In Refs. [51,60] a parallel correlation length $\xi_{\parallel}$ is defined on this footing, by studying the crossover in the finite-volume correlation functions considered for displacements along the field, i.e. $G_l(x_{\parallel}) \equiv G(x_{\parallel}, \mathbf{x}_{\perp} = \mathbf{0})$. Then $\xi_{\parallel}$ is obtained by fitting $G_l^{-1}(x_{\parallel})$ with $1 + x_{\parallel}^2/\xi_{\parallel}^2$. However, this definition is not able to capture the crossover to the critical power law and thus can be regarded only as a phenomenological one (see the discussion in Ref. [35]), leading also to results for the exponent $\nu_{\parallel}$ which are not in agreement with the standard[8] theory [51].

Even more difficult appears the definition of a transverse correlation length because of the presence of negative correlations at large distances [35, 51].

To overcome the difficulties of the real-space strategy we will define the correlation length by using the two-point function for small momenta. We follow closely Ref. [109], where we discussed the possible definitions of correlation length in the absence of the zero mode, as it is the case here.

To take into account the absence of the zero mode also in the DLG we follow the analogy with the studied model, heuristically extending our findings. The basic observation is that, in the DLG, the infinite-volume transverse *wall-wall*[9] correlation function decays exponentially, so that a transverse

[8] We term "standard" the theory described in Sect. 3.2.

[9] We do not consider the standard point-point correlation but the mean correlation between two walls, i.e. between two parallel lines along the direction of the external field.

correlation length can be naturally defined in the thermodynamic limit. Differently stated, we can say that, restricting to $n_\parallel = 0$ and outside the origin (where $\tilde{G}(\mathbf{0}) = 0$ as a consequence of the conservation law), the plot of $\tilde{G}(\mathbf{k})$ in Fig. 2.3 has the usual Ornstein-Zernike form (and thus its Fourier transform has an exponential decay at large distances from which we can extract a sensible correlation length).

We consider, thus, the structure factor (2.27) in finite volume at zero longitudinal momenta

$$\tilde{G}_\perp(q; L_\parallel, L_\perp) \equiv \tilde{G}((0,q); L_\parallel, L_\perp) \;, \tag{2.37}$$

(note that the conservation law implies $\tilde{G}_\perp(0; L_\parallel, L_\perp) = 0$) and introduce a finite-volume (transverse) correlation length (which is the analogous of $\xi_L^{(2e)}$ in Eq. (2.36) with $\mathbf{q}_{\min} \mapsto \mathbf{q}_1$) as

$$\xi_{ij}(L_\parallel, L_\perp) \equiv \sqrt{\frac{1}{\hat{q}_j^2 - \hat{q}_i^2}\left(\frac{\tilde{G}_\perp(q_i; L_\parallel, L_\perp)}{\tilde{G}_\perp(q_j; L_\parallel, L_\perp)} - 1\right)}, \tag{2.38}$$

where $\hat{q}_n = 2\sin(\pi n / L_\perp)$ is the lattice momentum.

Some comments are in order:

(i) If we consider an equilibrium system or a steady state in which correlations decay exponentially, then we have for $q \to 0$ that

$$\tilde{G}_\perp^{-1}(q; L_\parallel, L_\perp) = \chi(L_\parallel, L_\perp)^{-1}[1 + \xi_{ij}^2(L_\parallel, L_\perp)\, q^2 + O(q^4, L^{-2})] \;, \tag{2.39}$$

where $\chi(L_\parallel, L_\perp)$ is the susceptibility. Thus, $\xi_{ij}^2(\infty, \infty)$ is a good definition of correlation length which has an infinite-volume limit independently of i and j.

(ii) Since $\tilde{G}_\perp(0; L_\parallel, L_\perp) = 0$, q_i and q_j must not vanish. Moreover, as discussed in Ref. [109], the definition should be valid for all T in finite volume. Since the system orders in an even number of stripes, for i even $\tilde{G}_\perp(q_i; L_\parallel, L_\perp) = 0$ is zero as $T \to 0$. Therefore, if our definition should capture the nature of the phase transition, we must require i and j to be odd. Although any choice of i, j is conceptually good, finite-size corrections increase with i, j, a phenomenon which should be expected since the critical modes correspond to $q \to 0$. Thus, we will choose $(i, j) = (1, 3)$.

Another quantity which is considered in the analysis is the amplitude A_{13} defined by

$$A_{13}(L_\parallel, L_\perp) \equiv \frac{\xi_{13}^2}{\chi} \;. \tag{2.40}$$

Chapter 3

Non-equilibrium Critical Phenomena

This Chapter is devoted to a review of the field-theoretical approach to the DLG *phase transition. The main ideas underlying such a description of (non-)equilibrium critical phenomena is briefly recalled in §3.1. In §3.2 we sum up the results of Refs. [39,40] in which critical exponents for the* DLG *phase transition have been obtained by means of the renormalization-group (*RG*) analysis for a suitable Langevin equation. Recently these results have been questioned, also on the basis of some discrepancies observed between theoretical predictions and numerical simulations. In §3.3 we make a critical review of this open debate, giving a survey of the relevant literature and analyzing the alternative theories that have been proposed.*

3.1 Field-theoretical Approach

There are many examples of non-equilibrium systems in which, by adjusting the value of some parameter, a phase transition can occur. See, for some examples, Refs. [21,35] and references therein. Among lattice models we want to recall percolation, reaction-diffusion processes, low dimensional models as one dimensional non-equilibrium systems (for recent reviews see Refs. [18–20, 24]), and many generalizations of the standard DLG as the *randomly driven* lattice gas [35, 44, 45], the *two-temperatures* lattice gas [35, 41–43], the DLG with *tilted or open* boundary conditions [46, 47] and the DLG *with quenched disorder* [48], to cite only some of them.

All these models are defined on a lattice. However, in a neighborhood of the critical point (critical region) we can limit ourselves to consider slowly-varying (in space and time) observables. At criticality (corresponding to the onset of long-range order) the lattice spacing a is negligible compared to the length and time scales at which long-range order is established so that a can be removed from the problem by taking the formal limit $a \to 0$. In this way, it is possible to formulate a description of the system in terms of *mesoscopic* variables defined on a continuum space. In principle, the dynamics of such variables can be obtained by coarse graining the microscopic system. However, given the difficulty of performing a rigorous coarse-graining procedure, one postulates[1] a continuum field theory, in the form of a stochastic Langevin equation (as that given in Eq. (1.5)) for

[1] In some simple cases it is possible to derive, at least heuristically and in a mean-field approximation (factorization of joint probabilities in the Master Equation), the mesoscopic equation from the microscopic model [68].

the order parameter, that has all the symmetries of the microscopic lattice model. We will discuss this point again in Section 3.3, giving an overview of a recent and still ongoing debate.

By universality [5] the continuum model should have the same critical behavior of the microscopic (lattice) one. This statement has quite rigorous foundations in the theory of equilibrium critical phenomena, from both static and dynamical point of view, and may be explained by means of the RG approach to the problem. As far as equilibrium dynamical aspects are concerned we would point out that dynamics is expected to play a role in the problem only in determining conservation laws to which the system is subjected during time evolution. We expect no dependence of the system behavior on the exact realization of the lattice dynamics employed to generate the equilibrium state.

On the other hand this fact is not evident at all in the case of non-equilibrium critical phenomena which depend strongly on dynamical realization of the system. To what extent universality applies to this case is not clear (see the overview in Ref. [73]). We discuss this issue in Section 3.3.

3.2 Field Theory for the DLG

Assuming universality, a field theory (see discussion in Sect. 3.3) has been proposed [39, 40] (see also Ref. [35]) and analyzed, giving exact predictions for critical exponents in space dimension d with $2 < d < 5$[2].

Using standard methods it is possible to analyze the continuum theory in terms of a dynamical functional [12–14] (see Sect. 8.1 for a brief introduction) which reads (neglecting terms irrelevant by power counting) [39]

$$J[s,\tilde{s}] = \int \mathrm{d}^d\mathbf{x}\,\mathrm{d}t\;\lambda\left\{\tilde{s}[\lambda^{-1}\partial_t + \Delta_\perp(\Delta_\perp - \tau) - \rho\Delta_\parallel]s + \frac{1}{2}u_0\nabla_\parallel\tilde{s}\,s^2 + \tilde{s}\Delta_\perp\tilde{s}\right\}\;, \tag{3.1}$$

where $s(\mathbf{x},t)$ is the local "density" field (actually, the coarse-grained version of $s_\mathbf{i} = 2n_\mathbf{i} - 1$), $\tilde{s}$ is the Martin-Siggia-Rose response field [12]. The subscripts $\parallel$ and $\perp$ mean spatial directions parallel and perpendicular to the external field. τ is the effective distance from the critical point, ρ is a parameter and u_0 the coupling constant of the theory, which is proportional to the coarse-grained microscopic force field, and takes into account its leading effects. The upper critical dimension for this theory turns out to be $d_c = 5$. Power counting leads to the conclusion that only the parameter ρ is renormalized by interactions. A dangerous irrelevant operator is also present. Renormalization-group analysis gives the following scaling form for $\Gamma_{\tilde{n}\,n}$ (one-particle irreducible vertex functions with $\tilde{n}$ fields $\tilde{s}$ and n fields s) in momentum space [39]

$$\Gamma_{\tilde{n}\,n}(\{p_\parallel,\mathbf{p}_\perp,\omega\};\tau,u,v,\rho,\mu) = l^{Q_{\tilde{n},n}}\Gamma_{\tilde{n}\,n}(\{\frac{p_\parallel}{l^{2+\eta}},\frac{\mathbf{p}_\perp}{l},\frac{\omega}{l^4}\};\frac{\tau}{l^2},u^*,l^{\kappa^*}v,\rho,\mu)\;, \tag{3.2}$$

where $u \propto \mu^{-\epsilon}\rho^{-\frac{3}{2}}u_0^2$, $\epsilon = 5-d$, μ is a momentum scale, $l \ll 1$ in the scaling limit, $u^* = O(\epsilon)$ is the non-trivial infrared (IR) fixed-point value of the coupling u, v is the coupling of the dangerous irrelevant operator. $\eta = (5-d)/3$ exactly, $\kappa^* = \frac{2}{3}(d-2)$,

$$Q_{\tilde{n},n} = -2\,\eta(\frac{n+\tilde{n}}{4} - \frac{1}{2}) + d + 5 - \tilde{n}\frac{d+3}{2} - n\frac{d-1}{2}\;.$$

From Eq. (3.2) we see that when considering time-independent observables at vanishing $p_\parallel$ the scaling form obtained is that of a *mean-field* theory for $2 < d < 5$ (with a dangerous irrelevant operator). The strongly anisotropic scaling is explicit in Eq. (3.2), and the exponent Δ (defined in Sect. 2.3.2) is readily found: $\Delta = 2 + \eta = (8-d)/3$.

[2] A field theory for the DLG was also derived in Ref. [38], starting from the standard Model B dynamics. The external drive partially breaks the supersymmetry (SUSY) of Model B, giving rise to a crossover towards a new fixed point in $d = 5$, with a residual symmetry ($\frac{1}{2}$SUSY of Ref. [38]).

3.3 DLG: Which Universality Class?

We said in Sect. 3.1 that the mapping between lattice models and the corresponding continuum field theories is rather difficult and seldom rigorously obtained (this problem is even harder when dynamics is involved). Then, in principle, every postulated field theory may be questioned. In recent years the field theory given in Eq. (3.1) and proposed to describe the physics of the DLG has been criticized by some authors. We want here to take a quick survey of this open debate (see also Ref. [73]), to which we wish to contribute with our findings [69, 70].

Episode I: 1986

Shortly after the introduction of the DLG a field-theoretical approach to the problem was attempted. The theory proposed in Refs. [38–40], from various perspectives, is based on a Langevin equation for the order parameter, and it is derived from the heuristic arguments that we would describe briefly.

First of all we expect that the description of the DLG from a mesoscopic point of view could be formulated in terms of the order parameter which is readily identified with the scalar field of particle density. We will be interested in its fluctuations around the mean spatial value (fixed by some initial condition), i.e. in the fluctuating field $s(\mathbf{x}, t)$. The DLG dynamics is conservative: This means that $s(\mathbf{x}, t)$ satisfies the continuity equation

$$\partial_t s + \nabla \cdot \mathbf{J} = 0 \, . \tag{3.3}$$

In the theory of dynamic critical phenomena [1,4,5] we assume that $\mathbf{J}$, the particle current, is given by Model B [1]:

$$\mathbf{J} = -\lambda \nabla \frac{\delta \mathcal{H}}{\delta s} + \mathbf{J}_L \, , \tag{3.4}$$

where λ plays the role of a diffusion constant and $\mathcal{H}$ is assumed to be a Landau-Ginzburg Hamiltonian:

$$\mathcal{H} = \int \mathrm{d}^d \mathbf{x} \left\{ \frac{1}{2} (\nabla s)^2 + \frac{\tau}{2} s^2 + \frac{f}{4!} s^4 \right\} \, , \tag{3.5}$$

where τ is the deviation from a reference temperature T_0, i.e. $\tau \propto T - T_0$ and f is the coupling constant of the theory. The choice of Eq. (3.5) is due to the fact that it includes all those operators (according to the RG classification) that are relevant at the Gaussian fixed point. $\mathbf{J}_L$ is a stochastic current that takes into account microscopic fluctuations around the deterministic part of the evolution equation for s (with $\langle \cdots \rangle$ we mean an average over possible noise realizations),

$$\begin{aligned} \langle J_{L,i}(\mathbf{r}, t) \rangle &= 0 \, , \\ \langle J_{L,i}(\mathbf{r}, t) J_{L,j}(\mathbf{r}', t') \rangle &= 2\lambda \delta^{(d)}(\mathbf{r} - \mathbf{r}') \delta(t - t') \delta_{ij} \, , \end{aligned} \tag{3.6}$$

we assume $\mathbf{J}$ to have a Gaussian distribution.

Remark: These are standard definitions in the context of weak perturbation around a thermodynamical equilibrium state. For example Eq. (3.4) is usually assumed when dealing with the linear response theory [8].

By means of standard manipulations one gets

$$\begin{gathered} \partial_t s = \lambda \Delta \frac{\delta \mathcal{H}}{\delta s} + \nu_L \, , \quad \text{where} \quad \nu_L = -\nabla \cdot \mathbf{J}_L \quad \text{and} \\ \langle \nu_L(\mathbf{r}, t) \rangle = 0 \, , \\ \langle \nu_L(\mathbf{r}, t) \nu_L(\mathbf{r}', t') = -2 \, \lambda \, \Delta_{\mathbf{r}} \delta^{(d)}(\mathbf{r} - \mathbf{r}') \delta(t - t') \, , \end{gathered} \tag{3.7}$$

which is exactly the Model B. If one now introduces the external field $\mathbf{E}$ we expect (a) an additional contribution to $\mathbf{J}$ in Eq. (3.3), due to the mesoscopic version of enhanced transitions in the direction of the field (a sort of "conduction"), of the form $\mathbf{J}^{(\mathbf{E})} = \sigma(s)\mathbf{E}$ (linear approximation is assumed) and (b) anisotropy of diffusion coefficients. The latter means that the breaking of space isotropy may give rise to mesoscopic anisotropic coefficients, as it has been showed in Ref. [38]. Moreover we also expect anisotropic expression for the Landau-Ginzburg Hamiltonian. In RG language we can say that the anisotropy introduced by the field E could drive the RG isotropic fixed point towards an anisotropic one (this means that even the field propagators show anisotropic scaling).

Taking into account all these factors one ends up with the Langevin equation [35]

$$\partial_t s = \lambda[\Delta_\perp(\tau_\perp - \kappa_\perp\Delta_\perp) + \rho\Delta_\parallel(\tau_\parallel - \kappa_\parallel\Delta_\parallel) - \kappa\Delta_\parallel\Delta_\perp]s - \mathbf{E}\cdot\nabla\sigma(s) + \nu_L \ , \tag{3.8}$$

with the noise

$$\langle\nu_L(\mathbf{r},t)\nu_L(\mathbf{r}',t')\rangle = -2\lambda(\gamma\Delta_\perp + \varsigma\Delta_\parallel)\delta^{(d)}(\mathbf{r}-\mathbf{r}')\delta(t-t') \ , \tag{3.9}$$

where we assumed a constant $\mathbf{E}$. As in Sect. 3.2, $\parallel$ and $\perp$ subscripts mean spatial directions parallel and perpendicular to $\mathbf{E}$, respectively. All the parameters in this equation have been introduced to account for the anisotropy. Let us note that we now have two temperature parameters, namely $\tau_\perp$ and $\tau_\parallel$, on which the onset of transverse or longitudinal order depends. We have, in general

$$\sigma(s) = \sigma_0 + \sigma_1 s + \sigma_2 s^2 + \cdots \ , \tag{3.10}$$

but, by means of symmetry arguments, it is easily shown that only σ_2 matters as the leading non-linearity [39]. Now it is possible to discuss the dynamical functional associated with the Langevin equation (3.8) and determine the critical dimensions of its possible fixed points. To this end we take advantage of the classification of operators according their scaling dimensions and behavior under RG flow into relevant, irrelevant and marginal ones [5]. It's not difficult to realize that the case corresponding to the ordered state numerically observed (see Fig. 2.1) is the one giving rise to the dynamic functional written in Eq. (3.1).

Now the question is whether the field-theoretical results obtained from the standard RG analysis of Eq. (3.1) agree with numerical data or not.

As we can see from Tab. 3.2, early numerical simulations [60] seemed to find agreement with theoretical predictions apart from a quite different value of the critical exponent β (we want to remark that the theoretical result $\beta = 1/2$ may be affected by logarithmic corrections in $d = 2$, given the presence of a marginal operator). A better understanding of FSS in anisotropic systems (we discuss this issue in Chapter 4), led to a reconciliation between numerics and theory (see Refs. [52,53]). Indeed in Ref. [52] (whose expanded version is Ref. [53]) it was shown (in a quite clear way) that an effective exponents $\beta_{\text{eff}} \approx 1/3$ may be a consequence of an incorrect FSS, in which one tries to collect on a single scaling plot, data coming from systems with different and small shape factors S (see Sect. 4.2). In a sense, β_{eff} describes the crossover to the case $S = 0$. Nevertheless, some doubts remained, and numerical analysis was debated [57,62].

To have a flavor of such a debate let us give a look at literature. In Ref. [55] the main concern is the two-layers DLG[3] but, as a byproduct of the authors' numerical analysis, it is claimed that Leung's results in Refs. [52,53] are incorrect, and that the correct scaling plots ruled out the value $\beta = 1/2$. A reply to these criticism appear in Ref. [56]: There it has been shown (using as an example the well-known 2D Ising model) that the results presented in Ref. [55] are due to the

[3]It is defined as the union of a pair of parallel copies of the DLG, so that each site in one of them has a corresponding one into the other. Inter-copy jumps are allowed only between corresponding sites, according to Metropolis rate, without any interaction Hamiltonian between copies.

inclusion, in scaling plots, of data well outside what we expect to be a reasonable critical region. Subsequent papers bear evidence supporting the standard picture [54] even if discrepancies are still numerically observed as in the case of Ref. [57] (dealing with two-layer DLG).

Episode II: May 1997

Following a proposed criticism [61] (also supported by some numerical observations [57]) to the widely accepted naïvely determined mesoscopic equation, the authors of Ref. [62] introduced a new Langevin equation for driven diffusive systems, in which the effects of the microscopic dynamics were carefully taken into account. They claimed that the above-mentioned discrepancy between field-theoretical results and MC simulations was due to the fact that the microscopic DLG Master Equation and the mesoscopic equation used to analyze the DLG critical behavior were not describing the same physics. In particular the mesoscopic equation derived in Ref. [62], has coefficients that depend in a quite precise way on the microscopic parameters defining the dynamics of the underlying lattice model (especially the microscopic driving field $\mathbf{E}$), while in the standard case [39, 40] it is not possible to work out this dependence. For finite value of $\mathbf{E}$ the equation introduced in Ref. [62] is the same as that of Refs. [39, 40][4], that is written in the form

$$\partial_t s = \frac{e(0)}{2}\left[-\Delta_\perp(\Delta_\perp - \tau)s + \frac{g}{3!}\Delta_\perp s^3\right] - \tau h'(E)\Delta_\parallel s - E\,h'(E)\nabla_\parallel s^2 + \sqrt{e(0)}\nabla_\perp\cdot\zeta_\perp\,, \quad (3.11)$$

where ζ is a δ-correlated Gaussian noise, $h'(E)$ is a function of the microscopic field strength E, and all others are given parameters. The current term is $-E\,h'(E)\nabla_\parallel s^2$, as in Eq. (3.8).

But for $|\mathbf{E}| = \infty$[5](this case is sometimes called infinitely fast driven lattice gas – IDLG), i.e. when jumps against the field are not allowed on the lattice, a non-trivial result is obtained only in the isotropic case (the same scaling for all directions at least naïvely, i.e. $\Delta = 0$ at tree level, see Tab. 3.1), with an upper critical dimension $d_c = 4$ instead of 5. The resulting equation turns out to be quite different from the previous one:

$$\partial_t s = \frac{e(0)}{2}\left[-\Delta_\perp(\Delta_\perp - \tau)s + \frac{g}{3!}\Delta_\perp s^3\right] - \frac{e(0)}{2}\Delta_\perp\Delta_\parallel s + \sqrt{e(0)}\nabla_\perp\cdot\zeta_\perp + \sqrt{\frac{e(0)}{2}}\nabla_\parallel\cdot\zeta_\parallel\,. \quad (3.12)$$

Indeed the term proportional to the current disappears, showing that the *particle current is not a relevant feature of the dynamics.* As a consequence of Eq. (3.12) we expect a different set of critical exponents (although, at variance with the standard case, not exactly computable), resulting also in a *different universality class.*

The observed discrepancy between simulations and theory is then traced back to the fact that the former may be affected by strong crossover effects between the two possible theories, depending on the value of E used in simulations.

Comment: Even though the statements made by the authors of Ref. [62] are all reasonable, we should notice that the arguments leading to their conclusions are quite questionable. Their "derivation" of the newly proposed Langevin equation has, to our concern, less rigor than claimed and, moreover, it fails to reproduce some well-established properties of the microscopic model (see Ref. [67]).

In a subsequent paper by the same authors [63] the details of the new derivation were given in a more extensive way, but again with some quite heuristic assumptions.

---

[4]In some papers, including Ref. [62], mesoscopic equations describing a diffusion mechanism coupled to an external drive, as it is the case of the DLG equation of Refs. [39, 40], are termed driven diffusive systems – DDS.

[5]We want to point out that even if microscopic driving field is infinite, the coarse-grained one may be finite.

Then a paper devoted to the one-loop RG analysis of the model of Ref. [62] for the IDLG appeared [64]. We checked the calculations reported therein and found a combinatoric error [65]. Even more severe were the generic infrared (IR) problems of this theory [65]. Meanwhile a paper by other authors appeared bearing strong evidences against the theory and pointing also out these problems [67]. In particular it is easy to realize that equation (3.12) obeys a spurious conservation law [65–67], given that if one defines a "row density", i.e.

$$\rho_r(r_\parallel, t) \equiv \int d^{d-1} r_\perp \, s(\mathbf{r}, t) \ ,$$

then, after averaging on the noise, it is a conserved quantity $\forall r_\parallel$ for the dynamics given by Eq. (3.11). This is an additional conservation law which is not present in the original model and it causes the IR problems of the theory (as one easily realize putting the theory on a finite volume) and an ill-defined static structure factor (with a line of singularities in momentum space instead of only one point of discontinuity).

Moreover in Ref. [67] it was pointed out that the Langevin equation of Ref. [62] has a symmetry not observed in MC simulations. Indeed the absence of a coupling to the external field results in a theory with Ising up-down symmetry (particle-hole symmetry $s \mapsto -s$, i.e. the C-symmetry of Eq. (2.6) for the density field), leading to a vanishing three-point correlation function for all $T \geq T_c$, in disagreement with existing numerical data. Thus, in a sense, mesoscopic theory has an higher degree of symmetry than the microscopic one. This may be justified only showing explicitly that the corresponding fixed point is stable against perturbations by symmetry-breaking operators [67].

Episode III: January 2000

A new paper by the same author of Ref. [62] (hereafter called "Granada Group") appeared [66] in order to correct the previously proposed Langevin equation, following suggestions and observations of Refs. [65, 67]. By means of heuristic arguments they introduce a new term $\rho \nabla_\parallel s(\mathbf{r}, t)$ in the Langevin equation (3.11), suitable for healing IR divergences, and due, in their opinion, to a correct evaluation of the "entropic term" that was overlooked in the previous derivation (we are still waiting for an analytic proof of the new term, see Ref. [18] in Ref. [66]). This term changes a lot of features of the theory previously proposed in Ref. [62]. The naïve (tree level) anisotropic scaling is recovered and, by power-counting analysis, the critical theory (there called *anisotropic diffusive system* – ADS) turns out to be a well-known Langevin equation, i.e. that of the *randomly driven lattice gas* (RDLG). This model was introduced in Ref. [44] (and discussed in a detailed way in Ref. [45]), to describe, from a mesoscopic point of view, a lattice gas with annealed randomness given by a fluctuating Gaussian random driving field (instead of a fixed one, as in the case of standard DLG). The naïve Langevin equation associated with this model has no current term, for obvious symmetry reason: The random field causes anisotropy but not an overall mesoscopic current. The relevant non-linearity is due to a cubic term in s, instead of the usual quadratic coupling to the mesoscopic external field, given by the non-linear dependence of the "conductivity" $\sigma(s)$ on the density (see Eq. (3.10)). Then the conclusion drawn in Ref. [66] was, again, that at least for the infinite-driving-field case, the *particle current is not the relevant features of the* DLG. This is due, in the authors' opinion, to a saturation of microscopic transition rates in the Master Equation, that, in a sense, wipes out any dependence on the precise value of the field and so on the current coupled to it [66]. For the ADS the upper critical dimension is $d_c = 3$ (compared to 5 of the standard case, see Tab. 3.1). At variance with the microscopic DLG model, the ADS (i.e. the RDLG) shows again an up-down symmetry ($s \mapsto -s$) resulting in a vanishing three point correlation function [66, 67], which might be irrelevant at the critical point. Indeed the closely related triangular anisotropies (observed during phase ordering) seem to disappear in the limit of large (compared to typical energy scale) external driving field [74, 75].

A brief summary of the theoretical predictions on these models is reported in Tab. 3.1.

A contribution to this debate appeared in Ref. [68], where a heuristic and approximate scheme is presented to derive the mesoscopic kinetic equations from the microscopic dynamics of the system. The method consists of two steps:

- A mean-field type factorization of joint probabilities, appearing into the Master Equation, into single variable ones (i.e. correlations are neglected),
- A naïve continuum expansion, in which probabilities are replaced by the corresponding mesoscopic density fields. In this way a *deterministic* (i.e. without any noise term) kinetic equation for these field is obtained.

By applying this method, it is possible to determine the dependence of the mesoscopic parameters on the microscopic ones. In Ref. [68] 1D, 2D and 3D Ising model with Glauber (i.e. spin flip) dynamics are considered, and quite good estimates for critical temperatures are obtained in the last two cases. The kinetic equation derived is, of course, a (deterministic) time-dependent Landau-Ginzburg model. The case of 1D (with only hard-core interaction) and 2D (with heat-bath rates) DLG is also considered, the latter leading to a deterministic kinetic equation in agreement with standard theory [38–40] (barring its noise term). Even the explicit temperature dependence of the mesoscopic transverse and parallel mass parameters ($\tau_\perp$, $\tau_\parallel$), is in qualitative agreement with what was found heuristically in Refs. [39,40]. Moreover for $|\mathbf{E}| = \infty$ (being $\mathbf{E}$ the microscopic field), the relevant non-linearity still come from the coupling of the current to the external field, at variance with the claims of Ref. [66].

	DLG [39,40]†	IDLG [64]‡	RDLG [44,45,66]
Current	Yes	No	No
Symmetries*	CP, CR, PR	C, P	C, P
d_c	5	4	3
$\eta_\perp^{**}$	0	$O(\epsilon^2)$	$\frac{4}{243}\epsilon^3 + O(\epsilon^4)$
$\nu_\perp^{**}$	$\frac{1}{2}$	$\frac{1}{2} + \frac{\epsilon}{12} + O(\epsilon^2)$	$\frac{1}{2} + \frac{\epsilon}{12} + \frac{\epsilon^2}{18}\left[\frac{67}{108} + \ln\frac{2}{\sqrt{3}}\right] + O(\epsilon^3)$
$z = z_\perp$	4	$4 + O(\epsilon^2)$	$4 - \frac{4}{243}\epsilon^3 + O(\epsilon^4) \equiv 4 - \eta$
β	$\frac{1}{2}$	$\frac{1}{2} - \frac{\epsilon}{6} + O(\epsilon^2)$	$\frac{1}{2} - \frac{\epsilon}{6} + \frac{\epsilon^2}{18}\left[-\frac{7}{54} + \ln\frac{2}{\sqrt{3}}\right] + O(\epsilon^3)$
Δ	$1 + \frac{\epsilon}{3}$	$O(\epsilon^2)$	$1 - \frac{2}{243}\epsilon^3 + O(\epsilon^4) \equiv 1 - \frac{\eta}{2}$

Table 3.1: Theoretical predictions for the (transverse) critical exponents, obtained from the Langevin equations proposed to describe the DLG phase transition. $\epsilon \equiv d_c - d$ where d_c is reported in the table. * We define these transformations: $s \overset{C}{\mapsto} -s$, $\mathbf{E} \overset{R}{\mapsto} -\mathbf{E}$, $\hat{\mathbf{x}} \overset{P}{\mapsto} -\hat{\mathbf{x}}$. We do not indicate the obvious $O(d-1)$ symmetry in transverse space, common to all these models. † Exponents *exactly* known for $2 < d < 5$. ‡ This theory has severe IR problems [65,67]. ** Exponent inferred from the scaling form in momentum space (for strongly anisotropic systems it differs from that emerging from real space scaling forms, see Sect. 2.3.2).

Episode IV: June 2001

We concluded our FSS analysis of the DLG, reported in Ref. [69], finding good agreement between numerical results and theoretical predictions of Refs. [39,40]. Recently, we have revised these results

$d=2$									
	DLG	IDLG	RDLG	MC					
	[39,40]	[64]	[66]*	[60]	[52]	[57]	[54]	[69,70]	[72]
Δ (†)	2	0	1	0	2	0	$1.98(4)^\ddagger$	2	~ 1
$\eta_\perp$	0	0	0						
$\nu_\perp$	1/2	2/3	0.626	$0.62(12)^a$	0.5	0.7		$0.4605(32)^b$	0.625
β	1/2	1/6	0.334	0.23(2)	0.5	0.3	$1.00(2)\nu_\perp$	$0.461(35)^c$	0.33
γ	1	4/3	1.25				$2.03(3)\nu_\perp$	$0.921(48)^d$	1.22

Table 3.2: Theoretical predictions for the (transverse) critical exponents of the two-dimensional DLG (these results come from ϵ-expansion series listed in Tab. 3.1, up to $O(\epsilon^2)$, and naïvely extended to the proper value of ϵ, without any summation attempt and neglecting possible logarithmic corrections due to marginal operators in $d=2$), compared to MC results. Remember that $\gamma = \nu_\perp(2-\eta_\perp)$. * See also Refs. [44,45]. † To perform an anisotropic FSS of MC data, the value of Δ has to be assumed. ‡ Assuming results from Ref. [59] it is possible to determine Δ (by using FSS crossover). Indeed it was found $\nu_\perp/\nu_\parallel = 2.98(4) \equiv 1+\Delta$. ^{a} This result is quoted in Ref. [60] as $0.55^{+0.20}_{-0.05}$. ^{b} See Eq. (5.6). ^{c} Value obtained taking into account the rough estimate $\beta/\nu_\perp = 1.00(7)$ (see Sect. 5.2.2) and the $\nu_\perp$ reported here in the table. ^{d} Value obtained from a first rough estimate $\gamma/\nu_\perp = 2.00(9)$ (see Sect. 5.2.2).

(finding a better agreement and clarifying some point not well understood in the first analysis), by means of simulations on bigger lattices (see Ref. [70]). In both cases we have used a different approach to FSS, described in Sect. 4.3.2, based on a suitably defined correlation length which has been introduced and discussed in Section 2.4.

Before entering into the details of our work, we have to say that shortly after our paper, a new one by the Granada group appeared [72], supporting their previous conclusions in a surprising way. By means of MC simulations and a suitable anisotropic FSS, they conclude that (quoting from Ref. [72]):

> ..., MC *results support strongly that both the* IDLG *and the* RDLG *belong in the same universality class, and share not only critical exponents and scaling functions, but also the scaling amplitudes.*

Summing up, they carried out MC simulations of both RDLG and IDLG, on lattices from 20×20, up to 125×50. By using Binder's cumulant crossing method (see Section 4.3) they determined the critical temperatures for both models and then performed an anisotropic FSS analysis (see Chap. 4) for the finite-volume magnetization, susceptibility and Binder's cumulant. In order to have a good data collapse (where the goodness is judged by eye inspection) one has to adjust some parameters, whose values are related to critical exponents, as explained in Chapter 4. Estimated values (though authors do not make any error analysis, judged to be " ... *inessential in this context.*"–quotation from Ref. [72]) of critical exponents are in agreement with theoretical ones (even though computed within ϵ-expansion) for RDLG, as easily seen from Tab. 3.1. Moreover, unexpectedly, FSS functions turns out to be exactly the same for the two models, without having to adjust any non-universal amplitude [72].

Episode V: April 2002

Very recently Ref. [77] has appeared in the literature, announcing unexpected numerical results and making the statement of Ref. [72], about universality classes, even stronger. At variance with

previous studies, the numerical investigation of the DLG and some related models, is there carried out by means of short-time dynamic MC method. This numerical technique has been extensively used to investigate dynamical and static properties of several well-known equilibrium models (see Ref. [150] for early works and reviews), giving exponents in good agreement with those obtained by standard MC simulations. We would not discuss here the details of the method. The general underlying ideas are related to the short-time universal scaling behavior observed in the relaxation processes starting from a prepared initial condition (fully ordered and completely disordered ones are considered in Ref. [77]). This subject is described briefly in Section 8.2. Remarkably enough, short-time MC simulations do not suffer the problem of critical slowing down [150] and even finite-size effects do not have the same relevance (at least in the very early stages of relaxation) as they have in standard MC simulations. In Ref. [77] the DLG with finite and infinite driving field (there called FKLS and IKLS, respectively), the RDLG with infinite random field (called IRDLG) and the driven lattice gas with an oscillatory field[6] (introduced in Ref. [49]) in the limit of infinite field (IOKLS) are studied to clarify the long-standing controversy about the universality class of the DLG. At variance with previous works, the analysis of the numerical results should not be influenced by the problem of the strongly anisotropic FSS (see Section 4.2), and this should make the results more reliable and unbiased by theoretical expectations (no value of the anisotropy exponent Δ is required and, indeed, it is possible to measure it). The main results of Ref. [77] are that

- As a consequence of the short-time scaling forms assumed in the paper, the critical exponents[7] of all the models studied are the same as those predicted by the field theory of the RDLG [44,45], while there is a quantitative disagreement with the prediction of Refs. [39, 40]. Short-time scaling forms differ only for non-universal amplitudes.
- The models IKLS, FKLS, with a macroscopic current and IRKLS and IOKLS, without any current, have the same critical exponents, and thus belong to the same universality class. This observation support the conclusion of Ref. [72], that the relevant feature of the DLG is the anisotropy and not the current (which does not play any role neither to determine the universality class nor to give rise to the strong anisotropy).

First of all we note that these results go well beyond the statements originally done in Refs. [64,72], where it was argued that the IKLS, i.e. the DLG driven with an infinite field, should be in the same universality class as the RDLG, while for finite driving (FKLS) the field theory of Refs. [39, 40] should be the correct one to describe critical properties. In a sense the limit of infinite driving was previously regarded as a singular one. Here the stronger statement is made that in *all the cases* discussed the critical behavior is that of the RDLG.

We remark that the conclusions of Ref. [77] depend crucially on some assumptions made in the paper on the short-time scaling forms. These generalize in a non-trivial way standard scaling arguments usually applied when dealing with short-time scaling forms in finite systems. For example the authors implicitly assume that there is only one exponent $z = z_{\|}$, instead of the two standard $z_{\perp}$, $z_{\|}$ and that, depending on the chosen initial condition, $t \sim \tau^{-\nu_{\|} z}$, or $t \sim \tau^{-\nu_{\perp} z}$ (t is the typical time scale of the dynamics and τ measures the distance from the critical point). This is not usually the case. In Ref. [77] there is no attempt to justify these unnatural assumptions. Moreover, if one tries to analyze the results of this paper following a more reasonable extension of short-time scaling forms[8], one finds these results in quantitative disagreement with both the field-theoretical

[6]The field acts along a given lattice axis exactly as in the standard definition of the DLG but its sign is reversed once every n MC sweeps ($n = 10$ in the specific case studied in Ref. [49]).

[7]At variance with previous MC studies, the dynamical exponent $z_{\|}$ is measured (actually it is called z by the authors of Ref. [77]).

[8]For example keeping in mind that, at least in principle $z_{\perp} \neq z_{\|}$, as also predicted by field-theoretical approach of both Refs. [39, 40] and Ref. [72].

descriptions proposed. We refer to Ref. [77] for the numerical results of that paper, not reported in Table 3.2.

We believe that these unclear aspects of the work presented in Ref. [77] should be clarified before making any statement based on it.

Chapter 4

Finite-Size Scaling

To compare numerical results (about a finite system) with theoretical predictions for the critical behavior (observed only in the thermodynamic limit), obtained from a field-theoretical approach, it is of fundamental importance to exploit finite-size scaling properties. In §4.1 we discuss this problem for isotropic systems, within a phenomenological approach. Then we describe how it is possible to generalize it to the case of strongly anisotropic systems, as the DLG. *In §4.3 we discuss how this phenomenological approach can be used to get, from* MC *simulations, estimates of critical exponents (and, more generally, critical properties). In particular we compare the standard method (§4.3.1) with that introduced in Ref. [90] (§4.3.2), which heavily relies on the definition of a finite-volume correlation length. We also stress the fact that the latter method does not require any parameter tuning, at variance with the former. In §4.4 we exploit the predictions that can be obtained for* FSS *function from the field theory described in §3.2.*

Phase transitions are characterized by a non-analytic behavior of the partition function, and thus of some observables, at the critical point [2, 3, 5]. These non-analyticities can be observed only in the infinite-volume limit performed keeping constant the density of degrees of freedom in the system (thermodynamic limit [3] – TD) and, generally, temperature. If the system is finite, all thermodynamic functions are analytic in the thermodynamic parameters as the temperature, the applied magnetic field, and so on: There cannot be any phase transition. However, even in a finite sample, observables show an anomalous behavior as a function of temperature, from which it is possible to obtain many informations on the critical behavior. Indeed, large but finite systems[1] show a *universal* behavior called *finite-size scaling* (FSS). The FSS hypothesis, formulated for the first time by Fisher [6, 82–84] and justified theoretically by using renormalized continuum field theory [81, 85] (a collection of relevant articles on the subject appears in Ref. [87] and a recent monograph is Ref. [89]), is a very powerful method to extrapolate to the thermodynamic limit the results obtained from a finite sample, both in experiments and in numerical simulations. In particular, the most recent Monte Carlo studies rely heavily on FSS for the determination of critical properties (see, e.g., Refs. [90,91,93,98,100–105] for recent applications in two and three dimensions; the list is of course far from being exhaustive).

[1] A confined system generally also exhibits *surface effects*, due to the presence of boundaries. They can be easily avoided (at least in numerical simulations and analytic calculations) assuming periodic boundary conditions [84]. The presence of surfaces in critical system makes the phenomenology more complicated (see Ref. [17] for a filed-theoretical approach).

4.1 Isotropic FSS

The most commonly studied systems are those showing a second-order phase transition at a critical temperature T_c (for the FSS effects on first-order phase transitions see Ref. [107]). In this case the distance from the critical point may be measured in terms of an infinite-volume correlation length ξ_∞ (in units of some microscopic scale, as the lattice spacing a), diverging for $T \to T_c$ (ξ_∞ is the inverse renormalized mass in quantum field theory). For a finite system of typical size L (expressed with respect to a) we can consider two different limits:

TD: $L \to \infty$, $\xi_\infty \to \infty$, $\xi_\infty/L \to 0$;

FSS: $L \to \infty$, $\xi_\infty \to \infty$, $\xi_\infty/L =$constant;

In these limits the lattice spacing becomes negligible with respect to the length scales relevant for collective phenomena, i.e. L and ξ_∞. For this reason the system may be effectively described at an arbitrary intermediate scale (i.e. from a mesoscopic point of view) in terms of a suitable field theory on the continuum, renormalized at that scale. Physics must be independent of this arbitrary scale. This reason leads to the Callan–Symanzik equation from which one can determine scaling forms (in the scaling limit) and critical exponents [4].

Now we want to give a brief description of a phenomenological approach to the FSS problem [82, 84] (see also Ref. [89]). In the case we are interested in, i.e. that of the second-order phase transitions, there are quantities $\mathcal{O}$ which, in infinite volume, behave as

$$\mathcal{O}_\infty(t) \equiv \langle \mathcal{O} \rangle_\infty \sim |t|^{-x_\mathcal{O}} \qquad \text{for} \quad t \to 0 \,, \tag{4.1}$$

where $t \equiv (T - T_c)/T_c$ is the reduced temperature and $\langle \cdot \rangle_\infty$ denote averaging in the infinite-volume system. In a finite sample of length L in all directions, the finite-volume mean values $\mathcal{O}_L(t) \equiv \langle \mathcal{O} \rangle_L$ are analytic functions of t. However, for large L, the FSS theory predicts a scaling behavior of the form

$$\mathcal{O}_L(t) = G_\mathcal{O}(t, L) \approx L^{x_\mathcal{O}/\nu} \, F_{2,\mathcal{O}} \left(t^{-\nu}/L \right) \,, \tag{4.2}$$

where $\nu \equiv x_\xi$ is the critical exponent which, according to Eq. (4.2), controls the divergence of the bulk correlation length ξ[2]. The function $F_{2,\mathcal{O}}(z)$ is finite and non-vanishing in zero[3], and should satisfy[4]

$$F_{2,\mathcal{O}}(z) \sim |z|^{-x_\mathcal{O}} \qquad \text{for} \quad z \to \infty \,. \tag{4.3}$$

Equation (4.2) can be conveniently rewritten in terms of the bulk correlation length, in order to avoid the knowledge of the critical temperature, otherwise required,

$$\mathcal{O}_L(t) \approx L^{x_\mathcal{O}/\nu} \, F_{3,\mathcal{O}} \left(\frac{\xi_\infty(t)}{L} \right) , \tag{4.4}$$

where $F_{3,\mathcal{O}}(z)$ is finite for $z \to \infty$ and

$$F_{3,\mathcal{O}}(z) \sim |z|^{x_\mathcal{O}/\nu} \qquad \text{for} \quad z \to 0 \,. \tag{4.5}$$

[2] We expect corrections to Eq. (4.2) of order $L^{-\alpha} g_\alpha(t^{-\nu}/L)$ with $\alpha > 0$.

[3] If it is not the case we have *violations* of FSS and hyperscaling relations fail, generally because of dangerously irrelevant operators [7].

[4] Note that the behavior of $|z|^{x_\mathcal{O}} F_{2,\mathcal{O}}(z)$ for $z \to \infty$ is not directly related to the finite-size corrections to $\mathcal{O}_L(t)$ for $L \to \infty$ at t fixed in the limit of small t. See the detailed discussion in Refs. [106, 108].

Eq. (4.4) clarifies the physical meaning of Eq. (4.2): There are many length scales in a statistical system, some of them being of microscopic nature (as the lattice spacing) others macroscopic (as the physical size), but when approaching a critical point only one relevant length scale emerges, i.e. ξ_∞. The statement that critical behavior is controlled only by this length is the so called *scaling hypothesis* [5], nowadays justified in the RG perspective. So it is natural to expect that in a finite system of size L only the ratio ξ_∞/L is relevant.

Let us note that Eq. (4.4) involves both finite- and infinite-volume observables (i.e. the finite-volume value of $\mathcal{O}$ and ξ_∞), but in numerical simulations one determines only the finite-volume ones. So it is convenient to recast the previous relations in a different form, following Ref. [90]. Indeed from Eq. (4.4) we can derive a general relation for the ratio of $\mathcal{O}_L$ at two different sizes L and αL,

$$\frac{\mathcal{O}_{\alpha L}(\beta)}{\mathcal{O}_L(\beta)} = F_{\mathcal{O}}\left(\frac{\xi_L(\beta)}{L}\right) , \tag{4.6}$$

(β is the inverse temperature) where we have traded ξ_∞/L for ξ_L/L by inverting $\xi_L \approx L F_{3,\xi}(\xi_\infty/L)$.

If we define $z = \xi_L/L$, then, varying β in a fixed geometry, z varies between 0 (we expect negligible correlations in the high-temperature phase, so ξ_L very small) and z^*, where z^* is defined by

$$z^* = F_{3,\xi}(\infty) . \tag{4.7}$$

The value z^* is directly related to the behavior of the finite-size correlation length at the critical point, since $\xi_L(\beta_c) \approx z^* L$. For ordinary phase transitions z^* is finite. At the critical point it also holds

$$\mathcal{O}_L(\beta_c) \propto L^{x_{\mathcal{O}}/\nu}. \tag{4.8}$$

Then

$$F_{\mathcal{O}}(z^*) = \frac{\mathcal{O}_{\alpha L}(\beta_c)}{\mathcal{O}_L(\beta_c)} = \alpha^{x_{\mathcal{O}}/\nu}, \tag{4.9}$$

and therefore

$$\frac{x_{\mathcal{O}}}{\nu} = \frac{\log F_{\mathcal{O}}(z^*)}{\log \alpha}. \tag{4.10}$$

From this relation it is easy to determine ratios between critical exponents (see Section 4.3).

To get the set of critical exponents we have to determine ν from the scaling functions obtained. To this end let us observe that, calling $z_L = \xi_L/L$,

$$z_L = z^* + G'_\xi(0)(tL^{1/\nu}) + O((tL^{1/\nu})^2) , \tag{4.11}$$

where $G_\xi(u) = F_{2,\xi}(u^{-\nu})$ (see Eq. (4.2)) and z^* is defined in Eq. (4.7). As a consequence

$$\frac{z_{\alpha L}}{z_L} = 1 + \frac{G'_\xi(0)}{z^*}(\alpha^{1/\nu} - 1)(tL^{1/\nu}) + O((tL^{1/\nu})^2) . \tag{4.12}$$

Eq. (4.12) together with Eq. (4.11), implies that

$$\frac{\mathrm{d}}{\mathrm{d}z_L}\left.\frac{z_{\alpha L}}{z_L}\right|_{z_L = z^*} = \frac{\alpha^{1/\nu} - 1}{z^*} , \tag{4.13}$$

and thus, using the fact that $F_\xi(z^*) = \alpha$,

$$z\frac{\mathrm{d}}{\mathrm{d}z}\log F_\xi(z)\Big|_{z=z^*} = \alpha^{1/\nu} - 1 \,. \tag{4.14}$$

The value of ν can be obtained by means of the function F_ξ only.

The function $F_{\mathcal{O}}(z)$ is universal and directly accessible, e.g., to MC simulations. It depends on α and on global features of the considered geometry, such as shape, boundary conditions, etc. If one considers, for example, a two-dimensional finite lattice of dimension $L_\perp \times L_\parallel$, then we expect that $F_{\mathcal{O}}(z)$ depends on the ratio $L_\perp/L_\parallel$. The appropriate FSS limit is then achieved by taking the limit $L_\perp, L_\parallel, \xi_L \to \infty$ with $L_\perp/L_\parallel$ and ξ_L/L fixed.

4.2 Anisotropic FSS

The results presented above are valid for an isotropic or weakly anisotropic systems (see Sect. 2.3.2 for a phenomenological discussion of strong anisotropy).

On the other hand, there are phase transitions strongly anisotropic in nature, as in the case of the DLG we are interested in (numerical evidences) and of some equilibrium system with anisotropic interactions, mentioned in Sect. 2.3.2 to which we refer. In the specific case of the DLG, the continuum field theories introduced (see Sect. 3.3) to describe its critical singularities predict a non-trivial anisotropy exponent Δ (see Tab. 3.1). This facts calls for an extension of the FSS arguments presented in the case of isotropic systems ($\Delta = 0$). For example we should make clear how to manage the two (or even more!) correlation length $\xi_\parallel$, $\xi_\perp$ that generally emerge as a consequence of the strong anisotropy (see Sect. 2.3.2 for details), when doing FSS. Although what follows is quite general, we restrict ourself to the case of the DLG. A phenomenological approach to the FSS for this model has been developed in Ref. [60], keeping into account the strong anisotropy observed in the transition (for $d = 2$ see Refs. [53, 54, 59], for $d = 3$ see Ref. [58]). Following this approach, we will assume for our numerical investigations that all observables have a finite FSS limit obtained by taking the longitudinal size $L_\parallel$ and the transverse one $L_\perp$ to infinity keeping constant

- the *anisotropic aspect ratio* $S = S_\Delta \equiv L_\parallel^{1/(1+\Delta)}/L_\perp$;
- the FSS *parameter* $\xi_{\perp,\infty}(\beta)/L_\perp$ (or equivalently its longitudinal counterpart).

Then, Eq. (4.4) still holds by using the correct FSS parameter. In terms of transverse quantities we may rewrite

$$\mathcal{O}_L(\beta) \approx L_\perp^{x_{\mathcal{O}}/\nu_\perp} F_{2,\mathcal{O}}(t^{-\nu_\perp}/L_\perp) \approx L_\perp^{x_{\mathcal{O}}/\nu_\perp} F_{3,\mathcal{O}}(\xi_{\perp,\infty}/L_\perp). \tag{4.15}$$

Analogously, Eq. (4.6) is recast in the form

$$\frac{\mathcal{O}_{\alpha L_\perp}(\beta, S)}{\mathcal{O}_{L_\perp}(\beta, S)} = F_{\mathcal{O}}\left(\frac{\xi_{\perp,L_\perp}(\beta)}{L_\perp}, \alpha, S\right) \,, \tag{4.16}$$

where we have shown explicitly the dependence on α and on the aspect ratio S. Equation (4.16) will be the basis for our analysis of the phase transition in the DLG. For the finite-volume transverse correlation length we will use ξ_{13} as defined in Sect. 2.4.2, Eq. (2.38). Moreover, as much of our efforts are aimed at testing accurately the theoretical predictions of Refs. [39, 40], we *assume* that $\Delta = 2$ for $d = 2$ as described in Chap. 5.

4.3 FSS and Numerical Simulations.

Without entering too much into details (to which several papers and books are devoted) we would outline here the basic methods usually employed to apply the general FSS argument to the numerical simulations. We will give only a pedagogical introduction without discussing such relevant problems as statistical errors, corrections to FSS forms and so on.

4.3.1 Standard Method

To take advantage of the scaling forms (4.4), one usually follows these steps.

- *Determination of the critical temperature:* One easy way to do that is to consider an observable as the Binder's cumulant $g_L(T)$, for which $x_{\mathcal{O}} = 0$. The scaling form (4.2) tells us that if one collects data taken from lattices with different sizes $L_1, L_2, \ldots, L_n$, and plots them as a function of the temperature T, then there will be a point where all the curves, no matter the L which they refer to, cross each other. This point correspond to $t = 0$, i.e. $T = T_c$. The same procedure can be applied to the finite-volume correlation length, for which $x_\xi = \nu$, so, instead of $g_L(T)$, one can consider $\xi_L(T)/L$.

- *Determination of ν:* For all the lattice sizes L from which data have been collected, we plot $g_L(T)$ vs. a suitably rescaled T, given by $(T - T_c)L^x$, where x is an arbitrarily fixed parameter (generally $x \sim 2$). Then we change x and replot the data, looking for the value x_b of x that ensures the best data collapse, i.e. a superposition of curves referring to different L. This value gives the estimate for the critical exponent $\nu = 1/x_b$.

- *Determination of the critical exponents:* Once T_c and ν have been determined, it is quite obvious how to get all the other exponents. Again by using Eq. (4.4), one can determine the value r_b of r such that plots of $L^{-r}\mathcal{O}_L(T)$ vs. $(T - T_c)L^{x_b}$ for different L collapse onto the same curve. The estimate is then $x_{\mathcal{O}} = r_b/x_b$. By analyzing data referring to different observables (as susceptibility, magnetization, etc.) one can determine all the critical exponents.

Several cross-checks are possible, given that usually the number of independent critical exponents is smaller than the number of observables.

4.3.2 Improved Method

We can take advantage of Eq. (4.6) to determine critical exponents. To this end we need row MC data, at given temperatures, from *pairs* of lattices with sizes L and αL where $\alpha > 1$ is a fixed number (if, as it is usually the case, α is not an integer, an interpolation procedure is required). Then we can follow these steps.

- *Determination of F_ξ:* Once we have measured the finite-volume correlation length $\xi_L(T)$ for several values of the temperature T, we can determine F_ξ by means of (see Eq. (4.6))

$$\frac{\xi_{\alpha L}(T)}{\xi_L(T)} = F_\xi(\xi_L(T)/L) \; , \tag{4.17}$$

  plotting the l.h.s. ratio as a function of $\xi_L(T)/L$. A fit to the data can be performed to get our estimate for F_ξ.

- *Determination of z^*:* To compute critical exponents by using Eq. (4.10), we have to know z^* as defined in Eq. (4.7). By using Eqs. (4.6) and (4.4) we have

$$\alpha = F_\xi(z^*) \; , \tag{4.18}$$

so that z^* can be easily determined from the fitted F_ξ.

- *Determination of the critical exponents:* Knowing the value of z^* all the critical exponents may be computed by means of Eqs. (4.14) and (4.10). To determine $F_{\mathcal{O}}$ one has to apply the same method used for F_ξ.

An alternative method to that now discussed, uses the infinite-volume extrapolation of the observables. Indeed once F_ξ and $F_{\mathcal{O}}$ are determined (the latter for each observable we are interested in), we can construct the following sequence, for fixed temperature T, by using Eqs. (4.17) and (4.6)

$$\begin{aligned}(L, \xi_L(T), \mathcal{O}_L(T)) \mapsto (\alpha L, \xi_{\alpha L}(T), \mathcal{O}_{\alpha L}(T)) \mapsto (\alpha^2 L, \xi_{\alpha^2 L}(T), \mathcal{O}_{\alpha^2 L}(T)) \mapsto \\ \mapsto \ldots \mapsto (\infty, \xi_\infty(T), \mathcal{O}_\infty(T)) \,,\end{aligned} \tag{4.19}$$

that leads to the infinite-volume extrapolations. In principle these are independent of the starting value of L, but corrections to the FSS may give such a dependence. If it is not the case, we can estimate T_c and the critical exponents, in a very direct way, by analyzing the singular behavior of the extrapolated observables. This method is particularly efficient and it has been applied successfully to many different equilibrium models [93–99]. For a discussion of the error sources in this procedure see Refs. [90,93].

4.4 Field Theory for the DLG and FSS

In Section 3.2 we explained why a lattice model as the DLG may be described, in the critical region, with suitable field theories, outlining its derivation in Section 3.3. Here we want to draw further conclusions from the theory represented by the dynamic functional (3.1).

For the structure factor the renormalization-group analysis gives the scaling form (see Eq. (3.2))

$$\tilde{G}(k_\parallel, k_\perp; \tau) = \mu^{-2} \tilde{G}(k_\parallel \mu^{-1-\Delta}, k_\perp \mu^{-1}; \tau \mu^{-1/\nu}), \tag{4.20}$$

where, in d dimensions (see Tab. 3.1),

$$\nu = \frac{1}{2}, \tag{4.21}$$

$$\Delta = \frac{1}{3}(8 - d), \tag{4.22}$$

and $\tau \propto T - T_c$. In two dimensions, for the transverse structure factor (see Eq. (2.37)), this implies the simple scaling form

$$\tilde{G}_\perp(k; \tau) = \tau^{-1} f(k^2/\tau). \tag{4.23}$$

Thus, in infinite volume we have, by using the definition (2.38),

$$\xi_{ij} \sim \tau^{-\nu}, \qquad \chi \sim \tau^{-\gamma}, \tag{4.24}$$

where ν is given in Eq. (4.21) and

$$\gamma = 1. \tag{4.25}$$

The function $f(x)$ defined in Eq. (4.23) is trivial. Indeed, keeping into account the causality and the form of the interaction vertex one can see that for $k_\parallel = 0$ there are no loop contributions to

the two-point function (and also to the response one $\langle \tilde{s}_0 s_x \rangle$). Thus, for all $2 \leq d \leq 5$, $\tilde{G}_\perp(k,\tau)$ is simply given by its tree-level expression

$$\tilde{G}_\perp(k;\tau) = \frac{1}{k^2+\tau}. \tag{4.26}$$

Two observations are here in order. First it is usually assumed that τ is an analytic function of $t(\equiv (T-T_c)/T_c)$ such that $\tau = 0$ at criticality and $\tau = bt$ for $t \to 0$ with b positive constant. Second, the function that appears in Eq. (4.26) refers to the coarse-grained fields, which, in the critical limit, differ by a finite renormalization from the lattice ones. Thus, for the lattice function we are interested in, in the scaling limit $t \to 0$, $k \to 0$, with k^2/t fixed, we have

$$\tilde{G}_{\perp,\mathrm{latt}}(k;t) = \frac{Z}{k^2+bt}\ , \tag{4.27}$$

where Z and b are positive constants.

On the same footing, we can conclude that all correlation functions with vanishing longitudinal momenta behave as in a free theory. In particular, the Binder's cumulant defined in Eq. (2.29) vanishes (although some attention should be paid, due to the presence of a dangerous irrelevant operator, see below). It is also important to notice that Eq. (4.27) implies the exponential decay of

$$G_{\perp,\mathrm{latt}}(x_\perp;t) = \int d^{d-1}k\, e^{ikx_\perp}\ \tilde{G}_{\perp,\mathrm{latt}}(k;t)\ , \tag{4.28}$$

which fully justifies our definition of transverse correlation length.

In Section 5.2, we study the FSS behavior of the model. Here, we want to analyze the corresponding continuum field theory in a finite geometry following the method applied in equilibrium spin systems (see, e.g., Refs. [4, 89] and references therein). The idea is quite simple. Consider the system in a finite box with periodic boundary conditions. The finite geometry has the only effect of quantizing the momenta. Thus, the perturbative finite-volume correlation functions are obtained by replacing momentum integrals by sums over the allowed momenta. Ultraviolet divergences are not affected by the presence of the box [81] and thus one can use the infinite-volume renormalization constants [85, 86] to render the theory finite when the regularization is removed. Once the renormalization is carried out, one obtains the geometry-dependent finite-size correlation functions (see, for some examples, Ref. [89]).

Following this idea, if we consider a finite box of size $L_\parallel \times L_\perp$, Eq. (4.20) becomes

$$\tilde{G}(k_\parallel, k_\perp; \tau; L_\parallel, L_\perp) = \mu^{-2}\tilde{G}(k_\parallel \mu^{-1-\Delta}, k_\perp \mu^{-1}; \tau\mu^{-2}; L_\parallel \mu^{-1-\Delta}, L_\perp \mu^{-1})\ , \tag{4.29}$$

which shows that at $T = T_c$

$$\xi_{ij}(T_c) \sim L_\perp \qquad \text{and} \qquad \chi(T_c) \sim L_\perp^{\gamma/\nu} \sim L_\perp^2\ . \tag{4.30}$$

Moreover, Eq. (4.26) holds in finite volume. Keeping again into account the relation between coarse-grained and lattice quantities, we obtain for the lattice correlation function in a finite volume in the continuum limit (i.e. in the FSS limit with $k \to 0$ keeping k^2/t fixed)

$$\tilde{G}_{\perp,\mathrm{latt}}(k;t;L_\parallel,L_\perp) = \frac{Z(t;L_\parallel,L_\perp)}{k^2+\tau(t;L_\parallel,L_\perp)}\ , \tag{4.31}$$

where Z and τ are analytic functions of their arguments. In the FSS limit, we expect

$$Z(t;L_\parallel,L_\perp) = \tilde{Z}(tL_\perp^2, S_\Delta)\ , \tag{4.32}$$

$$\tau(t;L_\parallel,L_\perp) = L_\perp^{-2}\,\tilde{\tau}(tL_\perp^2, S_\Delta)\ . \tag{4.33}$$

Using these expressions, in the FSS limit we find

$$\frac{\xi_{13}(t;L_\parallel,L_\perp)}{L_\perp} = \left((2\pi)^2+\tilde{\tau}(tL_\perp^2,S_\Delta)\right)^{-1/2}, \tag{4.34}$$

$$A_{13} \equiv \frac{\xi_{13}^2(t;L_\parallel,L_\perp)}{\chi(t;L_\parallel,L_\perp)} = \left[\tilde{Z}(tL_\perp^2,S_\Delta)\right]^{-1}, \tag{4.35}$$

valid for $t\to 0$, $L_\parallel, L_\perp \to \infty$ with S_2 and $tL_\perp^2$ fixed. Therefore, from the scaling of the correlation length and of the amplitude A_{13} we can derive the scaling functions $\tilde{Z}$ and $\tilde{\tau}$.

If we make, as usually done, the simplest approximations $\tilde{Z}(tL_\perp^2,S_\Delta)=$ const and $\tilde{\tau}(tL_\perp^2,S_\Delta) =$ const $\times\, tL_\perp^2$, we obtain for the scaling functions defined in Eq. (4.16) the forms

$$F_\xi(z) = \left[1-\left(1-\alpha^{-2}\right)(2\pi)^2 z^2\right]^{-1/2}, \tag{4.36}$$

$$F_\chi(z) = F_\xi^2(z) = \left[1-\left(1-\alpha^{-2}\right)(2\pi)^2 z^2\right]^{-1}. \tag{4.37}$$

As we shall see, numerical data are in very good agreement with these expressions (see Chap. 5).

In the previous discussion we have neglected the possible presence of a dangerously irrelevant operator that becomes marginal at $d=2$. Its presence may modify the scaling relations (4.20), (4.23), and (4.29). Considering $\tilde{G}_\perp(k)$ (defined in Eq. (2.37)) we have

$$\tilde{G}_\perp(k;\tau;L_\parallel,L_\perp;u) = \mu^{-2}\tilde{G}_\perp\left(k\mu^{-1};\tau\mu^{-2};L_\parallel\mu^{-1-\Delta},L_\perp\mu^{-1};u\mu^{2\sigma}\right), \tag{4.38}$$

where, $\sigma=(d-2)/3$ in d dimensions, and u is the irrelevant coupling. If the scaling function vanishes for $u\to 0$, one obtains an anomalous scaling behavior. In two dimensions, since the operator is marginal ($\sigma=0$), we expect logarithmic corrections to the formulae previously computed. It is also possible that logarithmic terms modify Eq. (4.16). In the absence of any prediction, we will neglect these logarithmic violations. As it has been observed in previous numerical studies, if present, they are small [53]. As we will discuss, this is confirmed by our numerical results.

Finally, we want to notice that the Gaussian nature of the fields at zero longitudinal momenta allow us to write down the probability distribution of $\phi(\mathbf{k}_{0,n})$. Indeed, the previous results give

$$P(\phi(\mathbf{k}_{0,n})) = \frac{1}{N}\exp\left[-\frac{1}{L_\parallel L_\perp}\phi(-\mathbf{k}_{0,n})\tilde{G}^{-1}_{\perp,\mathrm{latt}}(\mathbf{k}_{0,n})\phi(\mathbf{k}_{0,n})\right], \tag{4.39}$$

where N is a normalization factor. From this expression we can derive the probability distribution of $M^2=|\phi(\mathbf{k}_{0,1})|^2/L_\parallel^2 L_\perp^2$. Of course, $\langle M\rangle = m$, $\langle M^2\rangle = \chi/(L_\parallel L_\perp)$ (see Eqs. (2.26), (2.27), and (2.28)). We obtain

$$P(M^2)dM^2 = \frac{1}{\sigma^2}e^{-M^2/\sigma^2}dM^2, \tag{4.40}$$

where

$$\sigma^2 = \frac{1}{L_\parallel L_\perp}\tilde{G}_{\perp,\mathrm{latt}}(2\pi/L_\perp) = \frac{1}{L_\parallel L_\perp}\chi(L_\parallel,L_\perp). \tag{4.41}$$

Chapter 5

Numerical Simulations

In the previous Chapters we introduced the definition of a finite-volume correlation length (overcoming the difficulties described in §2.3), to be used when dealing with the FSS *of the* DLG *phase transition. Moreover we exploited the predictions for scaling functions coming from the field theory described in §3.2. In this Chapter we would take advantage of these achievements in order to drawn, from our* MC *simulations, some conclusions about the universality class of the* DLG *and thus contribute also to the debate discussed in §3.3. In §5.1 we give some detail on the setup of our numerical simulations. In §5.2 we discuss the* FSS *of data. In particular we take care to verify the good behavior (in the sense described §5.2.1) of the correlation length in the thermodynamic limit. Then we perform the* FSS *analysis of our data, finding very good agreement with theoretical predictions. Our findings seem to confirm the standard picture and then rule out the alternative field theories discussed in §3.3. In §5.3 we present the preliminary results that one can obtain when performing the* FSS *analysis without keeping correctly into account the anisotropy. This kind of investigation should be relevant, as discussed in §5.3.1, to understand some numerical results which have been interpreted as evidences against the validity of the standard field theory for the* DLG *phase transition. In §5.4 we sum up our results. For further details we refer to Refs. [69, 70].*

5.1 Setup

We studied the phase transition of the DLG in two dimensions by Monte Carlo simulations. Our aim was to check the validity of the FSS assumptions and eventually use the FSS to compute the critical exponents. The observables we consider are those described in Section 2.4. We use the dynamics discussed in Sect. 2.1, with Metropolis rates, i.e. we set

$$w(x) = \min(1, e^{-x}). \tag{5.1}$$

Simulations were performed at infinite driving field E: Forward (backward) jumps in the direction of the field are always accepted (rejected).

The dynamics of the DLG is diffusive and the dynamic critical exponent is expected to be $z_\perp = 4$ [39]. Thus, it is important to have an efficient implementation of the Monte Carlo sampling algorithm in order to cope with the severe critical slowing down. Details of the algorithmic implementation used can be found in Ref. [69]. A multi-spin coding technique is used to evolve simultaneously 128 independent spin configurations (this number has been chosen to optimize the

number of single-spin sweeps per second, see Ref. [69] for details) with a speed of $2.7 \cdot 10^8$ spin-flip/sec on a Pentium processor.

First of all our aim has been the test of the theoretical predictions of the standard field theory for the DLG, see Sect. 3.2 and Sect. 4.4. Thus we assume that the "correct" FSS limit has to be done with $S_2 = L_\parallel / L_\perp^3$ kept constant, i.e. $\Delta = 2$[1].

The sizes of the lattices we have considered are $(L_\parallel, L_\perp)$: $(21,14)$, $(32,16)$, $(46,18)$, $(64,20)$, $(88,22)$, $(110,24)$, $(168,28)$, $(216,30)$, $(262,32)$, $(373,36)$, $(512,40)$, $(592,42)$, $(681,44)$, $(778,46)$, $(884,48)$, for which $S_2 \simeq 0.2$. The temperatures at which we have simulated the DLG are β: 0.28, 0.29, 0.3, 0.305, 0.3075, 0.31, 0.3105, 0.311, 0.31125, 0.3115, 0.31175, 0.312, which all lie in the high-temperature disordered phase (albeit very near to the critical point).

It is very important to be sure that the system has reached the steady-state distribution before sampling. Metastable configurations in which the Markov chain could be trapped for times much longer than the typical relaxation times in the steady state are a dangerous source of bias. In the DLG, configurations in which multiple stripes aligned with the external field are present are very long-lived and it is possible that they persist for times comparable to those of typical simulation runs (an analysis of the dynamics of DLG below the critical temperature and thus of metastabilities in domain growth, can be found in Ref. [76]), thus effectively inducing a spurious geometry on the system. To avoid the formation of stripes, we took care to initialize the larger systems by rescaling suitably the thermalized configurations of the smaller ones (where the metastable states decay faster) with the same temperature and value of S_2.

We computed the autocorrelation time τ_χ for the susceptibility χ. Such an observable is expected to have a good overlap with the slowest modes of the system, so that τ_χ should give a good indication of the number of sweeps required to generate independent configurations. We found that, for one of the lowest temperature we considered ($\beta = 0.311$), $\tau_\chi \approx 900$, 1400, 2700 sweeps, for $L = 20, 24, 28$ respectively, where a MC sweep is conventionally defined as the number of moves equal to the volume of the lattice. For this reason, in order to have approximately independent configurations, we measured once every 1500 sweeps for every value of β.

For each geometry and β we collected approximately $3 \cdot 10^5$ measures. We would not report here the raw MC data, as they can be found in Ref. [69].

The statistical variance of the observables is estimated by using the jackknife method [80]. To take into account the possible residual correlations of the samples, we used a blocking technique in the jackknife analysis. In the standard jackknife method the variance estimator is obtained discarding single data points. In the blocking technique, several variance estimators are considered, discarding blocks of data of increasing length and monitoring the estimated variance until it reaches a maximum.

5.2 FSS Analysis of Numerical Data

Here we discuss some of our numerical results concerning the FSS analysis of the DLG, done following the general strategy described in Section. 4.3.2, which heavily relies on the correlation length, see Sect. 2.4.2.

5.2.1 Thermodynamic Limit for ξ_L

In Sect. 2.4.2 we introduced a definition for the finite-volume correlation length. We would test, first of all, that it has a well-defined thermodynamic limit, independently of the particular geometry chosen. Indeed for fixed temperature $T \neq T_c$ (T_c being the critical one), we expect an infinite-volume

[1] This value is obtained by a naïve extrapolation of the exact result Eq. (4.22) down to $d = 2$.

limit independent of how this limit has been taken, given that whenever both sizes (we have in mind the two-dimensional DLG) exceed the typical length through which correlations are established, the observables should not change with the actual geometry of the system. This statement is nothing but the very requirement of the existence of a thermodynamic limit. Of course there are systems (for examples those with long-range interactions, see the discussion and references in Ref. [33]) for which this is not true. Given the generic long-range correlations in the DLG, it is not obvious *a priori* what the behavior of the introduced correlation length could be. So we test numerically that ξ_{13} (which in the following will be called ξ_L), introduced in Sect. 2.4.2, has a good thermodynamic limit independently of the chosen geometry, that is, in particular, of the specific S_Δ kept constant.

To this end we considered not only the lattices mentioned above with S_2 constant, but also a sequence of systems for which S_1 is constant and with $L_\perp$ ranging from 14 to 48 as above. With the aim to test the theoretical prediction on the finite-size corrections to the correlation length:

$$\xi_L^{-2}(\beta) = \xi_\infty^{-2}(\beta) + \frac{4\pi^2}{L^2} + \text{corrections}\,, \tag{5.2}$$

we introduce the following quantity

$$\tau_L(\beta) \equiv \xi_L^{-2}(\beta) - \frac{4\pi^2}{L^2}, \tag{5.3}$$

where, hereafter, $L \equiv L_\perp$. A good behavior of ξ_L as $L \to \infty$ is reflected in a good behavior of τ_L and vice-versa. Moreover we expect from Eq. (5.2) that τ_L will be constant (apart from corrections) for large L when the shape factor S_2 is kept constant, but not otherwise. Indeed, as Fig. 5.1 shows, a good thermodynamic limit seems to exist for every value of β. As expected, when the temperature approaches the critical value, it is necessary to use larger and larger lattices to see the convergence to the infinite-volume limit (as a consequence of the fact that correlations are established on a much bigger scale). At β fixed we expect the convergence to become eventually exponential in L. However, for lattices with S_2 fixed we observe an intermediate region of values of L in which τ_L is apparently constant. Such a region widens as β approaches the critical point and is therefore consistent with the relation (5.2), that is

$$\xi_\infty^{-2}(\beta) \approx \tau_L(\beta) = \xi_L^{-2}(\beta) - \frac{4\pi^2}{L^2}\,, \tag{5.4}$$

in the FSS limit $L \to \infty$, $T \to T_c$. But this happens only for the geometries with S_2 constant. Of course we are neglecting, in the previous equation, the subleading corrections that will depend in general on the specific value chosen for S_2 and are particularly small for our choice $S_2 \approx 0.200$. Note also that when S_1 is kept constant, the corrections to the infinite-volume limit are larger. This has to be expected since the geometries with S_1 constant tend to be smaller than those with S_2 constant when comparing system with the same transverse size, as we do here.

5.2.2 FSS for the Observables

The good behavior of τ_L hints that it should be possible to extract the infinite-volume limit τ_∞ directly by fitting τ_L, for large enough L, with the constant value $\tau_\infty = 1/\xi_\infty^2$.

Table 5.1 shows the results of fitting $\tau_L(\beta)$ as a function of L within the linear approximation $\tau_\infty(\beta) + a(\beta)L^{-2}$ discarding the observations with $L < L_{\min}$ where $L_{\min}$ has been chosen to have a reasonable value of the sum of squared residuals R^2. In the table the critical values of R^2 at the 95% confidence level based on the χ^2 statistics are also reported and show that almost all the fits are consistent (only two of them have $R^2 > R_c^2$ and this is statistically compatible with the 95% confidence level). The value of the parameter $\tau_\infty(\beta)$ gives then our preferred estimate for the infinite-volume correlation length $\xi_\infty(\beta) = 1/\sqrt{\tau_\infty(\beta)}$.

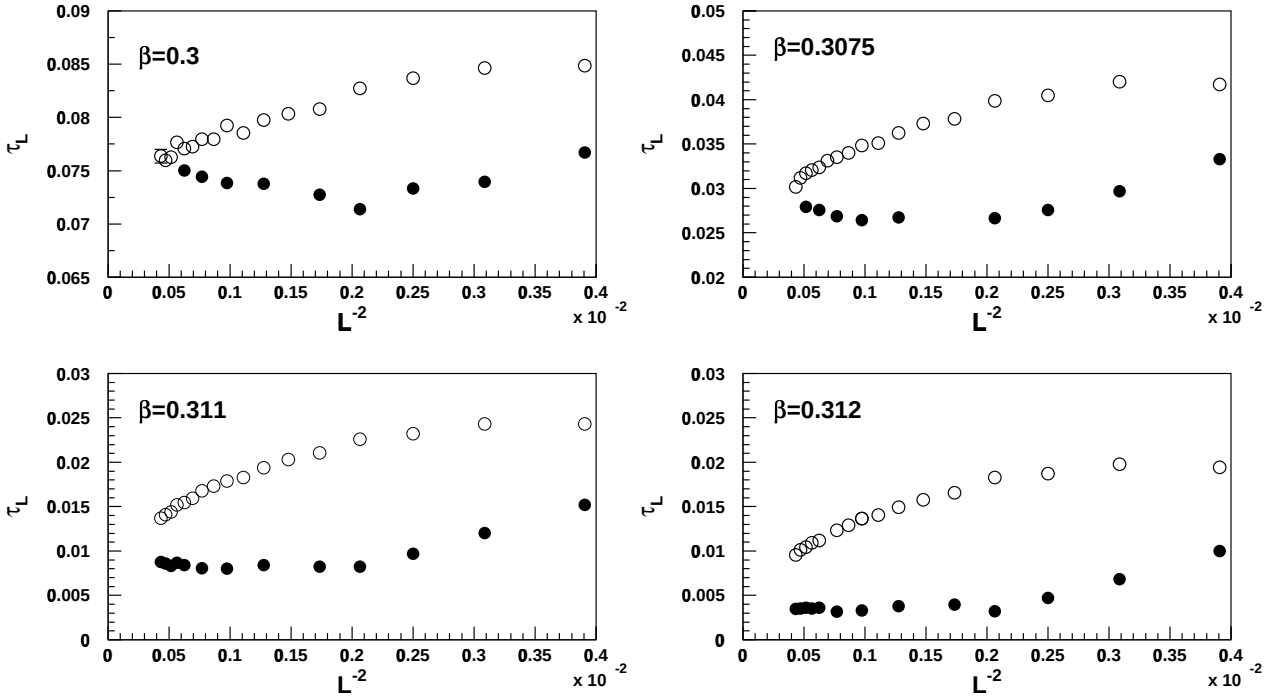

Figure 5.1: τ_L for different geometries as a function of the inverse temperature β. Filled (respectively empty) points refer to geometries with S_2 (respectively S_1) fixed. Here $S_2 \approx 0.200$, $S_1 \approx 0.106$. Errors are smaller than the sizes of the points.

The same kind of analysis on the data referring to geometries with S_1 constant is not reliable. Indeed they are clearly affected by larger corrections and thus any extrapolation could not be reliable without the knowledge of their analytic forms.

A simple argument shows that Eq. (5.2) implies $\nu = 1/2$. Then, given the values of $\tau_\infty(\beta)$ we can both check the expected value of ν and take advantage of it to estimate the critical value of β.

We fitted

$$\tau_\infty(\beta) = A \left| \frac{\beta}{\beta_c} - 1 \right|^{2\nu} , \tag{5.5}$$

for $\beta > \beta_{\min}$ choosing for $\beta_{\min}$ the lowest value for which $R^2 < R_c^2$ (here and in the following we will use always critical values at the 95% confidence level) and we obtained $\beta_{\min} = 0.31$, $N = 4$, $R^2 = 4.2$ ($p = 0.38$[2], $R_c^2 = 9.48$), $A = 1.09(31)$, $\beta_c = 0.312557(93)$,

$$\nu = 0.4605(32) . \tag{5.6}$$

Adding analytic corrections to scaling does not give better results.

A better estimate of β_c is obtained by fixing $\nu = 1/2$. In this case $\beta_{\min} = 0.31$, $N = 5$, $R^2 = 5.56$ ($p = 0.35$, $R_c^2 = 11.07$), $A = 1.540(24)$, $\beta_c = 0.312670(26)$. Adding the first analytic correction to scaling, i.e. fitting with

$$\tau_\infty(\beta) = A \left|\beta/\beta_c - 1\right|^{2\nu} \left(1 + B \left|\beta/\beta_c - 1\right|\right) , \tag{5.7}$$

[2]With p we indicate the probability for R to be bigger than the value found in the fit, assuming a χ^2_N distribution.

β	$L_{\min}$	N	R^2	R_c^2	τ_∞	a
0.28	22	4	3.12	9.49	0.2397(13)	-5.44(87)
0.29	22	4	2.76	9.49	0.15309(87)	-4.19(56)
0.3	22	4	5.09	9.49	0.07607(35)	-2.02(24)
0.3025	22	4	5.19	9.49	0.05864(36)	-1.30(25)
0.305	24	8	14.63	15.50	0.04382(26)	-1.91(26)
0.3075	26	2	0.70	6.00	0.02961(52)	-3.33(67)
0.31	22	4	8.29	9.49	0.01309(11)	0.310(74)
0.3105	22	4	7.57	9.49	0.01069(18)	0.09(13)
0.311	24	7	14.78	14.08	0.00852(21)	-0.17(18)
0.31125	22	4	2.65	9.49	0.00703(11)	-0.012(72)
0.3115	22	4	8.56	9.49	0.00586(14)	0.01(13)
0.31175	24	3	9.21	7.82	0.00421(20)	0.49(19)
0.312	28	6	11.46	12.59	0.00348(16)	0.01(20)

Table 5.1: Fit of $\tau_L(\beta)$ with $\tau_\infty + aL^{-2}$ (for S_2 constant): $L_{\min}$ is the minimum value of L allowed in the fit, N are the degrees of freedom, R^2 is the sum of square residuals and R_c^2 is the critical value for R^2 at the 95% confidence level based on a χ^2 distribution with N degrees of freedom.

gives (with the same value of $\beta_{\min} = 0.31$) $N = 4$, $R^2 = 4.02$ ($p = 0.40$, $R_c^2 = 11.07$), $A = 1.70(13)$, $\beta_c = 0.312603(54)$ and $B = -15(12)$.

Then we consider as our best estimate of the critical temperature:

$$\beta_c \quad = 0.312603(54). \tag{5.8}$$

This result should be compared with the existing determinations:

$$\beta_c = \begin{cases} 0.3108(11) & \text{Ref. [52];} \\ 0.3125(13) & \text{Ref. [54];} \\ 0.3155(9) & \text{Ref. [72];} \\ 0.31250(97) & \text{Ref. [77].} \end{cases} \tag{5.9}$$

Our estimate Eq. (5.8) is in fairly good agreement with all of them (the agreement not so good in the case of Ref. [72]), although more precise.

The good FSS behavior of the correlation length is witnessed by the plot of ξ_{2L}/ξ_L vs. ξ_L/L in Fig. 5.2. The solid line is the theoretical prediction Eq. (4.36) with $\alpha = 2$. It is clear that as the size of the system increases the points converge towards the theoretical curve. Let us emphasize that in this plot *there are no tunable parameters involved*, at variance with the case of usual FSS plots, as discussed in Sect. 4.3. So the observed collapse is very remarkable. To get rid of the quite small corrections to FSS still present, in Fig. 5.3 we plotted ξ_{2L}/ξ_L vs. $\xi_{2L}/2L$. In this way, the values on the abscissa, should have smaller corrections given they refer to bigger lattices, improving the quality of the plot.

Next we checked the FSS behavior of various observables, plotting $\mathcal{O}_{2L}/\mathcal{O}_L$ vs. $\xi_{2L}/(2L)$. The plot of the susceptibility is reported in Fig. 5.5 and it has the same features already discussed for the plot of ξ. In Fig. 5.4 we report the amplitude A, defined in Eq. (2.40), which the theory predicts a dimensionless quantity in the RG sense (no anomalous dimension). The error-bars seem quite large, due to the very small range in the vertical axis. We note that the points show the right trend towards the theoretical prediction, shown as a dotted line.

The plot for the magnetization, in Fig. 5.7, shows a reasonably good collapse of data points.

As we described in Sect. 4.3.2, it is possible to determine the ratio between critical exponents by looking at the curve $\mathcal{O}_{2L}/\mathcal{O}_L$ vs. $\xi_{2L}/(2L)$, as those presented here. To this end we have to determine, first of all, the value of $\xi_{2L}/2L$ at criticality, which is nothing but the value corresponding to $\xi_{2L}/\xi_L = 2$ in Fig. 5.3. Given the good agreement between numerical data and analytic prediction Eq. (4.36), we assume for critical $\xi_{2L}/2L$ the theoretical value $1/2\pi \simeq 0.159$. We look at the value of the ratio m_{2L}/m_L at the critical point, i.e. corresponding, in Fig. 5.7 to the abscissa 0.159, which turns out around 0.5 (without any precise determination or fitting procedure we can say that a reasonable range of values is 0.500(25)) By using Eq. (4.10) we can conclude that $\beta/\nu \simeq 1$ (1.00(7) using the previous estimate) in agreement with the theoretical prediction, see Tab. 3.1, and definitely different from $\beta \sim 1/3$ ($\nu = 0.4605(32)$), found by some authors (see Tab. 3.2). As far as γ is concerned, it may be computed from the FSS plot of the susceptibility. Assuming as a rough estimate of χ_{2L}/χ_L at criticality the value 4.00(25), we find $\gamma/\nu = 2.00(9)$. We sum up these (rough) estimates in Tab. 3.2.

Following the general strategy outlined in Sect. 4.3.2 it is possible to give much more precise estimates of critical exponents. We have reported here only the results of a preliminary analysis (details can be found in the revised version of Ref. [69], to appear), giving rough, but already satisfactory, estimates of critical exponents. Also the extrapolation to the thermodynamic limit of the considered observable should give, as above, results consistent with the theoretical predictions reviewed in Sect. 4.4. Indeed, give data points collapse quite well onto the theoretical predictions for the scaling functions, we expect that the extrapolations based on suitable fits of data will give the expected results. Of course a careful analysis of statistical uncertainties has to be done.

The behavior of the Binder's parameter, reported in Fig. 5.6, seems to lead to a good data collapse. A rough estimate of the anomalous dimensions of g would give in this case $x_g/\nu \simeq -0.4$ meaning that $g = 0$ at the critical point and $g(L) \sim L^{-0.2}$ for $L \to \infty$. This is in agreement with the idea that transverse fluctuations are Gaussian (nevertheless some attention has to be paid when making statements about the behavior of the finite-size Binder's cumulant, see Ref. [71] for details).

The plot in Fig. 5.8 shows some *preliminary* results about the parallel correlation length $\xi_\perp$, defined analogously to the transverse one by looking at the structure factor for small parallel momenta (and vanishing transverse ones). The correlation length plotted in Fig. 5.8 is obtained, in particular, by using the first and the second non-zero parallel momenta (it is the analogous of ξ_{12}). This plot is not very illuminating given the presence of very strong corrections to scaling. We remark only the fact that increasing the lattice sizes, points move downwards and leftwards. To get some useful information we plotted in Fig. 5.9, $\xi_{\parallel,L}/L_\parallel$ vs. ξ_L/L. The huge corrections to FSS are still evident, but the general trend is now clear. With a given marker we indicate a specific temperature, and points corresponding to increasing lattice sizes move from right to left. We can see that at least for sufficiently large sizes, points collapse onto a well-defined FSS curve. This fact allows us to conclude that $\xi_{\parallel,L}(\beta_c) \propto L_\parallel = L^3$, and thus $\nu_\parallel = 3\nu$. The same conclusion could be drawn from Fig. 5.8, having now in mind that there is an underlying scaling plot, although hidden by huge corrections in the smallest lattices. Looking only at the biggest ones ($L = 22(\Diamond)$, $24(\bigstar)$) we can say that $\xi_{\parallel,2L}/\xi_{\parallel,L}(\beta_c) \approx 8$ and thus, again, $\nu_\parallel/\nu \approx 3$ (of course a more careful analysis is required).

5.3 FSS with S_1 fixed

The results reviewed in Sect. 5.2 make us fairly confident that S_2 is the right shape factor to be kept constant when doing a FSS analysis for the two-dimensional DLG. Nevertheless we will explore in this Section the possibility of having a good FSS behavior (with somehow "effective" exponents) also for S_2 not constant. In particular the striking results of Ref. [72] which we would compare with, are obtained, as discussed in Sect. 3.3 with a FSS analysis done keeping constant S_1, that

implies a vanishing S_2 as the size increases.

5.3.1 Aim

It has been shown, in Refs. [52, 53], that crossover effects could play a crucial role when discussing FSS of strongly anisotropic systems. Generally speaking, it is a well-known fact, supported also by exact solutions (see, e.g. the work on the Kasteleyn model of dimers on the brick lattice [88]), that keeping constant the "wrong" shape factor (i.e. changing the correct one with the size) may lead to a crossover between finite geometries and striped ones. The exponents appearing in the FSS functions are exactly those expected for the limit geometry, keeping into account the strong anisotropy, and do not depend on the specific way with which the correct shape factor is changed with the geometry. In some cases, however, it seem possible to have a non-trivial FSS limit of observables in which the exponents appearing in the FSS functions have such a dependence. This leads to effective exponents depending on the particular way in which the FSS limit is performed (see Ref. [71] for details and for an analysis of the behavior of the Spherical Model, in which such a strange behavior can be traced back to the presence of Goldstone bosons in the low-temperature phase). In the specific case of the DLG the situation is even less clear given the additional presence of the dangerous irrelevant operator (see Eq. (4.38)), leading to a violation of hyperscaling relations, whose effects on the scaling behavior are not well-understood at least with respect to FSS. In particular the presence of such an operator is expected to give rise, as in equilibrium, to an "effective" length scale which should appear somewhere in scaling functions. In Refs. [52,53] a scaling theory has been developed, following closely the analogy with the case of the dangerous irrelevant coupling of ϕ^4 theory above the upper critical dimension, to take into account both the presence of this operator and the possible singular behavior arising when the correct shape factor is not kept fixed. This problem has been also discussed in Ref. [59], following again a phenomenological approach for finite-size observables right at the critical point.

It seems to us worthwhile to study this problem by using the approach to FSS described in Sect. 4.3.2. We expect that FSS plots done in that way (with no tunable parameters and thus more robust) could give some useful hints, also in view of the debate on the universality class of the DLG. Some of the claims done in the literature (see Sect. 3.3) could be accounted for once the possible crossover towards a non-trivial scaling function has emerged also in the case of "wrong" FSS.

5.3.2 Preliminary Results

Here we report the preliminary results of simulations done in lattices with a fixed value of $S_1 = L_\parallel / L_\perp^2$.

We considered the following geometries with $S_1 \approx 0.106$ constant: $(20, 14)$, $(27, 16)$, $(34, 18)$, $(42, 20)$, $(51, 22)$, $(61, 24)$, $(72, 26)$, $(83, 28)$, $(96, 30)$, $(109, 132)$, $(123, 34)$, $(138, 36)$, $(154, 38)$, $(170, 40)$, $(188, 42)$, $(206, 44)$, $(225, 46)$, $(245, 48)$. And the following values of β: 0.27, 0.28, 0.29, 0.3, 0.305, 0.3075, 0.31, 0.3105, 0.311, 0.312. We do not report here the raw data, which can be found in Ref. [71].

In Fig. 5.10 we reported the plot for ξ_{2L}/ξ_L vs. ξ_L/L in the case of fixed S_1. It shows larger corrections (i.e. the scaling looks worser) compared to that obtained with S_2 constant (see Fig. 5.3). This fact is somewhat natural given that the geometries considered here are smaller compared to the those with S_2 constant and the same L. In any case (whatever the scaling holds or not), the most relevant feature of the plot is that $\xi_{2L}/\xi_L \leq 1.85$, in the range of values assumed by ξ_L/L. We expect, on the other hand, that at criticality $\xi_{2L}/\xi_L = 2$. This could mean that the values of β considered here are still too far from the critical point. But this does not seem the case given that the temperatures reported in Fig. 5.10 are the same as those used when studying FSS with S_2 constant and we have data up to $\beta = 0.312$, quite near to the determined $\beta_c \approx 0.3126$ (we

remark that the critical temperature, being referred to the thermodynamic limit, should be well-defined whenever the latter exists). Thus even if we assume that the spread of data in Fig. (5.10) is simply a consequence of important corrections and that when they are vanishing a well-defined FSS curve is recovered, something peculiar is happening. This point of view is consistent with the idea that an "effective" scaling could be obtained, albeit with stronger corrections, also when the FSS is performed keeping constant the "wrong" shape factor.

To understand the scaling behavior of ξ_L at β_c we took the data with $\beta = 0.312$ and, assuming $\xi_L(\beta_c) \propto L^{a_\xi}$, we tried to estimate a_ξ. To do this we proceeded as follows: Given that L_n is an increasing sequence of values of L at our disposal we computed the ratios

$$r_n = \frac{\log(\xi_{L_{n+1}}(\beta)) - \log(\xi_{L_n}(\beta))}{\log(L_{n+1}) - \log(L_n)} , \tag{5.10}$$

with the corresponding statistical errors. Note that if $\xi_{L_n} \propto L_n^{a_\xi}$ we have $r_n = a_\xi$. We estimated a_ξ fitting the r_n with a constant. The best fit is obtained considering data with $L \geq L_{\min} = 24$ and gives $a_\xi = 0.847(13)$ with $R^2 = 3.765$ and $N = 10$. The same procedure may be applied for the susceptibility χ, whose plot is given in Fig. 5.11. Assuming the same value of $L_{\min}$ we get, $a_\chi = 1.676(16)$ with $R^2 = 6.210$ and $N = 10$. For m (with the same $L_{\min}$): $a_m = -0.6787(91)$ with $R^2 = 8.260$ and $N = 10$.

Note that the determinations of a_ξ, a_χ and a_m are consistent with the equations $a_\chi = 2a_\xi$, $a_m = a_\chi/2 - 3/2$ obtained from the relations

$$\chi_L \propto \xi_L^2, \qquad m_L^2 \propto \frac{\chi_L}{L_\parallel L_\perp} , \tag{5.11}$$

valid for the mean-field theory.

These findings suggest that the appropriate FSS form in this case could be

$$\xi_L/L_{\text{eff}} = F_\xi^\flat(\xi_\infty/L_{\text{eff}}), \qquad \chi_L/L_{\text{eff}} = F_\chi^\flat(\xi_\infty/L_{\text{eff}}), \tag{5.12}$$

where $L_{\text{eff}} = L^{a_\xi}$ is an effective length scale entering the FSS functions (related to the dangerous irrelevant operator?). Note that a similar result was found (in the same limit $S_2 \to 0$) by Leung [52, 53]. Fig. 5.13 show the good data collapse obtained by plotting ξ_{2L}/ξ_L against $\xi_{2L}/(2L_{\text{eff}})$, as it should be if Eq. (5.12) is correct.

We would not discuss this point further given, that our investigation is still in a preliminary stage (see Ref. [71] for more details and conjectures). We are confident, however, that partial explanation of some of the numerical controversies originate from peculiarities in the FSS of anisotropic system.

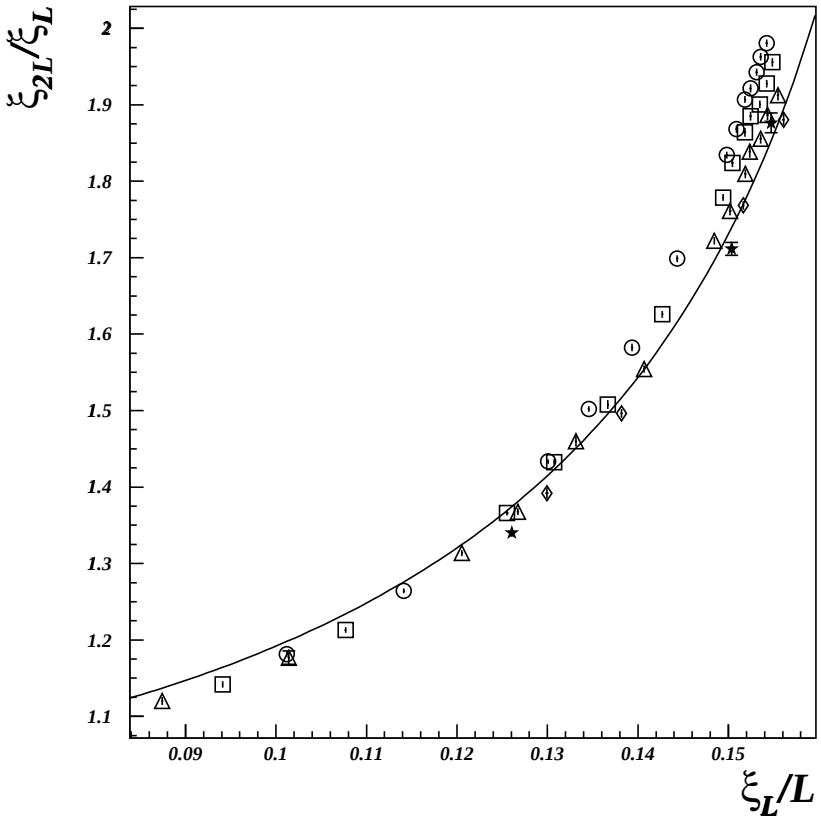

Figure 5.2: FSS plot for ξ with $\alpha = 2$. Marks are as follows : $L = 16(\circ)$, $18(\square)$, $20(\triangle)$, $22(\Diamond)$, $24(\bigstar)$. On the right ξ_{2L}/ξ_L is plotted against $\xi_{2L}/(2L)$ to reduce the effects of corrections to FSS. The lines are the theoretical prediction.

5.4 Summary

Summing up, in Refs. [69,70] we have performed a thorough check of the theoretical predictions for the DLG.

First of all we checked the existence (in the sense specified in Sect. 5.2.1) of the thermodynamic limit for the correlation length defined in Sect. 2.4.2, and on which our FSS analysis is based. We remark that, at least to our knowledge, we determine for the first time a sensible correlation length, measurable in MC simulations, with a good behavior in finite volume. Assuming $\Delta = 2$, we checked that the transverse susceptibility χ and the transverse correlation length ξ_{13} have the correct behavior in the sense that, apart quite small corrections, data point collapse onto some curves and the resulting FSS plots agree with theoretical predictions. Moreover we have been able to probe the FSS regime of the DLG in much deeper detail than done in previous works in the literature, first of all avoiding the quite questionable technique of data collapse to determine the critical exponents. Indeed, the goodness of the observed collapse, is usually judged by eyes inspection: In doubtful situations like ours, a more quantitative and constrained approach is required to make strong checks

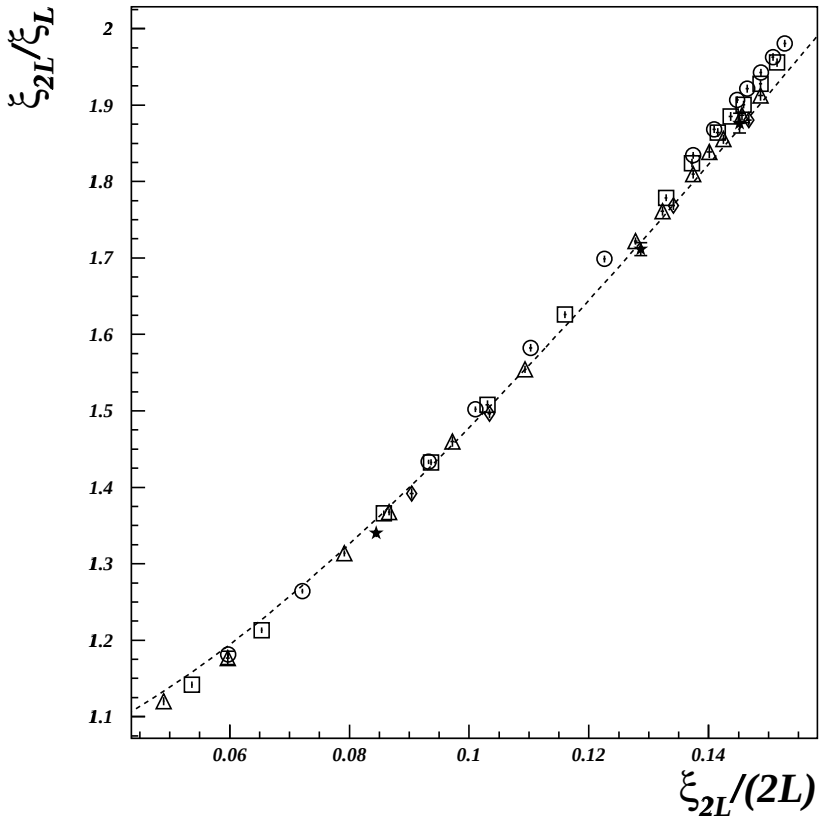

Figure 5.3: FSS plot for ξ. Marks are as in fig. 5.2. ξ_{2L}/ξ_L is plotted against $\xi_{2L}/(2L)$ to reduce the effects of corrections to FSS. The line is the theoretical prediction.

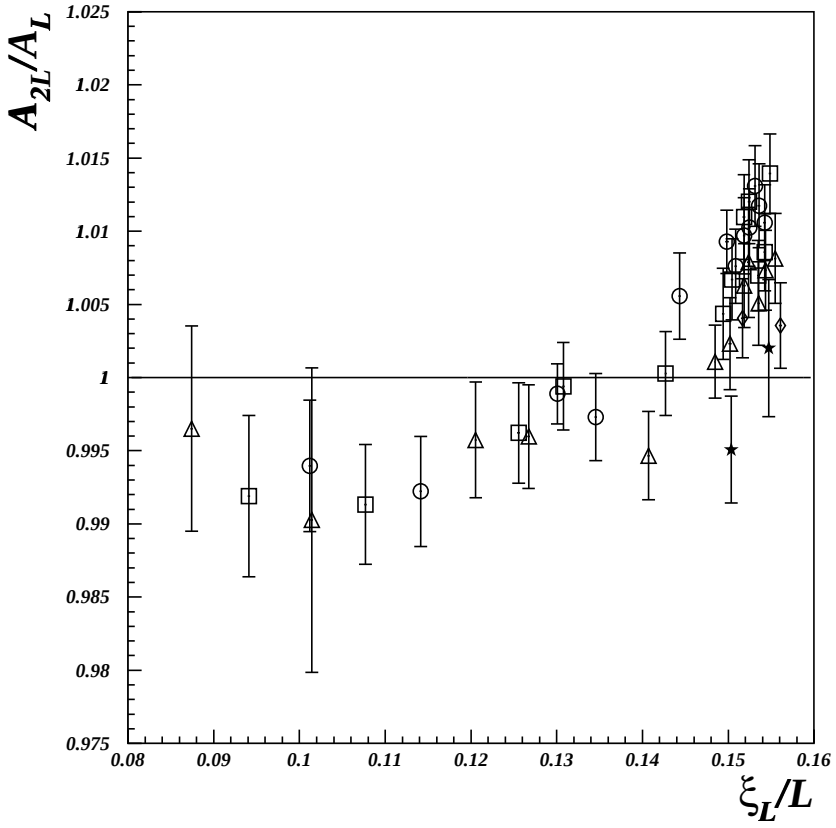

Figure 5.4: FSS plot for A. Marks are as in fig. 5.2. The solid line is the theoretical prediction.

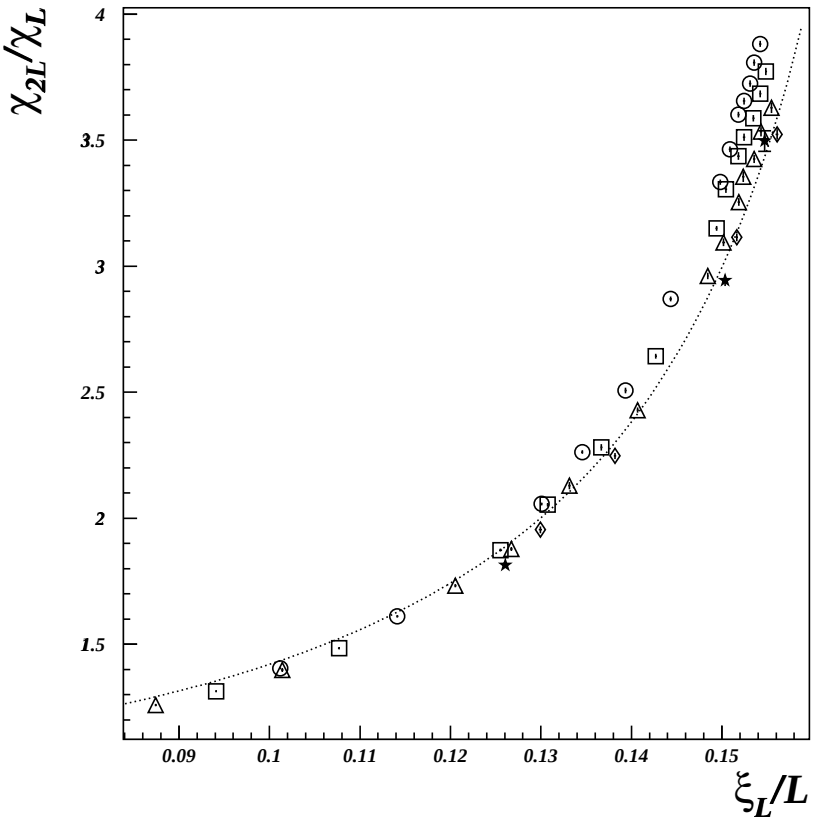

Figure 5.5: FSS plot for χ. Marks are as in fig. 5.2. The line is the theoretical prediction.

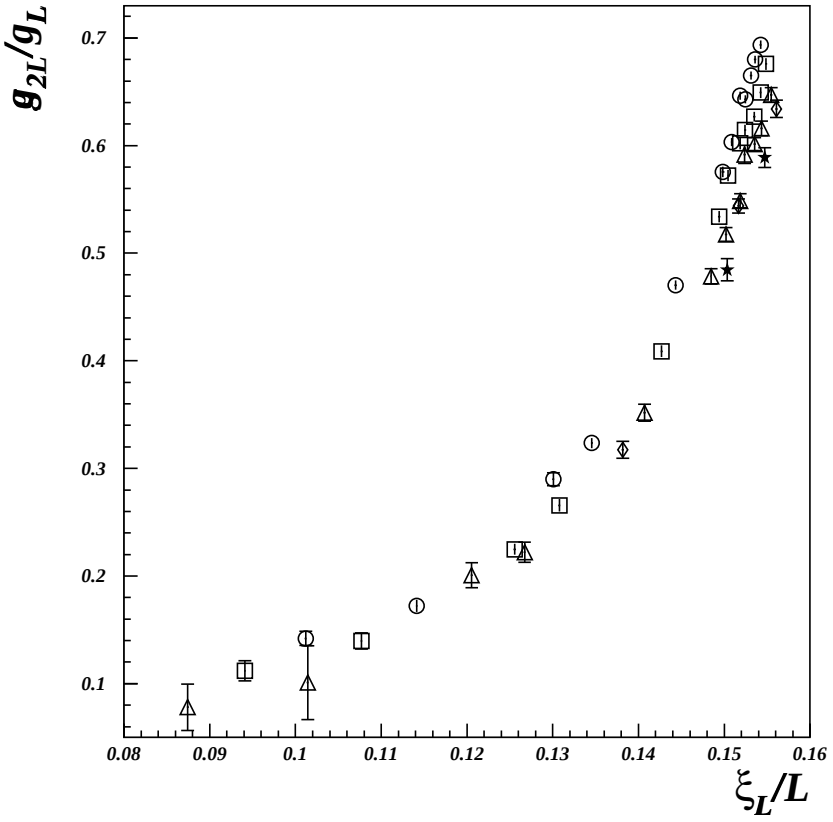

Figure 5.6: FSS plot for g. Marks are as in fig. 5.2.

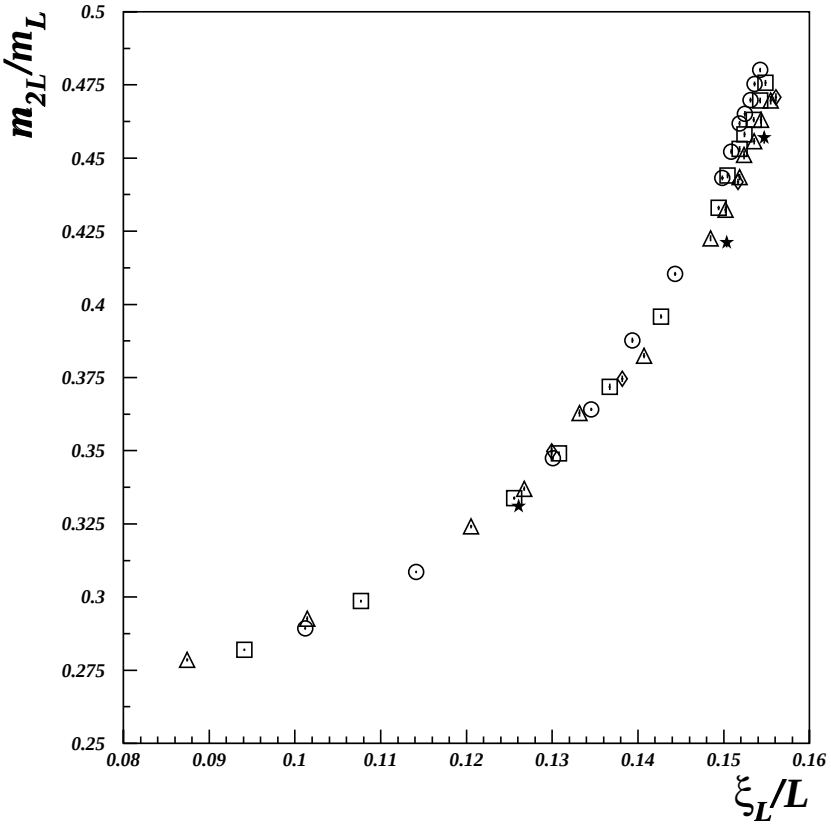

Figure 5.7: FSS plot for m. Marks are as in fig. 5.2.

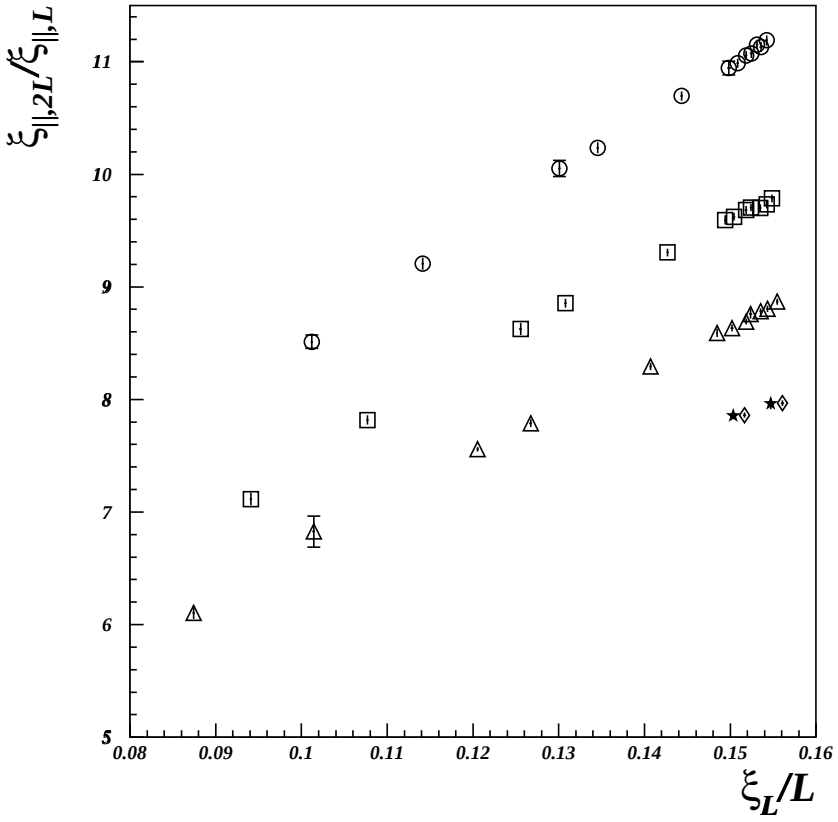

Figure 5.8: FSS plot for $\xi_{\|}$. Marks are as in fig. 5.2.

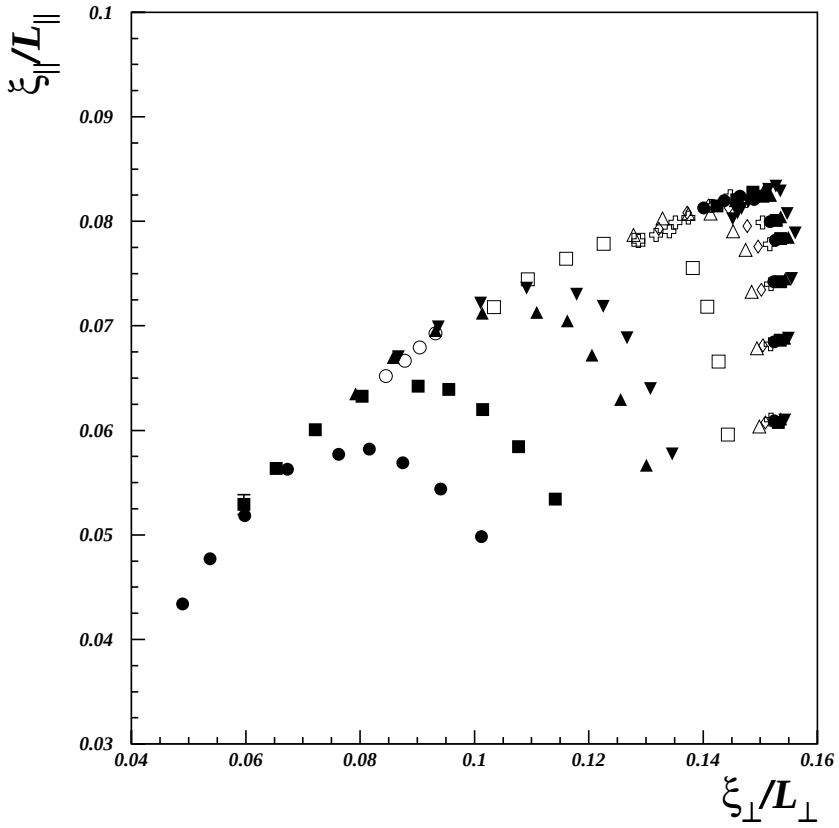

Figure 5.9: FSS plot of $\xi_{\parallel}/L_{\parallel}$ versus ξ/L. All the data points are shown. For the same value of β (same marker) the larger geometries are on the left of smaller ones. The plot clearly shows that corrections to FSS dies out as L increases.

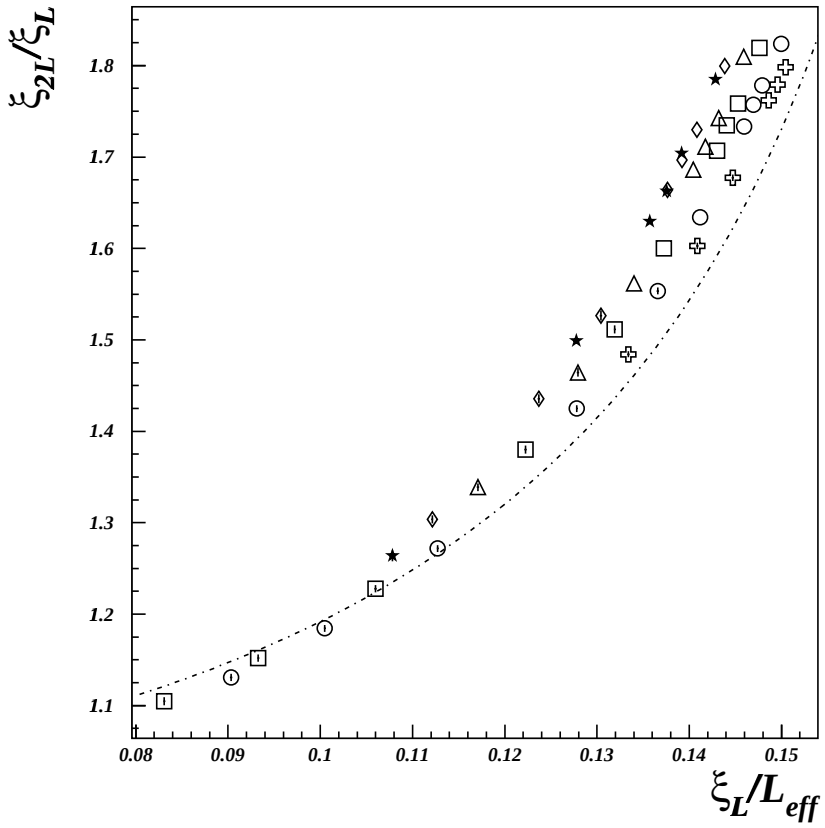

Figure 5.10: FSS plot for ξ with S_1 fixed. Marks are as in fig. 5.2.The line is the theoretical prediction of FSS with S_2 fixed, for comparison.

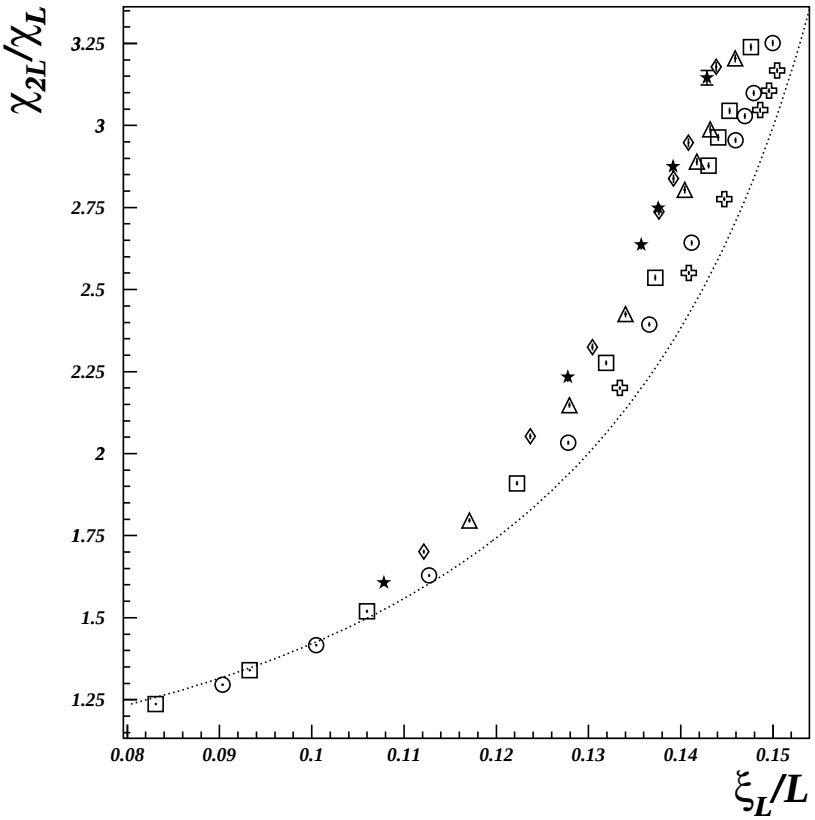

Figure 5.11: FSS plot for χ with S_1 fixed. Marks are as in fig. 5.2. The line is the theoretical prediction of FSS with S_2 fixed, for comparison.

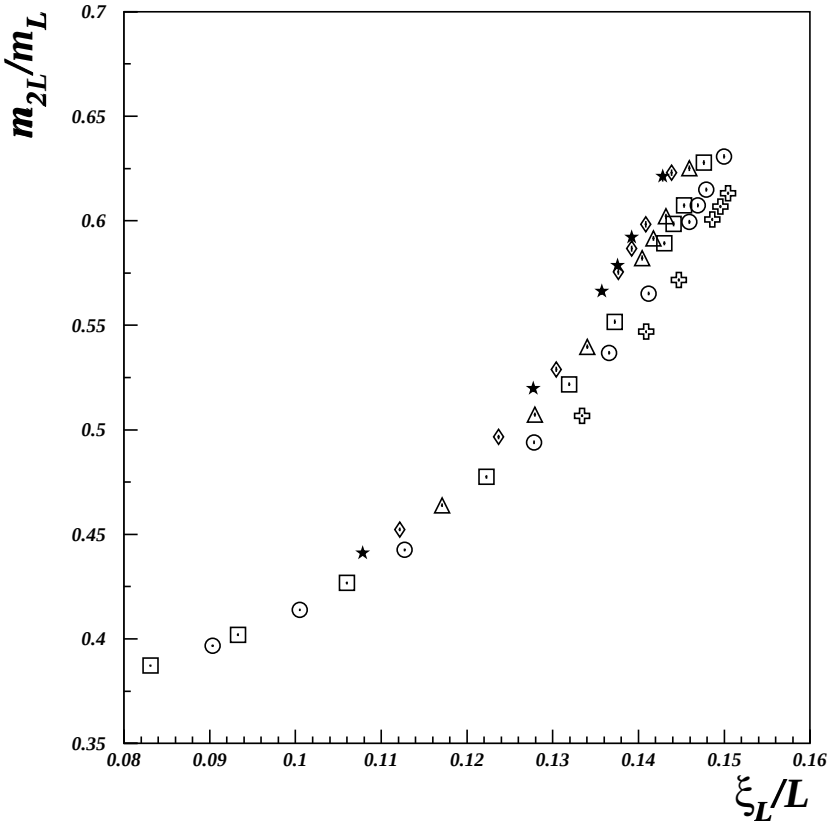

Figure 5.12: FSS plot for m with S_1 fixed. Marks are as in fig. 5.2.

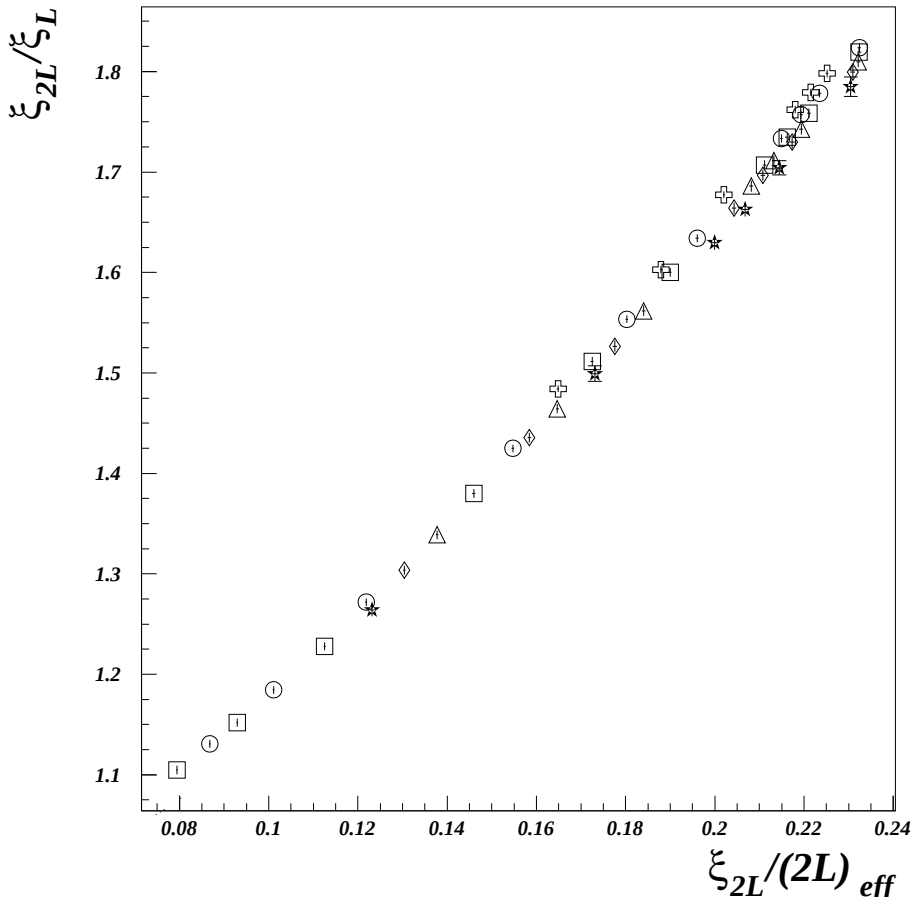

Figure 5.13: FSS plot for ξ with S_1 fixed . Marks are as in fig. 5.2. Here $L_{\rm eff} = L_\perp^{a_\xi}$ ($a_\xi = 0.847$). The data collapse is remarkable.

on the FSS behavior. We want to stress again that the FSS functions obtained from numerical data referring to lattices with S_2 kept constant agree fairly well with the theory *without* any parameter tuning. This give strong evidences that the correct scaling limit is that obtained in this way. The prediction of ν, γ and β are consistent with the mean-field behavior of the transverse correlations as predicted by the standard field-theoretical approach described in Chap. 3.

It is important to notice that in all these analyses we have not found any evidence of the presence of logarithmic corrections. As it has been observed in previous studies [53], if they are really there, they are quite small.

Our result for the Binder's parameter g seems to be not in agreement with that of Refs. [52,53] where it was found $g \neq 0$ at criticality, but confirms the results of Wang [54] that could not find a satisfactory collapse for the Binder's parameter. He traced back this fact to possible correction to FSS and effects due to the interfaces [54]. Our result $g = 0$ is compatible with the idea that in the scaling limit transverse correlations (both in infinite volume and in the finite-size scaling regime) are Gaussian, so that $g = 0$ at criticality.

We mention that it is also possible that g decreases as a power of $\log L$ because of the marginal operator, but that, in our range of values of L, the complicated logarithmic dependence is mimicked by a single power. Note that, if $g_\infty(\beta_c) = 0$, the Binder's parameter cannot be used to compute β_c: The crossing method should not work. We refer for further comments and discussions on this point, to Ref. [71].

An analysis of the data taken from geometries with S_1 constant is under consideration in order to understand the nature of the discrepancy between the recent claims made in the literature [72] and our results [71].

Chapter 6

DLG: Conclusions

In this Chapter we summarize our results and the main perspectives of the work described in the previous Chapters.

6.1 Results

Following the ongoing discussion on the field-theoretical approach to the DLG phase transition (briefly reviewed in Section 3.3), we pointed out some troubles in the field theory proposed in Ref. [62], particularly evident when trying to study the theory in finite volume (in order to determine analytically the FSS functions).

To clarify some aspects of the FSS in the DLG we studied a simple exactly solvable equilibrium model. We investigate possible definitions of finite-volume correlation length, taking into account peculiarities due to the absence of the zero mode (as it is the case of the Lattice Gas) [109].

Then, by a heuristic extension of these findings, we defined a suitable correlation length also for the DLG.

By using it, it was possible to apply the FSS analysis of Ref. [90] to the numerical data from the MC simulations of the DLG, for the first time in non-equilibrium phase transition.

Results of the anisotropic FSS analysis seem to confirm the standard picture of this phase transition, even though some aspects require further investigations, see Section 5.4.

6.2 Perspectives

As we said, a new challenge is issued by Refs. [72, 77]. There are several things to understand:

- Are scaling plots in Ref. [72] affected by a shape crossover as pointed out in Refs. [52, 53] for data in Ref. [60]? If this is the case, why there is such a surprising overlap with FSS functions for RDLG?
- If numerical result of Ref. [72] are not affected by such an effect and their claims are correct, why our results do not agree with theirs? Are they affected by correction to FSS? We have to say, to this respect, that lattice sizes employed in Ref. [72] (from 20×20 to 125×50) are comparable with ours (from 32×16 to 512×40).
- If, eventually, the standard picture of DLG is not right, what we can say about the field theoretical approach to the DLG phase transition? And if the criticisms in Refs. [61, 64, 66, 72] are correct, why does their proposed alternative field theory work?

- Are standard methods to detect FSS sufficiently robust also in the case of non-equilibrium phase transitions?
- The dangerous irrelevant operator neglected so far is really negligible in two dimensions?
- What is going on in the striking short-time dynamic MC results of Ref. [77]?

Answers to these questions in the simplest case of the DLG may be quite relevant to the whole field of non-equilibrium phase transitions, and to their theoretical understanding.

DLG Generalizations

Studying some of the many generalizations of the DLG (for a description see Ref. [35]) would allow us to collect evidences either against or supporting the various arguments proposed. We have to analyze (applying FSS technique described in Section 4.3.2) already collected MC data on the two-temperature model[1] and on the DLG in $d = 3$. The latter case may be especially relevant to determine the influence of the irrelevant coupling onto the two dimensional DLG. We would also get insight into this problem by studying simplified one dimensional models, where it is possible to check some conjectures on general properties of non-equilibrium phase transitions.

[1] It is defined as a lattice gas with Kawasaki dynamics in which Metropolis rates are determined according to the Hamiltonian (2.4), with $J > 0$, but different temperatures $T_\perp$, $T_\parallel$ according to the direction of the proposed particle-hole exchange, see Refs. [21, 35, 41–43].

Chapter 7

Aging

In this Chapter we briefly introduce the phenomenology of aging phenomena as observed in the dynamics of various physical systems, in particular spin glasses and other disordered models (systems with slow dynamics). Then, in §7.2 we focus our attention on aging in the case of unfrustrated, non-disordered systems, reviewing some results on the (low-temperature) coarsening dynamics, in §7.2.1, and on the (high-temperature) relaxation from an initial state in §7.2.2. Then, in §7.2.3, we introduce the fluctuation-dissipation ratio which will be our main concern in Chapters 8–9. We discuss, in §7.2.4 some general properties of non-equilibrium critical dynamics, reviewing also some analytical results available on the Spherical Model. The importance of a field-theoretical approach to determine the universal aspects of aging behavior is also stressed in §7.2.5.

7.1 Aging Phenomena

Complex systems such as glasses, spin glasses and, more generally, disordered systems with quenched disorder show very interesting dynamical behaviors depending on temperature and time-scale ranges. After some successes in describing the putative equilibrium state of such systems, much more attention has been paid to their dynamics. Recent reviews of progresses in this direction are listed in Ref. [111]. One of the most striking dynamical behavior is that of *aging* (observed for the first time in amorphous polymers, see the early account in Ref. [112]), characterized by the fact that physical properties of the system depend on its thermal history. Many different aging systems have been studied both numerically and experimentally, and these evidences have called for a theoretical investigation of the phenomenon.

Aging is mainly due to the fact that the system, say, for example, a spin glass at low temperature, does not reach thermal equilibrium even after a "macroscopic" time has elapsed since the last perturbation on the system. In real experiments (see, e.g. Ref. [117]) and numerical simulations (references can be found in Ref. [111]) it is possible to observe this kind of behavior by looking at the slow time dependence of the properties of the system under study. For example consider a spin-glass sample at high temperature and quench it rapidly to a temperature T below the glassy transition, so that T is reached at time $t = 0$. Then apply a weak oscillating external field of a given frequency ω, and measure the susceptibility χ of the sample. As a consequence of aging, we observe a slow continuous decrease of the amplitude of χ as a function of the time t elapsed since the sample has reached the final temperature T. Thus $\chi = \chi(\omega, t)$, i.e. the response of the system to a perturbation depends on its thermal history. For many spin glasses the shape of $\chi(\omega, t)$ may

be well approximated as (see Ref. [111] and references therein)

$$\chi(\omega,t) = A(\omega t)^{-b} + \chi_{ST}(\omega) \ , \tag{7.1}$$

at least when $\omega t \gg 1$. A is a temperature-dependent amplitude and b takes usually value in the range $0.1 - -0.4$. The parameterization (7.1) shows that there are two distinct contributions: One is the stationary part of the response $\chi_{ST}(\omega)$ which is independent of the waiting time t. The other is not stationary, and indeed it depends on t, the age of the system. Moreover it is a function of the scaling variable ωt. Generally, in a system with a finite relaxation time t_R, the susceptibility χ is expected to be a function of ωt_R. Thus, for an aging systems, we can say that the "effective" relaxation time is given by the age of the system itself.

Many quantities and various methods have been introduced to characterize aging behavior, as well as suitable theories to account for it (see, e.g. Ref. [113]), but we would not further discuss this point in the case of disordered systems (we refer to Ref. [111]).

7.2 Aging in Non-disordered Systems

Although firstly studied in glassy and disordered systems [112], aging phenomena may be observed also in non-disordered ones [118,137].

7.2.1 Coarsening Dynamics

Consider a ferromagnetic model in its high-temperature (disordered) phase, at the initial time $t = 0$, and quench it to a given temperature T. We first discuss briefly the case $T < T_c$, in which the relevant feature of the dynamics is the growth of order through domain coarsening (see Ref. [137] for a comprehensive review). Calling ϕ the order-parameter field, we can study the dynamics of its fluctuations by looking at the two-point correlation function $C_{\mathbf{x}}(t,s) = \langle \phi_{\mathbf{x}}(t)\phi_{\mathbf{0}}(s)\rangle$, where $\langle\cdot\rangle$ stands for the mean over the stochastic dynamics. Of course, the presence of an initial condition for the dynamics causes a breaking of the time-translational invariance of the systems, i.e. we expect that $C_{\mathbf{x}}(s+\tau,s)$ (with $\tau = t - s$, assumed to be > 0 in the following) differs from $C_{\mathbf{x}}(\tau,0)$. This translates into the fact that the Fourier transform of this function depends on both ω and s, as observed in typical experiments (see the discussion at the end of Sect. 7.1).

Consider, now, the simpler case of an Ising ferromagnet[1]. In that case we expect that after the quench, domains of positive and negative magnetization start coarsening. The typical domain size $\ell(s)$ at time s after the quench, is expected to grow as a power law (or even slower when impurities are present). Equilibrium[2] is reached after a relaxation time t_R such that $\ell(t_R) \sim L$, where L is the typical size of the sample. As a consequence, for a macroscopic sample (or in the thermodynamic limit), the non-equilibrium behavior will persist long enough to be observed on macroscopic time scales. We expect that, in this regime, some aspects of dynamics should be universal, in the sense that they do not depend on the microscopic features of the system, provided they refer to time scales much longer than the typical microscopic ones. In the large N limit, the problem of coarsening dynamics for a non-conserved N-component vector field may be solved exactly [121, 137]. The model displays an aging behavior, as we can see from the form of the correlation function

$$C_{\mathbf{0}}(\tau+s,s) = C_{ST}(\tau) + C_{AG}(\ell(s)/\ell(\tau+s)) \ . \tag{7.2}$$

[1] In the case of more complicated order parameters the coarsening dynamics involves the formation of topological defects as vortex, strings, monopoles, etc. See Sect. 3 of Ref. [137] for a discussion.

[2] We mean, here, equilibrium (and ergodicity) within one ergodic component, in the sense that time averages and ensemble ones may be exchanged only if $t_R < t < t_{ERG}$, where t_{ERG} is the typical time required to reverse the magnetization of the sample, see, e.g. Ref. [113].

The first term describes the spin correlations inside a domain and it is equal to that in equilibrium, when only one infinite domain is present. The second term, responsible for the aging behavior, is related to the motion of domain walls (see Ref. [111]). We note that the system behavior for $s \to \infty$ may be different depending on whether τ is finite or not. In the former case a stationary non-equilibrium regime is reached, while in the latter, characterized by $\ell(s)/\ell(\tau + s) < 1$, the systems is in the aging or coarsening regime. Moreover we expect

$$\lim_{\tau\to\infty} \lim_{s\to\infty} C_{\mathbf{0}}(\tau + s, s) = M^2 \ , \tag{7.3}$$

where M is the spontaneous magnetization.

7.2.2 High-temperature Relaxation

Our main concern, in the following, will be the case of a quench to a temperature $T \geq T_c$. During the relaxation a small external field h is applied at $\mathbf{x} = 0$ after a waiting time s. At time t the order parameter response to h is given by the response function $R_{\mathbf{x}}(t, s) = \delta\langle\phi_{\mathbf{x}}(t)\rangle/\delta h(s)$, which is nothing but the susceptibility χ measured in experiments. The time evolution of the system may be characterized by two different regimes: A transient behavior with off-equilibrium evolution, for $t < t_R$, and a stationary equilibrium evolution for $t > t_R$, where t_R is the relaxation time. In the former a dependence of the behavior of the system on initial conditions is expected, while in the latter time homogeneity and time-reversal symmetry (at least in the absence of external fields) are recovered; as a consequence we expect that for $t_R \ll s, t$, $R_{\mathbf{x}}(t, s) = R^{eq}_{\mathbf{x}}(t-s)$, $C_{\mathbf{x}}(t, s) = C^{eq}_{\mathbf{x}}(t-s)$ where R^{eq} and C^{eq} are determined by the "equilibrium" dynamics of the system, with a characteristic time scale diverging at the critical point (critical slowing down). Moreover the fluctuation-dissipation theorem (discussed in some detail in Sect. 1.2) implies that

$$R^{eq}_{\mathbf{x}}(\tau) = -\frac{1}{T}\frac{\mathrm{d}C^{eq}_{\mathbf{x}}(\tau)}{\mathrm{d}\tau} \ . \tag{7.4}$$

When the system is not in thermal equilibrium all the previous functions will depend both on s (the "age" of the system) and t.

7.2.3 The Fluctuation-Dissipation Ratio

To characterize the distance from equilibrium of an aging system, evolving at a fixed temperature T, the *fluctuation-dissipation ratio* (FDR) is usually introduced [116]:

$$X_{\mathbf{x}}(t, s) = \frac{T\, R_{\mathbf{x}}(t, s)}{\partial_s C_{\mathbf{x}}(t, s)} \ . \tag{7.5}$$

This ratio is equal to 1 whenever the fluctuation-dissipation theorem applies. On the other hand, if aging takes place, $X_{\mathbf{x}}(t, s)$ is expected to be a non-trivial function of both the time arguments.

For a wide class of systems in their low-temperature phase, ranging from glassy one to ferromagnetic models, it has been found that $X_{\mathbf{0}}$ can be expressed as a function of $C_{\mathbf{0}}(t, s)$, i.e.

$$X_{\mathbf{0}}(t, s) = X(C_{\mathbf{0}}(t, s)) \ , \tag{7.6}$$

for $1 \ll s \sim t$. Many attention has been recently paid to the function X defined above, given it has been proved to provide very useful links between static equilibrium properties and non-equilibrium dynamics [34]. Moreover, by using X, one can distinguishes three main types of low-temperature behaviors (see Ref. [115] for a summary). When domain growth takes place, $X(C)$ is discontinuous in C, taking a first value equals to 1, in the non-equilibrium stationary regime discussed above, and

a second one equals to 0. For spin glass models with p-spin interactions $X(C)$ is discontinuous as in the previous case, but the second value it takes is different from 0. For continuous spin glass model, instead, $X(C)$ is non-trivial.

In recent years, several works [34, 111, 114, 118–120, 123] have been devoted to the study of the FDR for systems exhibiting domain growth (see Sect. 7.2.1), and for aging systems, showing, as expected, that in the low-temperature phase $X(t,s)$ turns out to be a non-trivial function of its two arguments. In particular analytical and numerical studies indicate that the limit

$$X^{\infty}_{\mathbf{x}=0} = \lim_{s\to\infty}\lim_{t\to\infty} X_{\mathbf{x}=0}(t,s), \tag{7.7}$$

vanishes throughout the low-temperature phase both for glasses and simple ferromagnetic systems [114, 119].

Only recently [118, 122, 124–127] attention has been paid to the FDR, for non-equilibrium, non-disordered, and unfrustrated systems at criticality. It has been argued that the FDR (7.7) is a novel universal quantity of non-equilibrium critical dynamics (see Sect. 9.1).

The value of $X^{\infty}_{\mathbf{x}=0}$ has been determined for the models reported in Tab. 7.1. In all cases it has values ranging between 0 and $\frac{1}{2}$ while for some urn models a different range has been found [131].

Model		$T < T_c$	$T = T_c$	$T > T_c$
Random Walk[a]	[118]	—	1/2	—
Free Gaussian Field[a]	[118]	—	1/2	1
d-dim. Spherical Model[a]	[125]	0	$(d-2)/d^{\dagger}$	1
Ising–Glauber Chain[a]	[122]	—	1/2	1
2-dim. Ising Model[b]	[125]		0.26(1)	
3-dim. Ising Model[b]	[125]		0.40	

Table 7.1: X^{∞} for some models. [a] Exact solution, [b] Monte Carlo simulations. † $2 < d < 4$.

7.2.4 Non-equilibrium Critical Dynamics and the FDR

Let us consider, in more detail, non-equilibrium critical dynamics of a spin system in d dimensions (see Ref. [127] for a recent summary), quenched from $T = \infty$ down to T_c at time $t = 0$[3]. Soon after the quench, correlations start growing in the system, just as in equilibrium critical state, but they develop only over a length scale ℓ_c growing in time as

$$\ell_c(t) \sim t^{1/z} , \tag{7.8}$$

where z is the dynamic critical exponent. On length scales smaller than ℓ_c the system is effectively critical, while for length scales much bigger than ℓ_c it is still disordered. This behavior is encoded in the scaling form for the equal-time correlation function [127]

$$C_{\mathbf{x}}(t,t) \sim |\mathbf{x}|^{-2\beta/\nu} f(|\mathbf{x}|/\ell_c(t)) , \tag{7.9}$$

where $f(v)$ is a constant for $v = 0$ and rapidly decreases for $v \to \infty$. β and ν are the usual static critical exponents. Given that $2\beta/\nu = d - 2 + \eta$, in the limit $t \to \infty$ and $\mathbf{x}$ fixed, we recover the standard behavior of correlations in the critical state. As far as the two-time autocorrelation

[3] A rigorous discussion of aging behavior of one-dimensional q-state Potts model, quenched from $T = \infty$ down to $T = 0$ has been done in Ref. [128].

function $C_{\mathbf{0}}(s+\tau,s)$ (we assume $\tau > 0$) is concerned we should distinguish various regimes, as already discussed in the case of the low-temperature phase (see Sect. 7.2.3). For $s \gg \tau \gg 1$ the system reaches the stationary equilibrium state, and thus fluctuation-dissipation theorem applies. The scaling regime, instead, is reached when $\tau \sim s \gg 1$, and correlations scale according to

$$C_{\mathbf{0}}(t,s) \sim s^{-b} f_C(t/s) \,, \tag{7.10}$$

where $b = 2\beta/\nu z$. When $x = t/s \to \infty$, $f_C(x)$ is expected to behave as

$$f_C(x) \sim A_C x^{-\lambda_c/z} \,, \tag{7.11}$$

where λ_c is the autocorrelation exponent [139]. It is related to the initial-slip exponent θ' of the magnetization (see Chapter 8) by the relation

$$\lambda_c = d - z\theta' \,. \tag{7.12}$$

In the same regime, the response function behaves as

$$R_{\mathbf{0}}(t,s) \sim s^{-1-b} f_R(t/s) \,, \tag{7.13}$$

with $f_R(x) \sim A_R x^{-\lambda_c/z}$, for $x \gg 1$. All the scaling behaviors presented above may be deduce from a renormalization-group analysis, as discussed in Sect. 8.3. So far we can consider them as phenomenological scalings. From Eq. (7.10) we deduce the scaling function for $\partial_s C_{\mathbf{0}}(t,s)$, i.e.

$$\partial_s C_{\mathbf{0}}(t,s) \sim s^{-1-b} f_{C'}(t/s) \,, \tag{7.14}$$

where $f_{C'}$ may be easily derived from f_C, Eq. (7.10). In particular we expect $f_{C'}(x) \sim (\lambda_c/z - b) A_C x^{-\lambda_c/z}$. We can compute the fluctuation-dissipation ratio

$$X_{\mathbf{0}}(t,s) = T_C \frac{f_R(t/s)}{f_{C'}(t/s)} \,, \tag{7.15}$$

which is, as expected in the aging regime, a function of t/s only. Its long-time limit is

$$X^{\infty} = \lim_{s\to\infty} \lim_{t\to\infty} X_{\mathbf{0}}(t,s) = \lim_{x\to\infty} T_c \frac{f_R(x)}{f_{C'}(x)} = T_c \frac{A_R}{(\lambda_c/z - b) A_C} \,. \tag{7.16}$$

To give a concrete example of the scaling relations introduced so far, let us consider in more detail the results for the Spherical Model (see Ref. [125]). Consider a d-dimensional lattice Λ_N with N sites, labeled by $\mathbf{x} \in \Lambda_N$. A continuous variable $\sigma_{\mathbf{x}}$ is assigned to each site in such a way that the constraint

$$\sum_{\mathbf{x}\in\Lambda_N} \sigma_{\mathbf{x}}^2 = N \,, \tag{7.17}$$

is fulfilled. In the configuration space $\mathbb{S}^{N-1}$, the Hamiltonian of the model in the presence of an external field $H_{\mathbf{x}}$ is given by

$$\mathcal{H}[\{\sigma\};\{H\}] = -\sum_{\langle \mathbf{x},\mathbf{y}\rangle\in\Lambda_N} \sigma_{\mathbf{x}}\sigma_{\mathbf{y}} - \sum_{\mathbf{x}\in\Lambda_N} H_{\mathbf{x}}\sigma_{\mathbf{x}} \,, \tag{7.18}$$

where the first sum is extended only to nearest-neighbor sites. A possible dynamics for this model is given by the following Langevin equation for the time evolution of configurations

$$\frac{\mathrm{d}\sigma_{\mathbf{x}}}{\mathrm{d}t} = -\frac{\delta\mathcal{H}}{\delta\sigma_{\mathbf{x}}} - \lambda(t)\sigma_{\mathbf{x}} + \eta_{\mathbf{x}}(t) \,, \tag{7.19}$$

where $\lambda(t)$ is a Lagrange multiplier used to enforce the constraint, while $\eta_{\mathbf{x}}(t)$ is a Gaussian noise with correlations

$$\langle \eta_{\mathbf{x}}(t)\eta_{\mathbf{y}}(t')\rangle = \delta_{\mathbf{x},\mathbf{y}}\delta(t-t') \; . \tag{7.20}$$

Equation (7.19) is used to compute exactly [125], in the large-N limit, the evolution of the field $\sigma_{\mathbf{x}}(t)$ starting from a completely disordered and homogeneous initial state with

$$C_{\mathbf{x}}(0,0) = \delta_{\mathbf{x},\mathbf{0}} \; , \tag{7.21}$$

i.e. characterized by the absence of correlations.

The two-time correlation function reads [125]

$$C_{\mathbf{0}}(t,s) \sim s^{-(d/2-1)} f_C(t/s) \; , \tag{7.22}$$

where [125]

$$f_C(x) = \begin{cases} T_c \dfrac{4(4\pi)^{-d/2}}{d-2} \dfrac{x^{1-d/4}(x-1)^{1-d/2}}{x+1} & 2 < d < 4 \; , \\ T_c \dfrac{2(4\pi)^{-d/2}}{d-2} [(x-1)^{1-d/2} - (x+1)^{1-d/2}] & d > 4 \; , \end{cases} \tag{7.23}$$

given that for this model $z = 2$, we can determine from the expected asymptotic behavior Eq. (7.11) above, the value of the exponent λ_c

$$\lambda_c = \begin{cases} 3d/2 - 2 & 2 < d < 4 \; , \\ d & d > 4 \; . \end{cases} \tag{7.24}$$

For the response function, instead,

$$R_{\mathbf{0}}(t,s) \sim s^{-d/2} f_R(t/s) \; , \tag{7.25}$$

where

$$f_R(x) = \begin{cases} (4\pi)^{-d/2} x^{1-d/4}(x-1)^{-d/2} & 2 < d < 4 \; , \\ (4\pi)^{-d/2}(x-1)^{-d/2} & d > 4 \; , \end{cases} \tag{7.26}$$

in agreement with the expected scaling form of $f_R(x)$ for $x \gg 1$ and the value of λ_c in Eq. (7.24).

The computation of X^{∞} for this model is straightforward, leading to

$$X^{\infty} = \begin{cases} 1 - 2/d & 2 < d < 4 \; , \\ 1/2 & d > 4 \; . \end{cases} \tag{7.27}$$

Scaling laws introduced in Eqs. (7.10) and (7.13) may be also numerically tested by means of Monte Carlo simulations. As an example, we report in Fig. 7.1 the results presented in Ref. [125] for the critical autocorrelation function $C_{\mathbf{0}}(t,s)$ of the two-dimensional Ising model, quenched at criticality from a completely disordered initial state. The very good collapse of data taken at fixed s by varying t, rescaled with $s^{2\beta/\nu z}$ and plotted against t/s, is a clear indication that the scaling form Eq. (7.10) holds.

A similar plot may be done for the integrated response (which is easier to be measured in numerical simulations than the response function), defined as the system response, at time t, to a constant and homogeneous field applied during the time interval $[0,s]$ with $s < t$, i.e.

$$\rho_{\mathbf{0}}(t,s) = T_c \int_0^s \mathrm{d}s' R_{\mathbf{0}}(t,s') \; . \tag{7.28}$$

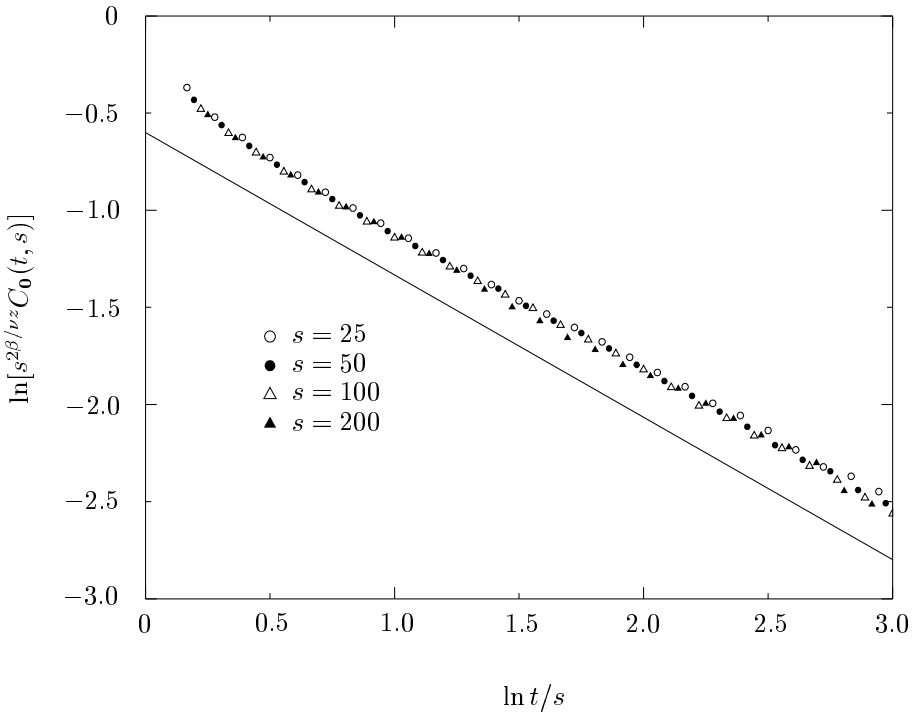

Figure 7.1: Plot of the critical autocorrelation function $C_{\mathbf{0}}(t,s)$ for the two-dimensional Ising model. Data are multiplied by $s^{2\beta/\nu z}$, in order to check the collapse into the scaling function $f_C(t/s)$, according to Eq. (7.10). The straight line has a slope ~ -0.73 and gives a numerical estimate for the exponent of the fall-off of $f_C(t/s)$ for large t/s, i.e. $-\lambda/z$. From Ref. [125].

From the scaling functions Eqs. (7.10), (7.13) and the expression Eq. (7.16) for X^∞, it is easy to see that

$$\rho_{\mathbf{0}}(t,s) \sim X^\infty C_{\mathbf{0}}(t,s) \quad \text{for} \quad 1 \ll s \ll t \,, \tag{7.29}$$

and thus X^∞ can be determined once the scaling plots for $C_{\mathbf{0}}(t,s)$ and $\rho_{\mathbf{0}}(t,s)$ have been measured. For an example of this way of measuring X^∞ we refer to Ref. [125].

7.2.5 FDR from Field-theoretical Models

It is easy to see, by looking at the contents of the works whose results are listed in Tab. 7.1, and by an inspection of the available literature, that only exact solutions have been analytically determined, so far, for the FDR.

Exactly solvable models are very useful because they can be analyzed without relying on any approximation scheme that, in some cases, could hide physical (e.g. non-perturbative) phenomena. On the other hand they constitute a small subset of the whole set of physically relevant models, and the specific solution method is generally not extendible to systems which, in some sense, are "close" to the exactly solvable one. For example, as far as the FDR is concerned, it is not a priori obvious to what extent we can trust the value found for the Spherical Model in $d = 3$ as an estimate for FDR of the three dimensional Ising model. Or it is very difficult to understand, from exact solutions, which would be the effect of small changes in the model as, e.g., the coupling to another field or the introduction of conservation laws in the dynamics.

As we discussed in Sect. 7.2, there should be some universal aspect in the non-equilibrium dynamics. In particular we expect, as we will discuss in more detail in Section 9.1, that $X(t,s)$ is a universal function associated with a given non-equilibrium dynamics. As such it should be possible, at least in principle, to compute it for those mesoscopic models of dynamics which have the same critical behavior of the lattice models that have been considered, so far, in the literature. For example X^{∞}, being universal, should attract the same interest as the critical exponents do. Once a suitable mesoscopic model of dynamics (usually in the form of a Langevin equation) has been singled out, it is possible to deal with the problem of the critical relaxation from an initial disordered state, by using field-theoretical methods. This allows also the use of well-known techniques to compute universal quantities and give estimates for them.

Chapter 8

Time Homogeneity Breaking

In this Chapter we discuss the field-theoretical approach to the critical non-equilibrium dynamics following a quench or, in general, to a relaxation from a given initial state. In both cases there is a breaking of time homogeneity which has remarkable effects on the critical dynamics, such as the emergence of aging behavior. The approach discussed here plays a central role in the perturbative determination of the scaling functions in the aging regime and of the fluctuation-dissipation ratio (which will be the subject of Section 9). We summarize briefly the contents of the seminal work by Janssen, Schaub, and Schmittmann [140], following Ref. [141]. In particular, in §8.1 we describe the basic step that allows one to analyze the Langevin equations (describing the dynamics of the system) within a field-theoretical approach. From this point of view we discuss briefly in §8.2 how to deal with critical dynamics and relaxation processes. In §8.3 we review the renormalization-group (RG) analysis of the field theory introduced to describe dynamics. Finally we introduce briefly the ideas underlying the recently proposed local scale invariance (LSI). It amounts to a requirement of covariance under a suitably constructed group of transformations, and allows one to obtain analytic informations on dynamical scaling forms in the aging regime, which go, in some cases, beyond those provided by RG analysis.

8.1 Path-Integral Representation of Dynamics

In Section 3.1 we described briefly the ideas underlying a field-theoretical approach to (non-equilibrium) critical phenomena. We would spend here some more words on this problem. A statistical model is usually defined on a lattice with spacing a, which in some sense is related to "real" lattices of, say, a condensed-matter system. If the model undergoes a second-order phase transition (when its parameters are suitably tuned), then the physically relevant length scales are essentially two (we are considering an infinite system). One, a, is of microscopic nature, while the other, ξ is a consequence of the emerging collective behavior and diverges at criticality. If we are interested in the long-time, large-distance behaviors we expect that only the length ξ matters. Thus when μ^{-1}, the typical length scale of interest, is $\mu^{-1} \gg a$ and $\xi \gg a$, we expect that an effective "mesoscopic" description of the lattice model could be given on the continuum in terms of fields. These ones are usually associated with the order parameter and conserved densities, and generally with "slow" variables of the system. Moreover, we expect that "microscopic" quantities, defining the system on the lattice, should not affect the long-time, large-distance behavior in a crucial way and thus do not significantly change the "mesoscopic" description. The resulting field-theoretical

model is plagued by divergences in the limit $\mu a \to 0$, but they can be removed by a suitable renormalization of the bare parameters. The existence of this limit in well-specified cases is itself a central result of the renormalization theory and important consequences follow. For example the renormalization-group equations may be viewed as the statement of the independence of the bare theory from the length scale μ^{-1}, characterizing the effective description.

The field-theoretical approach to dynamical critical phenomena relies on a path-integral description of stochastic processes. The microscopic dynamics of the model is specified, as discussed in Section 2.1 for the lattice gas, in terms of a Master Equation with assigned transition probabilities. Approaching a critical point the typical time scale of dynamics diverges as $\sim \xi^z$, and thus also dynamics could be described at "mesoscopic" level. This description is usually done in term of a first-order (in the time variable) stochastic differential equation of the Langevin type, for the slow variables. The effects of the microscopic dynamics is summed up in the functional form of the equation and in the stochastic noise (usually assumed Gaussian), playing the role of a random force acting on the system and summing to the deterministic force. We briefly recall the basic steps which allow a construction of a path-integral representation for a dynamical process. All details can be found in the literature [4,14,141]. Consider, for example, the following equation for the field φ

$$\partial_t \varphi(\mathbf{x},t) = \mathcal{F}[\varphi(\mathbf{x},t)] + \zeta(\mathbf{x},t) \ , \tag{8.1}$$

where $\mathcal{F}[\varphi(\mathbf{x},t)]$ is a local functional of $\varphi(\mathbf{x},t)$, $\zeta(\mathbf{x},t)$ is a zero-mean Gaussian noise with correlation

$$\langle \zeta(\mathbf{x},t)\zeta(\mathbf{x}',t')\rangle = \mathcal{N}(\varphi(\mathbf{x},t))\delta(t-t')\delta(\mathbf{x}-\mathbf{x}') \ , \tag{8.2}$$

and $\mathcal{N}$ a local functional depending on the field. This equation may be viewed as the continuum limit of a Markov process defined on the fields $\varphi_k(\mathbf{x}) = \varphi(\mathbf{x},t_k)$, at given discretized times t_k, $k = 0,1,\ldots$, with Gaussian transition probabilities (see Ref. [141] for details). We remark that different discretizations of Eq. (8.1) are possible and they give rise to an ambiguity in the path integral we are going to derive (see Refs. [16,141] for details and the footnote 2 below). Given an initial condition $\varphi(\mathbf{x},t_0)$, we would compute the mean of a generic observable $\mathcal{O}$ over all possible realizations of the noise ζ. Of course this mean may be written as

$$\langle \mathcal{O} \rangle = \int [\mathrm{d}\varphi]\, \mathcal{O} \left\{ \int [\mathrm{d}\zeta] \delta(\varphi - \varphi_\zeta) P[\zeta] \right\} \ , \tag{8.3}$$

where $P[\zeta]$ is the functional Gaussian probability distribution function for the noise and φ_ζ is the solution of Eq. (8.1) for a given realization of the noise, with the specified $\varphi(\mathbf{x},t_0)$ as initial condition. Taking into account that

$$\delta(\varphi - \varphi_\zeta) = \delta(\partial_t \varphi - \mathcal{F}[\varphi] - \zeta) \det \left[\partial_t - \frac{\delta \mathcal{F}}{\delta \varphi} \right] \ , \tag{8.4}$$

it is possible to express the functional δ-function as an exponential by introducing a complex auxiliary field $\tilde{\varphi}$. Then the average over the Gaussian noise is straightforward and leads to

$$\langle \mathcal{O} \rangle = \int [\mathrm{d}\varphi \mathrm{d}\tilde{\varphi}]\, \mathcal{O}\, e^{-\mathcal{J}_{t_0}[\varphi,\tilde{\varphi}]} \ , \tag{8.5}$$

where

$$\mathcal{J}_{t_0}[\varphi,\tilde{\varphi}] = \int_{t_0}^{\infty} \mathrm{d}t \int \mathrm{d}^d x \left\{ \tilde{\varphi}[\partial_t \varphi - \mathcal{F}[\varphi]] - \frac{1}{2}\mathcal{N}(\varphi)\tilde{\varphi}^2 \right\} \ . \tag{8.6}$$

The functional $\mathcal{J}_{t_0}[\varphi, \tilde{\varphi}]$ is termed dynamic functional and it is the starting point for the field-theoretical approach to dynamics. We remark that in Eq. (8.6) the term corresponding to the determinant in Eq. (8.4) is missing. This does not change the perturbative expansion, provided that one assumes $\theta(0) = 0$[1], where $\theta(t)$ is the Heaviside step function[2]. In Chap. 1 we introduced the ideas of detailed balance and fluctuation-dissipation theorem for equilibrium systems. In particular we saw that to get a stationary state with the expected probability measure (proper to the specified Hamiltonian) from the dynamics described by a Langevin equation as Eq. (1.5) the condition $\mathbb{N} \propto \mathbb{D}$ (see the definitions in Chap. 1) has to be satisfied. How does this translate for the dynamical functional (8.6)? First of all we note that for the Langevin equation (8.1) to represent the continuum version of a Markov process, the functional $\mathcal{F}$ should be local in time (so that the evolution at time t does not depend on the preceding evolution). Let us assume that we can write $\mathcal{F}$ as

$$\mathcal{F}[\varphi(\mathbf{x}, t)] = \mathcal{D}(\varphi(\mathbf{x}, t)) \frac{\delta \mathcal{M}}{\delta \varphi(\mathbf{x}, t)} \tag{8.7}$$

where $\mathcal{D}$ is a local functional depending on φ and $\mathcal{M}$ is another functional. In a sense we are assuming that $\mathcal{F}$ is obtained from some kind of Hamiltonian $\mathcal{M}$, with a diffusion operator given by $\mathcal{D}$. To have time-reversal symmetry and thus a convergence towards an equilibrium measure, it is possible to see that the condition $\mathcal{D} \propto \mathcal{N}$ has to be fulfilled (see Refs. [4, 14, 15]) which is the analogous of the condition mentioned above. Causality is another crucial issue when dealing with Langevin equations. In fact they could have also non-causal solutions, which should be discarded when discussing physical processes. From the field-theoretical point of view the most remarkable result is that, once causality has been imposed (by suitable initial condition on the field $\tilde{\varphi}$, see Sect. 8.3) at the tree level, it is preserved when the effects of fluctuations are taken into account [4, 14, 15].

The functional $\mathcal{J}_{t_0}[\varphi, \tilde{\varphi}]$ may now be analyzed by field-theoretical methods [4, 14, 141]. Once the renormalizability by power counting has been verified, the renormalizations may be computed by standard methods. Moreover, as said in the previous Section, the existence of a well-defined renormalized theory allows one to derive the RG equations. Their scaling solutions show a universal behavior at the infrared (IR) stable fixed point and the universal quantities may be computed by means of the renormalized perturbation theory (see, e.g., Ref. [4]).

8.2 Critical Dynamics and Relaxation Processes

As we said in the previous Section, the renormalizability allows the computation, by means of the renormalized field theory, of the universal scaling functions. Their validity is, of course, restricted to the range of long times and large distances compared to the microscopic ones. We would briefly describe the relaxation process from a prepared initial condition. Shortly after the relaxation process has started, dynamics is governed by microscopic parameters and thus, it has no universal character. This microscopic initial-slip dynamics may be described only in terms of a microscopic theory (and thus a mesoscopic description of the phenomenon can not be done). It has been pointed out [140, 141], however, that a new universal behavior may be identified in the intermediate stage of relaxation, which eventually crosses to the expected long-time behavior. This early stage of

[1] From the diagrammatic point of view this means that self-loops of the response propagator have to be neglected in the perturbative expansion [15].

[2] This correspond to the Îto prescription in the stochastic calculus. This arbitrariness is related to the possible different discretizations of the same stochastic differential equation, as discussed in details in Ref. [141]. The introduction of Grassmann field to take into account the determinant is also possible, and this makes explicit the BRS symmetry of the resulting functional [4].

universal relaxation has been termed "critical initial slip" and has an analogous in the field of surface phase transitions (see the review in Ref. [17]). From a field-theoretical point of view we know that the universal behaviors emerge as a consequence of the RG equations, and thus they are related to the presence of divergences in perturbation theory. Thus we expect that the new critical initial-slip behavior is somehow related to "new" divergences, due to the presence of the "time surface", i.e. the initial condition, in the dynamics. In this sense there is a strong link with the critical behavior of a semi-infinite system near an uncritical surface (for a comprehensive review see Ref. [17]), even though causality plays, here, a central role[3].

For illustration purposes we focus on the behavior of the one-point function, i.e. the mean value of the order parameter (which we will refer to as the magnetization $M(t)$, having in mind ferromagnetic systems). A very simple scaling argument may be used to determine the long-time limit of the relaxation process at criticality (see, e.g., Ref. [138]), leading to

$$M(t) \sim t^{-\beta/\nu z} \ . \tag{8.8}$$

Let us consider in more detail the process in the Ising model, starting from a configuration with $T \gg T_c$. Being in the high-temperature phase, all correlations are short-ranged. We assume that a small initial magnetization M_0 is prepared in this uncorrelated state. When the system is quenched rapidly at its critical point, the correlations start growing, as discussed in Sect. 7.2. We remark that the critical temperature of the corresponding mean-field model T_c^{mf} is higher than the real one, so that, as long as the correlations are small (and thus the mean-field theory applies), the magnetization grows given that the system is in an "effective" low-temperature phase. Once correlations are established on a larger length scale, mean-field theory fails and the magnetization starts decreasing towards a vanishing value, as expected in the long-time limit. For times t larger than the typical microscopic scale the evolution of the magnetization may be written in the following scaling form

$$M(t) = M_0 \, t^{\theta'} \, \mathcal{M}(M_0 t^{\theta'+\beta/\nu z}) \ , \tag{8.9}$$

where θ' is a new exponent, called "initial-slip exponent" of the magnetization [140, 141]. The universal scaling function $\mathcal{M}(x)$ is defined so that $\mathcal{M}(0) \sim 1$ and $\mathcal{M}(x) \sim 1/x$, for $x \to \infty$. It is useful to introduce also the exponent

$$\theta = \theta' - \frac{2 - z - \nu}{z} \ , \tag{8.10}$$

which is related the magnetization one by means of well-known critical exponents. We remark that the emerging of an initial-slip behavior is essentially due to the "mismatch" between the uncritical initial state and the critical dynamics according to which it evolves. When the initial state is also critical we do not expect any crossover. The exponent θ appears also in the scaling form of the autocorrelation function $A(t) = \langle \sigma_{\mathbf{x}}(t) \sigma_{\mathbf{0}}(t) \rangle$ [141] (where $\sigma_{\mathbf{x}}$ is the spin variable of the ferromagnetic system we have in mind) that, at criticality, behaves as $A(t) \sim t^{\theta' - d/z}$. The universal character of the relaxation process in its early stage (on a time scale much bigger than the microscopic one) may be used to determine the critical exponents, without facing critical slowing down, as shown in many (recent) numerical works [150]. We mention also that the effects on the initial-slip behavior of a finite volume have been investigated in Ref. [151], while those of a (spatial) surface have been discussed in Ref. [152].

To study aging dynamics we will focus, in Chapter 9, on two-time quantities whose scaling behaviors depend on θ as well. In Sect. 8.3 we briefly recall how the renormalization of the field

[3] At variance with surface phase transitions [17] there can not be any influence of the bulk on the surface behavior (because of causality).

theory, suitable to describe the relaxation processes, has to be done, establishing also the scaling forms (useful for the discussion in Chapter 9).

8.3 Renormalization and Scaling Forms for Model A

We recall here the basic steps required to determine, in the context of renormalized field theory, the exponent θ introduced in Sect. 8.2. All details may be found in Refs. [140,141]. The simplest model of dynamics displaying the initial-slip behavior is the purely relaxational dynamics (Model A in the classification of Halperin, Hohenberg and Ma, see Ref. [1]) of an N-component field $\varphi(\mathbf{x},t)$, with a Landau-Ginzburg Hamiltonian $\mathcal{H}[\varphi]$. Its static (i.e. time-independent) critical properties describe the behavior of a wide class of lattice spin systems near their critical points [4,10]. The dynamics is specified in terms of the stochastic Langevin equation (of the same form as Eq. (8.1) discussed in Sect. 8.1)

$$\partial_t \varphi(\mathbf{x},t) = -\Omega \frac{\delta \mathcal{H}[\varphi]}{\delta \varphi(\mathbf{x},t)} + \xi(\mathbf{x},t) \ , \tag{8.11}$$

where Ω is the kinetic coefficient, $\xi(\mathbf{x},t)$ a zero-mean stochastic Gaussian noise with correlations

$$\langle \xi_i(\mathbf{x},t)\xi_j(\mathbf{x}',t')\rangle = 2\Omega\, \delta(\mathbf{x}-\mathbf{x}')\delta(t-t')\delta_{ij} \ , \tag{8.12}$$

and $\mathcal{H}[\varphi]$ is the static Hamiltonian. Near the critical point, the leading IR behavior of the system is described by the Landau-Ginzburg Hamiltonian

$$\mathcal{H}[\varphi] = \int \mathrm{d}^d x \left[\frac{1}{2}(\nabla\varphi)^2 + \frac{1}{2} r_0 \varphi^2 + \frac{1}{4!} g_0 \varphi^4 \right] \ , \tag{8.13}$$

where $r_0 \propto T - T_c$ (T_c being the critical temperature of the model[4]).

All dynamical properties may be worked out by representing the Langevin equation (8.11) by a dynamical functional, following the method outlined in Sect. 8.1. The resulting field-theoretical action is [4,14,141]

$$S[\varphi,\tilde{\varphi}] = \int \mathrm{d}t \int \mathrm{d}^d x \left[\tilde{\varphi} \frac{\partial \varphi}{\partial t} + \Omega \tilde{\varphi} \frac{\delta \mathcal{H}[\varphi]}{\delta \varphi} - \tilde{\varphi} \Omega \tilde{\varphi} \right] . \tag{8.14}$$

Here $\tilde{\varphi}(\mathbf{x},t)$ is the auxiliary field. We notice that it has also a physical meaning. Indeed, given an external field h, coupled to the order parameter, we have $\mathcal{H}[\varphi,h] = \mathcal{H}[\varphi] - \int d^d x\, h\, \varphi$. This implies, following Eq. (8.14), that $\tilde{\varphi}$ is conjugated, in $S[\varphi,\tilde{\varphi}]$, to the external field h. As a consequence, the linear response to the field h of a generic observable $\mathcal{O}$ is given by

$$\frac{\delta \langle \mathcal{O} \rangle}{\delta h(\mathbf{x},s)} = \Omega \langle \tilde{\varphi}(\mathbf{x},s) \mathcal{O} \rangle \ , \tag{8.15}$$

for this reason $\tilde{\varphi}(\mathbf{x},t)$ is termed *response field*.

To completely specify the dynamics we should give the initial condition for the field $\varphi(\mathbf{x},t)$, i.e., assuming as the initial time $t_0 = 0$, $\varphi_0(\mathbf{x}) = \varphi(\mathbf{x}, t=0)$. More generally we could give the probability distribution function for the initial condition, and thus average on the initial field $\varphi_0(\mathbf{x})$ with a weight $e^{-\mathcal{H}_0[\varphi_0]}$. If the system is already in thermal equilibrium at time $t = 0$, then

[4] In the following calculations we always use the dimensional regularization and so no additive renormalizations of r_0 are expected.

$\mathcal{H}_0[\varphi_0] = \mathcal{H}[\varphi_0]$ and we can equivalently extend the time integration in $S[\varphi, \tilde{\varphi}]$, from $-\infty$ to ∞. This is possible given that, assuming ergodicity, whatever the initial condition in the far past was, the same stationary order-parameter distribution is reached at time $t = 0$. The resulting theory is translational invariant both in space and time, and given that the condition in Eq. (1.7) (see Sect. 1.2 for the discussion) is fulfilled, equal-time correlation functions could be computed directly using the functional distribution $e^{-\mathcal{H}[\varphi]}$. In this case there is no "surface" effect and divergences appearing in the theory are related, as usual, to the singular behavior of correlators and propagators at small distances and times. In momentum space this amount to ultraviolet (UV) divergences in Feynman diagrams, due to the bad large-momentum large-frequency behavior of integrands. Standard regularization methods could be applied to give meaning to the perturbative expansion, and in the following we will adopt dimensional regularization. By means of a suitable redefinition of bare parameters (renormalization), it is possible (at least for renormalizable theories) to render finite all the correlation functions of fields even in the limit in which, formally, the regulator disappears. This is the standard way to deal with the dynamics in critical phenomena [4, 14, 141].

Let us consider the case in which the initial condition is a non-equilibrium one. As long as $\mathcal{H}_0$ has the same form as $\mathcal{H}$ with different bare couplings, the usual renormalizations are enough to render the theory finite, i.e. no new UV singularities are expected [140, 141]. This is no more true if, for example, the initial state is an uncritical one, for example an high-temperature state with short-range correlations and a small initially prepared magnetization, $\langle \varphi_0(\mathbf{x}) \rangle = a(\mathbf{x})$ and

$$\langle [\varphi_0(\mathbf{x}) - a(\mathbf{x})][\varphi_0(\mathbf{x}') - a(\mathbf{x}')] \rangle = \tau_0^{-1} \delta(\mathbf{x} - \mathbf{x}') \ . \tag{8.16}$$

The corresponding $\mathcal{H}_0[\varphi_0]$ is a Gaussian one

$$\mathcal{H}_0[\varphi_0] = \int \mathrm{d}^d x \, \frac{\tau_0}{2} (\varphi_0(\mathbf{x}) - a(\mathbf{x}))^2 \ . \tag{8.17}$$

Any addition of anharmonic terms in $H_0[\varphi_0]$ is not expected to be relevant as long as the harmonic term is there (as it is the case when the initial state is in the high-temperature phase). Instead, an initial condition with long-range correlations may lead to a different universality class, as recently shown for the d-dimensional Spherical Model with non-conservative dynamics [129]. Following standard methods [4, 14], the response and correlation functions may be obtained by a perturbative expansion of the functional weight $e^{-(S[\varphi,\tilde{\varphi}]+H_0[\varphi_0])}$ in terms of the coupling constant g_0 (appearing in the vertex $g_0 \varphi^3 \tilde{\varphi}/3!$). The propagators (Gaussian two-point functions of the fields φ and $\tilde{\varphi}$) of the resulting theory can be found by looking at the quadratic part of $S[\varphi, \tilde{\varphi}] + H_0[\varphi_0]$ [140], which we call $S^{(2)}_{tot}[\varphi, \tilde{\varphi}, \varphi_0]$. A convenient way to determine the inverse of the operator appearing in $S^{(2)}_{tot}$ is to compute the Gaussian integral with sources for both φ and $\tilde{\varphi}$, called ψ and $\tilde{\psi}$ respectively, i.e.

$$Z[\psi, \tilde{\psi}] = \int [\mathrm{d}\varphi \mathrm{d}\tilde{\varphi} \mathrm{d}\varphi_0] e^{-S^{(2)}_{tot}[\varphi,\tilde{\varphi},\varphi_0] - \int \mathrm{d}^d x \mathrm{d}t (\psi\varphi + \tilde{\psi}\tilde{\varphi})} \ . \tag{8.18}$$

To this end we determine the fields φ_m and $\tilde{\varphi}_m$ which minimizes the quadratic form, i.e. solve the equations (transformed in momentum space)

$$\begin{cases} [\partial_t + \Omega(q^2 + r_0)]\varphi_m - 2\Omega\tilde{\varphi}_m + \tilde{\psi} = 0 \ , \\ [-\partial_t + \Omega(q^2 + r_0)]\tilde{\varphi}_m - \tilde{\varphi}_m \delta(t) + \tau_0(\varphi_m - a)\delta(t) + \psi = 0 \ , \end{cases} \tag{8.19}$$

where the second term in the second equation comes from the boundary term in $t = 0$ when integration by parts is performed. The terms on the second line with a $\delta(t)$ could be written in the form of an initial condition,

$$\tilde{\varphi}_m(\mathbf{q}, 0) = \tau_0(\varphi_m(\mathbf{q}, 0) - a(\mathbf{q})) \ , \tag{8.20}$$

for the system

$$\begin{cases} [\partial_t + \Omega(q^2 + r_0)]\varphi_m - 2\Omega\tilde{\varphi}_m + \tilde{\psi} = 0 \ , \\ [-\partial_t + \Omega(q^2 + r_0)]\tilde{\varphi}_m + \psi = 0 \ . \end{cases} \tag{8.21}$$

The second initial condition required to solve this system of first-order differential equations is $\tilde{\varphi}_m(\mathbf{q}, \infty) = 0$, which enforce the causality of the solution selected. Once this has been determined, the functional integral in Eq. (8.18) can be computed

$$Z[\psi, \tilde{\psi}] = Z[0,0] e^{-\int_0^\infty \mathrm{d}t \int \frac{\mathrm{d}^d q}{(2\pi)^d} \frac{1}{2}(\varphi_m \psi + \tilde{\varphi}_m \tilde{\psi})} \ , \tag{8.22}$$

and the part of the exponential which is quadratic in the fields ψ, $\tilde{\psi}$ (remember that φ_m and $\tilde{\varphi}_m$ depend on them) may be written as

$$\tilde{\psi}(\mathbf{q}, s) R_q^0(t, s) \psi(-\mathbf{q}, t) + \frac{1}{2} \psi(\mathbf{q}, s) C_q^0(t, s) \psi(-\mathbf{q}, t) \ . \tag{8.23}$$

Thus, computing the functional derivatives of $Z[\psi, \tilde{\psi}]$ with respect to its arguments one finds [140, 141]

$$\begin{cases} \langle \tilde{\varphi}_i(\mathbf{q}, s) \varphi_j(-\mathbf{q}, t) \rangle_0 = & \delta_{ij} R_q^0(t, s) = & \delta_{ij}\, \theta(t - s) G(t - s) \ , \\ \langle \varphi_i(\mathbf{q}, s) \varphi_j(-\mathbf{q}, t) \rangle_0 = & \delta_{ij} C_q^0(t, s) \ , & \end{cases} \tag{8.24}$$

with

$$C_q^0(t, s) = \frac{1}{q^2 + r_0} \Big[G(|t - s|) + \left(\frac{r_0 + q^2}{\tau_0} - 1 \right) G(t + s) \Big] \ , \tag{8.25}$$

where

$$G(t) = e^{-\Omega(q^2 + r_0)t} . \tag{8.26}$$

The response function in Eq. (8.24) is the same as in equilibrium. Eq. (8.25), instead, reduces to the equilibrium form when both times t and s go to infinity and $\tau = t - s$ is kept fixed. By power counting it is easy to see that τ_0^{-1} is an irrelevant variable, so that to study the leading scaling behavior it is possible to assume $\tau_0^{-1} = 0$, and thus use the Dirichlet correlator

$$C_q^D(t, s) = \frac{1}{q^2 + r_0} \Big[G(|t - s|) - G(t + s) \Big] \ . \tag{8.27}$$

This is characterized by the properties $C_q^D(t, s) = C_q^D(s, t)$, and $C_q^D(t, 0) = 0$. The second term in $C_q^D(t, s)$ ("image" term) gives rise to new divergences in perturbation theory whenever both t and s approach the "time surface" located at 0. As it has been shown in Ref. [17] for the case of surface critical phenomena, it is possible to remove these singularities by counterterms "located" at that time surface. Moreover, naïve power counting gives $t \sim (\Omega \mu^2)^{-1}$ (where μ is the external momentum scale) and thus the degree of divergence of a generic Green function should decrease by 2 for each vanishing time argument. As a consequence the new renormalizations are required only in the case of two-point functions[5]. A detailed analysis shows that only one new renormalization

[5] We remark that if the dynamics is conservative (Model B [1]), then $t \sim (\Omega \mu^2)^{-2}$, thus no new divergences are expected.

constant is sufficient to renormalize both the correlation and the response functions. Thus, if in the case of Model A dynamics without any time surface, the following renormalizations are required, $\varphi \mapsto Z^{1/2}\varphi$, $\tilde{\varphi} \mapsto \tilde{Z}^{1/2}\tilde{\varphi}$, $\Omega \mapsto (Z/\tilde{Z})^{1/2}\Omega$, $g_0 \mapsto G_d^{-1}\mu^{4-d}Z^{-2}Z_g g$ (where $G_d = \Gamma(3-d/2)/(4\pi)^{d/2}$), $r_0 \mapsto Z^{-1}Z_r r$, now we have also to renormalize the field $\tilde{\varphi}_0(\mathbf{x}) = \tilde{\varphi}(\mathbf{x}, t=0)$ according to

$$\tilde{\varphi}_0(\mathbf{x}) \mapsto (Z_0\tilde{Z})^{1/2}\tilde{\varphi}_0(\mathbf{x}), \tag{8.28}$$

where Z_0 is the new renormalization constant.

From the technical point of view, the breaking of time homogeneity makes the renormalization procedure in terms of one-particle irreducible (1PI) correlation functions less straightforward than in standard cases (see Refs. [17, 140, 141]). Thus, usually, the computations are done in terms of connected functions.

We remark that it is easy to realize, by giving a look at the diagrammatic contributions, that the correlation functions with at least one external φ-leg at the time surface, vanish. This is essentially related to the choice of Dirichlet correlators, and a non-vanishing result is found only taking into account τ_0^{-1} [140,141]. In terms of the constants above it is possible to renormalize also the initial magnetization $a(\mathbf{x})$ and τ_0^{-1}. As one can naïvely expect, the renormalization constants are the same as those of Model A, given that the image term in the Dirichlet correlator, being exponentially convergent for large momenta, can not change divergences related to the "time bulk".

The computation of Z_0 is straightforward, and it has been done up to two-loop order by determining the response function [140, 141]. The result is

$$Z_0 = 1 + \frac{N+2}{3}\frac{g}{\epsilon}\left[1 + \left(\frac{N+5}{3\epsilon} + \frac{\ln 4 - 1}{2}\right)g\right] + O(g^3)\,, \tag{8.29}$$

and all the other renormalizations may be found in the literature [4, 14].

The scaling properties of the connected Green functions

$$G^{\tilde{n}_0}_{n,\tilde{n}} = \langle [\varphi]^n [\tilde{\varphi}]^{\tilde{n}} [\tilde{\varphi}_0]^{\tilde{n}_0} \rangle\,, \tag{8.30}$$

may be exploited by using the RG equations. To renormalize $G^{\tilde{n}_0}_{n,\tilde{n}}$ we use the previously introduced Z-factors, obtaining

$$G^{\tilde{n}_0}_{n,\tilde{n}} \mapsto \overset{\circ}{G}{}^{\tilde{n}_0}_{n,\tilde{n}} = Z^{n/2}\tilde{Z}^{\tilde{n}/2}(\tilde{Z}Z_0)^{\tilde{n}_0/2} G^{\tilde{n}_0}_{n,\tilde{n}}\,, \tag{8.31}$$

where on the r.h.s. everything is expressed in terms of renormalized quantities. The RG equations may be derived by exploiting the fact that the bare correlation functions are independent of the momentum scale μ introduced to define the renormalized theory, i.e.

$$\mu\partial_\mu \left.\overset{\circ}{G}{}^{\tilde{n}_0}_{n,\tilde{n}}\right|_0 = 0\,, \tag{8.32}$$

at fixed bare quantities. As usual, Eq. (8.32) may be rewritten introducing the Wilson's functions $\gamma = \mu\partial_\mu \ln Z|_0$, $\tilde{\gamma} = \mu\partial_\mu \ln \tilde{Z}|_0$, $\gamma_0 = \mu\partial_\mu \ln Z_0|_0$, $\beta = \mu\partial_\mu g|_0$, $\kappa = \mu\partial_\mu \ln r|_0$, $\zeta = \mu\partial_\mu \ln \Omega|_0 = (\tilde{\gamma} - \gamma)/2$. This last equality is a consequence of the fluctuation-dissipation theorem, which does not apply to the non-equilibrium dynamics we are discussing, but it still holds for the "bulk" renormalizations required to make the theory finite (as noted before, the "image" term in $C_q^D(t,s)$ does not affect bulk divergences). Thus, apart from γ_0, all the others are the well-known functions for Model A dynamics with equilibrium initial conditions. The long-time large-distance behavior of the model may be derived by determining the scaling solutions of Eq. (8.32) at the stable IR fixed point g^* ($\beta(g^*) = 0$). Taking advantage of the dimensional analysis and solving Eq. (8.32) with the

standard methods of characteristic functions (see, e.g., Ref. [4]), the leading scaling behavior of the correlation functions is easily obtained

$$G^{\tilde{n}_0}_{n,\tilde{n}}(\{\mathbf{x},t\};r) = l^{\delta(n,\tilde{n},\tilde{n}_0)} G^{\tilde{n}_0}_{n,\tilde{n}}(\{l\mathbf{x}, l^z t\}; l^{-1/\nu} r) \ , \tag{8.33}$$

with

$$\delta(n,\tilde{n},\tilde{n}_0) = n\frac{d-2+\eta}{2} + \tilde{n}\frac{d+2+\tilde{\eta}}{2} + \tilde{n}_0\frac{d+2+\tilde{\eta}+\eta_0}{2} \ . \tag{8.34}$$

In terms of the RG functions, the exponents are given by $\eta = \gamma(g^*)$, $\tilde{\eta} = \tilde{\gamma}(g^*)$, $z = 2 + (\tilde{\eta} - \eta)/2$, $\nu^{-1} = 2 - \kappa(g^*)$, and $\eta_0 = \gamma_0(g^*)$. The only new one is η_0, in term of which θ' (introduced in Eq. (8.9)) is given by[6]

$$\theta' = \frac{2 - z - \eta - \eta_0/2}{z} = -\frac{\eta + \tilde{\eta} + \eta_0}{2z} \ , \tag{8.35}$$

whereas $\theta = -\eta_0/(2z)$. It has been computed up to two-loop order in Refs. [140,141] (see footnote 6), for the model we are dealing with

$$\theta = \frac{N+2}{N+8}\left[1 + \frac{6}{N+8}\left(\frac{N+3}{N+8} + \ln 2\right)\epsilon\right]\frac{\epsilon}{4} + O(\epsilon^3) \ . \tag{8.36}$$

Following the same lines as those we have summarized, the analysis has been extended to other models. In particular Model C dynamics has been analyzed in Ref. [142] (see also Sect. 9.3), while the dynamics of an order parameter reversibly coupled to conserved densities, i.e. Models E (usually used to describe planar (anti-)ferromagnets) and G (isotropic antiferromagnets) is studied in Ref. [143]. Model A dynamics at a tricritical point has been investigated in Ref. [144]. The initial-slip behavior of systems belonging to the important class of reaction-diffusion processes (as directed percolation, see Ref. [19]) is analyzed in Ref. [145], while that of growing interfaces is discussed in Ref. [146]. Also models with quench disorder have been studied in this respect. In particular in Refs. [147, 148, 175] the Ising model with uncorrelated quenched disorder (i.e. the random-temperature Landau-Ginzburg model, see also Sect. 9.4) is considered in the case of uncorrelated initial conditions and short-range interactions. This analysis has been extended to the case of the Landau-Ginzburg model with long-range interaction, and quenched disorder with long-range correlations, in Ref. [149].

We observe that (see Eqs. (8.33) and (8.34)) whenever $\tilde{n}_0 = 0$ the exponent θ does not appear explicitly in the scaling forms. On the other hand it is easy to see that when the relaxation of an initial condition is studied, Eq. (8.9) is found (see details in Refs. [140,141]).

Let us look more closely at the scaling form for the two-point critical (i.e. with $r = 0$) correlation function $C_q(t,s)$ and for the response one $R_q(t,s)$, with both times in the "bulk". From Eq. (8.33) and Eq. (8.34) we have

$$\begin{cases} C_q(t,s) &= l^{\eta-2} C_{l^{-1}q}(l^z t, l^z s) \ , \\ R_q(t,s) &= l^{\eta+z-2} R_{l^{-1}q}(l^z t, l^z s) \ . \end{cases} \tag{8.37}$$

These scaling forms, expected also for equilibrium initial conditions, may be rewritten, considering $l = (t-s)^{-1/z}$ $(t > s)$

$$\begin{cases} C_q(t,s) &= (t-s)^{(2-\eta)/z} \tilde{\mathcal{F}}_C(q(t-s)^{1/z}, s/t) \ , \\ R_q(t,s) &= (t-s)^{(2-\eta-z)/z} \tilde{\mathcal{F}}_R(q(t-s)^{1/z}, s/t) \ . \end{cases} \tag{8.38}$$

[6] We are following the notations of Ref. [140]. In Ref. [141] only the exponent $\Theta = \theta'$ is introduced.

We observe that the introduced scaling functions $\tilde{\mathcal{F}}_C$ and $\tilde{\mathcal{F}}_R$ are not expected regular when s approaches the time surface, i.e. when $s \to 0$. We should make the small-s behavior more explicit, since in both functions it is related to the large-t behavior (and fixed s with $q = 0$) that we would investigate to study aging effects. So far we have exploited the scaling forms by studying the RG equations. It is also possible to determine the functional forms of the correlation and response functions when some of their arguments approach exceptional points, by using the *short-distance expansion* (SDE, see for general reference Ref. [4], Cardy in Ref. [5], and Ref. [17] for applications to surface critical phenomena). The starting point is a formal expansion of the fields $\varphi(\mathbf{x}, s)$ and $\tilde{\varphi}(\mathbf{x}, s)$ around $s = 0$. First of all we note that, when inserted into correlation functions with bulk fields, the following relations hold [140, 141] (we are considering the relaxation after a quench from high temperature, so that $a(\mathbf{x}) = 0$, and $\tau_0^{-1} = 0$ to get only the leading behavior)

$$\varphi(\mathbf{x}, 0) = \varphi_0(\mathbf{x}) = 0 \quad \text{and} \quad \partial_s \varphi(\mathbf{x}, s)|_{s=0} \equiv \dot{\varphi}_0(\mathbf{x}) = 2\Omega \tilde{\varphi}_0(\mathbf{x}) \; . \tag{8.39}$$

As a consequence, for small s, we can formally expand the fields as

$$\left\{ \begin{array}{lcl} \varphi(\mathbf{x}, s) & \sim & \phi(s)\tilde{\varphi}_0(\mathbf{x}) + \text{h.o.c.f.} \; , \\ \tilde{\varphi}(\mathbf{x}, s) & \sim & \tilde{\phi}(s)\tilde{\varphi}_0(\mathbf{x}) + \text{h.o.c.f.} \; , \end{array} \right. \tag{8.40}$$

where h.o.c.f stands for higher-order composite fields which could be neglected if one is interested only in the leading contributions. Inserting relations (8.40) into correlation functions and taking into account the scaling behavior Eq. (8.33), one deduces that, at criticality [140, 141],

$$\left\{ \begin{array}{lcl} \phi(s) & = & a_C s^{1-\theta} \; , \\ \tilde{\phi}(s) & = & a_R s^{-\theta} \; , \end{array} \right. \tag{8.41}$$

where a_C and a_R are two (non-vanishing) constants. Thus, for small s, we have

$$\left\{ \begin{array}{lcl} C_q(t, s) & = & \phi(s) \langle \varphi(\mathbf{q}, t) \tilde{\varphi}_0(-\mathbf{q}) \rangle \; , \\ R_q(t, s) & = & \tilde{\phi}(s) \langle \varphi(\mathbf{q}, t) \tilde{\varphi}_0(-\mathbf{q}) \rangle \; . \end{array} \right. \tag{8.42}$$

From Eq. (8.33) the scaling form of $\langle \varphi(\mathbf{q}, t) \tilde{\varphi}_0(-\mathbf{q}) \rangle \equiv G^1_{1,0}(\{\mathbf{q}, t\}; r)$ can be determined, and at criticality one finds

$$G^1_{1,0}(\{\mathbf{q}, t\}; 0) = l^{-\theta z - (2 - z - \eta)} G^1_{1,0}(\{l^{-1}\mathbf{q}, l^z t\}; 0) \; . \tag{8.43}$$

Taking into account the previous three relations, the following conclusion may be drawn

$$\left\{ \begin{array}{lcl} C_q(t, s) & = & a_C t^{(2-\eta)/z} (t/s)^{\theta - 1} f(q t^{1/z}) \; , \\ R_q(t, s) & = & a_R t^{(2 - z - \eta)/z} (t/s)^{\theta} f(q t^{1/z}) \; . \end{array} \right. \tag{8.44}$$

Comparing these forms with Eq. (8.38) we can conclude that

$$\left\{ \begin{array}{lcl} \tilde{\mathcal{F}}_C(x, y) & \sim & a_C y^{-\theta + 1} f(x) \; , \\ \tilde{\mathcal{F}}_R(x, y) & \sim & a_R y^{-\theta} f(x) \; , \end{array} \right. \quad \text{for} \quad y \to 0 \; . \tag{8.45}$$

It is possible to rewrite Eq. (8.38) in terms of scaling functions $\tilde{F}_C(x, y)$ and $\tilde{F}_R(x, y)$ with a good behavior (i.e. non-vanishing and non-singular) for $y \to 0$, i.e.

$$\left\{ \begin{array}{lcl} C_q(t, s) & = & (t - s)^{(2-\eta)/z} (t/s)^{\theta - 1} \tilde{F}_C(q(t - s)^{1/z}, s/t) \; , \\ R_q(t, s) & = & (t - s)^{(2 - \eta - z)/z} (t/s)^{\theta} \tilde{F}_R(q(t - s)^{1/z}, s/t) \; . \end{array} \right. \tag{8.46}$$

Summing up we combined the general critical scaling forms as given by the RG analysis, with their short-time expansion, in such a way to obtain scaling forms suited for investigating the aging effects also in the long-time limit. Indeed Eq. (8.46) tell us, e.g., that for $q = 0$, in the long time limit $t \gg s$, $R_{q=0}(t, s) \sim t^{(2 - \eta - z)/z} (t/s)^{\theta}$. We will discuss the consequences of these scaling forms in Chap. 9.

8.4 Local Scale Invariance

Let us remark that the equilibrium dynamics enjoys some remarkable invariances, i.e. time and space translations and time reversal (some care has to be taken when there are external fields) as already discussed in Sect. 1.1. Although the dynamics in the aging regime does not enjoy these symmetries any more, it is not the most general non-equilibrium one, given it still has properties of "covariance". This amounts to the statement that the evolution of a system of age s is the same as that of a younger one of age, say, $s/2$, up to a suitable rescaling of time. This property is evident from scaling relations Eqs. (7.10), (7.13) and from the explicit results for the Spherical Model Eqs. (7.22), (7.25). Moreover, it clearly emerges in the RG context, as shown by the resulting scaling forms Eq. (8.46), which are covariant under a simultaneous rescaling of the age s of the system, of the time t and momentum q, i.e. under

$$\begin{cases} s & \mapsto & b^z s \,, \\ t & \mapsto & b^z t \,, \\ q & \mapsto & b^{-1} q \,, \end{cases} \tag{8.47}$$

as it is expected at criticality.

Recently much emphasis has been put on this covariance and on its generalization to the case of a space-time dependent rescaling factor [160,164]. The main question is whether it is possible or not to construct a theory of *local scale invariance* (LSI) pretty in the same way as conformal invariance extends critical isotropic scale invariance. Indeed we know that in local field theories scale and rotational covariances imply covariance under the larger group of conformal transformations. To be concrete let us recall briefly the main line along which conformal invariance develops in critical phenomena. Many properties of equilibrium critical phenomena are understood in the context of the RG theory. In particular, exactly at critical point, we expect that the n-point correlation function of scaling operators ψ_i, $G^{(n)}(\mathbf{x}_1, \ldots, \mathbf{x}_n) \equiv \langle \psi_1(\mathbf{x}_1) \cdots \psi_n(\mathbf{x}_n) \rangle$ are covariant under a global, isotropic, scaling transformation of space, given by $\mathbf{x}_i \mapsto b\mathbf{x}_i$, $i = 1, \ldots, n$. Thus

$$G^{(n)}(b\mathbf{x}_1, \ldots, b\mathbf{x}_n) = b^{-(y_1 + \cdots + y_n)} G^{(n)}(\mathbf{x}_1, \ldots, \mathbf{x}_n) \,, \tag{8.48}$$

where y_i is the scaling dimension of the operator ψ_i. Formally, covariance (8.48), may be expressed as $\psi_i(b\mathbf{x}) = b^{-y_i} \psi_i(\mathbf{x})$. Usually ψ_i are composite operators of the order parameter of the system. It is a well-known fact that, at least for systems with sufficiently short-range interactions, the correlation functions $G^{(n)}$ are covariant under a larger group of transformations, i.e. under the conformal group. It is given by the group of all those coordinate transformations which leave the metric invariant up to a space-dependent scale (see, e.g., Ref. [11]). They are locally equivalent to a rotation and a dilatation (i.e. we can say, roughly, that they amounts to $\mathbf{x} \mapsto b(\mathbf{x})\mathbf{x}$), and have the property that the angle formed by two arbitrary curves meeting at some point is unchanged after the transformation. Covariance under this group gives constraint on the functional forms of equilibrium critical correlation functions, in any space dimension. Moreover, in two dimensions the Lie algebra of the conformal group is the infinite-dimensional Virasoro algebra and this fact gives strong restrictions on the scaling dimensions and operators allowed in the theory. Furthermore conformal invariance allows also a classification of the universality classes and of the values of the associated critical exponents.

There are many critical systems which are covariant under an anisotropic scale transformation, in the sense that

$$G^{(n)}(b^\Theta t_1, b\mathbf{x}_1, \ldots, b^\Theta t_n, b\mathbf{x}_n) = b^{-(y_1 + \cdots + y_n)} G^{(n)}(t_1, \mathbf{x}_1, \ldots, t_n, \mathbf{x}_n) \,, \tag{8.49}$$

with $\Theta \neq 1$, where with t_i we mean either the time variable in the case of dynamic critical phenomena (and thus $\Theta = z$, z being the dynamic critical exponent), or the spatial coordinate in some direction

(and thus $\Theta = 1 + \Delta$, where Δ is the anisotropy exponent introduced in Sect. 2.3.2). Examples of such scalings range from equilibrium systems with strong anisotropy due to strong uniaxial dipolar forces (see, e.g., Ref. [4]), Lifshitz points (see, for a recent review, Ref. [166] and references therein), to the general class of dynamical and quantum critical phenomena. In Sect. 2.2 we have encountered the case of the DLG, whose scaling is characterized by a "two-fold" anisotropic scaling in the sense that both space and time coordinates scale with different exponents. Scaling form as Eq. (8.49) are quite common, as discussed in Sect. 2.3.2, in the field of non-equilibrium steady states, from driven diffusive systems to directed percolation and surface growth phenomena.

It is natural to address the problem of local scale invariance, i.e. the extension of the anisotropic scaling Eq. (8.49) towards a space-time-dependent rescaling factor $b = b(t, \mathbf{x})$ in such a way that n-point functions are still covariant under these transformations. For a comprehensive introduction to this kind of question as well as to the technical developments we refer to Ref. [160]. For $\Theta = 2$ the analogous of conformal group (known as Schrödinger group) is known and it provides useful dynamical informations on the systems whose correlation functions covariantly transform under it (see Ref. [159]). The approach to the problem, for generic Θ, is the following: First of all one should determine a "reasonable" set of transformations under which one wants to preserve the covariance of (some) correlation functions. Then one exploits the consequences of this covariance to give predictions for, say, the response functions in dynamical critical phenomena or correlation function for static ones. Possibly a constraint on the critical exponents could emerge. To test the physical relevance of the whole construction it is *crucial* to compare its predictions with the results obtained by independent methods which do not rely on the LSI (as MC simulations, exact solutions, field-theoretical computations).

Two-point correlation functions at criticality were predicted by using LSI, and they have been found in good agreement with the analytic results for some Spherical Models [161]. Recent MC results for equilibrium system (ANNNI, i.e. axial next-nearest-neighbor Ising model, which has a uniaxial Lifshitz point) agree with those predictions [163]. Moreover, LSI has been also applied in order to predict the scaling form for the response function in the aging regime at criticality and in the low-temperature phase, after a quench from a disordered initial state. This is, basically, a prediction for the critical function $\tilde{F}_R$, Eq. (8.46), in real space. Numerical simulation for the two- and three-dimensional Ising model with Glauber (non-conserved) dynamics have been done and a very good agreement has been found [164]. On the other hand, when attempting an explicit construction of the LSI transformations suitable to describe Lifshitz points, as in Ref. [162], the crucial assumption that $\Theta \in \{2/N, N \in \mathbb{N}\}$ is required to ensure that a subalgebra of the generators of these transformations closes. This seems not to be the case, even though in Ref. [163] a very good agreement was found between numerical simulations for the ANNNI model and the prediction of the scaling function for spin-spin correlations as computed from LSI with $N = 4$. Indeed recent analytical computations [167] show that Θ for the ANNNI model differs from $1/2$ at order ϵ^2[7] and in the case of the uniaxial Lifshitz point in $d = 3$ (as that studied in Ref. [163]), $\Theta \simeq 0.487$, pretty equal to $1/2$, and thus it could be difficult to distinguish them numerically.

Let us give a closer look at the prediction of (assumed) LSI for scaling functions in the aging regime (following a quench at or below the critical point). The key point is that, because of the presence of the time surface, the time homogeneity is broken. As a consequence, the response functions should be covariant under a subalgebra of the algebra of the (Type II – following the classification of Ref. [160]) LSI generators which leaves invariant the time surface at $t = 0$. This covariance may be expressed in terms of differential equations for the scaling functions (pretty in the same way as in conformal invariance) which can be solved to determine them. For the autoresponse

[7]Where $\epsilon = 4 + m/2 - d$, and m stands for the number of dimensions scaling with $\Theta \neq 1$. In the case of uniaxial Lifshitz point, $m = 1$.

function $R_{\mathbf{x}=\mathbf{0}}(t,s)$ it has been found [160, 164] (with the notations of Sect. 8.3) that

$$R_{\mathbf{x}=\mathbf{0}}(t,s) = \rho_0 (t-s)^{-(x_1+x_2)/z} \left(\frac{t}{s}\right)^{(x_1-x_2)/z} , \tag{8.50}$$

where ρ_0 is a constant, x_1 and x_2 are the scaling dimensions of the order parameter and response field, respectively.

The agreement of this prediction with the result for Spherical Model, Eqs. (7.25) and (7.26) is striking [161].

For $R_{\mathbf{x}}(t,s)$, LSI implies the following form

$$R_{\mathbf{x}}(t,s) = R_{\mathbf{x}=\mathbf{0}}(t,s) \Phi(|\mathbf{x}|(t-s)^{-1/z}) , \tag{8.51}$$

where the function Φ is given in Ref. [160] in terms of its convergent power series expansion.

We would remark that Eqs. (8.50) and (8.51) give a stronger constraint on response function than that given by RG equations (8.46). Indeed, from the latter one should expect, in Eq. (8.51), an explicit dependence of Φ on the ratio s/t, that the LSI seems to rule out. Moreover the predictions Eqs. (8.50) and (8.51) make reference to the physical system under investigation only through the indices z, x_1, x_2 and the constant ρ_0. As a consequence, if LSI holds, the space dependence of $R_{\mathbf{x}}(t,s)$, encoded in the function Φ, should be observed in the relaxation after a quench of a variety of different systems. For future reference let us note that Eq. (8.51), implies, in momentum space[8]

$$R_{\mathbf{q}=\mathbf{0}}(t,s) = \tilde{\rho}_0 (t-s)^{(d-x_1-x_2)/z} \left(\frac{t}{s}\right)^{(x_1-x_2)/z} , \tag{8.52}$$

where d is the dimensionality of the system.

We will further discuss the problem of the test of LSI predictions in Section 9.5.

[8] We assume, here, that Eq. (8.51) is Fourier-transformable and that the limit $q \to 0$ can be taken. See Sect. 9.2.5 and 9.5 for further discussion.

Chapter 9

Aging in Field-Theoretical Models

In this Chapter we present the analytic determination of the universal scaling functions and the fluctuation-dissipation ratio in the aging regime, for some field-theoretical models of dynamics. We take advantage of the approach described in Chap. 8. This kind of analysis provide useful informations also on the aging dynamics of classical spin models, given it concerns only universal quantities which are, thus, completely independent, at criticality, of the specific realization of the system. In particular, in § 9.1 we introduce a useful definition of the fluctuation-dissipation ratio (already discussed in § 7.2.3) and we argue about its universality. In §§ 9.2, 9.3, 9.4 we present in some details the computation that we have done on some relevant models of dynamics which share their universal properties (and thus the fluctuation-dissipation ratio and universal scaling forms) with some well-known classical spin models, also briefly described. Finally, in § 9.5, we give a summary of the results obtained, of the comparison with the existing numerical data and we stress the relevance of our findings for the issue of applicability of the local scale invariance to the models analyzed. In particular we can check some of its predictions, summed up in Sect. 8.4.

9.1 Fluctuation-Dissipation Ratio and its Universality

As discussed at the end of Sect. 7.2, the fact that X^∞ is a universal quantity of the critical dynamics allows us to compute it for an arbitrary system belonging to the same (dynamical) universality class as that of the system we are interested in. Following this line, the fluctuation-dissipation ratio for the Ising, XY, Heisenberg ferromagnets with a non-conservative dynamics (e.g. a Glauber dynamics on the lattice), could be computed in terms of the Model A dynamics of an N-component field (introduced in Sect. 8.3), using a field-theoretical approach. On the same footing, conservative dynamics (e.g. Kawasaki dynamics on the lattice) of these models could be analyzed in terms of Model B [1] for the same field. The effect of a dynamic coupling to a conserved density (e.g. the energy) in the above mentioned spin models (with non-conservative dynamics) may be studied by means of Model C, whose fluctuation-dissipation ratio and scaling forms can be computed as well. In this sense, field-theoretical approach to the problem of aging is more flexible with respect to the exact solutions discussed so far in the literature (partially reviewed in Sect. 7.2, see also Tab. 7.1).

The only drawback of this approach is that, in order to have reliable estimates of the quantities one is interested in (for example X^∞) it is important to perform high-order perturbative expansions. We will see, however, that quite good agreement is found also at low orders.

Within the field-theoretical approach to critical dynamics, computations are simpler if done

in momentum space, thus we are interested in momentum-dependent response and correlation functions.

To work in momentum space it is worthwhile to introduce a quantity that, just as $X_{\mathbf{x}}(t,s)$ (Eq. (7.5)), "measures" the distance from equilibrium. It is given by [132]

$$\mathcal{X}_{\mathbf{q}}(t,s) = \frac{T R_{\mathbf{q}}(t,s)}{\partial_s C_{\mathbf{q}}(t,s)} , \tag{9.1}$$

where T is the temperature of the thermal bath in contact with the system. We note that for field-theoretical models, this ratio (or, equivalently, $X_{\mathbf{x}}$) has to be normalized in such a way that it is equals to 1 when the system is in equilibrium, and fluctuation-dissipation theorem applies. Thus T in Eq. (9.1) should be replaced with some suitable parameter (appearing in the dynamical functional) to get the correct normalization.

To compare our results with $X^{\infty}_{\mathbf{x}=0}$ considered in the literature [118,125], defined as in Eq. (7.7), we have to relate $\mathcal{X}_{\mathbf{q}}(t,s)$ to $X_{\mathbf{x}}(t,s)$. We note that, in the limit we are interested in,

$$X^{\infty}_{\mathbf{x}=0} = \mathcal{X}^{\infty}_{\mathbf{q}=0} \equiv \lim_{s\to\infty}\lim_{t\to\infty} \mathcal{X}_{\mathbf{q}=0}(t,s) . \tag{9.2}$$

Indeed, we may rewrite the FDR in real $\mathbf{x}$ space as a mean value of that in momentum space with a weight given by $R_{\mathbf{q}}$:

$$X^{-1}_{\mathbf{x}=0} \equiv \frac{\int \mathrm{d}^d q\, \partial_s C_{\mathbf{q}}(t,s)}{T\int \mathrm{d}^d q\, R_{\mathbf{q}}(t,s)} = \frac{\int \mathrm{d}^d q\, R_{\mathbf{q}}(t,s)\, \frac{\partial_s C_{\mathbf{q}}(t,s)}{T R_{\mathbf{q}}(t,s)}}{\int \mathrm{d}^d q\, R_{\mathbf{q}}(t,s)} = \langle \mathcal{X}^{-1}_{\mathbf{q}} \rangle_{R_{\mathbf{q}}} . \tag{9.3}$$

Now, since we expect $R_{\mathbf{q}} \propto e^{-q^2(t-s)}$, in the limit $t\to\infty$ and fixed s (exactly the order used to compute X^{∞}, Eq. (7.7)) $X^{-1}_{\mathbf{x}=0}$ will take contributions only from the $q=0$ mode, i.e. apart a normalization, the weight function $R_{\mathbf{q}}$ is a $\delta^d(\mathbf{q})$.

At this point of the discussion we can make clear the sense in which the FDR (either given by Eq. (7.5) or Eq. (9.1)) is a *universal* quantity. We consider here the case of Model A dynamics, discussed in Sect. 8.3, but the same general arguments apply also for other dynamical models. It is clear from the RG scaling forms Eqs. (8.37), (8.38) and (8.44) that $R_q(t,s)$ and $\Omega\partial_s C_q(t,s)$ (or, in real space, $R_{\mathbf{x}}(t,s)$ and $\Omega\partial_s C_{\mathbf{x}}(t,s)$) scales in the same way, that is, they have the same scaling dimensions (both at criticality and not). As a consequence their ratio is a dimensionless quantity in the RG sense, and thus, as the fixed point is approached, it should converge to a function of, say, $q(t-s)^{1/z}$, and s/t (at least at criticality). This, in turn, is universal in the sense that (possibly apart some scaling amplitudes) it is independent of the bare parameters appearing in the dynamical functional, and thus of the particular realization of the microscopic model. At leading order the result is also independent of the perturbations introduced by operators which are irrelevant in the RG sense. Moreover, in the case of vanishing momenta $q=0$, and in the long-time limit with s fixed and $t\to\infty$, we are left with a universal number. It is worthwhile noting that, as long as the initial state is a disordered non-critical one with short-range interactions, the result is also independent of the particular form of the initial Hamiltonian $\mathcal{H}_0[\varphi_0]$, Eq. (8.17).

9.2 Model A

In this Section we present the results of our calculations for Model A dynamics. In particular we focus on the FDR and scaling forms for both response and correlation functions. Following the discussion in Section 8.3 we report here the expected scaling forms Eq. (8.46) in an equivalent way, convenient for the following discussions. We expect, in momentum space,

$$\begin{cases} C_q(t,s) &= (t-s)^{a+1}(t/s)^{\theta-1}\bar{F}_C(\Omega q^z(t-s), s/t) , \\ R_q(t,s) &= (t-s)^{a}(t/s)^{\theta}\bar{F}_R(\Omega q^z(t-s), s/t) , \end{cases} \tag{9.4}$$

where $a = (2 - \eta - z)/z$. We report also the expected scaling forms for $\partial_s C_{q=0}(t,s)$ and $R_{q=0}(t,s)$, i.e.

$$\begin{cases} \partial_s C_{q=0}(t,s) &= A_{\partial C}(t-s)^a (t/s)^\theta F_{\partial C}(s/t) \ , \\ R_{q=0}(t,s) &= A_R (t-s)^a (t/s)^\theta F_R(s/t) \ , \end{cases} \tag{9.5}$$

derived directly from Eq. (9.4), and where $A_{\partial C}$, A_R are non-universal amplitudes. The universal functions $F_{\partial C}(v)$ and $F_R(v)$ are defined in such a way that $F_{\partial C}(0) = 1$, $F_R(0) = 1$.

9.2.1 Gaussian Model

The effects of a quench on this model were firstly worked out in Ref. [140] where the main formulas can be found. However, a detailed analysis, in the perspective of studying the long-time behavior of the correlation and response functions and of the deviations from equilibrium theorems, was done only in Ref. [118]. For the Gaussian model we know exactly the response and correlations functions, so we can evaluate the FDR $\mathcal{X}_{\mathbf{q}}(t,s)$ (in Ref. [118] the related quantity $X_{\mathbf{x}}$ has been considered, see Sect. 9.1). From Eqs. (8.24), (8.25) and definition (9.1) we have

$$\mathcal{X}_q^0(t,s) = \left(\frac{\partial_s C_q^0}{\Omega R_q^0} \right)^{-1} = \left(1 + e^{-2\Omega(q^2+r_0)s} + \Omega q^2 \tau_0^{-1} e^{-2\Omega(q^2+r_0)s} \right)^{-1} . \tag{9.6}$$

If the theory is off-critical ($r_0 \neq 0$) the limit of this ratio for $s \to \infty$ is 1 for all values of q, in agreement with the idea that in the high-temperature phase all modes have a finite equilibration time, so that equilibrium is recovered and as a consequence the fluctuation-dissipation theorem holds. For the critical theory, i.e. $r_0 \propto T - T_c = 0$, if $q \neq 0$ the limit ratio is again equal to one, whereas for $q = 0$ we have $\mathcal{X}_{q=0}^0(t,s) = 1/2$. This analysis clearly shows that, as expected, the only mode characterized by aging, i.e. that "does not relax" to the equilibrium, is the zero mode in the critical limit.

9.2.2 One-loop Results

In Ref. [132] a detailed analysis of the one-loop critical FDR and of the scaling forms for both correlation and response functions is done. We report here the results there obtained, deferring some details of the computation to the Appendix 10.1.

To do analytic computations we use the method of renormalized field theory in the minimal subtraction scheme, as in Sect. 8.3. As already said, the breaking of time homogeneity makes less straightforward the renormalization procedure in terms of 1PI correlation functions (see Refs. [17, 140]), so our computations are done in terms of connected functions.

At one-loop order we have to evaluate, taking into account causality [14] (see also footnote 1 in Chapter 8), the three Feynman diagrams in Figure 9.1, one for the response function and two for the correlation one. In terms of them we have

$$\begin{aligned} R_q(t,s) &= R_q^0(t,s) - \frac{N+2}{6} g_0(a) + O(g_0^2) \ , \\ C_q(t,s) &= C_q^0(t,s) - \frac{N+2}{6} g_0[(b)+(c)] + O(g_0^2) \ . \end{aligned} \tag{9.7}$$

In order to evaluate the FDR at criticality we have to set in this perturbative expansion $r_0 = 0$ (massless theory). We also set $\tau_0^{-1} = 0$, since it is an irrelevant variable [140,141] (and thus it affects only the corrections to the leading scaling behavior), and $\Omega = 1$ to lighten the notations.

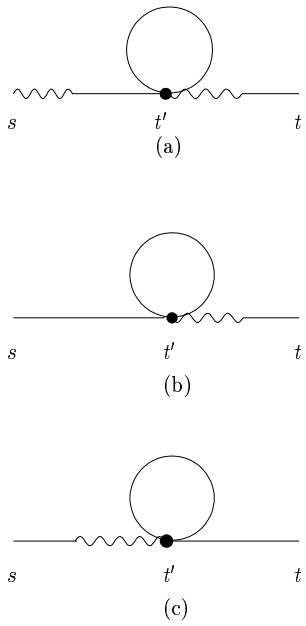

Figure 9.1: Feynman diagrams contributing to the one-loop response (a) and correlation function ((b)+(c)). Response functions are drawn as wavy-normal lines, whereas correlators are normal lines. A wavy line is attached to the response field and a normal one to the order parameter.

The first step in the calculation of the diagrams is the evaluations of the critical "bubble" $B_c(t)$, i.e. their common 1PI part. We have, in generic dimension d,

$$B_c(t) = \int \frac{\mathrm{d}^d q}{(2\pi)^d}\, C_q(t,t) = -\frac{1}{d/2-1}\frac{(2t)^{1-d/2}}{(4\pi)^{d/2}} = -N_d \frac{\Gamma(d/2-1)}{2^{d/2}} t^{1-d/2}, \tag{9.8}$$

where $N_d = \dfrac{2}{(4\pi)^{d/2}\Gamma(d/2)}$. Note that the equilibrium contribution to $B_c(t)$ is zero for $d > 2$.

Let us consider $t > s$ in the following. We may write, for generic $r_0 \geq 0$

$$\begin{aligned}
(a) &= \int_0^\infty \mathrm{d}t'\, R_q^0(t,t') B(t') R_q^0(t',s)\,, \\
(b) &= \int_0^\infty \mathrm{d}t'\, R_q^0(t,t') B(t') C_q^0(t',s)\,, \\
(c) &= \int_0^\infty \mathrm{d}t'\, R_q^0(s,t') B(t') C_q^0(t',t)\,,
\end{aligned} \tag{9.9}$$

where we set, now, $r_0 = 0$ in R_q^0 and C_q^0, and the bubble $B(t)$ is replaced with its critical expression $B_c(t)$.

Integrating and expanding in powers of $\epsilon = 4 - d$ we find for the response function

$$R_q(t,s) = G(t-s)\left(1 + \tilde{g}_0 \frac{N+2}{24} \ln\frac{t}{s}\right) + O(\epsilon^2, \tilde{g}_0^2), \tag{9.10}$$

and for the correlation one

$$C_q(t,s) = \frac{G(t-s)-G(t+s)}{q^2}\left(1+\tilde{g}_0\frac{N+2}{24}\ln\frac{t}{s}\right) - \tilde{g}_0\frac{N+2}{24}\frac{G(t+s)}{q^2}h(2q^2\,s) + O(\epsilon^2,\tilde{g}_0^2), \tag{9.11}$$

where

$$h(v) = 2\left[\int_0^v \mathrm{d}\xi\ \ln\xi\, e^{\xi} + (1-e^v)\ln v\right], \tag{9.12}$$

and $\tilde{g}_0 = N_d g_0$. Note that $h(0)=0$, $h'(0)=-2$ and $h(v)$ has the following asymptotic expansion, for $v \gg 1$

$$h(v) = -2\,\frac{e^v}{v}\left(1+\frac{1}{v}+\frac{2}{v^2}+\ldots+\frac{k!}{v^k}+\ldots\right). \tag{9.13}$$

In order to obtain the critical functions we have to set the renormalized coupling equal to its fixed point value. At first order in ϵ [4]

$$\tilde{g}_0 = \tilde{g}^* = \frac{6}{N+8}\epsilon + O(\epsilon^2). \tag{9.14}$$

Thus we get (called $P_N = \frac{N+2}{N+8}$)

$$R_q(t,s) = G(t-s)\left(1+\epsilon\frac{P_N}{4}\ln\frac{t}{s}\right) + O(\epsilon^2)\,, \tag{9.15}$$

$$C_q(t,s) = \frac{G(t-s)-G(t+s)}{q^2}\left(1+\epsilon\frac{P_N}{4}\ln\frac{t}{s}\right) - \epsilon\frac{P_N}{4}\frac{G(t+s)}{q^2}h(2q^2 s) + O(\epsilon^2)\,, \tag{9.16}$$

that are fully compatible with the scaling form given in Eq. (9.5), with

$$\bar{F}_R(x,y) = e^{-x} + O(\epsilon^2)\,, \tag{9.17}$$

and

$$\bar{F}_C(x,y) = \frac{e^{-x}}{xy} - \left[1+\epsilon\frac{P_N}{4}h\left(\frac{2xy}{1-y}\right)\right]\frac{e^{-x\frac{1+y}{1-y}}}{xy} + O(\epsilon^2)\,. \tag{9.18}$$

In particular we recognize the exponent $\theta = P_N\epsilon/4 + O(\epsilon^2)$ in agreement with Ref. [140], $z = 2 + O(\epsilon^2)$, $\eta = O(\epsilon^2)$ as expected, and that $\bar{F}_R(x,y)$ is not affected by $O(\epsilon)$ corrections.

Computing the derivative with respect to s of the two-time correlation function and taking its ratio with the response one we have

$$\mathcal{X}_q^{-1}(s) = 1 + e^{-2q^2 s} - \frac{P_N\epsilon}{4}e^{-2q^2 s}\left[\frac{e^{2q^2 s}-1}{q^2 s} - h(2q^2 s) + 2h'(2q^2 s)\right] + O(\epsilon^2)\,. \tag{9.19}$$

Note that, at least at this order, the result is independent of the observation time t. Using the large v behavior of $h(v)$, cf. Eq. (9.13), we find that the limit of the FDR for $s \to \infty$ is equal to 1 for all $q \neq 0$. Instead for $q = 0$ we get (using the expression Eq. (9.12))

$$\mathcal{X}_{q=0}^{\infty} = \frac{1}{2}\left(1-\epsilon\frac{P_N}{4}\right) + O(\epsilon^2)\,. \tag{9.20}$$

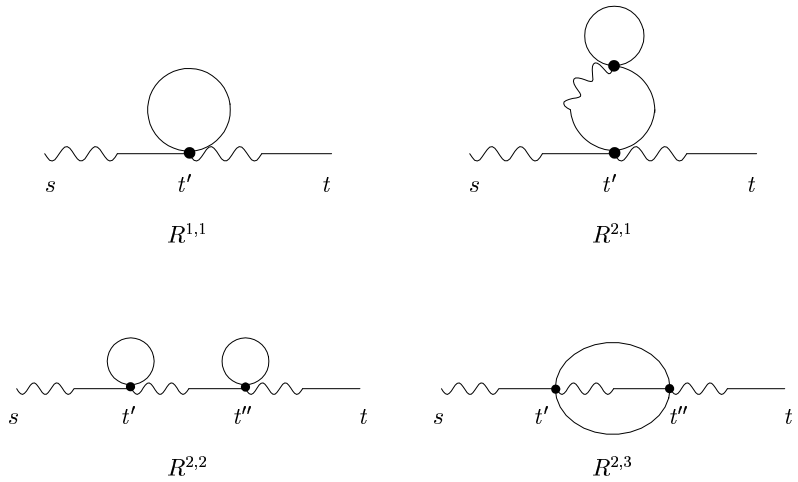

Figure 9.2: Two-loop Feynman diagrams contributing to the response function. Response propagators are drawn as wavy-normal lines, whereas correlators are normal lines. A wavy line is attached to the response field and a normal one to the order parameter.

Taking into account the effect of the mass r_0 (deviation from the critical temperature) in the previous computations, one obtains for the non-critical bubble (contributing to the mass renormalization)

$$B(t) = N_d \left[\frac{\pi}{2 \sin d\pi/2} - \frac{1}{2}\Gamma(d/2)\Gamma(1-d/2, 2r_0 t) \right] r_0^{d/2-1} , \tag{9.21}$$

where $\Gamma(x,y)$ is the incomplete Γ function [177]. Using this expression it is possible to determine, as previously done, the correlation and response functions. We report the basic formulas in the Appendix 10.1. The final result is obtained computing the ratio $\mathcal{X}_q$ in terms of the renormalized parameters of the theory. It is then trivial, but algebraically cumbersome, to show that $\mathcal{X}_q^{\infty}$ is equal to 1, in the high-temperature phase, for all q.

9.2.3 Two-loop Response Function

Up to the second order in perturbation theory there are four connected Feynman diagrams (without self-loops of the response propagator) that contribute to the response function. They are depicted in Figure 9.2. In terms of these diagrams and as a function of the bare couplings and fields (denoted in the following with φ_B, $\tilde{\varphi}_B$), the zero-momentum bare response function $R_B(t,s)$ is given by

$$\begin{aligned} R_B(t,s) = R^0_{q=0}(t,s) - g_0 \frac{N+2}{6} R^{1,1} \\ + g_0^2 \left[\left(\frac{N+2}{6} \right)^2 R^{2,1} + \frac{(N+2)^2}{18} R^{2,2} + \frac{N+2}{6} R^{2,3} \right] + O(g_0^3) . \end{aligned} \tag{9.22}$$

In the following we assume $t > s$ for simplicity. Using the results reported in the Appendix 10.2,

we get

$$
\begin{aligned}
R_B(t,s) = 1 + \tilde{g}_0 \frac{N+2}{24} \left\{ \log\frac{t}{s} + \frac{\epsilon}{2} \left[(\gamma_E + \log 2 + \log t) \log\frac{t}{s} - \frac{1}{2}\log^2\frac{t}{s} \right] \right\} \\
+ \tilde{g}_0^2 \frac{(N+2)^2}{144} \left\{ \frac{1}{8}\log^2\frac{t}{s} + \left[-\left(\frac{1}{\epsilon} + \log 2 + \gamma_E + \log t \right) \log\frac{t}{s} + \frac{1}{2}\log^2\frac{t}{s} \right] \right\} \\
- \tilde{g}_0^2 \frac{N+2}{24} \left[\frac{1}{\epsilon} \left(\log\frac{4}{3} + \log\frac{t}{s} \right) + \log\frac{t}{s} \left(\frac{1}{2} + \log t + \gamma_E \right) - \frac{1}{2}\log^2\frac{t}{s} \right. \\
\left. + (\log(t-s) + \gamma_E) \log\frac{4}{3} - \frac{f(s/t)}{4} \right] + O(g_0^3, g_0^2\epsilon, g_0\epsilon^2) \,, \qquad (9.23)
\end{aligned}
$$

where, as in Sect. 9.2.2, $\tilde{g}_0 = N_d g_0$, $N_d = 2/((4\pi)^{d/2}\Gamma(d/2))$ and $f(v)$ is a regular function defined in Eq. (10.40). To lighten the notations we set $\Omega = 1$ in the previous equations. The dependence on Ω of the final formulas may be simply obtained by $t \mapsto \Omega t$, where t is the generic time variable.

In order to cancel out the dimensional poles (i.e. singularities for $\epsilon \to 0$) appearing in this function, we have to renormalize the coupling constant according to [4]

$$
\tilde{g}_0 = \left(1 + \frac{N+8}{6} \frac{\tilde{g}}{\epsilon} \right) \tilde{g} + O(\tilde{g}^2), \qquad (9.24)
$$

and the fields φ and $\tilde{\varphi}$ via the relations [14] $\varphi_B = Z_\varphi^{1/2}\varphi$, $\tilde{\varphi}_B = Z_{\tilde{\varphi}}^{1/2}\tilde{\varphi}$, so that

$$
R(t,s) = (Z_\varphi Z_{\tilde{\varphi}})^{-1/2} R_B(t,s) = \left[1 + \frac{N+2}{24} \log\frac{4}{3} \frac{\tilde{g}^2}{\epsilon} + O(\tilde{g}^3) \right] R_B(t,s). \qquad (9.25)
$$

After this renormalization, $R(t,s)$ is a regular function of the dimensionality also for $\epsilon \to 0$. The critical response function is now obtained by fixing $\tilde{g}$ at its fixed point value [4]

$$
\tilde{g}^* = \frac{6\,\epsilon}{N+8} \left[1 + \frac{3(3N+14)}{(N+8)^2}\epsilon \right] + O(\epsilon^3) \,, \qquad (9.26)
$$

leading to

$$
\begin{aligned}
R(t,s) \;=\; & 1 + \epsilon \frac{N+2}{4(N+8)} \log\frac{t}{s} + \frac{\epsilon^2}{4} \left[\frac{6(N+2)}{(N+8)^2} \left(\frac{N+3}{N+8} + \log 2 \right) \log\frac{t}{s} \right. \\
& + \frac{(N+2)^2}{8(N+8)^2} \log^2\frac{t}{s} - \frac{6(N+2)}{(N+8)^2} \log\frac{4}{3} \log(t-s) \\
& \left. + \frac{3(N+2)}{2(N+8)^2} \left(f(s/t) - 4\gamma_E \log\frac{4}{3} \right) \right] + O(\epsilon^3) \,. \qquad (9.27)
\end{aligned}
$$

Note that the non-scaling terms, like $\log t \log t/s$ (appearing, for example, in $R^{2,3}$, see Eq. (10.39)), cancel each other out when the coupling constant is set equal to its fixed point value. Eq. (9.27) agrees with the expected scaling form in momentum space, Eq. (9.5),

$$
R(t,s) = A_R (t-s)^a (t/s)^\theta F_R(s/t) \,, \qquad (9.28)
$$

with the well-known exponents [4, 140, 141]

$$
\begin{aligned}
\theta &= \frac{N+2}{N+8}\frac{\epsilon}{4} \left[1 + \frac{6\epsilon}{N+8} \left(\frac{N+3}{N+8} + \log 2 \right) \right] + O(\epsilon^3) \,, & (9.29) \\
a &= \frac{2-\eta-z}{z} = -\frac{3(N+2)}{2(N+8)^2} \log\frac{4}{3}\,\epsilon^2 + O(\epsilon^3) \,, & (9.30)
\end{aligned}
$$

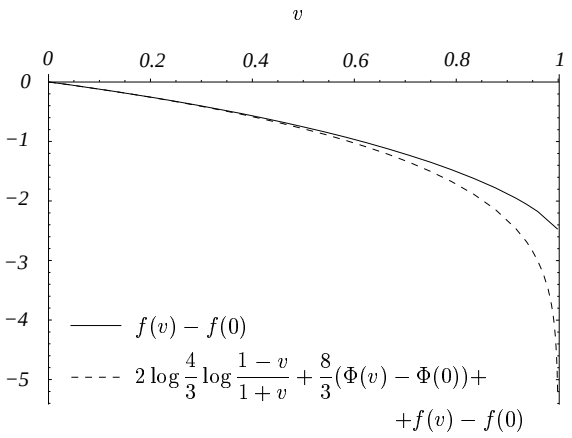

Figure 9.3: Plot of the two-loop contribution to the universal functions $F_R(v)$ (see Eq. (9.32)) and $F_{\partial C}(v)$ (see Eq. (9.42)).

and the non-universal amplitude

$$A_R = 1 + \epsilon^2 \frac{3(N+2)}{8(N+8)^2} \left(f(0) - 4\gamma_E \log \frac{4}{3} \right) + O(\epsilon^3) \ . \tag{9.31}$$

For the *new universal function* $F_R(v)$ we find

$$F_R(v) = 1 + \epsilon^2 \frac{3(N+2)}{8(N+8)^2} (f(v) - f(0)) + O(\epsilon^3) \ . \tag{9.32}$$

A plot of the quantity $f(v) - f(0)$ (defined in the Appendix 10.2, Eq. (10.40)), that completely characterizes the out-of-equilibrium corrections to the mean-field behavior up to the second order in the ϵ-expansion, is reported in Fig. 9.3. Due to the small prefactor ($\epsilon^2/72$ for the Ising model, $N = 1$), it might be very hard to detect this correction in numerical and experimental works, as it happens for the corrections to the mean-field behavior of the static [10] and equilibrium dynamics [178] two-point functions.

9.2.4 Two-loop Fluctuation-Dissipation Ratio

In this Section we evaluate the FDR up to the order ϵ^2. We do not compute the full two-point correlation function $C(t,s)$, since only $\partial_s C(t,s)$ is required to determine the FDR. This derivative may be computed by using the following diagrammatic identity.

Each amputated diagram $D_i(t,s)$ (with label i) contributing to the response function, also contributes to the correlation one in two diagrams, as graphically illustrated in Fig. 9.4. Taking into account the explicit form of the propagators (see Eqs. (8.24) and (8.25)) for $q^2 = 0$ and causality (which also implies that $D_i(t,s) \propto \theta(t-s)$ apart from contact terms) it is easy to find that

$$\partial_s C_i(t,s) = 2R_i(t,s) + 2 \int_0^\infty \mathrm{d}t'\, t' D_i(t',s), \tag{9.33}$$

where $C_i(t,s)$ is the contribution of this diagram to the correlation function, $R_i(t,s)$ the contribution to the response one, and $D_i(t',s)$ the common amputated part (the second term in the r.h.s. of Eq. (9.33) will be denoted by $(\partial C_i)_e$).

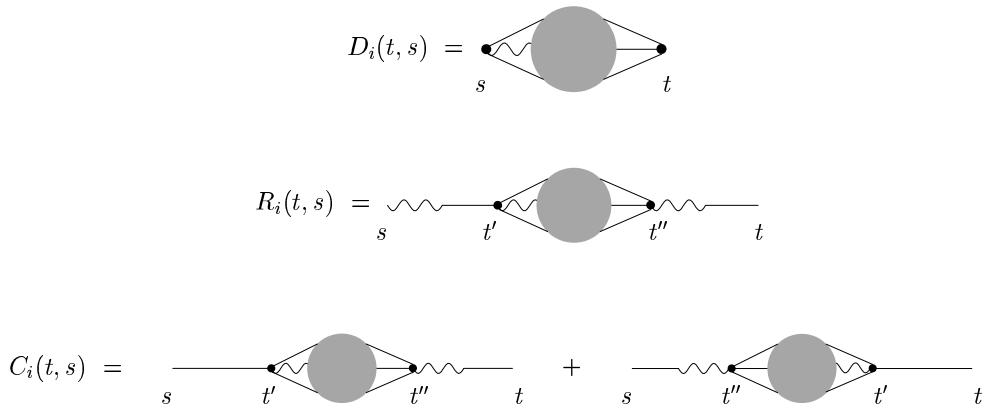

Figure 9.4: Diagrammatic trick.

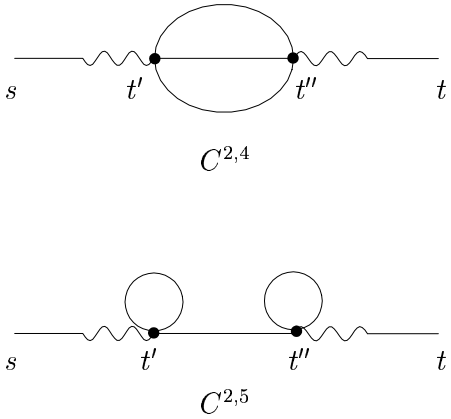

Figure 9.5: Diagrams contributing only to the correlation function.

Relation (9.33) is nothing but a particular case of a relation following an algebraic identity for the functional integral, i.e.

$$0 = \int [\mathrm{d}\varphi \mathrm{d}\tilde{\varphi} \mathrm{d}\varphi_0] \frac{\delta}{\delta \tilde{\varphi}(\mathbf{x}, s)} \left\{ \varphi(\mathbf{x}', t) e^{-S[\varphi,\tilde{\varphi}] - H_0[\varphi_0]} \right\} , \tag{9.34}$$

with $t > s > 0$. At criticality (i.e. $r_0 = 0$, using dimensional regularization) we get, in momentum space,

$$(\partial_s - \mathbf{q}^2) \langle \varphi(-\mathbf{q}, t) \varphi(\mathbf{q}, s) \rangle = 2 \langle \varphi(-\mathbf{q}, t) \tilde{\varphi}(\mathbf{q}, s) \rangle - \frac{g_0}{3!} \langle \varphi(-\mathbf{q}, t) \varphi^3(\mathbf{q}, s) \rangle , \tag{9.35}$$

which, in the limit $\mathbf{q}^2 \to 0$, is diagrammatically expressed by Eq. (9.33) as far as the amputated contributions common to the response and the correlation functions are concerned.

Diagrams contributing to the correlation function, but not to the response one do exist. They have to be computed without taking advantage of this identity. At two-loop order there are two of them, depicted in Fig. 9.5.

Summing the six contributions to the correlation function, we finally get

$$\frac{\partial_s C_B(t,s)}{2} = R(t,s) - g_0 \frac{N+2}{6}(\partial C)_e^{1,1} + g_0^2 \left\{ \left(\frac{N+2}{6}\right)^2 (\partial C)_e^{2,1} + \frac{(N+2)^2}{18}(\partial C)_e^{2,2} + \frac{N+2}{6}(\partial C)_e^{2,3} + \frac{1}{2}\left[\frac{N+2}{18}(\partial C)^{2,4} + \left(\frac{N+2}{6}\right)^2 (\partial C)^{2,5} \right] \right\} + O(g_0^3) . \tag{9.36}$$

Considering the explicit expression for the diagrams given in the Appendix 10.3 one obtains the derivative of the bare correlation function. This quantity is renormalized using Eqs. (9.24), (9.25) and

$$\Omega_B = Z_\Omega \Omega \qquad \text{with} \qquad Z_\Omega = \left(\frac{Z_\varphi}{Z_{\tilde\varphi}}\right)^{1/2} , \tag{9.37}$$

so that, taking into account the Ω we set equal to 1 in the previous relations,

$$\partial_s C(t,s) = Z_\Omega Z_\varphi^{-1}\, \partial_s C_B(t,s) = (Z_\varphi Z_{\tilde\varphi})^{-1/2}\, \partial_s C_B(t,s) . \tag{9.38}$$

The expression of $\partial_s C(t,s)$ in terms of the renormalized coupling has a multiplicative redefinition of its amplitude at the first order in $\tilde g$. Considering the fixed point value for $\tilde g$ (cf. Eq. (9.26)) one finally obtains

$$\begin{aligned} \frac{\partial_s C(t,s)}{2} &= \left[1 + \epsilon \frac{N+2}{4(N+8)} + \epsilon^2 \frac{3(N+2)(3N+14)}{4(N+8)^3}\right] \\ &\times \left\{ 1 + \epsilon \frac{N+2}{4(N+8)} \log\frac{t}{s} + \frac{\epsilon^2}{4}\left[\frac{6(N+2)}{(N+8)^2}\left(\frac{N+3}{N+8} + \log 2\right)\log\frac{t}{s} \right.\right. \\ &\left.\left. + \frac{(N+2)^2}{8(N+8)^2}\log^2\frac{t}{s} - \frac{6(N+2)}{(N+8)^2}\log\frac{4}{3}\log(t-s)\right]\right\} \\ &\times \left\{ 1 + \epsilon^2 \frac{N+2}{(N+8)^2}\left[\frac{3}{4}\log\frac{4}{3}\log\frac{t-s}{t+s} - \gamma_E \frac{3}{2}\log\frac{4}{3} \right.\right. \\ &\left.\left. + \Phi(s/t) + \frac{3}{8} f(s/t) + \frac{N+2}{8} + \tilde c\right]\right\} + O(\epsilon^3) , \end{aligned} \tag{9.39}$$

where the function $f(v)$ and $\Phi(v)$ are defined in Eqs. (10.40) and (10.53) respectively, Li_2 is the dilogarithmic function (its standard definition is recalled in Eq. (10.27)) and

$$\tilde c \equiv \frac{3}{2}\left(1 - \log\frac{4}{3}\right)\log 2 - \frac{3}{4}\left(1 + \log\frac{4}{3}\right) + \frac{3}{8}\log^2\frac{4}{3} + \frac{3}{4}\mathrm{Li}_2(1/4) . \tag{9.40}$$

Note that also for $\partial_s C(t,s)$ all the non-scaling terms cancel out when the coupling constant is set equal to its fixed point value. This result agrees with the scaling form in momentum space, Eq. (9.5),

$$\partial_s C(t,s) = A_{\partial C}(t-s)^a (t/s)^\theta F_{\partial C}(s/t), \tag{9.41}$$

with the same a and θ as those given in Eqs. (9.29), (9.30) and a new universal scaling function $F_{\partial C}(v)$ given by

$$F_{\partial C}(v) = 1 + \epsilon^2 \frac{3(N+2)}{8(N+8)^2}\left[2\log\frac{4}{3}\log\frac{1-v}{1+v} + \frac{8}{3}(\Phi(v) - \Phi(0)) + f(v) - f(0)\right] + O(\epsilon^3) . \tag{9.42}$$

A plot of the loop corrections in the above expression (apart from the factor $\frac{3(N+2)}{8(N+8)^2}$ appearing also in $F_R(v)$) is shown in Fig. 9.3. As already noticed for $F_R(v)$, effective corrections to mean-field behavior are quantitatively very small for $F_{\partial C}(v)$.

Taking the long-time limit (according to Eq. (9.2)) of both the correlation and response functions one obtains the limit of the critical fluctuation-dissipation ratio we are interested in:

$$\frac{(\mathcal{X}^{\infty}_{\mathbf{q}=0})^{-1}}{2} = 1 + \frac{N+2}{4(N+8)}\epsilon + \epsilon^2 \frac{N+2}{(N+8)^2}\left[\frac{N+2}{8} + \frac{3(3N+14)}{4(N+8)} + c\right] + O(\epsilon^3)\,, \tag{9.43}$$

with

$$\begin{aligned} c &= -\frac{3}{4} + \frac{3}{4}\log 2(2 + 11\log 2 - 3\log 3) - \frac{23}{8}\log^2 3 + \frac{3}{2}\mathrm{Li}_2(1/4) \\ &\quad -\frac{21}{4}\mathrm{Li}_2(1/3) + \frac{21}{8}\mathrm{Li}_2(3/4) - \frac{1}{8}\mathrm{Li}_2(8/9) = -0.0415\ldots\,. \end{aligned} \tag{9.44}$$

We note that the contribution of c to the FDR is quite small. For example, with $N = 1$ the sum of the first two terms in brackets is ~ 1, which is about 45 times larger than c.

9.2.5 Results and Discussions

In Section 9.2 we studied the off-equilibrium properties of the purely dissipative relaxational dynamics of the N-vector model in the framework of the field-theoretical ϵ-expansion [132, 133]. The scaling forms for the zero-momentum response function and for the derivative with respect to the waiting time of the two-time correlation function reads

$$R(t,s) = A_R(t-s)^a (t/s)^\theta F_R(s/t)\,, \tag{9.45}$$

$$\partial_s C(t,s) = A_{\partial C}(t-s)^a (t/s)^\theta F_{\partial C}(s/t). \tag{9.46}$$

The universal functions $F_R(s/t)$ and $F_{\partial C}(s/t)$ are given in Eqs. (9.32) and (9.42) respectively. In both cases the corrections to the Gaussian value 1 is of order ϵ^2. In principle these corrections should be detectable in computer and experimental works, but being quantitatively very small, it could be very difficult to observe them. We would remark that this fact does not mean that aging effects in this model are weak compared to the analogous phenomena in glassy systems. In fact aging manifests itself in the full scaling forms (e.g. $\theta \neq 0$) and in the violation of fluctuation-dissipation theorem, i.e. in $X^\infty \neq 1$ in a quantitative way.

We note that the $R(t,s)$ we found agrees with the general RG form (9.5), but at first sight it is not compatible with Eq. (8.52). This naïve comparison should be done very carefully because it involves the Fourier integral of Eq. (8.51) which could be divergent. The analysis of the full q-dependence of $R_{\mathbf{q}}(t,s)$ may give some insight into this problem. This dependence has been already worked out up to $O(\epsilon)$ [132], but it is very hard to determine it up to two loops. In other dynamical universality classes (see, e.g., Section 9.3) this discrepancy already arises at $O(\epsilon)$. The computation of the full q-dependence in these cases seems to be simpler and may provide some useful hints [136].

We computed the FDR $\mathcal{X}_{\mathbf{q}=\mathbf{0}}$ for general N, cf. Eq. (9.43). As shown in Sect. 9.1 [132] this quantity for zero momentum has the same long-time limit as the standard FDR X^∞. Using this fact we may compare our result with those presented in the literature (see Table 7.1).

In the limit $N \to \infty$, Eq. (9.43) reduces to $X^\infty = 1/2 - \epsilon/8 - \epsilon^2/32 + O(\epsilon^3)$, in agreement with the exact result for the Spherical Model $X^\infty = 1 - 2/d$ [125].

The formula for general N (cf. Eq. (9.43)) allows us to make quantitative predictions for a large class of systems. In Fig. 9.6 we report the dependence of X^∞ on the dimensionality at fixed N, while in Fig. 9.7 we show the dependence on N at fixed $d = 4 - \epsilon$. For each model we report two

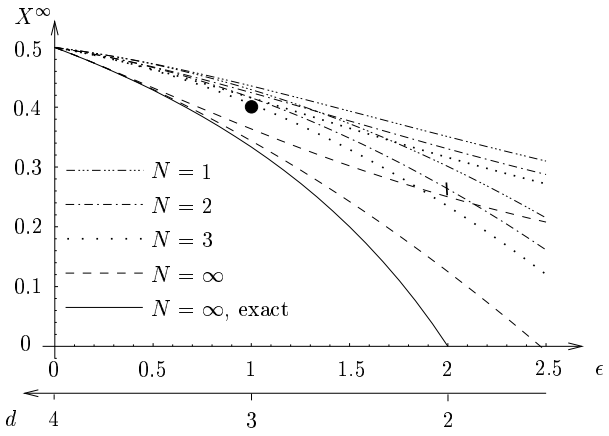

Figure 9.6: X^∞ as a function of the dimensionality $d = 4 - \epsilon$ for several N. For each N the upper curve is the $[2,0]$ Padé approximant and the lower one the $[0,2]$. The exact result for $N = \infty$ is reported as a solid line. The numerical Monte Carlo values for the Ising Model in two and three dimensions are also indicated (for the latter, there is no indication about the error).

values: One is obtained by direct summation (Padé approximant $[2,0]$) and the other by "inverse" summation (Padé approximant $[0,2]$). We do not show the $[1,1]$ approximant, since it has a pole in the range of ϵ we are interested in. From these figures some general trends may be understood:

- Decreasing the dimensionality, X^∞ always decreases, at least up to $\epsilon = 2$ (for the one-dimensional Ising model the value $X^\infty = 1/2$ is expected [125]);
- Increasing N, X^∞ decreases, approaching in a quite fast way the exact result for the Spherical Model;
- For $N = \infty$ the curve of the $[0,2]$ approximant reproduces better than the $[2,0]$ approximant the exact result in any dimension.

The last point suggests us to use the $[0,2]$ value as an estimate of X^∞, also for physical N. We quote as *indicative* error the difference between the two approximants. Using this procedure, we obtain $X^\infty = 0.429(6)$ for the three-dimensional $N = 1$ model, compared to $\simeq 0.46$ found at one-loop [132], in very good agreement with the Monte Carlo simulation value $X^\infty \simeq 0.40$ for the three-dimensional Ising Model [125] with non-conservative (heat-bath Glauber) dynamics. Considering $\epsilon = 2$ one obtains $X^\infty = 0.30(5)$ for $N = 1$, improving the one loop estimate $\simeq 0.42$ in the right direction towards the Monte Carlo result $X^\infty = 0.26(1)$ for the two-dimensional Ising Model with Glauber dynamics [125].

Using our results we can give predictions of X^∞ for systems that have not yet been analyzed by numerical simulations. We estimate $X^\infty = 0.416(8)$ for the three-dimensional XY model and $X^\infty = 0.405(10)$ for the three-dimensional Heisenberg model. These predictions may be tested by numerical simulations extending the results reported in Ref. [125].

9.3 Model C

In the previous Sections we have discussed the purely dissipative dynamics of the Landau-Ginzburg Hamiltonian. With "purely dissipative" we mean that during the evoultion (relaxation) there

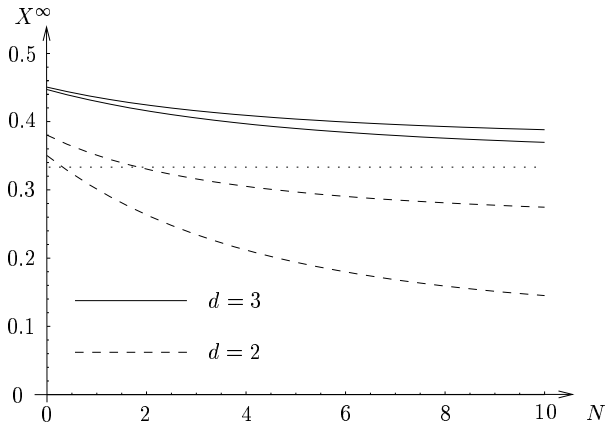

Figure 9.7: N-dependence of X^∞ for $d = 2$, 3. The upper curve is the $[2,0]$ Padé approximant and the lower one the $[0,2]$. The dotted line is the exact result for $N = \infty$ in $d = 3$ ($X^\infty = 1/3$)

are no conserved quantities. In some cases, however, it turns out that the dynamics of physical systems is such that some quantities are conserved, and thus a suitable field-theoretical description should account for this fact. One example is provided by the lattice Ising model with Kawasaki dynamics (lattice gas, see Sect. 2.1): Each elementary dynamical step amounts to a spin exchange between two chosen neighboring sites (see also the DLG in Sect. 2.2). Of course, in this case, the total magnetization of the system (well defined in finite volume) is conserved by the dynamics. To describe the critical properties of the model (which exhibits, as discussed in Section 2.1, a second-order phase transition when the density is 1/2), the Langevin equation for the corresponding field theory should be such that the integral over the whole space of the order parameter (which corresponds, in a mesoscopic description, to the spin field) does not change with time. This leads to Model B dynamics, discussed in Sect. 3.3 when dealing with DLG. Here, instead, we consider a different model, characterized by the fact that it is not the order parameter to be conserved, but a non-critical quantity, which is dynamically coupled to it. This quantity may describe, for example, the energy or the concentration of mobile impurities. The suitable field-theoretical description of this dynamics is given by Model C in the terminology of Ref. [1] (see also Ref. [4]), whose definition is briefly recalled in Section 9.3.1. It well describes, for example, the behavior of a phonon system close to the structural (*displacive*) phase transition [1]. Other physical realizations of this model are intermetallic alloys [153], adsorbed layers on solid substrates [154] and supercooled liquids [155]. In these last three systems the physically relevant processes are those of *decomposition* and *ordering*. In the case of the intermetallic alloys the system can be described as a lattice gas with two different species of atoms, A and B. The formation of structures in which an A atom is surrounded by B atoms is energetically favoured. As a consequence we expect that in the low-temperature region the ordered phase amounts to a segregation of A and B components into two different sublattices. The decomposition process is described by the conserved order parameter, corresponding to the local concentration of A atoms in the A-B alloy. The non-conserved order parameter, describing the ordering process, is essentially related to the local difference between the A concentration in each sublattice (somehow the analogous of the staggered magnetization in antiferromagnets). The phase diagram of this system is highly non-trivial and there are still unanswered questions (see Ref. [156] for recent discussions).

9.3.1 The Model

In this section we recall briefly the very definition of Model C dynamics. Let us consider an N-component field $\varphi(\mathbf{x},t)$ (the order parameter) dynamically coupled to a non-critical conserved density $\varepsilon(\mathbf{x},t)$. The joint dynamics of these two fields is given by the following stochastic Langevin equations

$$\partial_t\varphi(\mathbf{x},t) = -\Omega\frac{\delta\mathcal{H}[\varphi,\varepsilon]}{\delta\varphi(\mathbf{x},t)} + \xi(\mathbf{x},t)\ , \tag{9.47}$$

$$\partial_t\varepsilon(\mathbf{x},t) = \Omega\rho\nabla^2\frac{\delta\mathcal{H}[\varphi,\varepsilon]}{\delta\varepsilon(\mathbf{x},t)} + \zeta(\mathbf{x},t)\ , \tag{9.48}$$

where $\mathcal{H}[\varphi,\varepsilon]$ is the Landau-Ginzburg Hamiltonian for the field φ and ε with a coupling term γ between them

$$\mathcal{H}[\varphi,\varepsilon] = \int \mathrm{d}^d x\left[\frac{1}{2}(\nabla\varphi)^2 + \frac{1}{2}r_0\varphi^2 + \frac{1}{4!}g_0\varphi^4 + \frac{1}{2}\varepsilon^2 + \frac{1}{2}\gamma\varepsilon\varphi^2\right], \tag{9.49}$$

Ω is the kinetic coefficient, $\xi(\mathbf{x},t)$ and $\zeta(\mathbf{x},t)$ zero-mean stochastic Gaussian noises with

$$\langle\xi_i(\mathbf{x},t)\xi_j(\mathbf{x}',t')\rangle = 2\Omega\,\delta(\mathbf{x}-\mathbf{x}')\delta(t-t')\delta_{ij}, \tag{9.50}$$

$$\langle\zeta(\mathbf{x},t)\zeta(\mathbf{x}',t')\rangle = -2\rho\,\Omega\,\nabla^2\delta(\mathbf{x}-\mathbf{x}')\delta(t-t')\ . \tag{9.51}$$

We note that as a consequence of Eq. (9.48), $\int \mathrm{d}^d x\,\partial_t\varepsilon(\mathbf{x},t) = 0$, i.e. $\int \mathrm{d}^d x\,\varepsilon(\mathbf{x},t)$ is constant during the dynamical evolution. Introducing a source $e(\mathbf{x})$ for $\varepsilon(\mathbf{x})$ in Eq. (9.49), i.e. adding to it a term $-e(\mathbf{x})\varepsilon(\mathbf{x})$, it is easy to see that in the stationary regime (whose probability distribution is given by $e^{-\mathcal{H}[\varphi,\varepsilon]}$ due to the fact that the relation Eq. (1.7) between noise covariance and diffusion coefficient is satisfied), ε-field static correlation functions are related to φ^2-field correlation functions. Indeed the Gaussian integral over the field ε can be computed, finding an effective Hamiltonian for the φ field, given by

$$\mathcal{H}_{\mathrm{eff}}[\varphi,e] = \int \mathrm{d}^d x\left[\frac{1}{2}(\nabla\varphi)^2 + \frac{1}{2}r_0\varphi^2 + \frac{1}{4!}(g_0-3\gamma^2)\varphi^4 + \frac{1}{2}\gamma\varphi^2 e - \frac{1}{2}e^2\right]. \tag{9.52}$$

From this expression is easy to find that

$$\langle\varepsilon(-\mathbf{q})\varepsilon(\mathbf{q})\rangle = 1 + \frac{\gamma^2}{4}\langle\varphi^2(-\mathbf{q})\varphi^2(\mathbf{q})\rangle\ , \tag{9.53}$$

which establishes the relation with two-point energy-energy $(\varphi^2-\varphi^2)$ correlation function. Moreover, from $\mathcal{H}_{\mathrm{eff}}$ we see that the coupling of $\varepsilon(\mathbf{x},t)$ to $\varphi(\mathbf{x},t)$ does not change the static properties (i.e. the correlation functions), resulting only in a shift of the bare coupling-constant value (see Ref. [4] for details).

The dynamical correlation functions, generated by the Langevin equations (9.47) and (9.48), may be obtained by means of the field-theoretical action [4], derived as described in Sect. 8.1,

$$\begin{aligned} S[\varphi,\tilde\varphi,\varepsilon,\tilde\varepsilon] = \int \mathrm{d}t\int \mathrm{d}^d x\ \Bigg[&\tilde\varphi\partial_t\varphi + \Omega\tilde\varphi\frac{\delta\mathcal{H}[\varphi,\varepsilon]}{\delta\varphi} - \tilde\varphi\Omega\tilde\varphi \\ &+ \tilde\varepsilon\partial_t\varepsilon - \rho\,\Omega\tilde\varepsilon\nabla^2\frac{\delta\mathcal{H}[\varphi,\varepsilon]}{\delta\varepsilon} + \tilde\varepsilon\rho\,\Omega\,\nabla^2\tilde\varepsilon\Bigg]\ , \end{aligned} \tag{9.54}$$

where $\tilde\varphi(\mathbf{x},t)$ and $\tilde\varepsilon(\mathbf{x},t)$ are the response field associated with $\varphi(\mathbf{x},t)$ and $\varepsilon(\mathbf{x},t)$, respectively. It is easy to read from Eq. (9.54) and (8.13) the interaction vertices, given by $-\Omega g_0\tilde\varphi\varphi^3/3!$, as in the case of Model A, $-\Omega\gamma\varepsilon\tilde\varphi\varphi$ and $\rho\Omega\gamma\,\varphi^2\nabla^2\tilde\varepsilon/2$.

In Sect. 8.3, we described in detail how it is possible to deal with the effects of a macroscopically prepared initial state on the dynamics of Model A. In Ref. [142] the same formalism was applied to Model C. Following the same line as that explained in Sect. 8.3 one has to average also over the possible initial configuration of both order parameter $\varphi_0(\mathbf{x}) = \varphi(\mathbf{x}, t = 0)$ (as in Model A) and conserved density $\varepsilon_0(\mathbf{x}) = \varepsilon(\mathbf{x}, t = 0)$ with a probability distribution $e^{-H_0[\varphi_0, \varepsilon_0]}$ given by [142]

$$H_0[\varphi_0] = \int \mathrm{d}^d x \left[\frac{\tau_0}{2} (\varphi_0(\mathbf{x}) - u(\mathbf{x}))^2 + \frac{1}{2c_0} (\varepsilon_0(\mathbf{x}) - v(\mathbf{x}))^2 \right]. \tag{9.55}$$

This specifies an initial state $u(\mathbf{x})$ for $\varphi(\mathbf{x}, t)$ and $v(\mathbf{x})$ with correlations proportional to τ_0^{-1} and c_0, respectively. To deal with a quench from high temperature we set $u = v = 0$. The response and correlation functions may be obtained as in Sect. 8.3 by a perturbative expansion of the functional weight $e^{-(S[\varphi, \tilde{\varphi}, \varepsilon, \tilde{\varepsilon}] + H_0[\varphi_0, \varepsilon_0])}$.

The propagators of the resulting theory are [142]

$$\begin{aligned} \langle \tilde{\varphi}_i(\mathbf{q}, s) \varphi_j(-\mathbf{q}, t) \rangle_0 &= \delta_{ij} R_q^0(t, s) = \delta_{ij}\, \theta(t - s) G(t - s), & (9.56) \\ \langle \varphi_i(\mathbf{q}, s) \varphi_j(-\mathbf{q}, t) \rangle_0 &= \delta_{ij} C_q^0(t, s) \\ &= \frac{\delta_{ij}}{q^2 + r_0} \left[G(|t - s|) + \left(\frac{r_0 + q^2}{\tau_0} - 1 \right) G(t + s) \right], & (9.57) \end{aligned}$$

where $G(t)$ is given by Eq. (8.26),

$$G(t) = e^{-\Omega(q^2 + r_0)t}. \tag{9.58}$$

and

$$\begin{aligned} \langle \tilde{\varepsilon}(\mathbf{q}, s) \varepsilon(-\mathbf{q}, t) \rangle_0 &= R_{\varepsilon, q}^0(t, s) = \theta(t - s) G_\varepsilon(t - s), & (9.59) \\ \langle \varepsilon(\mathbf{q}, s) \varepsilon(-\mathbf{q}, t) \rangle_0 &= C_{\varepsilon, q}^0(t, s) = G_\varepsilon(|t - s|) + (c_0 - 1) G_\varepsilon(t + s)\,, & (9.60) \end{aligned}$$

where

$$G_\varepsilon(t) = e^{-\rho\Omega(q^2 + r_0)t}. \tag{9.61}$$

As in the case of Model A, it has been shown that τ_0^{-1} is irrelevant (in the renormalization-group sense) so that, as previously done, we will set $\tau_0^{-1} = 0$ [140, 142].

9.3.2 Gaussian FDR

The Gaussian part of Model C dynamics is the same as that of Model A as far as φ and $\tilde{\varphi}$ are concerned and of Model B (with some straightforward changes due to the non-critical behavior of the conserved field) for ε and $\tilde{\varepsilon}$. From Eq. (9.57) and definition (9.1) we can straightforwardly compute the FDR associated with the order parameter relaxation[1], and it is exactly the same as that of Model A (we refer to Sect. 9.2.1 for the discussion).

[1] Of course we could compute the FDR also for the conserved density ε. Being a non-critical field, we expect it to assume the trivial value 1.

9.3.3 One-loop Computations

In this Section we compute the non-equilibrium response and correlation functions for the Model C, defined in Sect. 9.3.1, up to one loop in an ϵ-expansion. As for Model A, time homogeneity breaking leads to some technical difficulties when making use of 1PI correlation functions. So, as in Sect. 9.2, we analyze only the connected ones. At one-loop order we have to evaluate, taking into account causality [14], the ten Feynman diagrams in Figure 9.8, three for the response function ((R_1), (R_2) and (R_3)) and seven for the correlation one ($(\mathrm{C}_{1a,b})$, $(\mathrm{C}_{2a,b})$, $(\mathrm{C}_{3a,b})$ and (C_4)). Let us note that all of them may be computed in terms of only four 1PI contributions which are common to all the diagrams depicted on the same line in Figure 9.8.

Grouping these contributions we have

$$\begin{aligned} R_q(t,s) &= R_q^0(t,s) - \frac{N+2}{6} g_0(\mathrm{R}_1) + \Omega^2\gamma^2(\mathrm{R}_2) + \rho\Omega^2\gamma^2(\mathrm{R}_3) + O(g_0^2, g_0\gamma^2, \gamma^4) \,, \\ C_q(t,s) &= C_q^0(t,s) - \frac{N+2}{6} g_0[(\mathrm{C}_{1a}) + (\mathrm{C}_{1b})] + \Omega^2\gamma^2[(\mathrm{C}_{2a}) + (\mathrm{C}_{2b})] \\ &\quad + \rho\Omega^2\gamma^2[(\mathrm{C}_{3a}) + (\mathrm{C}_{3b})] + \rho\Omega^2\gamma^2(\mathrm{C}_4) + O(g_0^2, g_0\gamma^2, \gamma^4) \,. \end{aligned} \tag{9.62}$$

In order to evaluate the FDR at criticality we have to set in this perturbative expansion $r_0 = 0$ (massless theory). We set $\Omega = 1$ to lighten the notations. The first step in the calculation of the diagrams is the evaluations of the critical "bubbles" $B_{1c}(t)$, $B_{2c}(t',t'')$, $B_{3c}(t',t'')$ and $B_{4c}(t',t'')$ i.e. the 1PI parts common to diagrams depicted on the first, second, third and fourth line of Figure 9.8, respectively. We have, in generic dimension d,

$$B_{1c}(t) = \int \frac{\mathrm{d}^d q}{(2\pi)^d}\, C_q(t,t) = -\frac{1}{d/2-1}\frac{(2t)^{1-d/2}}{(4\pi)^{d/2}} = -N_d \frac{\Gamma(d/2-1)}{2^{d/2}} t^{1-d/2}, \tag{9.63}$$

where, as usual, $N_d = 2/[(4\pi)^{d/2}\Gamma(d/2)]$. Note that the equilibrium contribution to $B_c(t)$ is zero for $d > 2$. Given we are interested in the value of the FDR (9.1) for $\mathbf{q} = \mathbf{0}$, in the following we evaluate the diagrams for vanishing external momenta. Then for $B_{2c}(t,s)$, $B_{3c}(t,s)$ and $B_{4c}(t,s)$ we have

$$\begin{aligned} B_{2c}(t,s) &= \int \frac{\mathrm{d}^d q}{(2\pi)^d}\, R_q^0(t,s)\, C_{\varepsilon,q}^0(t,s) = \\ &= \theta(t-s)[4\pi\Omega(1+\rho)]^{-d/2}\left[(t-s)^{-d/2} + (c_0-1)(t-\kappa\, s)^{-d/2}\right] \,, \end{aligned} \tag{9.64}$$

$$\begin{aligned} B_{3c}(t,s) &= \int \frac{\mathrm{d}^d q}{(2\pi)^d}\, q^2\, R_{\varepsilon,q}^0(t,s)\, C_q^0(t,s) = \\ &= \theta(t-s)[4\pi\Omega(1+\rho)]^{-d/2}\left[(t-s)^{-d/2} - (t+\kappa\, s)^{-d/2}\right] \,, \end{aligned} \tag{9.65}$$

$$\begin{aligned} B_{4c}(t>s,s) &= \int \frac{\mathrm{d}^d q}{(2\pi)^d}\, C_{\varepsilon,q}^0(t,s)\, C_q^0(t,s) = \frac{N_d}{2}\Gamma(d/2-1)[\Omega(1+\rho)]^{1-d/2} \cdot \\ &\quad \cdot\left\{(t-s)^{1-d/2} - (t+\kappa\, s)^{1-d/2} + (c_0-1)[(t-\kappa\, s)^{1-d/2} - (t+s)^{1-d/2}\right\} \,, \end{aligned} \tag{9.66}$$

where $\kappa = (1-\rho)/(1+\rho) < 1$ (given that for Model C to make sense, $\rho > 0$). Expression (9.66) for $B_{4c}(t,s)$ is valid only for $t > s$, while that for $s > t$ is easily found, given the property $B_{4c}(t,s) = B_{4c}(s,t)$. Once the critical bubbles have been determined, it is easy to compute each diagram in Figure 9.8.

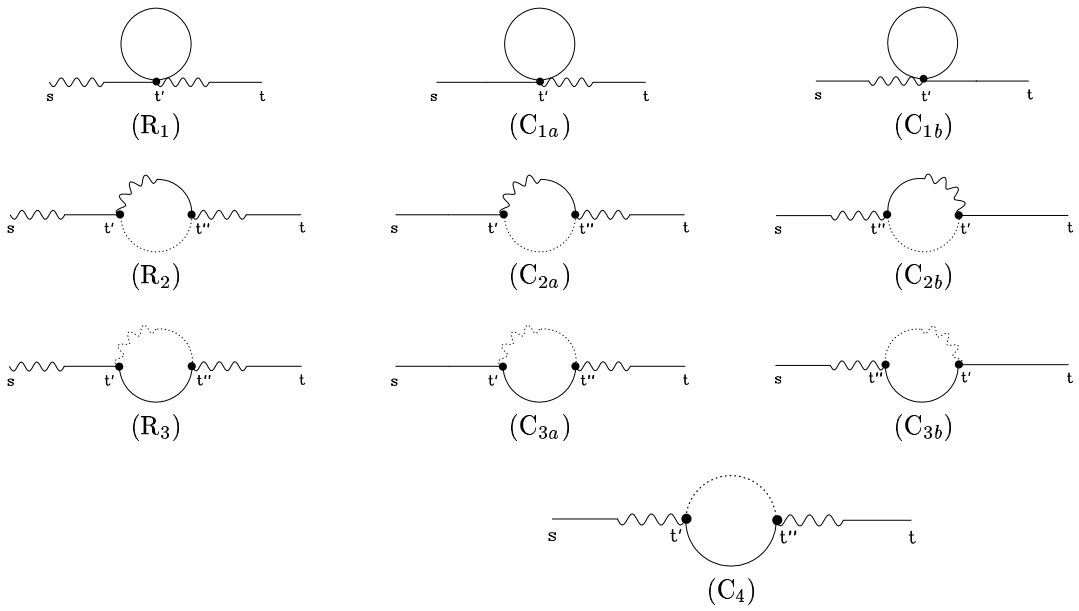

Figure 9.8: Feynman diagrams contributing to the one-loop order-parameter response ((R$_1$), (R$_2$), (R$_3$)) and correlation function ((C$_{1a,b}$), (C$_{2a,b}$), (C$_{3a,b}$), (C$_4$)). Response functions are drawn as wavy-normal lines, whereas correlators are normal lines. A wavy plain (wavy dotted) line is attached to the response field $\tilde{\varphi}$ ($\tilde{\varepsilon}$) and a normal plain (normal dotted) one to the order parameter φ (to the conserved density ε).

Performing the required integrations and expanding in powers of $\epsilon = 4-d$ we find for the critical response function

$$\begin{aligned} R_{q=0}(t,s) = &-\frac{2\tilde{\gamma_0}^2}{1+\rho}\frac{1}{\epsilon} + 1 + \left[\tilde{g}_0\frac{N+2}{24} - \tilde{\gamma_0}^2\frac{1+\rho^2-c_0}{2\rho(1+\rho)}\right]\ln\frac{t}{s} + \\ &-\frac{\tilde{\gamma_0}^2}{1+\rho}\ln[\Omega(t-s)] - \tilde{\gamma_0}^2 c_0\frac{1}{1-\rho^2}\ln\frac{1-\kappa v}{1-\kappa} + \tilde{\gamma_0}^2\mathcal{R}(s/t;\rho) + \\ &+O(\epsilon^2, \tilde{g}_0^2, \epsilon\tilde{g}_0, \tilde{\gamma}^4, \tilde{\gamma}^2\tilde{g}_0, \epsilon\tilde{\gamma}^2)\ , \end{aligned} \tag{9.67}$$

where

$$\mathcal{R}(v;\rho) = -\frac{\rho}{1-\rho^2}\ln\frac{1+\kappa v}{2} + \frac{1}{1-\rho^2}\ln\frac{1-\kappa v}{2\rho} - \frac{1}{1+\rho}\ , \tag{9.68}$$

and for the correlation function

$$\begin{aligned} C_{q=0}(t,s) \;=\; &-\frac{4\tilde{\gamma_0}^2\Omega s}{1+\rho}\frac{1}{\epsilon} + 2\Omega s\left\{1 + \tilde{g}_0\frac{N+2}{12} + \left[\tilde{g}_0\frac{N+2}{24} - \tilde{\gamma_0}^2\frac{1+\rho^2-c_0}{2\rho(1+\rho)}\right]\ln\frac{t}{s} + \right. \\ &-\frac{\tilde{\gamma_0}^2}{1+\rho}\ln[\Omega t] + \tilde{\gamma_0}^2\left[-c_0\mathcal{C}_1(\frac{s}{t};\rho) - c_0\mathcal{C}_2(\rho) - \frac{\ln[1+\rho]}{1+\rho} + \mathcal{C}_2(\rho) + \frac{1}{\rho}\mathcal{C}_2(\frac{1}{\rho})\right. \\ &\left.\left.+\mathcal{C}_1(\frac{s}{t};\rho) - \mathcal{C}_1(-\frac{s}{t};\rho)\right]\right\} + O(\epsilon^2, \tilde{g}_0^2, \epsilon\tilde{g}_0, \tilde{\gamma}^4, \tilde{\gamma}^2\tilde{g}_0, \epsilon\tilde{\gamma}^2)\ , \end{aligned} \tag{9.69}$$

where we assumed $t > s$ and we introduced $\tilde{g}_0 = N_d g_0$, $\tilde{\gamma}_0 = N_d\gamma_0$ and the functions

$$\mathcal{C}_1(v;\rho) \;=\; \frac{1+v}{2v(1+\rho)}\ln[1+v] - \frac{1-\kappa v}{2v(1+\rho)\kappa^2}\ln[1-\kappa v]\ , \tag{9.70}$$

$$\mathcal{C}_2(\rho) \;=\; -\frac{\ln[1-\kappa]}{(1-\rho)^2} - \frac{1}{(1-\rho)\rho}\ . \tag{9.71}$$

The first one is defined for $-1 < v < 1/\kappa$ and $\rho \neq 1$ (we are interested only in the case $\rho \geq 0$). We note that the contributions of $\mathcal{C}_i$ to Eq. (9.69) are regular in the limit $\rho \to 1$.

The previous expressions for the correlation and response functions have simple poles in ϵ, so renormalization of bare parameters is required. We use the minimal subtraction scheme in order to render the renormalized quantities finite for $\epsilon \to 0$. Up to one-loop order it is sufficient to perform the following renormalizations [4, 157],

$$\left\{\begin{array}{lcl} \tilde{\varphi} & \mapsto & \tilde{Z}^{-1/2}\tilde{\varphi} \\ \Omega & \mapsto & \tilde{Z}^{-1/2}\Omega \end{array}\right. \text{, with } \tilde{Z} = 1 - \frac{4\tilde{\gamma}^2}{1+\rho}\frac{1}{\epsilon} + O(\tilde{\gamma}^4, \tilde{\gamma}^2\tilde{g}, \tilde{g}^2)\ , \tag{9.72}$$

to have finite two-point functions.

In order to obtain the critical functions we have to set the renormalized couplings equal to their fixed point values. We recall the scenario of fixed points for Model C with initial condition [142]: As far as the coupling $\tilde{g}$ is concerned, there is only one stable fixed point value $\tilde{g}^*$ for $\epsilon > 0$, $\tilde{g}^* = \tilde{g}_A^* + 6\tilde{\gamma}^{2*}$, where $\tilde{g}_A^* = 6\epsilon/(N+8) + O(\epsilon^2)$ is the coupling-constant fixed-point value for Model A. In the (γ^2, ρ, c)-space, instead, we have

(I) $\alpha < 0$, i.e. $N > 4 + O(\epsilon)$ [2]: The stable fixed point for $\tilde{\gamma}$ is $\tilde{\gamma}^* = 0$, so the dynamics of the conserved density decouples from that of the order parameter and we get back to Model A (at least asymptotically).

[2] We recall that the specific-heat critical exponent for Model A is $\alpha = \frac{4-N}{2(N+8)}\epsilon + O(\epsilon^2)$ (see, e.g., Ref. [4]).

(II) $\alpha > 0$, i.e. $N < 4 + O(\epsilon)$ (see footnote 2): A non-trivial stable fixed point for $\tilde{\gamma}$ emerges,

$$\tilde{\gamma}^{2*} = \frac{4-N}{N(N+8)}\epsilon + O(\epsilon^2) \, .$$

As far as ρ is concerned we have two possible stable fixed points

(a) $N > 2 + O(\epsilon)$: $\rho^* = 0$, but this is a peculiar limit [4],

(b) $N < 2 + O(\epsilon)$: $\rho^* = 2/N - 1 + O(\epsilon)$.

It has been shown that whenever $\alpha > 0$ the fixed point value for c is $c^* = 0$ [142].

We focus our attention on the only relevant stable fixed point of the model, i.e. (IIb), for which

$$\tilde{g}^* = \frac{24}{N(N+8)}\epsilon + O(\epsilon^2). \tag{9.73}$$

9.3.4 Scaling Forms and Results

In Ref. [142] the scaling properties of the model and the effects of initial conditions are analyzed within the RG approach, along the same lines as those reviewed for Model A in Sect. 8.3. We do not give, here, any detail of the analysis but briefly sum up the results of Ref. [142]. The scaling forms predicted by the RG for the critical two-point response and correlation functions are the same as those for Model A, Eq. (8.46), with different critical exponent η, z, θ and scaling functions. We can write them as in Eq. (9.5)[3],

$$\left\{ \begin{array}{lcl} C_{q=0}(t,s) & = & A_C \, s(t-s)^a (t/s)^\theta F_C(s/t) \, , \\ R_{q=0}(t,s) & = & A_R \, (t-s)^a (t/s)^\theta F_R(s/t) \, , \end{array} \right. \tag{9.74}$$

where $a = (2-\eta-z)/z$ while A_C and A_R, as in the case of Model A (see Sect. 9.2), are non-universal amplitudes defined in such a way that $F_R(0) = F_C(0) = 1$. Given this normalization, F_R and F_C are universal. In Ref. [142] the expression for θ was determined up to two-loop order, at the fixed point with $c^* = 0$. Up to one loop, it reads

$$\theta = \tilde{g}^* \frac{N+2}{24} - \tilde{\gamma}^{2*} \frac{1+\rho^{*2}}{2\rho^*(1+\rho^*)} + O(\epsilon^2) \, . \tag{9.75}$$

The exponent a in Eq. (9.74) is given by well-known dynamical exponent for Model C (both η and z were computed up to two-loop order in Ref. [157], but recently it has been pointed out that the two-loop contribution to z is not correct, see Ref. [158]),

$$a = \frac{2-\eta-z}{z} = -\frac{\tilde{\gamma}^{2*}}{1+\rho^*} + O(\epsilon^2) \, . \tag{9.76}$$

Taking into account Eqs. (9.74), (9.75) and (9.76), the scaling functions F_R and F_C are easily identified in Eqs. (9.67) and (9.69). We find ($c^* = 0$) for the non-universal amplitudes

$$A_R = 1 + \tilde{\gamma}^{*2} \mathcal{R}(0;\rho^*) + O(\epsilon^2) \, , \tag{9.77}$$

$$\frac{A_C}{2} = 1 + \tilde{g}^* \frac{N+2}{24} + \tilde{\gamma}^{2*} \left[-\frac{\ln(1+\rho^*)}{1+\rho^*} + \mathcal{C}_2(\rho^*) + \frac{1}{\rho^*}\mathcal{C}_2(\frac{1}{\rho^*}) \right] + O(\epsilon^2) \, , \tag{9.78}$$

[3] We point out that the scaling form for $C_{q=0}(t,s)$ is written here in a slightly different form, compared to Eq. (9.5).

while, for the universal scaling functions,

$$F_R(v) = 1 + \tilde{\gamma}^{*2}[\mathcal{R}(v;\rho^*) - \mathcal{R}(0;\rho^*)] + O(\epsilon^2) \ , \tag{9.79}$$

$$F_C(v) = 1 + \tilde{g}^* \frac{N+2}{24} + \tilde{\gamma}^{2*}\left[\frac{\ln(1-v)}{1+\rho^*} + \mathcal{C}_1(v;\rho^*) - \mathcal{C}_1(-v;\rho^*)\right] + O(\epsilon^2) \ . \tag{9.80}$$

At variance with Model A [133], there is an $O(\epsilon)$ correction to F_R (cf. Eq. (9.32)). Moreover it is well-known that for the relevant fixed point of Model C, the coupling to a conserved density leads to a $O(\epsilon)$ contribution to z [157]. Computing the derivative with respect to s of the two-time correlation function and taking its ratio with the response one we have

$$\begin{aligned}\frac{1}{2}\mathcal{X}^{-1}_{q=0}(t,s) = 1 + \tilde{g}^*\frac{N+2}{24} + \tilde{\gamma}^{2*}\Bigg[&\frac{1}{1+\rho^*}\ln\frac{1-s/t}{1+\rho^*} + \mathcal{C}_2(\rho^*) + \frac{1}{\rho^*}\mathcal{C}_2(\frac{1}{\rho^*}) \\ &+ \mathcal{C}_1(\frac{s}{t};\rho^*) - \mathcal{C}_1(-\frac{s}{t};\rho^*) - \mathcal{R}(\frac{s}{t},\rho^*) + \frac{1+\rho^{*2}}{2\rho^*(1+\rho^*)}\Bigg] \\ &+ \tilde{\gamma}^{2*}\frac{s}{t}\left[\partial_1\mathcal{C}_1(\frac{s}{t},\rho^*) + \partial_1\mathcal{C}_1(-\frac{s}{t},\rho^*)\right] + O(\epsilon^2) \ .\end{aligned} \tag{9.81}$$

Note that, at variance with Model A, the result depends on the ratio s/t already at one loop..

In the limit $t \to \infty$, s fixed, we find an s-independent result, thus

$$\frac{1}{2}\mathcal{X}^{\infty\,-1}_{q=0} = 1 + \tilde{g}^*\frac{N+2}{24} + \tilde{\gamma}^{2*}\left[\frac{2\rho^*}{(1+\rho^*)(1-\rho^*)^2}\ln\frac{(1+\rho^*)^2}{4\rho^*} - \frac{1+\rho^*}{2\rho^*}\right] + O(\epsilon^2) \ . \tag{9.82}$$

Taking into account the fixed-point values of couplings we get

$$\mathcal{X}^{\infty}_{q=0} = \frac{1}{2}\left\{1 + \frac{4-N}{N(N+8)}\epsilon\left[\frac{N(N-1)}{(4-N)(2-N)} + \frac{N^2(2-N)}{4(N-1)^2}\ln[N(2-N)]\right]\right\} + O(\epsilon^2) \ . \tag{9.83}$$

For $N = 1$, which is the physically relevant case into which Model C is non-trivial, we find the following non-universal amplitudes

$$A_R = 1 - \frac{\ln 2}{6}\epsilon + O(\epsilon^2) \quad , \quad A_C = 2\left(1 - \frac{1+2\ln 2}{12}\epsilon\right) + O(\epsilon^2) \ , \tag{9.84}$$

and, for scaling functions,

$$F_R(v) = 1 - \frac{v}{6}\epsilon + O(\epsilon^2) \ , \tag{9.85}$$

$$F_C(v) = 1 + \frac{2}{3}\epsilon\left[\left(\frac{1-v}{v} + \frac{1}{4}\right)\ln(1-v) + \frac{1+v}{v}\ln(1+v) - v\right] + O(\epsilon^2). \tag{9.86}$$

The FDR turns out to be exactly the same as in Model A, $\mathcal{X}^{\infty}_{q=0} = 1/2(1-\epsilon/12) + O(\epsilon^2)$, i.e. the presence of a coupling to a conserved density does not affect the value of $\mathcal{X}^{\infty}_{q=0}$, at least up to one-loop order. Higher-loop calculations may clarify whether this fact is only a coincidence at one-loop or it is a deeper property. See Sect. 9.5 for further discussions.

9.4 Diluted Ising Model

In Sections 9.2 and 9.3 we have computed the scaling forms for the response and correlation functions in the aging regime (at least up to one-loop) and the FDR, basically for different dynamics of the

same Landau-Ginzburg Hamiltonian of an N-component order-parameter field. In this Section we extend these computations to Model A dynamics of a system with quench disorder. The extension of this kind of investigation to disordered systems is very interesting because, besides giving a check of the expected scaling laws, it predicts a new universal dynamical quantity (the long-time limit of the FDR) which could be measured in MC simulations and could be used to identify a universality class, as in the case of other universal quantities (see Sections 7.2 and 9.1).

As remarked in Sections 8.1 and 9.1, universality hypothesis implies that critical phenomena can be described in terms of quantities that do not depend on the microscopic details of the systems, but only on their global properties such as symmetries, dimensionality, etc. A question of theoretical and experimental interest is whether and how the critical behavior of a system is altered by introducing in it a small amount of uncorrelated impurities, considered as a quenched disorder.

Changes in the static critical behavior may be expected or not depending on the specific-heat exponent of the pure model, at least as long as the disorder is weak (in the sense that it is reasonable to treat it perturbatively). Indeed the Harris criterion [168] states that the addition of a small amount of quenched impurities to a system which undergoes a second-order phase transition does not change its critical behavior if the specific-heat critical exponent $\alpha_{\rm p}$ of the pure system is negative. If $\alpha_{\rm p}$ is positive, the transition is altered and its properties could change.

For the very important class of the three-dimensional $O(M)$-vector models it is known that $\alpha_{\rm p} < 0$ for $M \geq 2$ [10], and the critical behavior is unchanged by weak quenched disorder. Instead, the specific-heat exponent of the three-dimensional Ising model is positive [10], thus the existence of a new Random Ising Model (RIM) universality class is expected, as confirmed by RG analyses, MC simulations, and experimental works (see Refs. [10, 171] for a comprehensive review on the subject, and for an updated list of references).

The purely relaxational equilibrium dynamics (Model A of Ref. [1]) of this new universality class is under intensive investigation [172–176]. The dynamic critical exponent z differs from the mean-field value already at one-loop [172], at variance with the pure model. This exponent is known up to the three-loop order in a $\sqrt{\epsilon}$-expansion [175] and in the fixed-dimension ($d = 2, 3$) expansion [174], and has a value in good agreement with several MC simulations [176].

The out-of-equilibrium dynamics is, instead, less studied. The same field-theoretical methods described in Sect. 8.3 may be applied to study Model A dynamics of the suitable Hamiltonian $\mathcal{H}_\psi$ (see Eq. (9.89) below) for the diluted model (resulting in a different dynamical functional, Eq. (9.97)). In particular we are interested in the relaxation after a quench to the critical point, starting from an high-temperature disordered state. The initial-slip exponent θ has been determined up to two-loop order in Ref. [148] and the response function only at one-loop, both for conservative (Model B) and non-conservative (Model A) dynamics in Ref. [147]. Also the case with long-range interactions and quenched disorder with long-range correlations has been studied in detail in Ref. [149].

9.4.1 The Model

Before describing the field-theoretical model used to determine the critical properties of the Random Ising Model universality class, we present one possible lattice system belonging to it (see, e.g., Ref. [10]). Let us consider a ferromagnetic material described in terms of one-component spins on a lattice Λ. When non-magnetic impurities are introduced in the system they occupy lattice sites, causing a dilution of the spins. This fact can be described by introducing a set of uncorrelated random variables $\rho_i \in \{0, 1\}$, $i \in \Lambda$, such that $\rho_i = 1$ when the i-th site is occupied by a spin, 0 otherwise. The probabilities of these two occurrences are chosen equal to q and $1 - q$, so that the average spin concentration is q. The ferromagnetic Hamiltonian of this system is, assuming

nearest-neighbor interaction,

$$\mathcal{H}_q[\{s_i\};\{\rho_i\}] = -\sum_{\langle i,j\rangle} \rho_i \rho_j \; s_i s_j \; . \tag{9.87}$$

From a dynamical point of view, impurities (and thus the variables ρ_i) are assumed to be quenched, i.e. fixed on the typical time scale for the dynamics of the spins. As long as the concentration q is above the percolation threshold, the system undergoes a second-order phase transition at a temperature depending on q. The static properties of this model can be described (at least in the limit of small dilution $q \simeq 1$) by a suitable field-theoretical Hamiltonian, Eq. (9.89) [169]. In the case of microscopic non-conservative dynamics (e.g. Glauber dynamics), the corresponding one for the field-theoretical model is specified in term of the stochastic Langevin equation (as in Sections 8.3 and 9.3),

$$\partial_t \varphi(\mathbf{x},t) = -\Omega \frac{\delta \mathcal{H}_\psi[\varphi]}{\delta \varphi(\mathbf{x},t)} + \xi(\mathbf{x},t) \; , \tag{9.88}$$

where Ω is the kinetic coefficient, $\xi(\mathbf{x},t)$ a zero-mean stochastic Gaussian noise with correlations given in Eq. (8.12), and $\mathcal{H}_\psi[\varphi]$ the static Landau-Ginzburg Hamiltonian with "random temperature" [10]

$$\mathcal{H}_\psi[\varphi] = \int \mathrm{d}^d x \left[\frac{1}{2}(\nabla\varphi)^2 + \frac{1}{2}(r_0 + \psi(\mathbf{x}))\varphi^2 + \frac{1}{4!} g_0 \varphi^4 \right] . \tag{9.89}$$

Here $\psi(\mathbf{x})$ is a quenched (time-independent) spatially uncorrelated random field with Gaussian distribution and covariance $\propto w$, i.e.

$$P(\psi) = \frac{1}{\sqrt{4\pi w}} \exp\left[-\frac{\psi^2}{4w} \right] . \tag{9.90}$$

The dynamic correlation functions, generated by the Langevin equation (9.88) and averaged over the noise ξ, are obtained (as described in Sect. 8.1 and Sect. 8.3) by means of the following dynamical functional

$$S_\psi[\varphi,\tilde{\varphi}] = \int \mathrm{d}t \, \mathrm{d}^d x \left[\tilde{\varphi} \frac{\partial \varphi}{\partial t} + \Omega \tilde{\varphi} \frac{\delta \mathcal{H}_\psi[\varphi]}{\delta \varphi} - \tilde{\varphi} \Omega \tilde{\varphi} \right] . \tag{9.91}$$

To take into account the presence of an initial condition for the dynamics the same method as that described in Sect. 8.3, can be applied [148]. Thus we average over the initial configuration φ_0 with a weight $e^{-H_0[\varphi_0]}$, where

$$H_0[\varphi_0] = \int \mathrm{d}^d x \, \frac{\tau_0}{2} (\varphi_0(\mathbf{x}) - a(\mathbf{x}))^2 . \tag{9.92}$$

In this way all statistical means, for a given realization of $\psi(\mathbf{x})$, may be obtained as expectation value with the functional weight $\exp\{-(S_\psi[\varphi,\tilde{\varphi}] + H_0[\varphi_0])\} \equiv e^{-\mathcal{S}_\psi}$. For a generic observable $\mathcal{O}$, calling ϕ the set of all the fields involved in the calculation, we have

$$\langle \mathcal{O} \rangle_\psi = \frac{\int [\mathrm{d}\phi] \mathcal{O} e^{-\mathcal{S}_\psi[\phi]}}{\int [\mathrm{d}\phi] e^{-\mathcal{S}_\psi[\phi]}} \; . \tag{9.93}$$

Then, the average over all possible realizations of the noise can be computed,

$$\overline{\langle \mathcal{O} \rangle_\psi} = \int [\mathrm{d}\psi] P(\psi) \langle \mathcal{O} \rangle_\psi \; . \tag{9.94}$$

In the analysis of static critical behavior, the mean value over the quenched disorder ψ is usually computed by using the replica trick [10] which allows to transform the quenched average into an annealed one (whose computation is straightforward). If we are interested in dynamical processes the computation of the former, Eq. (9.94), is very simple. We remark that, for a generic dynamical functional $\mathcal{J}[\varphi,\tilde{\varphi}]$,

$$\int [\mathrm{d}\varphi \mathrm{d}\tilde{\varphi}] e^{-\mathcal{J}[\varphi,\tilde{\varphi}]} = 1 \,, \tag{9.95}$$

as a consequence of the fact that self-loops of the response propagator are vanishing and that all terms appearing in $\mathcal{J}[\varphi,\tilde{\varphi}]$ have at least one $\tilde{\varphi}$ (this is clear form Eq. (8.6) and from the fact that this structure is preserved by renormalization, see, e.g., Ref. [4]). Thus, Eq. (9.94) reduces to an annealed average [170], because of the denominator in Eq. (9.93) is equal to 1, whatever ψ is. The resulting effective dynamical action is given by

$$\overline{e^{-S_\psi[\varphi,\tilde{\varphi}]}} = \int [\mathrm{d}\psi] P(\psi) e^{-S_\psi[\varphi,\tilde{\varphi}]} \equiv e^{-S[\varphi,\tilde{\varphi}]} \,, \tag{9.96}$$

with the ψ-independent action [148]

$$\begin{aligned} S[\varphi,\tilde{\varphi}] = \int \mathrm{d}^d x \Bigg\{ & \int_0^\infty \mathrm{d}t\, \tilde{\varphi}[\partial_t \varphi + \Omega(r_0 - \Delta)\varphi - \Omega\tilde{\varphi}] \\ & + \frac{\Omega g_0}{3!} \int_0^\infty \mathrm{d}t\, \tilde{\varphi}\varphi^3 - \frac{\Omega^2 v_0}{2} \left(\int_0^\infty \mathrm{d}t\, \tilde{\varphi}\varphi \right)^2 \Bigg\} , \end{aligned} \tag{9.97}$$

where $v_0 \propto w$. In terms of it, the quenched average Eq. (9.94) is given by

$$\overline{\langle \cdots \rangle_\psi} = \int [\mathrm{d}\varphi \mathrm{d}\tilde{\varphi}] \cdots e^{-S[\varphi,\tilde{\varphi}]} \,. \tag{9.98}$$

The action $S[\varphi,\tilde{\varphi}]$ is similar to the standard one for Model A dynamics of the pure system Eq. (9.54) ($\mathcal{H}$ is given in Eq. (8.13)), with an extra-interaction term which is non-local in time.

The perturbative expansion is performed in terms of the two fourth-order couplings g_0 and v_0 and using the propagators of the free theory with an initial condition at $t = 0$, $\langle \tilde{\varphi}_i(\mathbf{q},s)\varphi_j(-\mathbf{q},t)\rangle_0 = \delta_{ij} R_q^0(t,s)$ and $\langle \varphi_i(\mathbf{q},s)\varphi_j(-\mathbf{q},t)\rangle_0 = \delta_{ij} C_q^0(t,s)$, given in Eqs. (8.24),(8.25) and (8.26) [140]. We observe that power counting, determined by the quadratic part of $S[\varphi,\tilde{\varphi}]$, is the same as that of the pure model and thus τ_0^{-1} is, again, irrelevant for large times behavior [140, 141, 148]. Thus, as far as the Gaussian model (tree-level quadratic action) is concerned, the theory is exactly the same as the pure Model A, discussed in Sect. 9.2. The Gaussian FDR is that reported in Eq. (9.6), and thus the remarks made in Sect. 9.2.1 applies also in this case.

9.4.2 Response and Correlation Functions

To compute the response function at one-loop order, we have to evaluate the two Feynman diagrams depicted in Fig. 9.9. In terms of them we may write

$$R_{\mathbf{q}}(t,s) = R_q^0(t,s) - \frac{1}{2} g_0(a) + v_0(b) + O(g_0^2, v_0^2, g_0 v_0) \,, \tag{9.99}$$

where we are considering the case $N = 1$ (RIM universality class), and we set $\Omega = 1$ to lighten the notation.

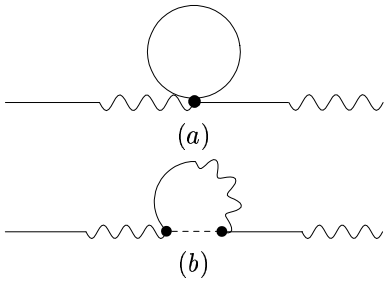

Figure 9.9: Feynman diagrams contributing to the one-loop response function. Response functions are drawn as wavy-normal lines, whereas correlators are normal lines. A wavy line is attached to the response field and a normal one to the order parameter. The dotted line is a non-local v-like vertex.

In the following we report the expressions of the Feynman diagrams at criticality ($r_0 = 0$ in dimensional regularization) for vanishing external momentum, since we are only interested in that limit, and since expressions for non-zero $\mathbf{q}$ are long and not very illuminating.

The diagram (a) in Fig. 9.9 contributes also the the response function of non-disordered models, and it has already been computed in Sect. 9.2.2 [132], obtaining (for $t > s$):

$$(a) = -N_d \frac{1}{4} \log \frac{t}{s} + O(\epsilon). \tag{9.100}$$

where $N_d = 2/[\Gamma(d/2)(4\pi)^{d/2}]$. For the diagram (b) we find

$$\begin{aligned}(b) &= \int_0^\infty \mathrm{d}t' \, \mathrm{d}t'' \int \frac{\mathrm{d}^d p}{(2\pi)^d} R^0_{q=0}(t,t') R_{\mathbf{p}}(t',t'') R^0_{q=0}(t'',s) \\ &= \frac{1}{(4\pi)^{d/2}} \frac{1}{1-d/2} \frac{1}{2-d/2} (t-s)^{2-d/2} \,. \end{aligned} \tag{9.101}$$

Inserting the expression for (a) and (b) in Eq. (9.99) and expanding (b) at first order in $\epsilon = 4-d$, one obtains

$$R_B(t,s) = 1 + \tilde{g}_0 \frac{1}{8} \ln \frac{t}{s} - \frac{\tilde{v}_0}{2} \left[\frac{2}{\epsilon} + \log(t-s) + \gamma_E \right] + O(\epsilon^2, \epsilon\tilde{g}_0, \epsilon\tilde{v}_0, \tilde{g}_0^2, \tilde{v}_0^2, \tilde{g}_0\tilde{v}_0) \,, \tag{9.102}$$

where $\tilde{g}_0 = N_d g_0$ and $\tilde{v}_0 = N_d v_0$.

There are five diagrams contributing to the correlation function. Four of them are obtained by the ones of Fig. 9.9 changing one of the two external response propagators with a correlation line (see Ref. [133] and Section 9.2.4 for a detailed explanation of this correspondence). We call these four diagrams (a_1), (a_2), (b_1), and (b_2). The sum $(a_1) + (a_2)$ was computed in Sect. 9.2.2 [132] leading to

$$(a_1) + (a_2) = -\frac{N_d}{2} s \left(\log \frac{t}{s} + 2 \right) + O(\epsilon) \,. \tag{9.103}$$

The sum $(b_1) + (b_2)$ is, instead,

$$(b_1) + (b_2) = -N_d \Gamma(d/2 - 3)[t^{3-d/2} + s^{3-d/2} - (t-s)^{3-d/2}]. \tag{9.104}$$

The octopus diagram in Fig 9.10 does not have a corresponding one contributing to the response function. It has the value

$$(c) = \frac{N_d \Gamma(d/2)}{(1-d/2)(2-d/2)(3-d/2)} \left[\frac{(t-s)^{3-d/2} + (t+s)^{3-d/2}}{2} - t^{3-d/2} - s^{3-d/2} \right] . \tag{9.105}$$

Collecting together these contributions and expanding in powers of ϵ, we find

$$\begin{aligned} C_B(t,s) =& 2s - \frac{g_0}{2}[(a_1)+(a_2)] + v_0[(b_1)+(b_2)+(c)] + O(g_0^2, v_0^2, g_0 v_0) \\ =& 2s + \frac{\tilde{g}_0}{4} s \left(\log \frac{t}{s} + 2 \right) + \tilde{v}_0 \Big[- \frac{2s}{\epsilon} - (\gamma_E - 1)s \\ &+ \frac{(t-s)\log(t-s)}{2} - \frac{(t+s)\log(t+s)}{2} \Big] + O(\epsilon^2, \epsilon\tilde{g}_0, \epsilon\tilde{v}_0, \tilde{g}_0^2, \tilde{v}_0^2, \tilde{g}_0\tilde{v}_0). \end{aligned} \tag{9.106}$$

The dimensional poles in Eqs. (9.102) and (9.106) can be canceled by a multiplicative renormalization of the fields φ, $\tilde{\varphi}$ and of the parameter Ω [148, 173, 175].

$$\left\{ \begin{array}{lcl} \varphi & \mapsto & Z^{1/2}\varphi \, , \\ \tilde{\varphi} & \mapsto & \tilde{Z}^{1/2}\tilde{\varphi} \, , \\ \Omega & \mapsto & (Z/\tilde{Z})^{1/2}\Omega \, , \end{array} \right. \quad \text{with} \quad \left\{ \begin{array}{lcl} Z & = & 1 + O(\tilde{v}_0^2, \tilde{g}_0^2, \tilde{g}_0\tilde{v}_0) \, , \\ \tilde{Z} & = & 1 + 2\frac{\tilde{v}_0}{\epsilon} + O(\tilde{v}_0^2, \tilde{g}_0^2, \tilde{g}_0\tilde{v}_0) \, . \end{array} \right. \tag{9.107}$$

For the response and correlation functions, these renormalizations imply

$$R(t,s) = Z^{-1/2}\tilde{Z}^{-1/2} R_B(t,s) \quad \text{and} \quad C(t,s) = Z^{-1/2} C_B(t,s) \, . \tag{9.108}$$

We remark that as far as the two point functions are concerned, bare ($\tilde{g}_0$, $\tilde{v}_0$) and renormalized ($\tilde{g}$, $\tilde{v}$) coupling constants are the same at this order in perturbation theory, i.e. $\tilde{g}_0 = \tilde{g} + O(\tilde{g}^2)$ and $\tilde{v}_0 = \tilde{v} + O(\tilde{v}^2)$. The critical response and correlation functions in ϵ-expansion are then obtained by setting the renormalized couplings at their fixed-point values. We remind that the stable fixed point of the RIM is of order $\sqrt{\epsilon}$ and not ϵ (see, e.g., Ref. [10]), due to the degeneracy of the one-loop β functions. The non-trivial fixed point values at the first non-vanishing order (i.e. two loops) are (see, e.g., Ref. [148])

$$\tilde{g} = \tilde{g}^* = 4\sqrt{\frac{6\epsilon}{53}} + O(\epsilon) \, , \; \tilde{v} = \tilde{v}^* = \sqrt{\frac{6\epsilon}{53}} + O(\epsilon). \tag{9.109}$$

Thus, we obtain

$$R(t,s) = 1 + \frac{1}{2}\sqrt{\frac{6\epsilon}{53}} \left[\ln \frac{t}{s} - \ln(t-s) - \gamma_E \right] + O(\epsilon) \, , \tag{9.110}$$

and

$$\frac{C(t,s)}{2} = s \left\{ 1 + \frac{1}{2}\sqrt{\frac{6\epsilon}{53}} \left[\log \frac{t}{s} + 3 - \gamma_E - \log(t-s) + \frac{t+s}{2s} \log \frac{t-s}{t+s} \right] \right\} + O(\epsilon) \, . \tag{9.111}$$

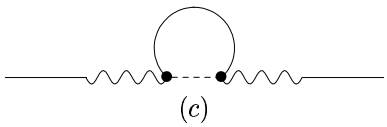

(c)

Figure 9.10: Feynman diagram contributing to the one-loop correlation function that does not have analogous in the response.

9.4.3 Scaling Forms and Results

In Refs. [147,148] the effects of initial conditions on the scaling properties of Model A with random impurities was studied within the RG approach. This analysis is done in Ref. [147] by applying the older standard method to deal with dynamical critical phenomena (see, e.g., S. K. Ma in Ref. [5]) while in Ref. [148] the analysis is carried out along the same lines as those reviewed for Model A in Sect. 8.3. We do not give, here, any detail of this analysis (discussed in some detail for Model A) but briefly sum up the results. The scaling forms predicted by RG for the critical two-point response and correlation functions are the same as those for Model A (Eq. (8.46)), with different critical exponent η, z, θ and scaling functions. We can write them as in Eq. (9.74),

$$\begin{cases} C_{q=0}(t,s) &= A_C\, s(t-s)^a (t/s)^\theta F_C(s/t)\,, \\ R_{q=0}(t,s) &= A_R\, (t-s)^a (t/s)^\theta F_R(s/t)\,, \end{cases} \tag{9.112}$$

where $a = (2-\eta-z)/z$ while A_C and A_R are, as in the case of Model A (see Sect. 9.2), non-universal amplitudes defined in such a way that $F_R(0) = F_C(0) = 1$. Given this normalization F_R and F_C are universal. In Ref. [147] θ was computed up to one-loop order and in Ref. [148] the computation was extended up to two loops (i.e. up to $O(\epsilon)$). At the order we are interested in its value is (at the fixed point Eq. (9.109))

$$\theta = \frac{1}{2}\sqrt{\frac{6\epsilon}{53}} + O(\epsilon)\,. \tag{9.113}$$

The exponent a in Eq. (9.112) is given in terms of exponents known in $\sqrt{\epsilon}$-expansion up to three-loop [175][4] in the case of static ones (η, required here, and ν) and up to two-loop for the dynamic exponent z [147,175]. At $O(\sqrt{\epsilon})$ it is

$$a = \frac{2-\eta-z}{z} = -\frac{1}{2}\sqrt{\frac{6\epsilon}{53}} + O(\epsilon)\,. \tag{9.114}$$

Taking into account Eqs. (9.112), (9.113) and (9.114), the scaling functions F_R and F_C are easily identified in Eqs. (9.110) and (9.111). We find the results $F_R(x) = 1 + O(\epsilon)$ and

$$A_R = 1 - \frac{1}{2}\sqrt{\frac{6\epsilon}{53}}\gamma_E + O(\epsilon)\,, \tag{9.115}$$

which are consistent, in the limit $q \to 0$, with the result of Ref. [147] about the q-dependent scaling form of the two-time response function (see Eq. (20) therein). For the two-time correlation function (in Ref. [147] only the structure factor $C_q(t,t)$ was considered), instead, the non-universal amplitude is given by

$$\frac{A_C}{2} = 1 + \frac{1}{2}\sqrt{\frac{6\epsilon}{53}}(2-\gamma_E) + O(\epsilon)\,, \tag{9.116}$$

while the universal regular scaling function is

$$F_C(x) = 1 + \frac{1}{2}\sqrt{\frac{6\epsilon}{53}}\left[1 + \frac{1}{2}\left(1+\frac{1}{x}\right)\log\frac{1-x}{1+x}\right] + O(\epsilon)\,, \tag{9.117}$$

which agrees with the result in Eq. (25) of Ref. [147], with $q = 0$, in the limit $t \to s$. Note that at variance with the pure model [132,133], the function $F_C(x)$ has a correction already at one-loop order which should be observable in MC simulations.

[4] Three-loop expansions have been determined in fixed dimension $d = 3$. See Ref. [174].

Using the definition (9.1) we compute the FDR for finite times,

$$\frac{\mathcal{X}^{-1}_{\mathbf{q}=\mathbf{0}}(t,s)}{2} = 1 + \frac{1}{2}\sqrt{\frac{6\epsilon}{53}}\left[1 + \frac{1}{2}\log\frac{t-s}{t+s}\right] + O(\epsilon)\ . \tag{9.118}$$

In the limit

$$\mathcal{X}^{\infty}_{\mathbf{q}=0} = \frac{1}{2} - \frac{1}{4}\sqrt{\frac{6\epsilon}{53}} + O(\epsilon)\ , \tag{9.119}$$

that, for $\epsilon = 1$ leads to $\mathcal{X}^{\infty}_{\mathbf{q}=0} \sim 0.416$, and ~ 0.381 for $\epsilon = 2$. It would be interesting to see if this one-loop result is in as good agreement with MC simulations as in the case of the pure model (cf. Refs. [132, 133]). To this order it is not even clear whether randomness really changes in a sensible way the limit of the FDR or not. Two-loop computations and MC simulations could clarify this point.

9.5 Summary and Conclusions

In this Section we summarize the results obtained for the models of dynamics previously described.

We have applied well-known field-theoretical methods in order to determine the new universal quantity X^{∞} (see Sect. 7.2 and 9.1) associated with the relaxational dynamics of a critical system after a quench from high temperature[5]. Our results extend previous studies of this quantity, summed up in Table 7.1, mainly based on exact solutions of simple models and on Monte Carlo simulations. The main virtue of the method applied here is that it allows to deal with systems that could be very difficultly solved exactly. On the other hand, only perturbative expressions can be found for X^{∞} and as a consequence to obtain reliable numerical estimates an higher-order loop expansion is required. We can note, however, that in some cases the one-loop result reproduces quite well the numerical value determined by Monte Carlo simulations (see Sect. 9.2.5).

We report in Table 9.1 the results obtained in the previous Sections for X^{∞}, in the form of an ϵ-expansion around the upper critical dimension which is 4 for all the models considered.
We refer to Sect. 9.2.5 for a comparison between the numerical estimates derived from our series for Model A and those obtained by Monte Carlo simulations of the Ising Model (with Glauber dynamics).

Some observations on our results are in order:

- We observe that in all the cases analyzed, the critical fluctuation-dissipation ratio in the aging regime turns out to be a number less than 1/2 (which is the value obtained for the free-field theory). To our knowledge there is neither a general proof or an argument showing that this result should be expected, nor any evidence against it.

- For Model C the result up to one-loop is the same as that for Model A with $N = 1$ (see Tab. 9.1). A two-loop computation would be very useful to determine whether this is simply a coincidence or a deeper property of the model. A comparison with Monte Carlo results (not yet available in the literature) could be useful as well.

- For the RIM the one-loop fluctuation-dissipation ratio is numerically very close to that for the pure model (Model A with $N = 1$). It is not clear whether the randomness present in the system really changes the fluctuation-dissipation ratio or not. Higher-loop computation and Monte Carlo simulations could be very useful to clarify this point.

[5] Very recently, the related problem of the long-time behavior of a Spherical Model in contact with a thermal bath having a time-dependent temperature, has been considered [130]. This correspond to the non-ideal case of a "slow" quench.

Model		$(2X^\infty)^{-1}$
Model A, $O(N)$ [a]	[132, 133]	$1+\frac{N+2}{4(N+8)}\epsilon+\epsilon^2\frac{N+2}{(N+8)^2}\left[\frac{N+2}{8}+\frac{3(3N+14)}{4(N+8)}+c^{\#}\right]+O(\epsilon^3)$
Model C [b,†]	[134]	$1+\frac{1}{12}\epsilon+O(\epsilon^2)$
RIM [c,‡]	[135]	$1+\frac{1}{2}\sqrt{\frac{6}{53}}\sqrt{\epsilon}+O(\epsilon)$

Table 9.1: $(2X^\infty)^{-1}$ for the field-theoretical models considered in [a] Sect. 9.2, [b] Sect 9.3 and [c] Sect. 9.4.# For the expression of this constant see Eq. (9.44). † We report only the result in the physically relevant case $N = 1$. ‡ With Model A dynamics.

We would stress here the relevance of our results for the problem of the validity of LSI, briefly introduced in Section 8.4. We recall that, assuming the covariance of the response function under a group of local anisotropic scale transformations, it is possible to determine its general form. In the cases we are interested in, i.e. those in which the time homogeneity is broken, the predictions of LSI are given in Eqs. (8.50), (8.51) and (8.52). As a consequence, we should expect that $F_R(v)$ in Eq. (9.45) for Model A, in Eq. (9.74) form Model C and in Eq. (9.112) for the RIM, are equal to 1, independently of v. This is not the case at least for Model A and Model C, in which a non-trivial dependence on v is explicitly found at two- and one-loop, respectively (cf. Eq. (9.32) for Model A and Eq. (9.85) for Model C). In the case of the RIM, instead, we do not find any correction to the value 1 at one-loop order, and thus LSI could hold. One possible objection [165] to these conclusions is that to compare our results in momentum space with the prediction coming from LSI as given in Eqs. (8.50) and (8.51), we have to Fourier-transform these scaling forms and take the limit $q \to 0$. This operation could not be safe if the starting formulas are singular. To reply to this criticism one should work out the full q-dependence of the response function and show explicitly that, at least at the perturbative order considered, it is Fourier-transformable. In the case of Model A the computation of this dependence up to two-loop is very difficult and the same is true for Model C up to one-loop. It is possible, however, to show that in simpler models the q-dependent response function does not agree with the LSI prediction already at one-loop and it is Fourier transformable [136]. Moreover we believe that also in the general case the generic large momentum behavior of the correlation function is exponentially decreasing (for generic times), so that its Fourier transform can be always computed. Thus, if the comparison is safe as we think, we have to account for the good agreement between the LSI predictions and the MC simulations for the two- and three-dimensional Ising model (with Glauber dynamics) in the aging regime, reported in Ref. [164] (see also Ref. [160]). In terms of the field-theoretical models analyzed, it corresponds to Model A dynamics of the $O(N)$ model with $N = 1$, whose scaling function is given in Eq. (9.32). We observe that, as remarked in Sect. 9.2.3, F_R, the scaling function of the response one, differs from 1 at $O(\epsilon^2)$. Furthermore, the correction bears a very small prefactor that makes it at most $\sim \epsilon^2/35$. Although not quantitative, from this result we can conclude that the dependence of $F_R(v)$ on v is expected quite small and thus difficult to be observed in Monte Carlo simulations. So the observed agreement with LSI could be more apparent than real. Note that in the case of Model C the correction to F_R are bigger by a factor ~ 6 in three dimensions and ~ 3 in two dimensions. A Monte Carlo simulation of this model could be helpful to detect deviations from LSI predictions. The nature of the above mentioned disagreement between perturbative results and LSI could be

probably found in the limits of applicability of the latter[6] which have not yet been investigated in the literature.

[6]A criticism of LSI, based on the disagreement between its prediction for critical exponents of Lifshitz points and field-theoretical calculation can be found in Ref. [166], see also Sect. 8.4.

Chapter 10

Model A: Two-loop Integrals

10.1 Some One-loop Results

We summarize here the main analytical results useful for the computation of the correlation and response functions for $r_0 \geq 0$ (i.e. at criticality or in the high-temperature phase) at one-loop order. Again one has to perform all the needed integrations over the times, as in Eq. (9.9) with the free field correlator and response functions given in Eqs. (8.24) and (8.25). At variance with the critical theory a renormalization of the parameter r_0 is now required to cancel the dimensional poles both in R_q and C_q.

Let us introduce the function

$$Y(t) \equiv \int_0^t \mathrm{d}\tau \, B(\tau) \; , \tag{10.1}$$

and

$$W(t) \equiv \int_0^t \mathrm{d}\tau \, G(-2\tau) \, B(\tau) \; , \tag{10.2}$$

where $G(t)$ and $B(t)$ are given in Eq. (8.26) and (9.21), respectively. In terms of Y and W we obtain (for $t > s$ and $\tau_0^{-1} = 0$, $\Omega = 1$), making reference to Fig. 9.1 in Sect. 9.2.2,

$$(a) = G(t-s)[Y(t) - Y(s)] \; , \tag{10.3}$$

and

$$(b) + (c) = \frac{1}{q^2 + r_0} \left\{ G(t-s)[Y(t) - Y(s)] - G(t+s)[Y(t) + Y(s)] + 2G(t+s)W(s) \right\} \; . \tag{10.4}$$

In the following with Y and W we mean also their analytic continuation in d.

An explicit computation leads to

$$Y(t) = \frac{r_0^{d/2-2}}{2(4\pi)^{d/2}} \left\{ (2r_0 t + d/2 - 1)[\Gamma(1 - d/2) - \Gamma(1 - d/2, 2r_0 t)] + (2r_0 t)^{1-d/2} e^{-2r_0 t} \right\} \; , \tag{10.5}$$

and

$$W(t) = \frac{1}{2(4\pi)^{d/2}} \frac{r_0^{d/2-1}}{q^2 + r_0} \Big\{ G(-2t)[\Gamma(1 - d/2) - \Gamma(1 - d/2, 2r_0 t)] - (q^2/r_0)^{d/2-1} \Delta(1 - d/2, 2q^2 t) \Big\} \; , \tag{10.6}$$

where we have introduced

$$\Delta(v,w) \equiv \int_0^w \mathrm{d}\tau\, \tau^{v-1}\, e^{\tau} \tag{10.7}$$

(for $v \leq 0$ its analytic continuation has to be considered).

Expanding Eqs. (10.5) and (10.6) in $\epsilon = 4-d$, we obtain

$$2(4\pi)^{d/2} Y(t) = -\frac{2}{\epsilon}(2r_0 t+1) - (2r_0 t+1)[\gamma(2r_0 t) - \ln r_0] + 1 + \frac{e^{-2r_0 t}}{2r_0 t} + O(\epsilon)\ , \tag{10.8}$$

and

$$\begin{aligned} &2(4\pi)^{d/2}(q^2+r_0)W(t) = \\ &\quad = -\frac{2}{\epsilon}[r_0 G(-2t) + q^2] + q^2[\ln q^2 - \delta(2q^2 t)] - r_0 G(-2t)[\gamma(2r_0 t) - \ln r_0] + O(\epsilon)\ , \end{aligned} \tag{10.9}$$

where

$$\gamma(v) \equiv 1 + e^{-v}\left(\ln v + \frac{1}{v}\right) + \int_0^v \mathrm{d}\xi\, \ln\xi\, e^{-\xi}\ , \tag{10.10}$$

and

$$\delta(v) \equiv 1 + e^{v}\left(\ln v - \frac{1}{v}\right) - \int_0^v \mathrm{d}\xi\, \ln\xi\, e^{\xi}\ . \tag{10.11}$$

It is easy to find that $h(v)$ in Eq. (9.12) is related to $\delta(v)$ by

$$h(v) = 2\left[1 + \ln v - \delta(v) - \frac{e^v}{v}\right]\ . \tag{10.12}$$

Plugging Eqs. (10.8) and (10.9) into Eqs. (10.3) and (10.4) and then into Eq. (9.7) it is easy to realize that to cancel the dimensional poles both in $R_q(t,s)$ and $C_q(t,s)$ a renormalization of the bare mass r_0 is sufficient (at least in the case $\tau_0^{-1} = 0$ we are considering)

$$r_0 = Z_r r \quad \text{with} \quad Z_r = 1 + \frac{N+2}{3}\frac{g_0}{(4\pi)^{d/2}}\frac{1}{\epsilon} + O(g_0^2)\ , \tag{10.13}$$

in agreement with what one would expect from the corresponding static field theory (see, for instance, Ref. [4]). All the previously stated results easily follow from the explicit expressions given above.

10.2 Connected Diagrams for the Response Function

The four diagrams contributing to the response function up to the two-loop order are reported in Fig. 9.2. The one-loop diagram was already discussed in Ref. [132] and Sect. 9.2.2. The expression of the critical bubble (i.e. for the 1PI part of the diagram) is given in Eq. (9.8). Thus the full connected one-loop diagram for the response function is given by Eq. (9.9), (b), i.e.

$$\begin{aligned} R^{1,1}(t,s) &= \int_s^t \mathrm{d}t' B_c(t') = -N_d \frac{\Gamma(d/2-1)}{2^{d/2}(2-d/2)}(t^{2-d/2} - s^{2-d/2}) \\ &= -N_d \frac{1}{4}\left[\log\frac{t}{s} + \frac{\epsilon}{2}\left((\gamma_E + \log 2 + \log t)\log\frac{t}{s} - \frac{1}{2}\log^2\frac{t}{s}\right)\right] + O(\epsilon^2)\ . \end{aligned} \tag{10.14}$$

From these one-loop expressions, it is quite simple to compute the two-loop integrals $R^{2,1}$ and $R^{2,2}$ of Fig. 9.2. Indeed the two-loop critical bubble (the 1PI part of $R^{2,1}$) can be computed in terms of $B_c(t)$ as

$$B_{c2}(t) = \int \frac{\mathrm{d}^d q_1}{(2\pi)^d} \int_0^\infty \mathrm{d}t' \; B_c(t') R^0_{q_1}(t,t') C^0_{q_1}(t,t') = N_d^2 \frac{b(d)}{4-d} t^{3-d} \,, \tag{10.15}$$

where

$$b(d) = \frac{\Gamma^2(d/2-1)}{2^{d-1}} \left[1 - \frac{(4-d)\Gamma^2(2-d/2)}{2\Gamma(4-d)} \right] = -\frac{1}{8} \left[1 + \epsilon(\log 2 + \gamma_E) + O(\epsilon^2) \right]. \tag{10.16}$$

By means of this expression, we compute $R^{2,1}$ taking into account the external legs with $q = 0$

$$R^{2,1}(s,t) = \int_s^t \mathrm{d}t' B_{2c}(t') = N_d^2 b(d) \frac{t^{4-d} - s^{4-d}}{(4-d)^2} \,, \tag{10.17}$$

that near four dimensions has the following series expansion

$$R^{2,1}(s,t) = \frac{N_d^2}{8} \left[-\log\frac{t}{s} \left(\frac{1}{\epsilon} + \log t + \log 2 + \gamma_E \right) + \frac{1}{2} \log^2 \frac{t}{s} \right] + O(\epsilon). \tag{10.18}$$

The computation of $R^{2,2}$ is simple once the expressions for $R^{1,1}$ and $B_c(t)$ are known. Indeed, from Eq. (10.14), we obtain

$$R^{2,2}(s,t) = \int_s^t \mathrm{d}t' R^{1,1}(t,t') B_c(t') = N_d^2 \frac{\Gamma^2(d/2-1)}{2^{d-1}} \left[\frac{t^{2-d/2} - s^{2-d/2}}{4-d} \right]^2 \,, \tag{10.19}$$

that is, expanding in ϵ,

$$R^{2,2}(s,t) = N_d^2 \frac{1}{32} \log^2 \frac{t}{s} + O(\epsilon) \,. \tag{10.20}$$

The last diagram $R^{2,3}$ is more difficult to be worked out and it requires a long calculation whose main steps are described in what follows. First of all we evaluate its 1PI contribution called $O_1(t,s)$

$$\begin{aligned} O_1(t,s) &= \int \frac{\mathrm{d}^d q_1}{(2\pi)^d} \int \frac{\mathrm{d}^d q_2}{(2\pi)^d} C^0_{q_1}(t,s) C^0_{q_2}(t,s) R^0_{q_1+q_2}(t,s) \\ &= \theta(t-s) \int \frac{\mathrm{d}^d q_1}{(2\pi)^d} \frac{\mathrm{d}^d q_2}{(2\pi)^d} \frac{1}{q_1^2 q_2^2} (e^{-q_1^2(t-s)} - e^{-q_1^2(t+s)})(e^{-q_2^2(t-s)} - e^{-q_2^2(t+s)}) e^{-(q_1+q_2)^2(t-s)} \\ &= \theta(t-s) \left[(t-s)^{2-d} J_d(1,1) + (t+s)^{2-d} J_d\left(1, \frac{t-s}{t+s}\right) - 2(t-s)^{2-d} J_d\left(\frac{t+s}{t-s}, 1\right) \right] \,, \end{aligned} \tag{10.21}$$

where

$$J_d(a,b) = \int \frac{\mathrm{d}^d q_1}{(2\pi)^d} \int \frac{\mathrm{d}^d q_2}{(2\pi)^d} e^{-q_1^2 - a q_2^2 - b(q_1+q_2)^2} = N_d^2 [(1+b)(a+b)]^{1-\frac{d}{2}} F_d\left(\frac{4b^2}{(b+1)(a+b)} \right) \,, \tag{10.22}$$

and

$$F_d(x) = \frac{\Gamma(d/2)}{4} \int_0^\infty \mathrm{d}s s^{d/2-2} e^{sx/4} \Gamma(0,s) = \frac{\Gamma(d/2)\Gamma(d/2-1)}{2(d-2)} \, {}_2F_1\left(\frac{d}{2} - 1, \frac{d}{2} - 1, \frac{d}{2}, \frac{x}{4} \right) \,. \tag{10.23}$$

In particular, for our calculations, we are interested in the limits

$$F_4(x) = -\frac{\log(1-x/4)}{x}, \tag{10.24}$$

$$F_{4-\epsilon}(1) = \log\frac{4}{3} + \epsilon\left[\left(\gamma_E - \frac{1}{2}\right)\log\frac{4}{3} - \frac{1}{4}\log^2\frac{4}{3} + \frac{1}{2}\mathrm{Li}_2\left(\frac{1}{4}\right)\right] + O(\epsilon^2)\,, \tag{10.25}$$

$$F_d(0) = \frac{\Gamma^2(d/2-1)}{4}. \tag{10.26}$$

Here $\mathrm{Li}_2(z)$ is the standard dilogarithm, defined as

$$\mathrm{Li}_2(z) = \sum_{k=1}^{\infty}\frac{z^k}{k^2}\,. \tag{10.27}$$

The final expression for $O_1(t,s)$, in generic dimension, is

$$O_1(t,s) = \frac{N_d^2\,\theta(t-s)}{2^{d-2}}\left[F_d(1)(t-s)^{2-d} + t^{2-d}F_d\left(\left(\frac{t-s}{t}\right)^2\right) - 2(t(t-s))^{1-d/2}F_d\left(\frac{t-s}{t}\right)\right]\,. \tag{10.28}$$

The full connected diagram $R^{2,3}(s,t)$ is thus given by the following expression

$$R^{2,3}(s,t) = \int_s^t \mathrm{d}t'' \int_{t''}^t \mathrm{d}t' O_1(t',t'') = N_d^2(A_1(s,t) + A_2(s,t) - 2A_3(s,t)), \tag{10.29}$$

where

$$A_1(s,t) = 2^{2-d}F_d(1)\frac{(t-s)^{4-d}}{(4-d)(3-d)}\,, \tag{10.30}$$

$$A_2(s,t) = 2^{2-d}t^{4-d}\int_{s/t}^1 \mathrm{d}y\, y^{3-d}\int_y^1 \mathrm{d}z\, z^{d-4}F_d((1-z)^2) = 2^{2-d}t^{4-d}I_1(s/t)\,, \tag{10.31}$$

$$A_3(s,t) = 2^{2-d}t^{4-d}\int_{s/t}^1 \mathrm{d}y\, y^{3-d}\int_y^1 \mathrm{d}z\, z^{d-4}(1-z)^{1-d/2}F_d(1-z) = 2^{2-d}t^{4-d}I_2(s/t)\,. \tag{10.32}$$

The evaluation of the two functions $I_1(v)$ and $I_2(v)$ is rather cumbersome but algebraically trivial. After some calculations one gets

$$I_1(v) = \frac{\Gamma^2(d/2-1)}{4}[\log v(8\log 2 - 6\log 3) + f_1(v) + O(\epsilon)], \tag{10.33}$$

$$I_2(v) = \frac{\Gamma^2(d/2-1)}{4}\left[-\frac{2}{\epsilon}\log v - \log^2 v - (1 - 6\log 2 + 3\log 3)\log v + f_2(v) + O(\epsilon)\right], \tag{10.34}$$

where $f_i(v)$ are given by

$$f_1(v)/4 = \log v\int_0^v \mathrm{d}z\, F_4((1-z)^2) + \int_v^1 \mathrm{d}z\,\log z\, F_4((1-z)^2), \tag{10.35}$$

$$f_2(v)/4 = \log v\int_0^v \mathrm{d}z\,\frac{F_4(1-z)-1}{1-z} + \int_v^1 \mathrm{d}z\,\frac{\log z}{1-z}[F_4(1-z)-1] + \int_v^1 \mathrm{d}z\frac{\log(1-z)}{z}, \tag{10.36}$$

and in particular these are regular functions in the limit $v \to 0$

$$f_1(0) = \log^2 2 + \log^2 \frac{8}{3} + 3\mathrm{Li}_2(1/4) - 4\mathrm{Li}_2(2/3)\,, \tag{10.37}$$

$$f_2(0) = -\frac{\pi^2}{6} + \frac{3}{2}\log^2 \frac{4}{3} - \mathrm{Li}_2(1/4). \tag{10.38}$$

Inserting all these contributions in Eq. (10.29), we get

$$\begin{aligned}\frac{4R^{2,3}(s,t)}{N_d^2} = -\frac{1}{\epsilon}\left(\log\frac{4}{3} + \log\frac{t}{s}\right) - \log\frac{4}{3}(\log(t-s) + \gamma_E) \\ - (\frac{1}{2} + \gamma_E + \log t)\log\frac{t}{s} + \frac{1}{2}\log^2\frac{t}{s} + \frac{f(s/t)}{4} + O(\epsilon),\end{aligned} \tag{10.39}$$

with

$$f(v) = f_1(v) - 2f_2(v) - \log\frac{4}{3}(2 + \log 12) - 2\mathrm{Li}_2(1/4), \tag{10.40}$$

$$f(0) = \frac{\pi^2}{3} - 2\log\frac{4}{3} + 3\log^2 2 - \log^2\frac{8}{3} + 3\mathrm{Li}_2(1/4) - 4\mathrm{Li}_2(2/3) = 0.663707\ldots. \tag{10.41}$$

10.3 Connected Diagrams for the FDR

In this Appendix we evaluate the rest of the diagrams required for the computation of the FDR. We do not evaluate the full integral for the correlation function, since we make use of the trick explained in details in Section 9.2.4. For this reason we consider first those diagrams contributing also to the response function and we evaluate only their extra-contributions (given by $\int_0^\infty \mathrm{d}t''t''D_i(t'',s)$ in Eq. (9.33) and denoted with the subscript "e" in what follows) to the derivative of the correlation function. For the first three diagrams these contributions are very simple:

$$(\partial C)_e^{1,1} = sB_c(s) = N_d\left[-\frac{1}{4} - \frac{\epsilon}{8}(\log s + \gamma_E + \log 2)\right] + O(\epsilon^2)\,, \tag{10.42}$$

$$(\partial C)_e^{2,1} = \int_0^s \mathrm{d}t''t''B_c(t'')B_c(s) = N_d^2\frac{\Gamma^2(d/2-1)}{2^d(3-d/2)}s^{4-d} = \frac{N_d^2}{16} + O(\epsilon), \tag{10.43}$$

$$(\partial C)_e^{2,2} = sB_{c2}(s) = -N_d^2\frac{1}{8}(\frac{1}{\epsilon} + \gamma_E + \log 2 + \log s) + O(\epsilon)\,. \tag{10.44}$$

The fourth contribution is less simple

$$\begin{aligned}(\partial C)_e^{2,3} = \int_0^s \mathrm{d}t''t''O_1(t'',s) = N_d^2 2^{2-d}s^{4-d}\Bigg[\frac{F_d(1)}{(4-d)(3-d)} + \int_0^1 \mathrm{d}z\, zF_d((1-z)^2) \\ - 2\int_0^1 \mathrm{d}z\, z(1-z)^{1-d/2}F_d(1-z)\Bigg].\end{aligned} \tag{10.45}$$

Using now the explicit form for $F_4(x)$ given in Eq. (10.24), one obtains

$$\frac{4(\partial C)_e^{2,3}}{N_d^2} = -\left(\frac{1}{\epsilon} + \log s + \gamma_E + \frac{1}{2}\right)(\log\frac{4}{3} + 1) + \mathrm{Li}_2(1/4) + \log\frac{4}{3}\left(\frac{1}{4}\log\frac{4}{3} - \log 2\right) + O(\epsilon)\,. \tag{10.46}$$

The diagrams whose amputated part do not contribute also to the response function are shown in Fig. 9.5. The sunset-type diagram $(\partial C)^{2,4}$ is quite difficult, thus we first compute its 1PI part $O_2(t,s)$. Introducing $q_3 = q_1 + q_2$, this contribution is given by (for $t > s$)

$$\begin{aligned} O_2(t,s) &= \int \frac{\mathrm{d}^d q_1}{(2\pi)^d} \int \frac{\mathrm{d}^d q_2}{(2\pi)^d} C^0_{q_1}(t,s) C^0_{q_2}(t,s) C^0_{q_3}(t,s) \\ &= \int \frac{\mathrm{d}^d q_1}{(2\pi)^d} \int \frac{\mathrm{d}^d q_2}{(2\pi)^d} \prod_i \frac{1}{q_i^2} (e^{-q_i^2(t-s)} - e^{-q_i^2(t+s)}) \\ &= N_d^2 \left[\Delta^{3-d} K_d(1) + 3\sigma^{3-d} K_d(\Delta/\sigma) - 3\Delta^{3-d} K_d(\sigma/\Delta) - \sigma^{3-d} K_d(1) \right], \end{aligned} \tag{10.47}$$

with $\Delta = t - s$, $\sigma = t + s$, and

$$\begin{aligned} K_d(x) &= \frac{1}{N_d^2} \int \frac{\mathrm{d}^d q_1}{(2\pi)^d} \int \frac{\mathrm{d}^d q_2}{(2\pi)^d} \frac{1}{q_1^2} \frac{1}{q_2^2} \frac{1}{(q_1+q_2)^2} e^{-q_1^2 - q_2^2 - x(q_1+q_2)^2} \\ &= \frac{\Gamma(d/2-1)\Gamma(d/2)}{4} \int_x^\infty \frac{\mathrm{d}u}{(1+u)^{d-2}} \int_0^1 \mathrm{d}v v^{d/2-2} \left[1 - \frac{vu^2}{(1+u)^2} \right]^{1-d/2}. \end{aligned} \tag{10.48}$$

In the following we are interested in the particular cases

$$K_4(x) = \frac{1}{2} \log \frac{2(1+x)}{1+2x} - \frac{1}{4x} \log \frac{1+2x}{(1+x)^2}, \tag{10.49}$$

$$K_{4-\epsilon}(1) = \frac{3}{4} \log \frac{4}{3} + \frac{\epsilon}{4} \left[3 \log \frac{4}{3} \left(\frac{1}{2} + \gamma_E \right) + \frac{1}{4} \log^2 3 + \frac{\mathrm{Li}_2(8/9)}{2} \right] + O(\epsilon^2). \tag{10.50}$$

Introducing these results in the expression for the connected diagram

$$(\partial C)^{2,4} = \int_0^t \mathrm{d}t' O_2(t',s) = \int_0^s O_2(s,t') + \int_s^t O_2(t',s), \tag{10.51}$$

one finds

$$\begin{aligned} \frac{(\partial C)^{2,4}}{N_d^2} =& \frac{K_d(1)}{4-d} \left(2s^{4-d} + (t-s)^{4-d} - (t+s)^{4-d} \right) \\ &+ 3 \int_0^s \mathrm{d}t' \left[(s+t')^{3-d} K_d \left(\frac{s-t'}{s+t'} \right) - (s-t')^{3-d} K_d \left(\frac{s+t'}{s-t'} \right) \right] \\ &+ 3 \int_s^t \mathrm{d}t' \left[(s+t')^{3-d} K_d \left(\frac{t'-s}{t'+s} \right) - (t'-s)^{3-d} K_d \left(\frac{s+t'}{t'-s} \right) \right] \\ =& \frac{K_d(1)}{4-d} \left(2s^{4-d} + (t-s)^{4-d} - (t+s)^{4-d} \right) \\ &+ 3(2s)^{4-d} \left[\int_0^1 \mathrm{d}y (1+y)^{d-5} [K_d(y) - y^{3-d} K_d(1/y)] \right. \\ &\left. + \int_0^{\frac{t-s}{t+s}} \mathrm{d}y (1-y)^{d-5} [K_d(y) - y^{3-d} K_d(1/y)] \right] \\ =& \frac{3}{2} \log \frac{4}{3} \left(\frac{1}{\epsilon} + \log s + \frac{1}{2} \log \frac{t-s}{t+s} + \gamma_E \right) + \Phi(s/t) + O(\epsilon), \end{aligned} \tag{10.52}$$

where

$$\begin{aligned}\Phi(v) =& 2K_4'(1) - \frac{3}{2}\gamma_E \log\frac{4}{3} \\ &+ 3\left[\int_0^1 \frac{\mathrm{d}y}{1+y}\left(K_4(y) - \frac{1}{y}K_4(1/y)\right) + \int_0^{\frac{1-v}{1+v}} \frac{\mathrm{d}y}{1-y}\left(K_4(y) - \frac{1}{y}K_4(1/y)\right)\right].\end{aligned} \tag{10.53}$$

In particular we are interested in the limit $v \to 0$, given by

$$\begin{aligned}\Phi(0) =& 2K_4'(1) + 6\int_0^1 \frac{\mathrm{d}y}{1-y^2}\left[K_4(y) - \frac{1}{y}K_4\left(\frac{1}{y}\right)\right] - \frac{3}{2}\gamma_E \log\frac{4}{3} \\ =& \frac{3}{4}\log\frac{4}{3} + \frac{39}{4}\log^2 2 - \frac{9}{4}\log 2 + \log 3 - \frac{13}{4}\log^2 3 - \frac{21}{4}\mathrm{Li}_2(1/3) \\ &+ \frac{21}{8}\mathrm{Li}_2(3/4) - \frac{1}{8}\mathrm{Li}_2(8/9) = -0.24889\ldots\end{aligned} \tag{10.54}$$

Now the only diagram left is $C^{2,5}$ of Fig. 9.5. It is given by

$$\begin{aligned}C^{2,5}(t,s) =& \int \mathrm{d}t'\mathrm{d}t'' R^0_{q=0}(t,t'')B_c(t'')C^0_{q=0}(t'',t')B_c(t')R^0_{q=0}(s,t) \\ =& N_d^2 \frac{\Gamma^2(d/2-1)}{2^{d-1}(3-d/2)(2-d/2)}\left[t^{2-d/2} - \frac{s^{2-d/2}}{5-d}\right]s^{3-d/2}.\end{aligned} \tag{10.55}$$

Its derivative with respect to s, near four dimensions, is

$$(\partial C)^{2,5} = \partial_s C^{2,5}(t,s) = N_d^2 \frac{1}{8}\left[\log\frac{t}{s} + 1\right] + O(\epsilon)\,. \tag{10.56}$$

Acknowledgments

I wish to express my deepest gratitude to Sergio Caracciolo, Andrea Pelissetto and Massimiliano Gubinelli who patiently guided me during these years of fruitful scientific collaboration.

I owe particular thanks to Royce Zia and Beate Schmittmann for interesting and stimulating discussions and for the kind hospitality at Virginia Tech and to Malte Henkel for useful correspondence and suggestions.

I warmly thank Pasquale Calabrese for the nice time we spent together during our joint works.

Bibliography

General references of Statistical Mechanics and Field Theory applied to Critical Phenomena and RG:

[1] P. C. Hohenberg and B. I. Halperin, *Theory of dynamic critical phenomena*, Rev. Mod. Phys. **49**, 435 (1977).

[2] C. N. Yang and T. D. Lee, Phys. Rev. Lett. **87**, 404 (1952); Phys. Rev. Lett. **87**, 410 (1952).

[3] D. Ruelle, *Statistical Mechanics: Rigorous Results* (Addison Wesley Publishing Company, New York, 1989).

[4] J. Zinn-Justin, *Quantum Field Theory and Critical Phenomena*, 3rd edition (Oxford Science Publication, Clarendon Press, Oxford, 1996).

[5] Basic concepts of the statistical theory of critical phenomena may be found in the following books:
J. Cardy, *Scaling and Renormalization in Statistical Physics*, Cambridge lecture notes in physics 5 (Cambridge University Press, 1996).
S. K. Ma, *Modern Theory of Critical Phenomena*, 12th printing (Addison–Wesley Publishing Company, 1994).
K. Huang, *Statistical Mechanics*, 2nd ed. (John Wiley & Sons, 1987).
G. Parisi *Statistical Field Theory* (Frontiers in Physics 66) (Addison–Wesley, Redwood City, 1988).
D. J. Amit *Field Theory, the Renormalization Group, and Critical Phenomena*, 2nd ed. (World Scientific, Singapore, 1984).
See also Ref. [4].

[6] M. E. Fisher, in *Critical Phenomena*, International School of Physics "Enrico Fermi", Course 51, edited by M. S. Green (Academic Press, New York, 1971).

[7] M. E. Fisher, in *Critical Phenomena*, Lecture Notes in Physics, Vol. 186, edited by F. J. W. Hahne (Springer, Berlin, 1983).

[8] R. Kubo, M. Toda, N. Hashitsume, *Statistical Physics* (Springer–Verlag, Berlin, 1985).

[9] N. G. van Kampen, *Stochastic processes in physics and chemistry* (North Holland Publishing Company, Amsterdam, 1983).

[10] A. Pelissetto and E. Vicari, *Critical Phenomena and Renormalization-Group Theory*, Phys. Rep. **368**, 549 (2002).

Applications of Conformal Invariance to critical phenomena:

[11] J. L. Cardy, *Conformal Invariance*, in *Phase Transitions and Critical Phenomena*, Vol. 11, C. Domb and J. L. Lebowitz eds. (Academic Press, 1987).
M. Henkel, *Conformal Invariance and Critical Phenomena* (Springer, Berlin, 1999).
J. L. Cardy, *Conformal invariance and critical dynamics*, J. Phys. A **18**, 2771 (1985).

Functional approach to dynamical critical phenomena:

[12] P. C. Martin, E. D. Siggia and H. A. Rose, Phys. Rev. A **8**, 423 (1973).
C. De Dominicis, Nuovo Cim. Lett. **12**, 567 (1975); J. Phys. (Paris) **37**, Colloque C247 (1976).
C. De Dominicis and L. Peliti, *Field-theory renormalization and critical dynamics above T_c: Helium, antiferromagnets, and liquid-gas systems*, Phys. Rev. B **18**, 353 (1978).

[13] H. K. Janssen, Z. Phys. B **23**, 377 (1976).

[14] R. Bausch, H. K. Janssen, and H. Wagner, Z. Phys. B **24**, 113 (1976).
See also Ref. [15].

[15] H. K. Janssen, *Field-theoretic method applied to critical dynamics*, in *Dynamical Critical Phenomena and Related Topics*, edited by C. P. Enz, Lecture Notes in Physics, Vol. 104, (Springer, Berlin–New York–Tokyo, 1979).

[16] F. Langouche, D. Roekaerts, and E. Tirapegui, Physica **95A**, 252 (1979).

Surface critical phenomena:

[17] H. W. Diehl, *Field-theoretical approach to critical behaviour at surfaces*, in *Phase Transitions and Critical Phenomena*, edited by C. Domb and J. L. Lebowitz, Vol. 10 (Academic Press, London, 1986).

General references for Non-equilibrium systems:

[18] M. R. Evans, *Phase Transitions in one–dimensional nonequilibrium systems*, Brazilian Journal of Physics **30**, 42 (2000), e-print `cond-mat/0007293`.
M. R. Evans and R. A. Blythe, *Nonequilibrium Dynamics in Low Dimensional Systems*, Lectures at the International Summer School on Fundamental Problems in Statistical Physics X, Aug.-Sept. 2001, Altenberg (Germany), Physica A **313**, 110 (2002), e-print `cond-mat/0110630`.

[19] H. Hinrichsen, *Nonequilibrium Critical Phenomena and Phase Transitions into Absorbing States*, Adv. in Phys. **49**, 815 (2000), e-print `cond-mat/0001070`.

[20] V. Privman, editor, *Nonequilibrium Statistical Mechanics in One Dimension* (Cambridge University Press, Cambridge, 1997).

[21] J. Marro and R. Dickman, *Nonequilibrium Phase Transitions in Lattice Models* (Cambridge University Press, Cambridge, 1999).

[22] G. Grinstein, *Generic scale invariance in classical nonequilibrium systems*, J. App. Phys. **69**, 5441 (1991).

[23] U. C. Täuber, V. K. Akkineni, and J. E. Santos, *The effects of violating detailed balance on critical dynamics*, Phys. Rev. Lett. **88**, 045702 (2002).

[24] Z. Rácz, *Nonequilibrium Phase Transitions*, Lecture Notes, Les Houches, July 2002, e-print `cond-mat/0210435`.

[25] R. K. P. Zia, E. L. Praestgaard, and O. G. Mouritsen, *Getting more from pushing less: Negative specific heat and conductivity in nonequilibrium steady states*, Am. J. Phys. **70**, 384 (2002).

Reversibility, Fluctuation theorems, Non-equilibrium, and all that:

[26] B. Derrida, J. L. Lebowitz, and E. R. Speer, Phys. Rev. Lett. **87**, 150601 (2001); J. Stat. Phys. **107**, 599 (2002); Phys. Rev. Lett. **89**, 030601 (2002); e-print `cond-mat/0205353`.
L. Bertini, A. De Sole, D. Gabrielli, G. Jona-Lasinio, and C. Landim, Phys. Rev. Lett. **87**, 040601 (2001); J. Stat. Phys. **107**, 635 (2002).
For an overview see D. Ruelle, Nature **411**, 27 (2001).

[27] J. Kurchan, *Fluctuation theorem for stochastic dynamics*, J. Phys. A **31**, 3719 (1998).
J. L. Lebowitz and H. Spohn, *A Gallavotti-Cohen Type Symmetry in the Large Deviation Functional for Stochastic Dynamics*, J. Stat. Phys. **95** 333 (1999), e-print `cond-mat/9811220`.

[28] D. Gabrielli, G. Jona-Lasinio, and C. Landim, *Onsager Reciprocity Relations without Microscopic Reversibility*, Phys. Rev. Lett. **77**, 1202 (1996).
See also the Comment by J. L. Lebowitz and H. Spohn, Phys. Rev. Lett. **78**, 394 (1997), and the authors' Reply.

[29] E. Gozzi, *Onsager principle of microscopic reversibility and supersymmetry*, Phys. Rev. D **30**, 1218 (1984).
S. Chaturvedi, A. K. Kapoor, and V. Srinivasan, *Ward Takahashi Identities and Fluctuation-Dissipation Theorem in a Superspace Formulation of the Langevin Equation*, Z. Phys. B **57**, 249 (1984).

[30] M. F. Zimmer, *Fluctuations in Nonequilibrium Systems and Broken Supersymmetry*, J. Stat. Phys. **73**, 751 (1993).

[31] E. Gozzi, *Fermionic zero modes and violation of the fluctuation-dissipation theorem*, Phys. Rev. D **33**, 584 (1986).
J. Kurchan, J. Phys. I (France) **1**, 1333 (1992).
See also Ref. [113].

[32] G. L. Eyink, J. L. Lebowitz, and H. Spohn, *Hydrodynamics of Fluctuations Outside of Local Equilibrium: Driven Diffusive Systems*, J. Stat. Phys. **83**, 385 (1996).

[33] F. J. Alexander, G. L. Eyink, *Shape-Dependent Thermodynamics and Non-Local Hydrodynamics in a Non-Gibbsian Steady-State of a Drift-Diffusion System*, Phys. Rev. E **57**, R6229 (1998).

Generalized Static-Dynamic connection for some glassy systems:

[34] S. Franz, M. Mézard, G. Parisi, and L. Peliti, Phys. Rev. Lett. **81**, 1758 (1998); J. Stat. Phys. **97**, 459 (1999).

Driven Lattice Gas and generalizations:

[35] B. Schmittmann and R. P. K. Zia, *Statistical mechanics of driven diffusive systems*, in *Phase Transitions and Critical Phenomena*, edited by C. Domb and J. L. Lebowitz, Vol. 17 (Academic Press, London, 1995).

[36] S. Katz, J. L. Lebowitz, and H. Spohn, Phys. Rev. B **28**, 1655 (1983); J. Stat. Phys. **34**, 497 (1984).

[37] H. van Beijeren and L. S. Schulman, Phys. Rev. Lett. **53**, 806 (1984).
J. Krug, J. L. Lebowitz, H. Spohn, and M. Q. Zhang, J. Stat. Phys. **44**, 535 (1986).

Field theoretical studies:

[38] K. Gawedzki and A. Kupiainen, Nucl. Phys. B **269**, 45 (1986).

[39] H. K. Janssen and B. Schmittmann, Z. Phys. B **64**, 503 (1986).

[40] K. -t. Leung and J. L. Cardy, J. Stat. Phys. **44**, 567 (1986); Erratum J. Stat. Phys. **45**, 1087 (1986).

Two temperatures DLG:

[41] P. L. Garrido, J. L. Lebowitz, C. Maes, and H. Spohn, *Long-range correlations for conservative dynamics*, Phys. Rev. A **42**, 1954 (1990).

[42] E. L. Præstgaard, H. Larsen, and R. K. P. Zia, *Finite-Size Scaling in a Two-Temperature Lattice Gas: a Monte Carlo Study of Critical Properties*, Europhys. Lett. **25**(6), 447 (1994).

[43] E. L. Præstgaard, B. Schmittmann, and R. K. P. Zia, *A Lattice Gas Coupled to Two Thermal Reservoirs: Monte Carlo and Field Theoretic Studies*, Eur. Phys. J. B **18**, 675 (2000), e-print `cond-mat/0010053`.

Random Field DLG:

[44] B. Schmittmann and R. K. P. Zia, *Critical Properties of a Randomly Driven Diffusive System*, Phys. Rev. Lett. **66**, 357 (1991).
Pay attention to a mistake pointed out in Ref. [45], footnote pag. 112.

[45] B. Schmittmann, *Fixed–Point Hamiltonian for a Randomly Driven Diffusive System*, Europhys. Lett. **24**, 109 (1993).

Further generalizations:

[46] K. Oerding and H. K. Janssen, *Surface Critical Behaviour of Driven Diffusive Systems with Open Boundaries*, Phys. Rev. E **58**,1446 (1998), e-print `cond-mat/9805189`.

[47] H. K. Janssen and K. Oerding, *Renormalized Field Theory and Particle Density Profile in Driven Diffusive Systems with Open Boundaries*, Phys. Rev. E **53**, 4544 (1996), e-print `cond-mat/9605175`.

[48] V. Becker, H. K. Janssen, *Field Theory of Critical Behaviour in Driven Diffusive Systems with Quenched Disorder*, e-print `cond-mat/9904216`.

[49] R. A. Monetti and E. V. Albano, *Critical behavior of a non-equilibrium interacting particle system driven by an oscillatory field*, Europhys. Lett. **56**, 400 (2001).

MC, FSS of DLG and alternative Field Theories:

[50] M. Gubinelli, *Leggi di Scala per Fenomeni Critici fuori dall'Equilibrio Termodinamico*, Laurea Thesis, University of Pisa, 1998 (unpublished).

[51] M. Q. Zhang, J. -S. Wang, J. L. Lebowitz, and J. L. Vallés, *Power Law Decay of Correlations in Stationary Nonequilibrium Lattice Gases with Conservative Dynamics*, J. Stat. Phys. **52**, 1461 (1988).

[52] K. -t. Leung, Phys. Rev. Lett. **66**, 453 (1991).
See also [53].

[53] K. -t. Leung, *Finite-size scaling at critical points with spatial anisotropies*, Int. J. Mod. Phys. C **3**, 367 (1992).

[54] J. S. Wang, J. Stat. Phys. **82**, 1409 (1996).

[55] A. Achahbar and J. Marro, *Phase Transitions in a Driven Lattice Gas in Two Planes*, J. Stat. Phys. **78**, 1493 (1995).

[56] K. -t. Leung and R. K. P. Zia, *Subtelties in Data Analysis Related to the Size of Critical Region*, J. Stat. Phys. **83**, 1219 (1996).

[57] J. Marro, A. Achahbar, P. L. Garrido, and J. J. Alonso, *Phase transitions in driven lattice gases*, Phy. Rev. E **53**, 6038 (1996).

[58] K. -t. Leung and J. S. Wang, Int. J. Mod. Phys. C **10**, 853 (1999).

[59] K. Binder and J. S. Wang, *Finite-Size Effects at Critical Points with Anisotropic Correlations: Phenomenological Scaling Theory and Monte Carlo Simulations*, J. Stat. Phys. **55**, 87 (1989).

[60] J. L. Vallés and J. Marro, *Nonequilibrium Phase Transitions in Stochastic Lattice Systems: Influence of the Hopping Rates*, J. Stat. Phys. **43**, 441 (1986); *Nonequilibrium Second-Order Phase Transitions in Stochastic Lattice Systems: A Finite-Size Scaling Analysis in Two Dimensions*, J. Stat. Phys. **49**, 89 (1987).

[61] P. L. Garrido, and M. A. Muñoz, *Fokker–Planck equation for nonequilibrium competing dynamics*, Phys. Rev. E **50**, 2458 (1994); *Continuum Description for Nonequilibrium Competing Dynamic Models*, Phy. Rev. Lett. **75**, 1875 (1995).

[62] P. L. Garrido, F. de los Santos, and M. A. Muñoz, *Langevin equation for driven diffusive systems*, Phys. Rev. E **57**, 752 (1998).

[63] P. L. Garrido and F. de los Santos, J. Stat. Phys. **96**, 303 (1999), e-print `cond-mat/9805211`.

[64] F. de los Santos and M. A. Muñoz, *Renormalized field theory of driven lattice gases under infinitely fast drive*, Phys. Rev. E **61**, 1161 (2000), e-print `cond-mat/9903053`.
Note that e-print version of the paper contains wrong critical exponents, as pointed out in Refs. [65, 67].

[65] S. Caracciolo, A. Gambassi, M. Gubinelli, and A. Pelissetto, private communication to M. A. Muñoz, November 1999.

[66] P. L. Garrido, M. A. Muñoz, and F. de los Santos, Phys. Rev. E **61**, R4683 (2000), e-print `cond-mat/0001165`.

[67] B. Schmittmann, H. K. Janssen, U. C. Täuber, R. K. P. Zia, K. -t. Leung, and J. L. Cardy, *Viability of competing field theories for the driven lattice gas*, Phys. Rev. E **61**, 5977 (2000), e-print `cond-mat/9912286`.

[68] K. -t. Leung, *Heuristic derivation of continuum kinetic equations from microscopic dynamics*, Phys. Rev. E **63**, 016102 (2001), e-print `cond-mat/0006217`.

[69] S. Caracciolo, A. Gambassi, M. Gubinelli, and A. Pelissetto, *Finite–Size Critical Behaviour of the Driven Lattice Gas*, e-print `cond-mat/0106221`.

[70] S. Caracciolo, A. Gambassi, M. Gubinelli, and A. Pelissetto, *Transverse Fluctuations in the Driven Lattice Gas*, to appear (2002).

[71] M. Gubinelli, *Finite-Size Scaling in Nonequilibrium Critical Phenomena*, Ph.D. Thesis, University of Pisa (Italy), 2002 (unpublished).
S. Caracciolo, A. Gambassi, M. Gubinelli, and A. Pelissetto, in preparation.

[72] A. Achahbar, P. L. Garrido, J. Marro, and M. A. Muñoz, *Is the Particle Current a Relevant Feature in Driven Lattice Gases?*, Phys. Rev. Lett. **87**, 195702 (2001), e-print `cond-mat/0106470`.

[73] M. A. Muñoz, *Some puzzling problems in nonequilibrium field theories*, e-print `cond-mat/0210645`.

Studies on dynamical aspects of the DLG phase transition:

[74] K. Hwang, B. Schmittmann, and R. K. P. Zia, *Three–point correlation functions in uniformly and randomly driven diffusive systems*, Phys. Rev. E **48**, 800 (1993).

[75] A. D. Rutenberg and C. Yeung, *Triangular anisotropies in driven diffusive systems: Reconciliation of up and down*, Phys. Rev. E **60**, 2710 (1999).

[76] E. Levine, Y. Kafri, and D. Mukamel, *Ordering dynamics of the driven lattice gas model*, Phys. Rev. E **64**, 026105 (2001), e-print `cond-mat/0101324`.

[77] E. V. Albano and G. Saracco, *Dynamic Behavior of Anisotropic Nonequilibrium Driving Lattice Gases*, Phys. Rev. Lett. **88**, 145701 (2002), e-print `cond-mat/0210141`.

General references on MC methods:

[78] A. D. Sokal, *Monte Carlo mehtods in statistical mechanics: Foundations and New Algorithms*, lectures given at the Cours de Troisième Cycle de la Physique en Suisse Romande, Lausanne, Switzerland, Jun 15-29, 1989.

[79] K. Kawasaki, in *Phase Transitions and Critical Phenomena*, edited by C. Domb and M. S. Green, Vol. 2 (Academic Press, New York, 1972).

[80] B. Efron, *The Jackknife, the Bootstrap and Other Resampling Plans*, Regional Conference Series in Applied Mathematics, Vol. 38 (SIAM, Philadelphia, 1982).

FSS in equilibrium systems (theory and MC simulations):

[81] E. Brézin, J. Physique **43**, 15 (1982).

[82] M. E. Fisher and M. N. Barber, Phys. Rev. Lett. **28**, 1516 (1972).

[83] Y. Imry and B. Bergman, Phys. Rev. A **3**, 1416 (1971).

[84] M. N. Barber, *Finite–Size Scaling*, in *Phase Transitions and Critical Phenomena*, edited by C. Domb and J. L. Lebowitz, Vol. 8 (Academic Press, London, 1983).

[85] E. Brézin and J. Zinn-Justin, Nucl. Phys. B **257** [FS14], 867 (1985).

[86] J. Rudnick, H. Guo, and D. Jasnow, J. Stat. Phys. **41**, 353 (1985).

[87] J. L. Cardy, editor, *Finite-Size Scaling* (North-Holland, Amsterdam, 1988).

[88] S. M. Bhattacharjee and J. F. Nagle, *Finite-size effect for the critical point of an anisotropic dimer model of domain walls*, Phys. Rev. A **31**, 3199 (1985).

[89] J. G. Brankov, D. M. Dantchev, and N. S. Tonchev, *Theory of Critical Phenomena in Finite-Size Systems. Scaling and Quantum Effects* (World Scientific, Singapore, 2000).

[90] S. Caracciolo, R. G. Edwards, S. J. Ferreira, A. Pelissetto, and A. D. Sokal, Phys. Rev. Lett. **74**, 2969 (1995), e-print `hep-lat/9409004`.
A similar method has been introduced in Refs. [91, 92].

[91] M. Lüscher, P. Weisz, and U. Wolff, Nucl. Phys. B **359**, 221 (1991).

[92] J. -K. Kim, Europhys. Lett. **28**, 211 (1994); Phys. Rev. D **50**, 4663 (1994); Nucl. Phys. B (Proc. Suppl.) **34**, 702 (1994).

[93] S. Caracciolo, R. G. Edwards, A. Pelissetto, and A. D. Sokal, Phys. Rev. Lett. **75**, 1891 (1995), e-print `hep-lat/9411009`.

[94] S. Caracciolo, R. G. Edwards, T. Mendes, A. Pelissetto, and A. D. Sokal, Nucl. Phys. B (Proc. Suppl.) **47**, 763 (1996), e-print `hep-lat/9509033`.

[95] G. Mana, A. Pelissetto, and A. D. Sokal, Phys. Rev. D **54**, 1252 (1996), e-print `hep-lat/9602015`.

[96] T. Mendes, A. Pelissetto, and A. D. Sokal, Nucl. Phys. B **477**, 203 (1996), e-print `hep-lat/9604015`.

[97] G. Mana, A. Pelissetto, and A. D. Sokal, Phys. Rev. D **55**, 3674 (1997), e-print `hep-lat/9610021`.

[98] S. J. Ferreira and A. D. Sokal, J. Stat. Phys. **96**, 461 (1999), e-print `cond-mat/9811345`.

[99] S. Caracciolo and M. Palassini, Phys. Rev. Lett. **82**, 5128 (1999), e-print `cond-mat/9904246`.

[100] M. Hasenbusch, J. Physique I **3**, 753 (1993).

[101] H. W. J. Blöte and G. Kamieniarz, Physica A **196**, 455 (1993).

[102] H. W. J. Blöte, E. Luijten, and J. R. Heringa, J. Phys. A **28**, 6289 (1995).

[103] J. Salas and A. D. Sokal, J. Stat. Phys. **88**, 567 (1997), e-print `hep-lat/9607030`.

[104] M. Hasenbusch, K. Pinn, and S. Vinti, Phys. Rev. B **59**, 11471 (1999).

[105] H. G. Ballesteros, L. A. Fernández, V. Martín-Mayor, A. Muñoz Sudupe, G. Parisi, and J. J. Ruiz-Lorenzo, J. Phys. A **32**, 1 (1999).

[106] X. S. Chen and V. Dohm, Eur. Phys. J. B **7**, 183 (1999); **15**, 283 (2000).

[107] V. Privman and M. E. Fisher, *Finite–Size Effects at First–Order Transitions*, J. Stat. Phys. **33**, 385 (1983).

[108] D. Dantchev and J. Rudnick, *Subleading long-range interactions and violations of finite size scaling*, Eur. Phys. J. B **21**, 251 (2001), e-print `cond-mat/0010478`.

[109] S. Caracciolo, A. Gambassi, M. Gubinelli, and A. Pelissetto, Eur. Phys. J. B **20**, 255 (2001), e-print `cond-mat/0010479`.

[110] A. Gambassi, internal note (2001).

General aspects of Aging Phenomena:

[111] E. Vincent, J. Hammann, M. Ocio, J. P. Bouchaud, and L. F. Cugliandolo, *Slow dynamics and aging in spin-glasses*, in *Complex Behavior of Glassy Systems*, Springer Lecture Notes in Physics **492**, 184 (1997).
J. P. Bouchaud, L. F. Cugliandolo, J. Kurchan, and M. Mézard, *Out of Equilibrium dynamics in Spin-Glasses and other Glassy Systems*, in *Spin Glasses and Random Fields*, Directions in Condensed Matter Physics, Vol. 12, edited by A. P. Young (World Scientific, Singapore, 1998).
See also Ref. [113]

[112] L. C. E. Struik, *Physical aging in amorphous polymers and other materials* (Elsevier, Amsterdam, 1978).

[113] L. F. Cugliandolo, *Dynamics of Glassy Systems*, Lecture Notes, Les Houches, July 2002, e-print `cond-mat/0210312`.

[114] L. F. Cugliandolo, J. Kurchan, and L. Peliti, *Energy flow, partial equilibration, and effective temperatures in systems with slow dynamics*, Phys. Rev. E **55**, 3898 (1997).
L. F. Cugliandolo and D. S. Dean, *Full dynamical solution for a spherical spin-glass model*, J. Phys. A **28**, 4213 (1995).
See also Ref. [116] and Zippold et al. in Ref. [119].

[115] L. F. Cugliandolo, *Effective temperatures out of equilibrium*, in *Trends in Theoretical Physics II*, H. Falomir et al, editors, AIP Conference Proceedings 484 (American Institute of Physics, New York, 1999), e-print `cond-mat/9903250`.

[116] L. F. Cugliandolo and J. Kurchan, *Analytical solution of the off-equilibrium dynamics of a long-range spin-glass model*, Phys. Rev. Lett. **71**, 173 (1993); *On the out-of-equilibrium relaxation of the Sherrington-Kirkpatrick model*, J. Phys. A **27**, 5749 (1994).

Experimental evidences of aging behavior:

[117] T. S. Grigera and N. E. Israeloff, *Observation of Fluctuation-Dissipation-Theorem Violations in a Structural Glass*, Phys. Rev. Lett. **83**, 5038 (1999).
L. Bellon and S. Ciliberto, *Experimental study of the Fluctuation-Dissipation-Relation during an aging process*, Physica D **168-169**, 325 (2002).
D. Hérisson and M. Ocio, *Fluctuation-dissipation ratio of a spin glass in the aging regime*, Phys. Rev. Lett. **88**, 257202 (2002).
F. Restagno, C. Ursini, H. Gayvallet, and É. Charlaix, *Aging in humid granular media*, Phys. Rev. E **66**, 021304 (2002).
This list, containing only some recent experiments, is far from being complete.

Non-equilibrium dynamic and aging in ferromagnetic systems:

[118] L. F. Cugliandolo, J. Kurchan, and G. Parisi, *Off equilibrium dynamics and aging in unfrustrated systems*, J. Phys. I (France) **4**, 1641 (1994), e-print `cond-mat/9406053`.

[119] W. Zippold, R. Kühn, and H. Horner, *Non-equilibrium dynamics of simple spherical spin models*, Eur. Phys. J. B **13**, 531 (2000).
S. A. Cannas, D. A. Stariolo, and F. A. Tamarit, *Dynamics of ferromagnetic spherical spin models with power law interactions: exact solution*, Physica A **294**, 362 (2001), e-print `cond-mat/0010319`.

[120] T. J. Newman and A. J. Bray, *Dynamic correlations in domain growth: a 1/n expansion*, J. Phys. A **23**, 4491 (1990).
J. G. Kissner and A. J. Bray, *Dynamic correlations in phase ordering: the 1/n-expansion reconsidered*, J. Phys. A **26**, 1571 (1993).
L. Berthier, J. L. Barrat, and J. Kurchan, *Response function of coarsening systems*, Eur. Phys. J. B **11**, 635 (1999).
A. Barrat, *Monte Carlo simulations of the violation of the fluctuation-dissipation theorem in domain growth processes*, Phys. Rev. E **57**, 3629 (1998).

[121] F. Corberi, E. Lippiello, and M. Zannetti, *Slow relaxation in the large N model for phase ordering*, Phys. Rev. E **65**, 046136 (2002).

[122] E. Lippiello and M. Zannetti, *Fluctuation dissipation ratio in the one-dimensional kinetic Ising model*, Phys. Rev. E **61**, 3369 (2000).

[123] F. Corberi, E. Lippiello, and M. Zannetti, *Interface fluctuations, bulk fluctuations, and dimensionality in the off-equilibrium response of coarsening systems*, Phys. Rev. E **63**, 061506 (2001); *Slow relaxation in the large N model for phase ordering*, Phys. Rev. E **65**, 046136 (2002).

[124] C. Godrèche and J. M. Luck, *Response of non-equilibrium systems at criticality: Exact results for the Glauber-Ising chain*, J. Phys. A **33**, 1151 (2000).

[125] C. Godrèche and J. M. Luck, *Response of non-equilibrium systems at criticality: Ferromagnetic models in dimension two and above*, J. Phys. A **33**, 9141 (2000).

[126] L. Berthier, P. C. W. Holdsworth, and M. Sellitto, *Nonequilibrium Critical Dynamics of the 2D XY model*, J. Phys. A **34**, 1805 (2001).

[127] C. Godrèche and J. M. Luck, *Nonequilibrium critical dynamics of ferromagnetic spin systems*, J. Phys. Cond. Matter **14**, 1589 (2002).

[128] L. R. Fontes, M. Isopi, C. M. Newman, and D. L. Stein, *Aging in 1D Discrete Spin Models and Equivalent Systems*, Phys. Rev. Lett. **87**, 110201 (2001).

[129] A. Picone and M. Henkel, *Response of non-equilibrium systems with long-range initial correlations*, J. Phys. A **35** 5575 (2002).

[130] A. Picone, M. Henkel, and J. Richert, *Competition between dynamic and thermal relaxation in non-equilibrium critical spin systems above the critical point*, e-print `cond-mat/0210330`.

Non-equilibrium dynamics in other models:

[131] S. Franz and F. Ritort, *Relaxation process and entropic traps in the Backgammon model*, J. Phys. A **30**, L359 (1997).
C. Godrèche and J. M. Luck, *Correlation and response in the backgammon model: the Ehrenfest legacy*, J. Phys. A **32**, 6033 (1999); *Nonequilibrium dynamics of the zeta urn model*, Eur. Phys. J. B **23**, 473 (2001); *Nonequilibrium dynamics of urn models*, J. Phys. Cond. Matter **14**, 1601 (2002).

Aging in ferromagnetic systems: field-theoretical approach

[132] P. Calabrese and A. Gambassi, *Aging in ferromagnetic systems at criticality near four dimensions*, Phys Rev. E **65**, 066120 (2002); Acta Phys. Slov. **52**, 335 (2002).

[133] P. Calabrese and A. Gambassi, *Two-loop Critical Fluctuation-Dissipation Ratio for the Relaxational Dynamics of the O(N) Landau-Ginzburg Hamiltonian*, Phys. Rev. E **66**, 0661XX (2002), e-print `cond-mat/0207452`.

[134] P. Calabrese and A. Gambassi, *Aging at Criticality in Model C Dynamics*, e-print `cond-mat/0211062`.

[135] P. Calabrese and A. Gambassi, *Aging and fluctuation-dissipation ratio for the diluted Ising Model*, Phys. Rev. B **67**, 0124XX (2003), e-print `cond-mat/0207487`.

[136] P. Calabrese, and A. Gambassi, in preparation.

General aspect of phase ordering dynamics:

[137] A. J. Bray, *Theory of Phase-ordering kinetics*, Adv. Phys. **43**, 357 (1994).

General aspects of relaxation in statistical systems:

[138] M. E. Fisher and Z. Rácz, *Scaling theory of nonlinear critical relaxation*, Phys. Rev. B **13**, 5039 (1976).
R. Bausch, E. Eisenriegler, and H. K. Janssen, *Nonlinear critical slowing down of the one component Ginzburg-Landau fields*, Z. Phys. B **36**, 179 (1979).

[139] D. A. Huse, Phys. Rev. B **40**, 304 (1989).

Initial-slip dynamics: general references

Non-disordered models:

[140] H. K. Janssen, B. Schaub, and B. Schmittmann, *New universal short-time scaling behaviour of critical relaxation process*, Z. Phys. B **73** 539 (1989).

[141] H. K. Janssen, *On the renormalized field theory of nonlinear critical relaxation*, in *From Phase Transitions to Chaos – Topics in Modern Statistical Physics*, G. Györgyi et al., editors (World Scientific, Singapore, 1992).

[142] K. Oerding and H. K. Janssen, *Non-equilibrium critical relaxation with coupling to a conserved density*, J. Phys. A **26**, 3369 (1993).

[143] K. Oerding and H. K. Janssen, *Non-equilibrium critical relaxation with reversible mode coupling*, J. Phys. A **26**, 5295 (1993).

[144] H. K. Janssen and K. Oerding, *Non-equilibrium relaxation at a tricritical point*, J. Phys. A **27**, 715 (1994).

[145] F. van Wijland, K. Oerding, and H. J. Hilhorst, *Wilson renormalization of reaction-diffusion process*, Physica A **234**, 103 (1997).
H. Hinrichsen and G. Ódor, *Correlated initial conditions in directed percolation*, Phys. Rev. E **58**, 311 (1998).
See also Ref. [19].

[146] M. Krech, *Short-time scaling behavior of growing interfaces*, Phys. Rev. E **56**, 668 (1997); Erratum Phys. Rev. E **56**, 1285 (1997).

Models with disorder:

[147] J. G. Kissner, *Nonequilibrium critical relaxation in the presence of random impurities*, Phys. Rev. B **46**, 2676 (1992).

[148] K. Oerding and H. K. Janssen, *Non-equilibrium critical relaxation in dilute Ising systems*, J. Phys. A **28**, 4271 (1995).

[149] Z. B. Li, Y. Chen, and S. H. Guo, *Short-time critical behavior of the Ginzburg-Landau model with quenched disorder*, Mod. Phys. Lett. B **15**, 43 (2001).

Application in Short-time Monte Carlo simulations:

[150] Z. B. Li, L. Schülke, and B. Zheng, *Dynamic Monte Carlo Measurement of Critical Exponents*, Phys. Rev. Lett. **74**, 3396 (1995).
K. Okano, L. Schülke, K. Yamagishi, and B. Zheng, *Universality and Scaling in Short-time Critical Dynamics*, Nucl. Phys. B **485**, 727 (1997).
B. Zheng, *Generalized Dynamic Scaling for Critical Magnetic Systems*, Int. J. Mod. Phys. B **12**, 1419 (1998); *Monte Carlo simulations and numerical solutions of short-time critical dynamics*, Physica A **283**, 80 (2000).

FSS ans Surface effects in Short-time dynamics:

[151] H. W. Diehl and U. Ritschel, J. Stat. Phys. **73**, 1 (1993).
U. Ritschel and H. W. Diehl, *Long-time traces of the initial condition in relaxation phenomena near criticality*, Phys. Rev. E **51**, 5392 (1995); *Dynamical Relaxation and Universal Short-Time Behavior in Finite Systems: The Renormalization Group Approach*, Nucl. Phys. B **464**, 512 (1996).

[152] U. Ritschel and P. Czerner, *Universal Short-Time Behavior in Critical Dynamics near Surfaces*, Phys. Rev. Lett. **75**, 3882 (1995).

Critical dynamics:

Models belonging to Model C universality class:

[153] V. I. Gorentsveig, P. Fratzl, and J. L. Lebowitz, *Kinetics of joint ordering and decomposition in binary alloys*, Phys. Rev. B **55**, 2912 (1997).

[154] K. Binder, W. Kinzel, and D. P. Landau, *Theoretical Aspects of Order-Disorder Transitions in Adsorbed Layers*, Surf. Sci. **117**, 232 (1982).

[155] H. Tanaka, *Two-order-parameter description of liquids: critical phenomena and phase separation of supercooled liquids*, J. Phys.: Condens. Matter **11**, L159 (1999).

[156] J. Kockelkoren and H. Chaté, *Late stages of coarsening in model C*, e-print `cond-mat/0209683`; *Comment on "Deterministic equations of motion and phase ordering dynamics"*, e-print `cond-mat/0209681`.

Dynamic critical exponents of Model C:

[157] B. I. Halperin, P. C. Hohenberg, and S. K. Ma, Phys. Rev. Lett. **29**, 1548 (1972); Phys. Rev. B **10**, 139 (1974).
E. Brézin and C. De Dominicis, Phys. Rev. B **12**, 4954 (1975).

[158] R. Folk and G. Moser, Acta Phys. Slov. **52**, 285 (2002); Phys. Rev. Lett. **89**, 125301 (2002).

Local Scale Invariance: general ideas and applications

[159] M. Henkel, *Schrödinger Invariance and Strongly Anisotropic Critical Systems*, J. Stat. Phys. **75**, 1023 (1994).

[160] M. Henkel, *Phenomenology of local scale invariance: from conformal invariance to dynamical scaling*, Nucl. Phys. B **641**[FS], 405 (2002); *Local scale invariance, conformal invariance and dynamical scaling*, e-print `cond-mat/0209039`.

[161] L. Frachebourg and M. Henkel, Physica A **195**, 577 (1993).

[162] M. Henkel, *Local scale invariance and strongly anisotropic equilibrium critical systems*, Phys. Rev. Lett. **78**, 1940 (1997).

[163] M. Pleimling and M. Henkel, *Anisotropic scaling and generalized conformal invariance at Lifshitz points*, Phys. Rev. Lett. **87**, 125702 (2001).

[164] M. Henkel, M. Pleimling, C. Godrèche, and J. M. Luck, *Aging, phase ordering and conformal invariance*, Phys. Rev. Lett. **87**, 265701 (2001).

[165] M. Henkel, private communication.

Some references on Lifshitz points:

[166] H. W. Diehl, *Critical behavior at m-axial Lifshitz points*, Acta Phys. Slov. **52**, 271 (2002).

[167] H. W. Diehl and M. Shpot, Phys. Rev. B **62**, 12338 (2000).
M. Shpot and H. W. Diehl, Nucl. Phys. B **612**, 340 (2001).

Statics and dynamics of diluted spin models:

[168] A. B. Harris, J. Phys. C **7**, 1671 (1974).

[169] V. J. Emery, *Critical properties of many-component systems*, Phys. Rev. B **11**, 239 (1975).
G. Grinstein and A. Luther, *Application of the renormalization group to phase transitions in disordered systems*, Phys. Rev. B **13**, 1329 (1976).

[170] C. De Dominicis, *Dynamics as a substitute for replicas in systems with quenched random impurities*, Phys. Rev. B **18**, 4913 (1978).

[171] R. Folk, Yu. Holovatch, and T. Yavors'kii, *Critical exponents of a three dimensional weakly diluted quenched Ising model*, e-print `cond-mat/0106468`.
A. Pelissetto and E. Vicari, *Randomly dilute spin models: A six-loop field-theoretic study*, Phys. Rev. B **62**, 6393 (2001).
P. Calabrese, V. Martín-Mayor, A. Pelissetto, and E. Vicari, *Random exchange Ising model*, to appear.
See also Ref. [10].

[172] G. Grinstein, S. K. Ma, and G. F. Mazenko, *Dynamics of spins interacting with quenched random impurities*, Phys. Rev. B **15**, 258 (1977).
U. Krey, Z. Phys. B **26**, 355 (1977).

[173] V. V. Prudnikov, J. Phys. C **16**, 3685 (1983).
I. D. Lawrie and V. V. Prudnikov, *Static and dynamic properties of systems with extended defects: two-loop approximation*, J. Phys. C **17**, 1655 (1984).

[174] V. V. Prudnikov, S. V. Belim, E. V. Osintsev, and A. A. Fedorenko, *Critical dynamics of disordered magnets in the three-loop approximation*, Phys. Sol. State **40**, 1383 (1998).
V. V. Prudnikov, S. V. Belim, A. V. Ivanov, E. V. Osintsev, and A. A. Fedorenko, *Critical dynamics of slightly disordered spin systems*, JETP **87**, 527 (1998).

[175] H. K. Janssen, K. Oerding, and E. Sengespeick, *On the crossover to universal criticality in dilute Ising systems*, J. Phys. A **28**, 6073 (1995).

Monte Carlo simulations of dynamics:

[176] V. V. Prudnikov and A. N. Vakilov, JETP **76** 469 (1993).
H. O. Heuer, J. Stat. Phys. **72**, 789 (1993); J. Phys. A **26**, L341 (1993).
G. Parisi, F. Ricci-Tersenghi, and J. J. Ruiz-Lorenzo, Phys. Rev. E **60**, 5198 (1999).

Other references

[177] I. S. Gradshteyn and I. M. Ryzhik, *Table of Integrals, Series, and Products*, Alan Jeffrey ed., 5th edition (Academic Press, New York, 1994).

[178] V. Martín-Mayor, P. Calabrese, A. Pelissetto, and E. Vicari, in preparation.